Keratan Sulphate metabolism in connective tissue proteoglycans

Thesis submitted in fulfilment of the requirements of the degree of

Doctor of Philosophy, University of Cardiff

September 2005

Briedgeen C. Kerr, BSc (Hons)

Connective Tissue Biology Laboratories

School of Biosciences

Cardiff University, Cardiff

UMI Number: U584769

All rights reserved

INFORMATION TO ALL USERS
The quality of this reproduction is dependent upon the quality of the copy submitted.

In the unlikely event that the author did not send a complete manuscript
and there are missing pages, these will be noted. Also, if material had to be removed,
a note will indicate the deletion.

UMI U584769
Published by ProQuest LLC 2013. Copyright in the Dissertation held by the Author.
Microform Edition © ProQuest LLC.
All rights reserved. This work is protected against
unauthorized copying under Title 17, United States Code.

ProQuest LLC
789 East Eisenhower Parkway
P.O. Box 1346
Ann Arbor, MI 48106-1346

Contents

Chapter 4: Production and characterisation of two new mAbs to bovine corneal keratan sulphate proteoglycans

Acknowledgments

Firstly I would like to thank my supervisors, Professor Bruce Caterson and Dr. Clare Hughes, for the opportunity to work with them in the Connective Tissue Laboratories. I would like to thank them for all their advice, support and encouragement over the course of my PhD.

I would also like to thank all my colleagues and friends in Connective Tissue Biology Laboratories, particularly Sam Hurst, Andrew Waggett, Amanda Hall, Liz Sowter, Amy Wright, Matt Heming, Iris Cheung, Tony Hayes, Aled Jones, Alison Rees, Debbie Tudor, Claire Gealy, Shane Wainright, Melody Liles and Kedar Deogaonkar who all made CTBL a great place to work over the past four years.

Thanks also to my sisters, Clodagh, Maureen, Adele and Joan, my brother Thomas. Also to my mother and father, Mary and Tommy, for all their support in everything I've done.

Finally, a special thanks to my fiancé Adrian, for all his unyielding support, patience and friendship, without him this would not have been possible.

Abbreviations

α	Anti
6-AHA	6 Amino Hexanoicacid
µg	Microgram
µl	Microlitre
µM	Micromolar
aa	Amino Acids
ADAM	A Disintegrin and Metalloproteinase Domain
ADAMTS	A Disintegrin and Metalloproteinase with ThromboSpondin motifs
Ag	Antigen
Ag 8	X 63 Ag 8.563 myeloma cell line
Ala	Alanine
Asn	Asparagine
BCIP	5-Bromo-4-Chloro-1-Indolyl Phosphate
BNC A1D1	Bovine Nasal Cartilage aggrecan
BNC (ABC) core	Chondroitinase ABC digested Bovine Nasal Cartilage aggrecan
BSA	Bovine Serum Albumin
C-terminal	Carboxyl terminal
Ca^{2+}	Calcium ions
cDNA	Complementary DNA
CH	Heavy Chain
COL	Collagenous Domain
C-4-S	Chondroitin-4-Sulphate

C-6-S	Chondroitin-6-Sulphate
C-0-S	Chondroitin-0-Sulphate
C6ST	Chondroitin Sulphate sulphotransferase
C6	Carbon 6
CS	Chondroitin Sulphate
CSI	Chondroitin Sulphate domain I
CSII	Chondroitin Sulphate domain II
CsCl	Caesium Chloride
dATP	Deoxyadenosine Triphosphate
dCTP	Deoxycytidine Triphosphate
DEA	Diethanolamine
dGTP	Deoxyguanidine Triphosphate
DIG	Digoxigenin
DMMB	Dimethylmethylene Blue
DMSO	Dimethyl Sulfoxide
DNA	Deoxyribonucleic Acid
dNTP	Deoxynucleoside Triphosphate
DS	Dermatan Sulphate
d(T)	Deoxythymidine
DTT	DL-Dithiothreitol
dTTP	Deoxythymidine Triphosphate
ECM	Extracellular Matrix
EDTA	Ethylenediaminetetraacetic Acid
EGF	Epidermal Growth Factor
ELISA	Enzyme Linked Immunosorbant Assay

ER	Endoplasmic Reticulum
Fab	Fragment Antigen Binding
Fc	Fragment Crystalline
FACIT	Fibril Associated Collagens with an Interrupted Triple Helix
FBS	Fetal Bovine Serum
Fuc	Fucose
G1	Globular Region 1
G2	Globular Region 2
G3	Globular Region 3
GAG	Glycosaminoglycan
Gal	Galactose
GalNAc	N-Acetylgalactosamine
GAPDH	Glyceraldehyde-3-Phosphate Dehydrogenase
GDP	Guanidine Diphosphate
GlcUA	Glucuronic acid
GlcNAc	N-Acetylglucosamine
$GlcNSO_3$	Glucosamine sulphate
Gln	Glutamine
Gly	Glycine
GNA	Galanthus Nivalis Agglutinin
GPI	Glycosyl Phosphatidylinositol
GTP	Guanidine Triphosphate
HA	Hyaluronic Acid
HABR	Hyaluronic Acid Binding Region
HAS	Hyaluronic Acid Synthase

HAT	Hypoxanthine, Aminopterin, Thymidine
HCl	Hydrochloric Acid
Hep	Heparin
hrs	Hours
HS	Heparan Sulphate
IdUA	Iduronic Acid
IgG	Immunoglobulin G
IGD	Interglobular Domain
IL-1	Interleukin-1
IvD	Intervertebral Disc
kb	Kilobase
kDa	Kilodalton
KS	Keratan Sulphate
KSI	KS type I
KSII	KS type II
KSIII	KS type III
KSGal6ST	Galactose-6-Sulphotransferase
KSPG	Keratan Sulphate Proteoglycan
Leu	Leucine
LLR	Leucine Rich Repeat
M	Molar
MAb	Monoclonal Antibody
Man	Mannose
MCD	Macular Corneal Dystrophy
mg	Milligram

MHC	Major Histocompatibility Complex
mins	Minutes
ml	Millilitre
mm	Millimetre
mM	Millimolar
MMP	Matrix Metalloproteinase
mRNA	Messenger RNA
MSF	Megakaryocyte Stimulating Factor
Mw	Molecular Weight
NaCl	Sodium Chloride
NAD	Nicotinamide Adenine Dinucleotide
NaOH	Sodium Hydroxide
NBT	Nitroblue Tetrazolium
NC	Non-Collagenous
NC3	Non-Collagenous Domain 3
Neu Ac	Neuraminic Acid
ng	Nanogram
N-linked	Nitrogen-linked
nm	Nanometres
OA	Osteoarthritis
°C	Degrees Celsius
O-linked	Oxygen-linked
PBS	Phosphate Buffered Saline
PCR	Polymerase Chain Reaction
pH	Per Hydrogen

Phe	Phenylalanine
PMSF	Phenylmethanesulfonyl Fluoride
Pro	Proline
PTR	Proteoglycan Tandem Repeat
RA	Rheumatoid Arthritis
RNA	Ribonucleic Acid
RNase	Ribonuclease
rpm	Rotations Per Minute
RT-PCR	Reverse Transcriptase Polymerase Chain Reaction
SDS-PAGE	Sodium Dodecyl Sulphate-Polyacrylamide Gel Electrophoresis
secs	Seconds
Ser	Serine
SO_4	Sulphate Group
SZP	Superficial Zone Protein
Thr	Threonine
TNF	Tumour Necrosis Factor
TSA	Tris Saline Azide
Tyr	Tyrosine
U	Unit
UV	Ultraviolet
v/v	Volume for Volume

Summary

The generally accepted structure for KS type I has been proposed to be composed of a pattern of non-sulphated N-acetyl-lactosamine disaccharides located next to the linkage region oligosaccharide, with mono-sulphated N-acetyl-lactosamine in the mid-regions of the KS GAG chain and disulphated N-acetyl-lactosamine disaccharides concentrated towards the non-reducing end of the KS chain (Oeben *et al.*, 1987; Stuhlsatz *et al.*, 1989). The generic structure for KS type II has been reported to occur with a similar pattern but with a predominance of disulphated and occasional interdispersed monosulphated N-acetyl-lactosamine residues present throughout the KS glycosaminoglycan chain (Stuhlsatz *et al.*, 1989). A novel KS monoclonal antibody (mAb) recognising a keratanase-generated KS 'stub' neoepitope was developed and used in conjunction with mAb 5D4 (recognising linear sulphated motifs) to analyse the sulphation pattern of KS from cornea and cartilage. The results of these analyses have demonstrated that KS types I and II chains both contain a combination of differentially sulphated (mono- versus di- versus unsulphated) N-acetyl-lactosamine domains. In the bovine model different tissue sources of KS most likely produce similar varieties of KS disaccharide structures, but that sulphation patterns are more randomly located along the KS chain than previously reported.

Two mAbs were also generated to the small leucine rich KS proteoglycans lumican and keratocan. They were used in the identification of low and increased levels of these 'corneal associated' PGs in musculoskeletal tissue locations with pathology.

Collectively the data challenges the generic structure for KS and proposes a range of KS chain structures that are more heterogeneous in nature, even from within the same tissue sources, than previously thought. The work also suggests that the expression of the KSPGs, lumican and keratocan, may be useful biomarkers to detect cellular changes in metabolism that lead to the onset of degenerative joint disease.

Chapter 1 – Introduction

1.1 Connective Tissues

Connective tissues are composed of a number of structurally and functionally organised extracellular matrix (ECM) components, including water, ground substance and matrix fibres that are produced and maintained by specific connective tissue cells. These all act together to provide a physiologically stable tissue environment where highly specific functions can proceed. Diversity in the amounts and type of the matrix molecules produced within a tissue give rise to variations in physical properties of a tissue. Traditionally, the ECM was thought of as a stability structure, a scaffold for the physical elements of a particular connective tissue. While it does act as such, it also assumes a detailed matrix composition where components display an active functional role in regulating a variety of developmental and physiological processes.

The major components of connective tissue ECMs include an intricate network of twisted collagen fibrils of indefinite length which act as an architectural scaffold to trap and position a matrix of highly hydrated proteoglycan molecules and matrix glycoproteins. The following subsections will review what is currently known about the structure and function of this matrix in different connective tissues with an emphasis on cartilage, intervertebral disc and cornea.

1.2 Connective Tissue Collagens

Collagen is an insoluble extracellular structural protein. It is found in abundance (25% of all body protein) through connective tissues of all multi-cellular animals and is an essential structural component of many connective tissues such as bone, cartilage, cornea, skin, tendon and ligaments. Through tissue specific expression, it functions in conjunction with other matrix molecules in providing tensile strength to a tissue.

Collagen is a heterogeneous population of molecules. Currently there are 27 different known collagens (Fitzgerald & Bateman, 2001; Koch *et al.*, 2001 and 2003; Hashimoto *et al.*, 2002; Sato, 2002; Tuckwell, 2002; Boot-Handford *et al.*, 2003) (table 1.1) based on the supra-molecular structures of a combination of different α chains, which are encoded by a number of genes (Robert *et al.*, 2001; Eyre, 2002; Gelse *et al.*, 2003; reviewed by Michelacci, 2003). They are divided into a number of classes based on these different molecular structures and assemblies: fibrillar; fibril associated collagens with interrupted triple helix (FACITs), network forming collagens, basement membrane collagens, microfibrillar collagens, anchoring collagens, transmembrane collagens and multiplexins. Despite the differences between collagens they all share a characteristic triple helical structure with [Gly-X-Y] repeats, where X and Y are often proline and hydroxyproline, respectively (Michelacci, 2003, review). The position of the glycine is essential for triple helical structure. Other amino acids face outwards and glycine faces inwards and form hydrogen bonds which are important in stabilisation of the collagen triple helical structure. Glycosylation may also occur on collagens in the endoplasmic reticulum and Golgi complex, resulting in a monosaccharide Galactose β - O linkage or a disaccharide Glucosamine α1 – 2 Galactose β1 - linkage to hydroxylysine with N-glycans linking to asparagine

in collagen types IV-VI and chondroitin sulphate (CS) attaching to serine in collagen types IX, XII and XIV.

Fibril forming collagens include types I, II, III, V, XI and XXIV (table 1.1). Three α chains twist into a left handed elongated triple helix through formation of disulphide bonds between chains to form a procollagen molecule which assemble into cross-striated fibrils, where three quarters of two procollagen molecules overlap, to form fibrils of uniform diameter, with each molecule showing displacement of 1/4 of its length along the axis relative to the next collagen molecule (reviewed by Kadler *et al.*, 1996). These organised structures are characteristic of the ECM and give the tissue its characteristic tensile strength.

FACITs do not form fibrils but associate with those that do. They include collagens IX, XII, XIV, XVI, XIX, XX, XXI and XXII (table 1.1) (Koch *et al.*, 2001; Tuckwell, 2002). They share a common motif and they all have one or two triple helical domains separated by non-triple helical domains giving them more flexibility than fibrillar collagens. They bind fibrillar collagens and are thought to mediate interactions between them and other matrix molecules (reviewed by Gelse *et al.*, 2003; Shaw & Olsen, 1991).

Network forming collagens include types IV, VIII and X. The collagens of this family assemble by association at the carboxyl and N-terminus to form two-dimensional cross-linked networks, which form stabilised structures.

The following discussion is primarily concerned with collagens which are present in cartilage and corneal stroma ECM, a brief description of each is given below.

Table 1.1
Collagen classification.

	Type
Fibril-forming	I, II, III, V, XI, XXIV
FACITs	IX, XII, XIV, XVI, XIX, XX, XXI
Network forming	VIII, X
Anchoring	VII
Transmembrane	XIII, XVII, XXV, XXIII
Multiplexins	XV, XVIII
Basement membrane	IV
Microfibrillar	VI
Other	XXII, XXVI

Adapted from Gelse *et al.*, 2003

Type I collagen:

This is a heterotrimer composed of $[\alpha 1\ (I)]_2$ and $\alpha 2$ (I) chains. It is a fibril forming collagen which accounts for a large portion of corneal collagen where it assembles with type V collagen to form single heterotypic fibrils which may be important in the regulation of uniform fibril diameter in the cornea which is essential for transparency (Birk *et al.*, 1988). It also accounts for 90% of the organic bone mass (reviewed by Gelse *et al.*, 2003). It is the major collagen found in large amounts in skin and tendon and is a minor component of cartilage where it is enriched in the lamina splendens of the superficial zone of articular cartilage (Duance, 1983).

Type II collagen:

This is a fibrillar collagen made up of a homotrimer of the form $[\alpha 1\ (II)]_3$ and possesses hydroxylysine-linked galactose residues. It is the main cartilage collagens, where it forms heterotypic fibres with collagens IX and XI. It is also expressed in the vitreous of the eye (Bishop *et al.*, 1994) in the notochord, the developing eye, foetal brain and in the developing skeleton where it is essential for endochondral ossification (Li *et al.*, 1995). There are only minor amounts of type II collagen found in the

cornea. Collagen II in non-pathological articular cartilage shows a turnover with a half life of over 100 years (Knudson & Knudson, 2001, review). Mutations of this collagen cause chondrodysplasia, a disorder characterised by dwarfism, joint and skeletal deformities (reviewed by Kuivaniemi *et al.*, 1997). Electron microscopic analysis shows collagen II fibril structures that have become crosslinked through head-to-tail hydroxylysyl pyridinoline residues (reviewed by Eyre, 2002).

Type III collagen:

This is a fibril forming collagen composed of 3 identical [α1 (III)]$_3$ chains (table 1.1). It is the major component of vascular tissues. In cartilage, it is found in low amounts (Young *et al.*, 2000) and the extent to which it is expressed depends on the ECM condition surrounding the chondrocyte. An increase is observed in chondrocytes of human osteoarthritic cartilage (Aigner *et al.*, 1993) and in wounded corneal tissue (Cintron *et al*, 1988; BenEzna & Foidart, 1981; reviewed by Steele, 1999) and may be made in response to matrix damage and inflammatory responses (Aigner *et al.*, 1993).

Type V collagen:

Type V collagen is a fibril forming collagen which has a [α1 (V)]$_2$ α2 (V) chain form (table 1.1). It is found in the corneal stroma where it co-polymerises together with collagen I monomers within the same fibril to help regulate fibril diameter, essential for transparency in the avian corneal stroma (Birk *et al.*, 1988).

Type VI collagen:

This is a non-fibrillar network forming collagen with a α1 (VI), α2 (VI) and α3 (VI) heterotrimer found in most connective tissues (table 1.1). It is a major component of human corneal connective tissue making up 17% of total corneal collagens

(Zimmermann *et al.*, 1986). It interacts with decorin core protein and other matrix proteins where it is thought to anchor cells to PGs and hence may have a role in regulating the structural organisation of the ECM (Bidanset *et al.*, 1992). In cartilage it forms a disulphide bonded structure involved in providing a fibrillar meshwork which surrounds and protects the chondrocytes (Chang & Poole, 1996). It is involved in regulation of fibril spacing and corneal transparency (Nakamura *et al.*, 1992). In cartilage it is predominantly found in lacunae surrounding the chondrocytes where it forms a fibrillar network that protects the chondrocytes from compressive loads.

Type IX collagen:

This is a FACIT collagen which is composed of three different chains, α1 (IX), α2 (IX) and α3 (IX) with three triple helical domains (COL 1, 2 and 3) flanked by four non-triple helical domains (NC 1, 2, 3 and 4) (Van der Rest *et al.*, 1985; Wu & Eyre, 1995). There are six possible sites where covalent crosslinks may occur with collagen II or collagen XI specifically (Wu *et al.*, 1992). Type IX collagen may also be classified as a proteoglycan since it has a chondroitin sulphate/dermatan sulphate glycosaminoglycan chain attached to the third non-helical domain (Mc Cormick *et al.*, 1987). Type IX collagen is found in developing avian cartilage (Mendler *et al.*, 1989) and in the developing avian corneal stroma (Fitch *et al.*, 1988). Homozygous mice with a mutation in collagen α1 (IX) were shown to be viable at birth. However, degenerative joint disease similar to OA was observed with age from 4 months and older (Fassler *et al.*, 1994). Histological analysis of eyes showed no apparent abnormalities even in older animals that had OA pathogenesis. Their results suggest that α1 (IX) collagen plays an important role in mechanical stability of articular cartilage.

Type X collagen:

Type X collagen is a short chain non-fibrillar network forming collagen composed of a homotrimer of α1 (X) chains with one triple helical domain and two non-triple helical domains. It is present at sites of new bone formation where it is thought to influence chondrocyte hypertrophy through α2β1 integrin cell-type X collagen interactions (Luckman *et al.*, 2003). Type X collagen is expressed in osteoarthritic and rheumatoid articular cartilage but not in normal cartilage (Von der Mark, 1992).

Type XI collagen:

This is a fibril forming collagen and a minor constituent of cartilage. It is a heterotrimer of three different chains, α1 (XI), α2 (XI) and α3 (XI). It contains two collagenous domains (COL 1 and 2) and three non-collagenous domains (NC 1, 2 and 3). The NC 2 domain forms a kink that produces an angle between COL 1 and COL 2. The proteins are cross-linked through head to tail bonds to other type XI collagen molecules and form lateral crosslinks to collagen II (Wu & Eyre, 1995; Eyre, 2002). It functions to promote nucleation of the cartilage type II collagen fibrils (Blaschke *et al.*, 2000)

Type XII collagen:

Type XII collagen is a FACIT collagen found in articular cartilage and the corneal stroma. In the developing avian cornea it has been localised in the subepithelial matrix on day 3 of embryonic development, in the primary stroma on days 5 of development and thereafter in the sub-epithelial and sub-endothelial matrices of the limbus before development of Descemet's and Bowman's membranes (Akimoto *et al.*, 2002; Young *et al.*, 2002).

1.3. Connective Tissue Proteoglycans

Properties of connective tissue ECM are dependent largely on protein and glycosaminoglycan (GAG) interactions, which together form the proteoglycan, a major functional component of connective tissues (Hassell *et al.*, 1986; reviewed by Roughley & Lee, 1994; Iozzo & Murdoch, 1996; Iozzo, 1998). Proteoglycans (PGs) are high molecular weight polyanionic elements of extracellular matrices that are synthesised and localized in accordance with the specific biological requirements of the tissue. They may be as diverse in function as they are in structure. In the ECM tissue they contribute to architectural organisation, and functions range from modulation of growth factor activities, collagen binding (Bindanset *et al.*, 1992; Scott, 1991; Rada *et al.*, 1993; Nakamura *et al.*, 1997), collagen fibrillogenesis (Chakravarti *et al.*, 1998), neurite outgrowth modulation (Cole & McCabe, 1991; Bovolenta & Fernaud, 2000), corneal transparency (Chakravarti *et al.*, 1998; Kao & Liu, 2003) and blood vessel elasticity (Bode-Lesniewska *et al.*, 1996).

In articular cartilage PGs, polyanionic side chains imbibe water and maintain an osmotic force in the ECM that allows cartilage to resist compressive deformation during movement. In corneal stroma, KS and CS/DS PGs are thought to influence corneal transparency by binding collagen fibrils and maintaining uniform fibril diameter and spacing (Chakravarti *et al.*, 1998; Kao & Liu, 2003). These properties are all essential for the proper organization and functioning of the ECM and the tissues associated with it.

1.3.1. Glycosaminoglycan and oligosaccharide attachments

Proteoglycans are formed from covalent interactions between a core protein and one or more glycosaminoglycan chains. GAGs are a family of extended linear polysaccharides and are classified by their characteristic disaccharide repeat structure

(figure 1.1) which are of variable length and can be classed into either sulphated or non-sulphated types. The most common sugar units that occur in GAGs include galactose (Gal), N-acetylglucosamine (GlcNAc), N-acetylgalactosamine (GalNAc), N-sulphated glucosamine ($GlcNSO_4$), uronic acid (UA) and iduronic acid (IdUA) with fucose (Fuc), mannose (Man) neuraminic acid (Neu) and xylose (Xyl) occurring to a lesser extent, mainly at linkage regions and capping structures (table 1.2).

There are six different types of GAG namely; chondroitin sulphate (CS), keratan sulphate (KS), dermatan sulphate (DS), heparan sulphate (HS), heparin (Hep) and hyaluronic acid (HA) (figure 1.1). CS, DS, KS, HS and Hep are all sulphated forms of GAG, which bind to a protein core to form proteoglycans (as described above in section 1.3). HA in cartilage and other tissues is an unsulphated GAG, which exists freely in the ECM (Hardingham & Muir, 1974; Hascall & Heinegard, 1974). Synthesis of HA by cartilage was first described by Gillard *et al.,* (1975).

PG forming GAGs can be bound through either specific O-glycosidic linkages between serine hydroxyl groups and Xyl in CS, DS, HS and Hep, through specific O-glycosidic linkages between serine or threonine and GalNAc in skeletal KS (Mathews & Cifonelli, 1965; Bray *et al.*, 1967), or through specific N-glycosidic linkages between asparagine and GlcNAc in corneal KS (Baker *et al.*, 1969; 1975; Nilsson *et al.*, 1983; Nakazawa *et al.*, 1983).

1.3.1.1. Keratan Sulphate

Keratan sulphate was first identified in the cornea by Suzuki in 1939, who established that the corneal mucoid contained galactose and glucose in equal amounts, as well as acetyl and sulphate groups. Keratosulphate was the name later given to this molecule when it was characterised by Meyer *et al.* in 1953 that we now call keratan sulphate (KS).

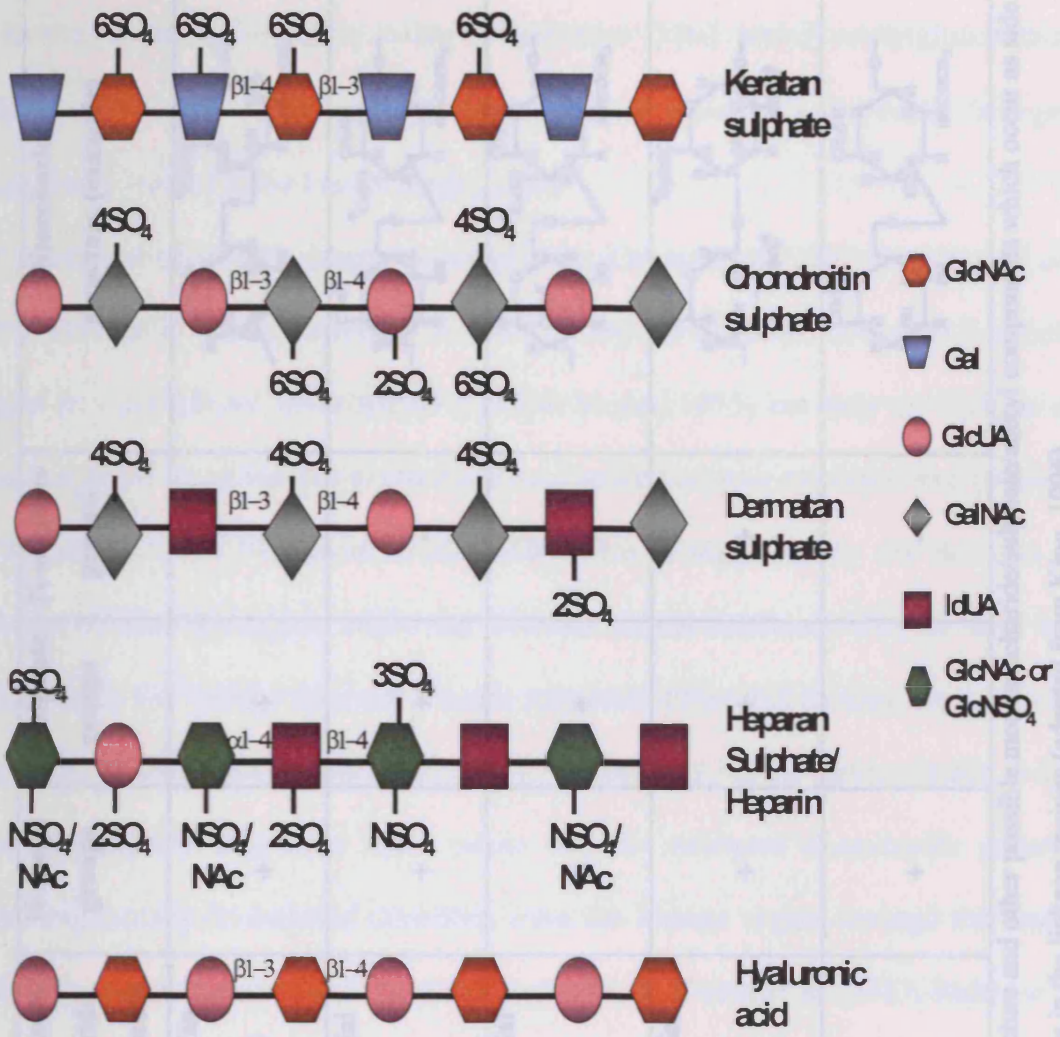

Figure 1.1 The disaccharide repeat structures characteristic of the different sulphated glycosaminoglycans (adapted from Hardingham & Fosang, 1992).

GAG	Repeat disaccharide components	Other mono-saccharide components	N-acetyl groups	O-sulphate groups	N-sulphate groups	Disaccharide structure (example)
Corneal KS I /Skeletal KS II	GlcNAc + Gal	Fuc, Man, Neu	+	+	-	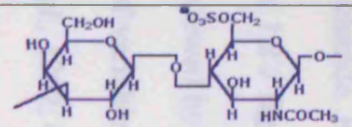
C-4-S /C-6-S /C-0-S	GalNAc + GlcUA	Xyl, Gal	+	+	-	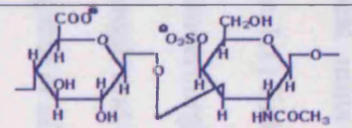
DS	GalNAc +GlcUA/IdUA	Xyl, Gal	+	+	-	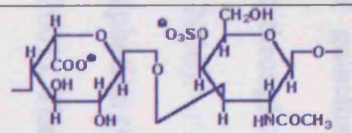
HS / Heparin	GlcNAc +GlcUA/IdUA	Xyl, Gal	+	+	+	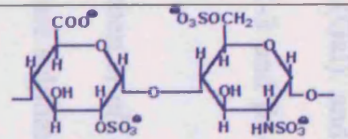
HA	GlcNAc + GlcUA		+	-	-	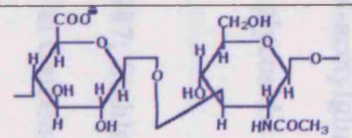

Table 1.2 The polysaccharide disaccharide structure and other possible monosaccharide/sulphate/acetyl components which occur as side branches or in the linkage regions (adapted from King, 1996).

Since then it has been further characterised into three types, KS I [corneal], KS II [skeletal] (Meyer, 1956) and KS III [brain] (Krusius *et al.*, 1986) all of which have the definitive disaccharide repeat units of galactose (Gal) and N-acetylglucosamine (GlcNAc) (table 1.2 / figure 1.1) linked through β1-3 and β1-4 glycosidic linkages, respectively (reviewed by Funderburgh, 2000).

KS chains are of variable length and sulphation (Oeben *et al.*, 1987; Stuhlsatz *et al.*, 1989; Block *et al.*, 1992; Oguma *et al.*, 2001). They are sulphated at Carbon-6 of both sugars in a disulphated disaccharide (Choi & Meyer, 1975) but only on GlcNAc of monosulphated disaccharides as this monosaccharide becomes sulphated first (Fukuda & Matsumra, 1976; Nakazawa *et al.*, 1998). This is supported by the fact that in macular corneal dystrophy, where the GlcNAc sulphotransferase enzyme does not function, the Gal residue does not become sulphated either and so may require initial sulphation of GlcNAc (Akama *et al.*, 2001), see section 1.4.3 for further details. It has been hypothesised that these non-, mono- and di- sulphated disaccharide patterns occur sequentially in domains stretching from the linkage region through the centre and to the non-reducing end of the chain, respectively (Oeben *et al.*, 1987; Stuhlsatz *et al.*, 1989) and this has been the accepted structure for the corneal KS chain since then. However, challenging this generic structure, Dickenson *et al.*, (1990) have identified a 6-sulphated GlcNAc residue occurring attached directly to the GalNAc of the linkage region. The extent to which KS sulphation occurs, and chain length proceeds, depends on tissue specific factors such as galactosyltransferase, glycosyltransferase and sulphotransferase expression (Nakazawa *et al.*, 1998; Sashima *et al.*, 2002; Kushe-Gullberg & Kjellen, 2003) which differ with specific requirements of the tissue (see section 1.4.1.3).

In vivo functions of KS include organogenesis (e.g. cartilage, heart, gonad, pancreas) during chick development (Hemming & Saxod, 1998), possible implications in diminishing the motility of lung cancer cells (Seko & Yamashita, 2004), cartilage maintenance and metabolism (Scott, 1994; Leroux *et al.*, 1996; Pratta *et al.*, 2000) and maintenance of corneal transparency (Cornuet et al., 1994; Nakazawa et al., 1984). KS substitution has been shown to increase with age in a variety of connective tissues (Kaplan & Meyer, 1959; Sweet *et al.*, 1979; Thonar *et al.*, 1986; Hering *et al.*, 1997). In addition, it has been shown that in the human cartilage KS increases in sulphation and molecular size from foetal up to 9 years of age, at which point there is a change in molecular size (Brown *et al.*, 1998).

KS type I (corneal specific), KS type II (skeletal specific) and KS type III (brain specific) are distinguished from each other by their different linkage regions, which are N- or O-linked (figures 1.2 – 1.5).

Type I KS (see figure 1.2) is characteristic of the KS found in cornea, but is not tissue specific as it has also been found in cartilage on small leucine-rich KSPGs (Funderburgh *et al.*, 1987) where as it is present in its unsulphated polylactosamine form. KS type I can also occur N-linked in the hyaluronic acid binding region of aggrecan (Barry *et al.*, 1995) where KS type II is the prevalent KS form in other GAG-attachment domains of aggrecan. Recently, Poon *et al.*, (2005) demonstrated that N-linked KS substituted onto Asparagine at position 368 in the IGD domain of aggrecan facilitated aggrecanase cleavage at the $E^{373} - E^{374}$ cleavage site. KS type I binds through N-glycosidic linkages from GlcNAc to asparagine residues of an Nx(S/T) site on the proteoglycan core protein (figure 1.2) (Choi & Meyer, 1975;

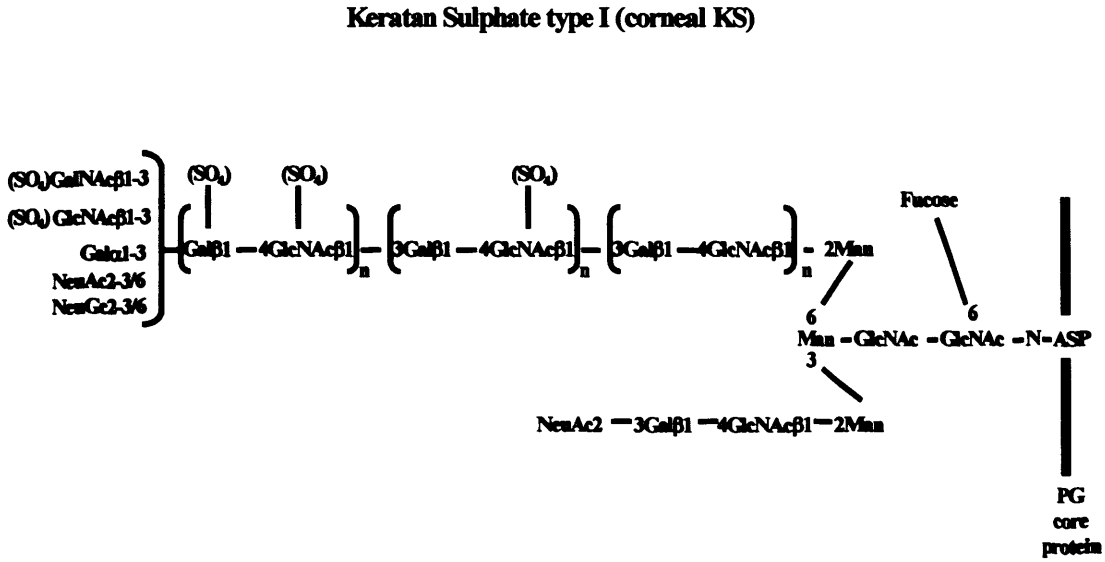

Figure 1.2 Keratan Sulphate type I structure is N-linked and found attached to SLRPs (Oeben *et al.*, 1987; Stuhlsatz *et al.*, 1989; Tai *et al.*, 1996; 1997; Funderburgh, 2000).

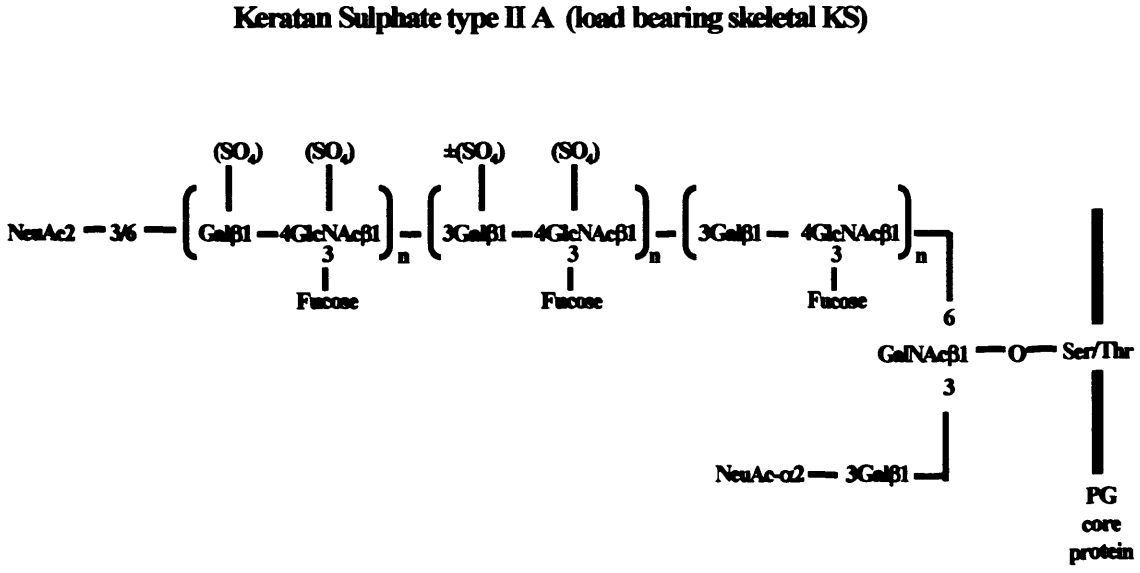

Figure 1.3 Keratan Sulphate type II A from load bearing tissues such as cartilage and IvD. KS II is O linked to serine or threonine (Stuhlsatz *et al.*, 1989; Nieduszynski *et al.*, 1990 B; Tai *et al.*, 1996. 1997; Funderburgh, 2000).

Keratan Sulphate type II B (non-load bearing skeletal KS)

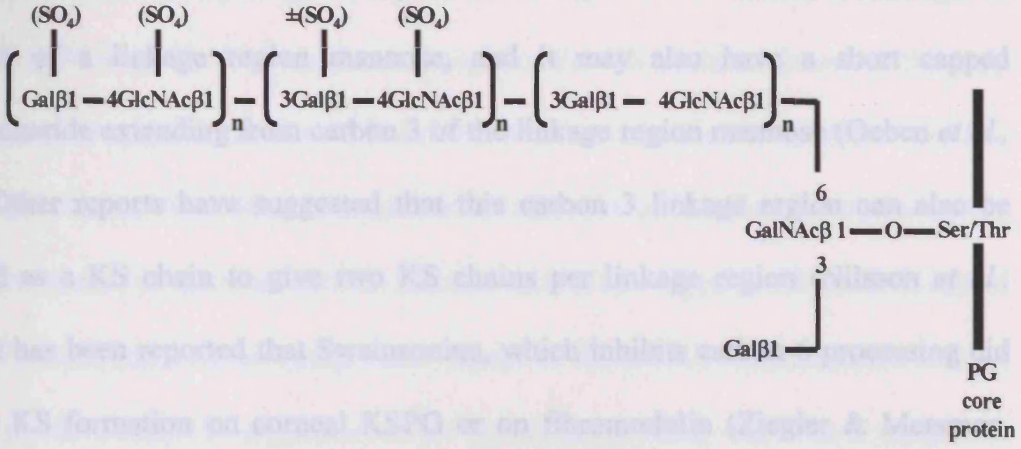

Figure 1.4 Keratan sulphate type II B from non-load bearing tissues such as trachea and nasal cartilage and is also O-linked to a core protein through serine or threonine (Nieduszynski *et al.*, 1990 B; Funderburgh, 2000).

Keratan Sulphate type III (brain KS)

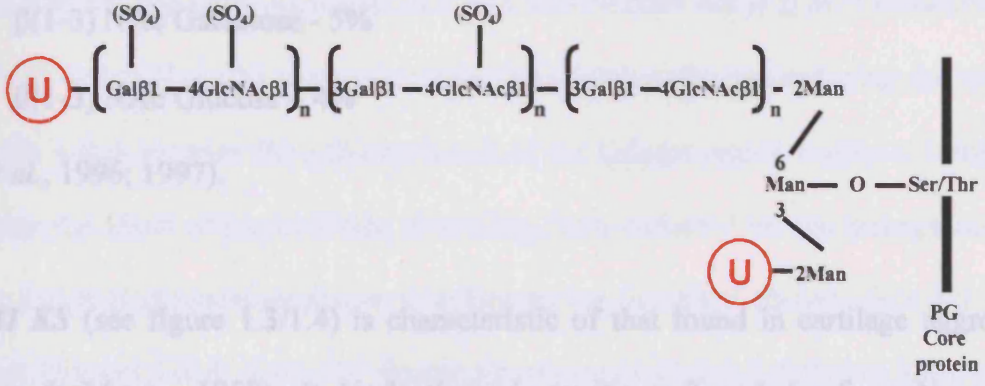

Figure 1.5 Keratan Sulphate type III structure from brain is O-linked through mannose to the core protein of nervous tissue KSPGs (**U** = unknown). It is lower sulphated than KS types I or II.

Nilsson *et al.*, 1983; Stuhlsatz *et al.*, 1989; Plaas *et al.*, 1990) where the presence of aromatic residues surrounding the Nx(S/T) sequence appears to be important in the attachment of KS at this site (Dunlevy *et al.*, 1998). The KS I chain extends from carbon 6 of a linkage region mannose, and it may also have a short capped oligosaccharide extending from carbon 3 of the linkage region mannose (Oeben *et al.*, 1987). Other reports have suggested that this carbon 3 linkage region can also be extended as a KS chain to give two KS chains per linkage region (Nilsson *et al.*, 1983). It has been reported that Swainsonine, which inhibits carbon 6 processing did not stop KS formation on corneal KSPG or on fibromodulin (Ziegler & Mersman, 1984; Plaas & Wong-Palms, 1993), indicating that it can be extended on carbon 3. The non reducing terminal of the KS I chain may be capped by any of the following:

- α(2-6) linked NAc Neuraminic acid - 41%
- α(2-3) linked NAc Neuraminic acid – 12%
- α(2-3) linked Glycosyl Neuraminic acid – 6%
- α(2-6) linked Glycosyl Neuraminic acid - 6%
- α(1-3) Galactose – 26%
- β(1-3) NAc Galactose - 5%
- β(1-3) NAc Glucose – 4%

(Tai *et al.*, 1996; 1997).

Type II KS (see figure 1.3/1.4) is characteristic of that found in cartilage aggrecan (Kalpan & Meyer, 1959). It binds through positions 3 and 6 of an N-acetyl-galactosamine (GalNAc) residue that is O-glycosidically linked to the hydroxyl group of serine or threonine on a core protein (figure 1.3/1.4) (Bray *et al.*, 1967; Choi & Meyer, 1975; Kikuchi *et al.*, 1987; reviewed by Stuhlsatz *et al.*, 1989). The KS II

chain may be capped by neuraminic acid at C-3 or C-6 of the terminal GlcNAc (Funderburgh, 2000, review). It can have α (1-3) fucose attachments with levels escalating with increasing length of the KS chain. The fucose residues are thought to attach to the C-3 of GlcNAc residues throughout the KS chain as these are the only sugars within the polylactosamine KS chain that are not already substituted on the C-3 position (Nieduszynski *et al.*, 1990 A). Fucose can also be found at the non-reducing capping structures of the extended KS chain, which when capped with α (2-3) linked N-acetyl neuraminic acid is a sulphated variant of the Vim-2 differentiation antigen (Brown *et al.*, 1996). When found in an unsulphated form, the Vim-2 antigen is thought to be an important structure in early cartilage development, whose structure may later become sulphated to mask the Vim-2 epitope when its role in development is complete. This idea is supported by the fact that fetal cartilage KS is found in an undersulphated form and that sulphated isoforms of KS increase dramatically with age.

KS II can be subdivided into either KS II A (Articular) or KS II B (Basic) (Nieduszynski *et al.*, 1990 B). Whilst KS II A is found in load bearing tissues such as intervertebral disc and articular cartilage, KS II B is found in non-load bearing tissues such as tracheal and nasal cartilage. KS II A differs from KS II B as it possesses an α (2 → 6) linked N-acetyl neuraminic acid (NeuNAc) at the non-reducing end of the KS chain which extends from the carbon 6 of the linkage region GalNAc. NeuNAc also caps the short oligosaccharide extending from carbon 3 of the linkage region residue and it also possesses fucose attachments (as described above) while KS II B does not (figures 1.3 & 1.4). The functional relevance of the 2 different KS type II structures is unknown, but perhaps may be a consequence of the load bearing properties of the tissues and fucose / NeuNAc attachments may play a role in binding or recognition of other articular cartilage molecules (Nieduszynski *et al.*, 1990 B).

Type III KS (see figure 1.5) is characteristic of KS found in the brain (Eronen *et al.*, 1985; Krusius *et al.*, 1986; Papageorgakopoulou *et al.*, 2001; 2002) where it is found attached to proteoglycans such as SV2, Phosphocan or Claustrin, and is thought to be involved in the modulation of cell interactions and neurite outgrowth in the developing brain (Margolis & Margolis, 1993, review). Its repeat disaccharide structure is composed of monosulphated disaccharide units of Gal β (1-4) – GlcNAc 6S – β (1-3), similar to KS types I and II (figure 1.5). It is lower sulphated than KS type I or II (Oguma *et al.*, 2001). It also differs from KS types I and II through differences in its linkage region, here the extended repeat disaccharide chain is O-glycosidically linked to serine or threonine of a proteoglycan core protein through mannose (figure 1.5). Structural heterogeneity and low concentrations have so far limited its isolation and a more detailed characterisation (Papageorgakopoulou *et al.*, 2001).

1.3.1.2. Chondroitin Sulphate

Chondroitin sulphate is a component of all connective tissues of the body, found primarily in cartilage and IvD. The specific chondroitin sulphate (CS) repeats are made up of disaccharide units of glucuronic acid (GlcUA) and GalNAc. Each chain consists of 20-40 disaccharide units (Mw 12-20 kDa), (table 1.2 / figure 1.1) which are linked through alternating β(1-3) and β(1-4) glycosidic linkages. Sulphation occurs at position 4 or 6 of GalNAc but the significance of these sulphation positions are at present unclear, although non-sulphation and / or C-4-sulphation has been shown to be more prominent in immature cartilage (Mourao et al., 1976) and in the corneal stroma (Hart, 1976; Midura & Hascall, 1989). Sulphation patterns have been shown to change with the onset of osteoarthritis and with age (Hardingham, 1995; Plaas *et al.*, 1998; Lauder *et al.*, 2001). Chain length can also vary through embryonic

development (Thonar & Sweet, 1981). CS biosynthetic attachment is signalled by a specific consensus sequence of 2 or 3 acidic amino acids followed by Ser - Gly - X - Gly where serine is the specific CS attachment site. Xylose is the initial attachment sugar attached through O-glycosidic linkages to the hydroxyl group of serine of the core protein (Lindahl & Roden, 1965). It is then followed by 2 galactose residues and a GlcUA residue. This Xyl - β (4-1) -Gal - β (3-1) - Gal - β (3-1) - GlcUA linkage region is followed by the addition of the characteristic series of repeat GalNAc and GlcUA residues. This is all dependent on the availability of specific glycosyltransferases and sulphotransferases and the availability of precursors (Telser *et al.*, 1965); this is discussed further in section 1.4.2.

1.3.1.3. Dermatan Sulphate

DS is a modified form of CS where it may contain GalNAc, GlcUA and Iduronic acid (IdUA) in its repeat disaccharide structure (table 1.2/figure 1.1). The IdUA is formed by epimerisation of GlcUA by C-5 uronosyl epimerase (Malmstrom & Aberg, 1982). It may have one to all of its glucuronic acids undergo this modification depending again upon tissue specific factors. The uronic acid residues undergo sulphation at position 2 of IdUA and at position 4 of GalNAc as with CS on GalNAc. It has a molecular weight of 15 - 40 kDa. It has been shown to bind collagen type V in vitro (Munakata *et al.*, 1999).

1.3.1.4. Heparan Sulphate

Heparan sulphate (HS) is a complex structure composed of a repeat disaccharide structure of GlcNAc (N-acetylated glucosamine) or $GlcNSO_4$ (N-sulphated glucosamine), iduronic acid (IdUA) and glucuronic acid (GlcUA) (table 1.2) with a molecular weight of 50 -100 kDa. Some of the GlcUA residues may undergo

epimerisation to become IdUA and are attached to a core protein in a similar manner to CS and DS (reviewed by Sugahara & Kitagawa, 2002). Sulphation occurs at position 6 or 3 of the $GlcNSO_4$ but only at the position C6 of GlcNAc and at the 2 position of IdUA residues, or they may not be sulphated at all, these multiple combinations adding to the structural heterogeneity of the HS chains (figure 1.1). HS is found mainly on cell surface proteoglycans, on some pericellular matrix proteoglycans and in basement membrane proteoglycans where it functions in binding cell growth factors such as fibroblast growth factor (FGF) (Imamura & Mitsui, 1987), vascular endothelial growth factor (VEGF) (Conrad, 1997 review), hepatocyte growth factor (HGF) and interleukins 3 and 7 for signal transduction. Its structure too is tightly controlled during the biosynthetic process so that it is also tissue specific.

1.3.1.5. Heparin

Heparin is an extensively modified and over sulphated form of HS (Conrad, 1997, review) with a molecular weight of 60 - 100 kDa. It is composed of the same repeat disaccharide pattern with GlcNAc and GlcUA or IdUA (table 1.2./figure 1.1) connected through a Xyl - β(4-1) -Gal - β(3-1) - Gal - β (3-1) - GlcUA linkage region sequence to peptides (reviewed by Sugahara & Kitagawa, 2002). Its synthesis appears to be restricted to the mast cell where it is found only in storage granules on serglycin proteoglycan. It functions as an anticoagulant of blood by blocking the action of thrombin and is widely used as an anticoagulant drug. It also regulates angiogenesis (Folkman & Shing, 1992). It has been shown to bind with collagen types V and IX, and with fibronectin, laminin and vitronectin in vitro (Munakata *et al.*, 1999).

1.3.1.6. Hyaluronic Acid

In contrast to other GAGs, hyaluronic acid (HA) is found as a free glycosaminoglycan lacking covalent attachment to a protein core (reviewed by Roughley & Lee, 1994). HA is synthesised on the internal surface of the cell plasma membrane and the polysaccharide chain is then released from the cell free of any protein attachments (Prehm, 1984). It is distributed widely through the body, in synovial fluid, vitreous humour, loose connective tissue and cartilage. It is made of repeat sugar units of β (1-4) GlcUA β(1-3) GlcNAc (table 1.2./figure 1.1) which are unsulphated giving it a much less complex structure than the other sulphated GAG. It has a variable molecular weight (M_w) ranging from 300 – 2000 kDa depending on the tissue function and stage of development. One of HAs most important functions in cartilage is its ability to non-covalently bind large numbers of aggrecan molecules to form multimolecular aggregates essential for the characteristic structural arrangement which is necessary for the normal functioning of articular cartilage (Hardingham & Muir, 1974; Hascall & Heinegard, 1974). In this aggregate it also non-covalently binds link protein, which stabilise the aggregate structure (Heinegard & Hascall, 1974; Baker & Caterson, 1979). It also interacts with a number of other proteoglycans e.g. versican, neurocan and brevican which all have hyaluronic binding regions similar to that found on aggrecan and are discussed further in section 1.3.2.1.

1.3.1.7. N- and O- linked oligosaccharides

Oligosaccharides are carbohydrate complexes which are often found as side chains on PG molecules. They attach to serine or threonine through O-glycosidic linkages or to asparagine through N-glycosidic linkages (Lohmander *et al.*, 1980). They have similar linkage regions to corneal and skeletal KS, but are not variably sulphated as with KS chains.

Oligosaccharide attachments to various peptide cores act in modifying peptide properties. They impart hydrophilic properties, protect against proteases, play essential roles in embryonic development and intramolecular regulation where they act as differentiation antigens, they target hormones to specific organs and they cover antigenic determinants. It is the N-linked oligosaccharides that become extensively modified with mannose, to a complex type oligosaccharide, which can be further processed to synthesise KS type II chains (Nilsson *et al.*, 1983; Dunlevy *et al.*, 1998).

1.3.2. Proteoglycans of cartilage and cornea

The general ECM proteoglycan structure consists of several distinct functional domains spanning a protein core, which may be variably glycosylated, and of different lengths and sequences. Some families may conserve a degree of sequence homology (reviewed by Roughley & Lee, 1994; Hardingham & Fosang, 1992; Iozzo, 1998; 1999). They may be classified into a number of families including the large hyaluronic acid binding extracellular proteoglycans and the small leucine rich proteoglycans (SLRPs).

1.3.2.1. Large Aggregating Proteoglycans

This group of proteoglycans include aggrecan, versican and the nervous tissue proteoglycans, brevican and neurocan (figure 1.6). All of these have a central GAG binding domain that is flanked by a hyaluronic acid binding region (HABR) at the N-terminal and a lectin binding domain at the C-terminal which led them to being termed as hyalectans (Doege *et al.*, 1987; Rauch *et al.*, 1992; Halberg *et al.*, 1988; Iozzo & Murdoch, 1996; reviewed by Iozzo, 1998). The general structural features of

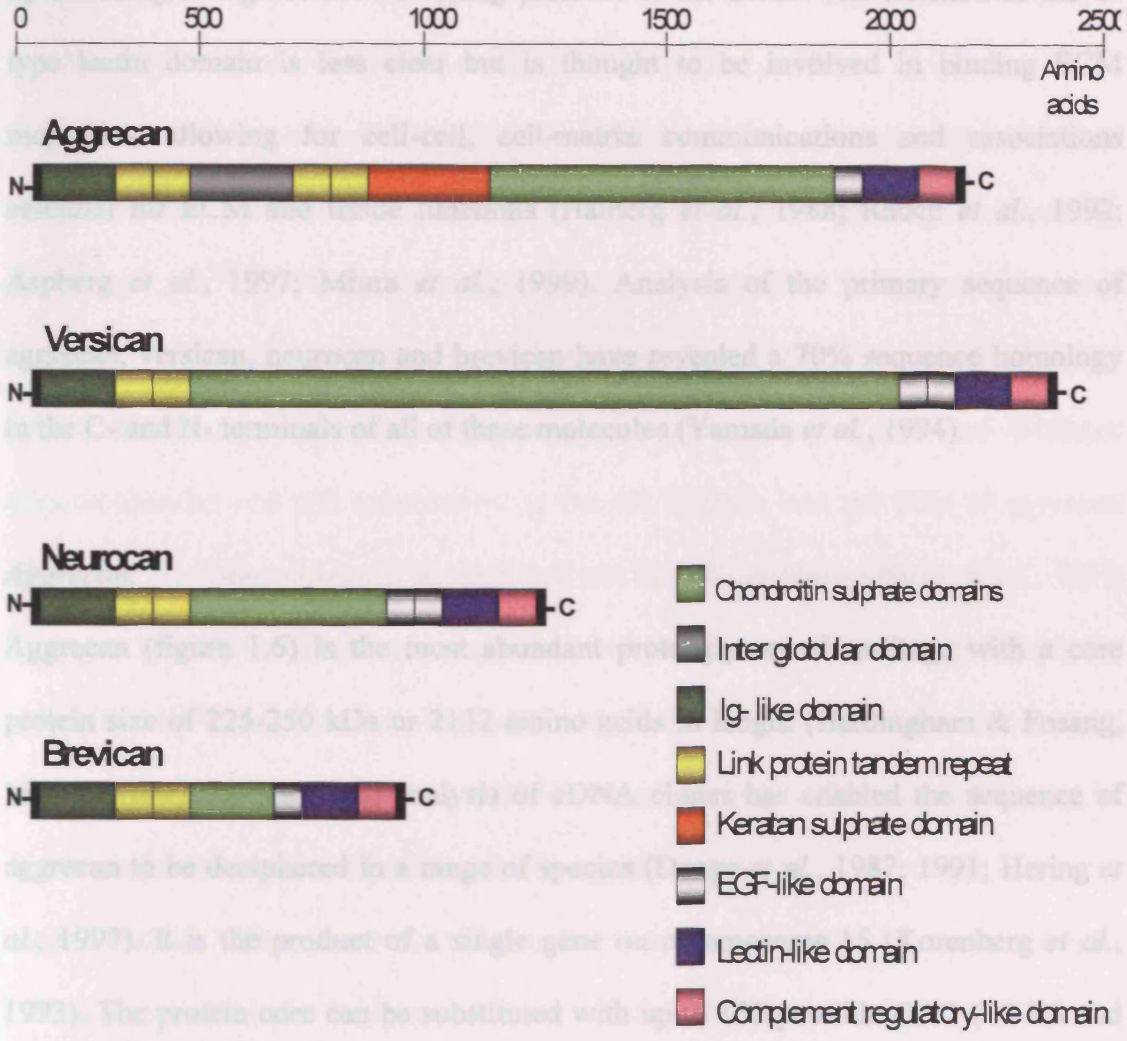

Figure 1.6 Structural domains of the Hyalectans (Adapted from Rauch *et al.*, 1992; Yamada *et al.*, 1994)

these proteoglycans allow the formation of large aggregates by interaction with HA and link protein. These large macromolecular aggregates are entrapped within the collagen fibrils and allow cartilage to resist compressive loading through the action of negatively charged sulphated GAG chains attached to the proteoglycan core proteins by affording a large osmotic swelling pressure to the tissue. The function of the C-type lectin domain is less clear but is thought to be involved in binding ECM molecules, allowing for cell-cell, cell-matrix communications and associations essential for ECM and tissue functions (Halberg *et al.*, 1988; Rauch *et al.*, 1992; Aspberg *et al.*, 1997; Miura *et al.*, 1999). Analysis of the primary sequence of aggrecan, versican, neurocan and brevican have revealed a 70% sequence homology in the C- and N- terminals of all of these molecules (Yamada *et al.*, 1994).

Aggrecan:

Aggrecan (figure 1.6) is the most abundant proteoglycan of cartilage with a core protein size of 225-250 kDa or 2132 amino acids in length (Hardingham & Fosang, 1992, review). Isolation and analysis of cDNA clones has enabled the sequence of aggrecan to be deciphered in a range of species (Doege *et al.*, 1987; 1991; Hering *et al.*, 1997). It is the product of a single gene on chromosome 15 (Korenberg *et al.*, 1993). The protein core can be substituted with up to 150 possible GAG (50 KS and 100 CS) attachments and a number of N- and O- linked oligosaccharides, although this number varies greatly with age and pathology (Lohmander *et al.*, 1980).

Aggrecan protein core structure is comprised of 3 globular domains G1, G2, and G3 N-terminal to C-terminal direction (figure 1.6). G1 (the HA binding domain) is of particular functional importance in the formation of cartilage aggregates. It is through this domain that aggrecan monomers bind non-covalently to HA and in non-covalent associations with link protein to form the large multimolecular weight aggregates. The

G1 domain occurs as a protein tandem repeat (PTR) loop with an immunoglobulin (Ig) like fold at the N-terminal of the protein core (Perkins *et al.*, 1989). As well as interacting with HA, the G1 domain also non-covalently interacts with a small glycoprotein termed link protein, which has similar PTR and Ig fold structures. The interaction helps stabilise the aggregate and without it HA-aggrecan interaction is considerably reduced (Buckwalter *et al.*, 1984; Tang *et al.*, 1996).

Adjacent to G1 is a short interglobular domain (IGD) where several N-linked oligosaccharide substitutions occur and several protease cleavage sites are found e.g. Glu^{373} and Ala^{374}, a designated aggrecanase cleavage site. Such proteases cause truncation of the aggrecan molecule with age and disease (Hering *et al.*, 1997; Little *et al.*, 2002). Age related changes occur in composition of N- and O-linked oligosaccharides and KS substitution in the G1 domain and the IGD of aggrecan where KS has been observed in steer but not in calf cartilage (Barry *et al.*, 1995; Hering *et al.*, 1997). It has been suggested that this age related substitution with KS may influence aggrecan catabolism at the aggrecanase cleavage site as its removal prevented cleavage (Pratta *et al.*, 2000; Poon *et al.*, 2005). Therefore, KS may be important for the recognition of this site by aggrecanases.

Adjacent to the IGD region is the G2 domain, which is structurally similar to G1 in its PTR motifs, but it lacks the Ig motif. The exact function of the G2 domain is yet to be determined. Between the G2 and G3 domains a longer GAG attachment region is found. At the amino terminal side of this GAG attachment region is a domain containing specific sequences for KS type II attachment (Heinegard & Axelsson, 1977). This is about 113 amino acids in length but can vary between species (Barry *et al.*, 1994). This KS attachment region may contain approximately 30 KS chains but this number varies greatly with animal species, development, age and pathology of the tissue (Sweet *et al.*, 1979; Thonar & Sweet, 1981). The amino acid sequence of the

bovine aggrecan KS attachment region has been determined (Antonsson *et al.*, 1989). It consists of a hexapeptide consecutively repeated 23 times and has 19-20 serine and 9-10 threonine sites for possible attachment of O-glycosidically linked carbohydrate chains, many of which may be further substituted with KS. KS content differs considerably between foetal and adult articular cartilage PGs (Sweet *et al.*, 1979; Thonar & Sweet, 1981; Inerot & Heinegard, 1983; Thonar *et al.*, 1986; Scott, 1994). In the KS domain the sum of O-glycosidically linked oligosaccharides plus KS remain constant, however KS content increases with development and age, presumably gradually replacing the O-linked oligosaccharides with increasing age (Inerot & Heinegard, 1983). The significance of the increase observed in KS substitution and the specific changes in sites of substitution at present remains unclear (possibilities are discussed in section 1.4.3).

Following the KS attachment region lies another GAG binding region, CS I, which possesses primarily CS chains but also some KS (Heinegard & Axelsson, 1977). This region is followed by another CS binding region CS II. Collectively, these regions may contain up to 100 CS chains. During development, age and disease the number of CS chains decreases substantially and the number of KS substitutions also increases considerably through the CS I and CS II domains of the protein core (Inerot & Heinegard, 1983). This has major functional and structural implications on cartilage and is discussed further in section 1.5.

Finally, the G3 domain is located at the C-terminal of the core protein and contains two epidermal growth factor (EGF)-like repeats, a complement regulatory protein and a lectin-like domain that are characteristic of this hyalectan family (Roughley & Lee, 1994). The G3 domain has been shown to selectively bind to sugars such as fucose or galactose with low affinity in a calcium dependent manner and thus can bind the galactose residues found on collagen type II (Halberg *et al.*, 1988; Iozzo & Murdoch,

1996; Iozzo, 1998). This G3 domain may act to link aggrecan with other cartilage ECM components and cells.

Versican:

Versican (figure 1.6) is the largest member of the hyalectan family of proteoglycans with a 2,389 amino acid core protein sequence and a molecular weight of 400kD (Krusius *et al.*, 1987). It is expressed by fibroblasts. It shares 3 characteristic domains with aggrecan, the HABR, the GAG binding region and the lectin binding region (Zimmermann & Ruoslahti, 1989). The HABR with an Ig and 2 protein tandem repeat motif structures, make it typical of this family allowing it to bind HA through non-covalent bonds to form aggregates, which are typically found in blood vessels (Bode-Lesniewska *et al.*, 1996) where it is thought to contribute to the elastic properties of this tissue allowing it to stretch and relax. It is also found in smooth muscle, fibrous and elastic cartilage, the central and peripheral nervous system, the epidermis and glandular epithelia (Bode-Lesniewska *et al.*, 1996). The GAG attachment domain is subdivided into two regions GAGα and GAGβ, respectively, which together contain up to 30 CS or DS GAG chains covalently bound to the core protein along with N- and O- linked oligosaccharides (review by Iozzo & Murdoch, 1996). At the C-terminal end it contains 2 of the common EGF-like repeats, a common C-type lectin and a complement regulatory protein motif which acts as it does in aggrecan to allow cell-cell and cell-matrix interactions.

Neurocan:

Neurocan, a brain specific proteoglycan, has been cloned and its primary structure deduced (Rauch *et al.*, 1992). It has 1,257 amino acids in its core protein sequence and has a molecular weight of 136 kDa. It is a member of the hyalectan family and is

composed of a HABR (G1 domain), a GAG binding region and 2 EGF like repeats (figure 1.6). The C-terminal area displays 60% sequence homology with the G3 domain of the fibroblast and cartilage PGs, versican and aggrecan (Margolis & Margolis, 1993, review). The central region of neurocan has no homology with other hyalectans. The primary structure (136 kDa) accounts for approximately ~60% of neurocans' 300 kDa molecular weight (Rauch *et al.*, 1991; 1992). The GAG attachment region consists of 3 CS attachments (~20% of total molecular weight) and several sites for N- and O- glycosylation (~20% total molecular weight). Friedlander *et al.*, (1994) have shown that neurocan binds to cell adhesion molecules N-CAM/L1/NILE and Ng-CAM with the CS glycosaminoglycans playing an active role in this process, which acts to inhibit neuronal outgrowth, an important occurrence during development.

Brevican:

Brevican is another member of the Hyalectan family that has been cloned and sequenced (Yamada *et al.*, 1994), and shown to possess 912 amino acid residues in its core protein. It possesses a hyaluronic acid binding region (containing an Ig like loop and 2 link protein tandem repeats) and lectin like (G3 domain) functional domains which are similar to aggrecan and versican. However, it only has one EGF-like repeat at the C-terminal region (figure 1.6). As its name suggests it has the shortest GAG attachment region where five serine-glycine and glycine-serine dipeptide sequences are present which are possible CS/DS attachment sites. It can also be found in the brain with no GAG attachments where it has been shown to run to the correct molecular weight on SDS-PAGE without prior chondroitinase ABC digestion (Yamada *et al.*, 1994). Brevican shows a high degree of sequence homology – 50 - 60% (review by Iozzo, 1998) to the other members of this family. Its expression is

confined to brain and central nervous system tissues and it was not located in bovine heart, lung or spleen. It may exist as a free ECM form or as a membrane bound form linked through a glycosyl phosphatidylinositol (GPI) moiety (Seidenbecher *et al.*, 1995). It can be found in processed forms that lack the GAG binding region and the N-terminal domain (Yamada *et al.*, 1995).

This group of large aggregating PGs have similar functional characteristics in that they all bind HA through a similar HABR and they also bind carbohydrates through their homologous lectin binding region, creating an extracellular network whereby HA is linked to cell surfaces through the carbohydrate/lectin binding region of these PGs. Although they share these functional capabilities, the differences in the central GAG binding regions and GAG attachment possibilities of each of these proteoglycans indicate different functional capacities for these regions of the PGs. The expression of and compensation for such molecules at different points of development or pathogenesis may be important aspects of such processes.

1.3.2.2. Small Leucine Rich Repeat Proteoglycans (SLRPs)

This family of PGs are particularly important in regulation of the collagen network assembly and maintenance. They include a series of lower molecular weight proteoglycans (25-40 kDa) such as decorin, biglycan, lumican, keratocan, fibromodulin and mimecan, which are structurally related but are the products of different genes and perform different functions (review by Iozzo, 1999). The amino terminal of these molecules may contain chondroitin sulphate or dermatan sulphate glycosaminoglycan (GAG) attachments or tyrosine sulphate attachments and N-linked oligosaccharides. Also found in this region are 4 conserved cystine repeats which form disulphide bonds (figure 1.7). Adjacent to the N-terminal lies a central protein core with a highly conserved region rich in a variable number of leucine repeat

residues (LRR) with the consensus sequence LxxLxLxxN/Cx (where x is any amino acid and L can be leucine, valine, isoleucine or phenylalanine). This LLR region may be involved in a range of functions such as cell adhesion, DNA repair, RNA processing and signal transduction (reviewed by Iozzo, 1999). Keratan sulphate GAGs may be found in this region. A further 2 conserved cystine repeats are found at the carboxyl terminal of the protein core which form disulphide bonds. The function of this region is yet poorly defined.

In general, the SLRPs bind with other ECM molecules to organise the matrix architecture. In the cornea, they are localised between collagen fibrils where they affect fibril assembly and play an important role in corneal transparency (Scott & Haigh, 1988; Funderburgh *et al.*, 1991 A; Scott, 1992; Rada *et al.*, 1993; Cornuet *et al.*, 1994; Chakravarti *et al.*, 1998). SLRP sequence alignment demonstrates a high degree of homology between this family of proteoglycans (reviews by Iozzo, 1998; 1999). They may be classed into groups according to the type of GAG attachment they possess (e.g. KS or CS / DS) and the degree of sequence homology between them (figures. 1.7 & 1.8).

Chondroitin sulphate / Dermatan sulphate containing SLRPs

This class of SLRPs contain CS or DS GAG attachments and include decorin (Krusius & Rouslahti, 1986) and biglycan (Fisher *et al.*, 1989). They possess 57% sequence homology at the amino acid level (reviewed by Iozzo, 1998). Both of these proteoglycans contain an amino terminal propeptide domain (reviewed by Roughley, 2001) that may be involved in the xylosyltransferase initiation of CS / DS GAG chain synthesis to the proteoglycan core protein (figure. 1.7).

Decorin is the product of an 8 exon gene located on chromosome 12 (Danielson *et al.*, 1993). Its core protein has 359 amino acids, which contains 10 leucine repeat residues

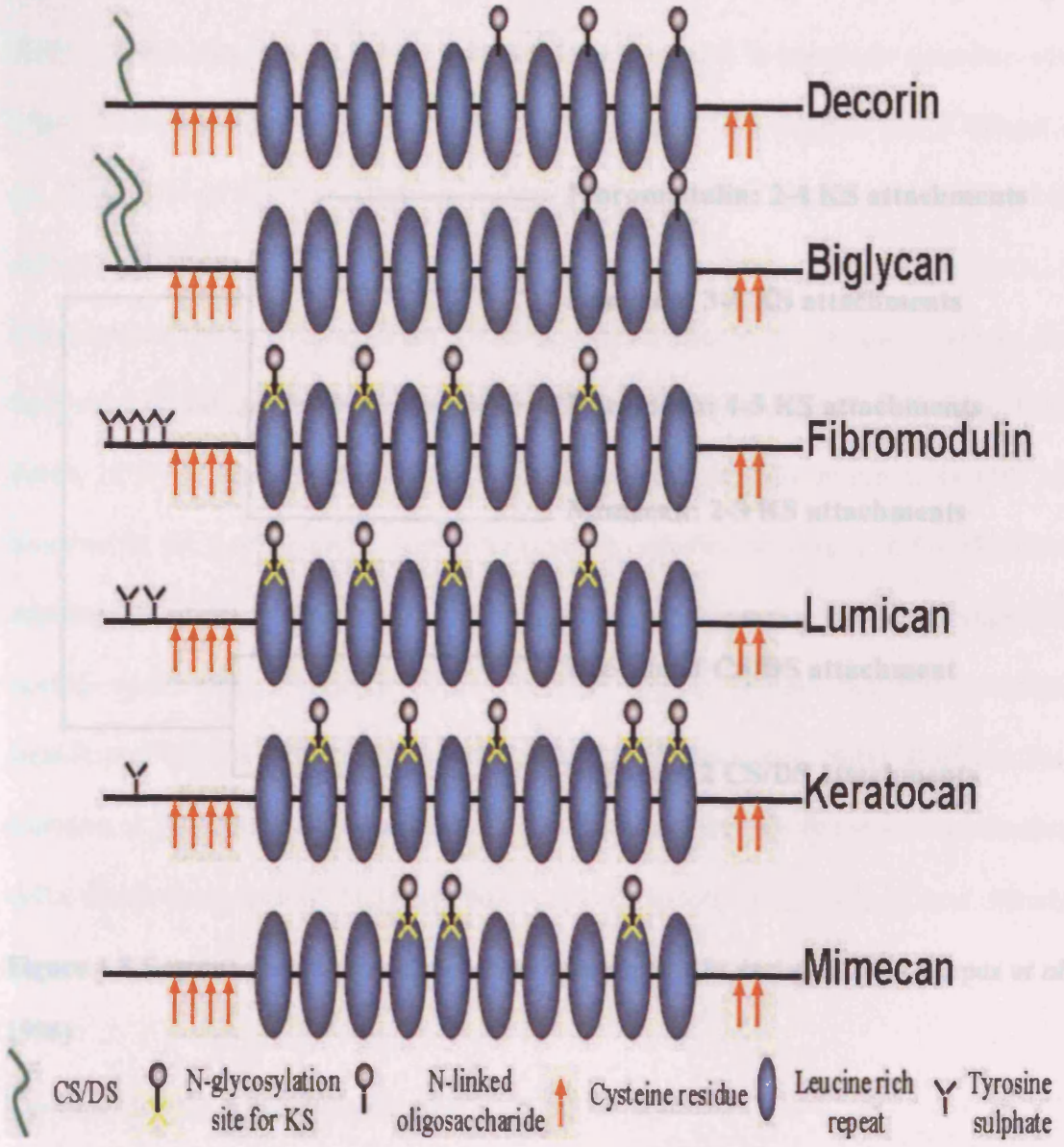

Figure 1.7 SLRPs of connective tissues (adapted from Mochizuki *et al.*, 1998)

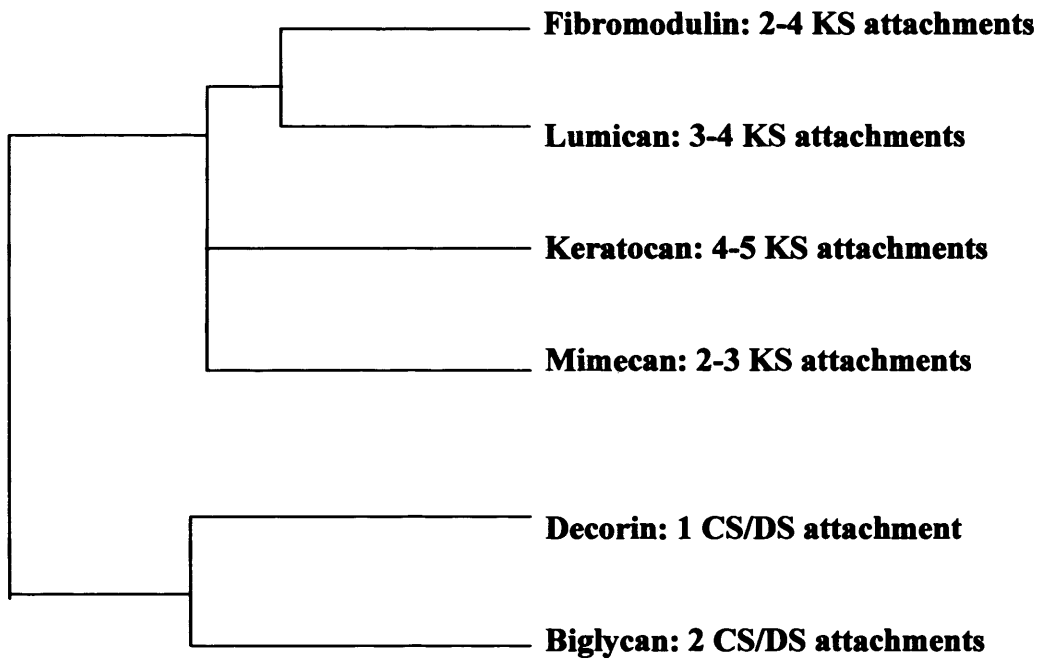

Figure 1.8 Sequence homology relationships between SLRPs (Adapted from Corpuz *et al.*, 1996)

of 24 amino acids (Krusius & Ruoslahti, 1986). Decorin may contain N-linked oligosaccharides (Abramson & Woessner, 1992) and it has one CS/DS GAG attachment at Ser^{11}. It controls cell proliferation and so is important in organising and maintaining ECM structure. Decorin is thought to be involved in regulating collagen fibrillogenesis (Rada *et al.*, 1993) and fibril diameter. DS is known to associate with other DS molecules and the decorin associates with collagen types I and II (Vogel *et al.*, 1984), two of the most abundant collagens of connective tissues, and with type VI collagen (Bindaset *et al.*, 1992).

The biglycan gene is located on the long arm of the X chromosome and is also composed of 8 exons (Fisher *et al.*, 1991; reviewed by Hardingham & Fosang, 1992; Iozzo, 1999). It, like decorin, has 10 leucine rich repeats of 24 amino acids with 368 residues in its protein core. The N-terminal is substituted with 2 CS / DS GAG attachments on Ser^{11}, Ser^{17} or Ser^{5}. Biglycan may undergo proteolytic cleavage with ageing where the N-terminal GAG bearing region is lost but the functional significance of this is as yet unknown (reviewed by Roughley, 2001). Biglycan may function in interactions with collagen VI to assist in network formation surrounding cells. Both decorin and biglycan bind growth factors (e.g. TGF-β) and thereby sequester them in extracellular matrices (Hildebrand *et al.*, 1994).

Keratan Sulphate containing SLRPs:

This family include proteoglycans such as lumican, fibromodulin, osteoglycin / mimecan and keratocan which all consist of a leucine rich core protein type structure with KS GAG attachments (figure 1.7) which are linked through N-glycosidic linkages to asparagine on the sequence Nx(S/T) as described previously in section 1.3.1.1. The presence of sulphated tyrosine on these SLRPs suggests that this may be an initiation signal for post-translational addition of KS (Corpuz *et al.*, 1996). They all

possess 10 repeats of 24 amino acids except for osteoglycin, which has only 6 LRRs (Hardingham & Fosang, 1992; Iozzo, 1998). Up to 10% of the mass of KSPGs can be attributed to the formation of N-linked mannose containing oligosaccharides on the core protein (Midura & Hascall, 1989; Funderburgh & Conrad, 1990).

Fibromodulin is expressed in many connective tissues with high levels in cartilage, it is also found in tendon and the sclera of the eye (Saamanen *et al.*, 2001). It is structurally related to other SLRPs and is composed of 4 N-terminal and 2 C-terminal cystines and a central region of 10 LLRs (Antonsson *et al.,* 1993). Its N-terminal domain is rich in tyrosine residues some of which may be sulphated (Antonsson *et al.*, 1991). It has type I KS GAG attachments which are N-glycosidically linked to Asn^{109}, Asn^{147}, Asn^{182} or Asn^{272} residues on bovine fibromodulin protein sequences (Plaas *et al.*, 1990). The unsulphated form of KS can also be found on fibromodulin. It associates with collagen types I and II and inhibits collagen fibril formation (Hedbom & Heinegard, 1989). Fibromodulin deficient mice have abnormal collagen fibrils in tendon (Svensson *et al.*, 1999). Lumican and fibromodulin bind to the same region of collagen type I indicating similar functions in collagen fibrillogenesis. This is supported by observations that lumican levels are increased in fibromodulin deficient mice and osteoarthritis is prevalent with age due to collagen disorganisation (Gill *et al.*, 2002).

Three different corneal PGs (two with a 37 kDa M_w core protein, and one with a 25 kDa M_w core protein) which have specific KS attachments, have been identified and cloned (Funderburgh & Conrad, 1990; Funderburgh *et al.,* 1991 A; 1997 A; Corpuz *et al.*, 1996). Lumican (Blochberger *et al.*, 1992) is a 37 kDa core protein that closely resembles fibromodulin with 48% sequence homology (figure 1.8). It has 4 - 5 potential KS attachment sites depending on species (Dunlevy *et al.*, 1998). In the avian cornea only half the potential sites are substituted with KS at Asn^{165}, Asn^{91} and

Asn ^{257}, while the rest have complex N-linked oligosaccharides, one out of four sites are substituted on bovine lumican (Funderburgh *et al.*, 1991 A). Lumican has been found at low levels with low-sulphated or un-sulphated KS depending on cytokines present (Melching & Roughley, 1999) in cartilaginous tissues (Grovner *et al.*, 1995; Melching *et al.*, 1997; Young *et al.*, 2005 A) and also in aorta, skin, skeletal muscle, lung, kidney, bone and IvD (Funderburgh *et al.*, 1987; 1991 B; Corpuz *et al.*, 1996; Chakravarti *et al.*, 1998; Raouf *et al.*, 2002; Yeh *et al.*, 2005; Young *et al.*, 2005 A). But it mainly occurs in a highly sulphated form in cornea where it is thought to have an important role in regulating collagen assembly by developing and maintaining corneal ECM ultrastructure. It has been identified as being an important molecule in inhibiting collagen fibrillogenesis (Rada *et al.*, 1993; Chakravarti *et al.*, 1998). Lumican deficient mice display corneal opacity and loose dermis with disrupted collagen organisation (discussed further in section 1.7).

Keratocan (Corpuz *et al.*, 1996) also has a 37 kDa core protein which has 4-5 possible KS attachment sites (figure 1.7) which are species dependent (Dunlevy *et al.*, 1998). Three of five possible sites are substituted with KS in bovine corneal keratocan (Midura & Hascall, 1989) and in chick cornea at Asn ^{94}, Asn ^{223}, Asn ^{261} and possibly Asn ^{299}. Keratocan expression has mainly been confined to the cornea to date where it is found with highly sulphated KS attachments, although it has been identified at the molecular level in some ocular and non-ocular tissues during early chick development (Conrad & Conrad, 2003). It may have a sulphated tyrosine residue at amino acid 27 in bovine corneal keratocan (Corpuz *et al.*, 1996). Sequence and distribution classify it as different from lumican. Keratocan knockout mice have larger collagen fibril diameters and loosely organised collagen fibrils (Liu *et al.*, 2003), this is discussed further in section 1.7.

Mimecan (Funderburgh *et al.*, 1997 A) is another typical leucine rich repeat proteoglycan which has characteristic sulphated KS attachments in corneal tissues where one out of four sites is substituted with KS in bovine mimecan (Funderburgh *et al.*, 1991 A; Dunlevy *et al.*, 1998). It is a full-length translation product of the osteoglycin producing gene and is synthesised by keratocytes in a 25 kDa M_w proteoglycan form (Funderburgh & Conrad, 1990). Osteoglycin is a small 12 kDa glycoprotein found in bone, which is also a product of the mimecan gene and appears to result from in situ proteolytic processing and / or alternative splicing of mRNA (Funderburgh *et al.*, 1997 A).

These groups of both large aggregating and small leucine rich proteoglycans show the enormous diversity in protein core sequence and length and in the type of GAG attachments that occur within this large family of macromolecules. The difference in core protein structures is clearly a gene related occurrence. However, post-translational modification associated changes in GAG types, amount, length and degree of sulphation, is dependent on various tissue specific factors and the relative functional requirements of the tissues and can change with development, age and pathological condition.

The degree to which these post-translational modifications occur and their implications on the healthy functioning of the tissues with which they are associated is therefore an important area of current research. In order to assess the modifications that occur with changing tissue needs, it is important to first understand the biosynthetic pathways and mechanisms by which they come about.

1.4. Proteoglycan Biosynthesis

1.4.1 General Overview

Proteoglycan biosynthesis begins when mRNA is transcribed from DNA and used to translate a specific core protein in the endoplasmic reticulum (ER) of the connective tissue cell. Through the synthetic process extensive co- and post-translational modifications occur. Major changes involve GAG substitution, N- and O- linked glycosylation, proteolytic processing and crosslinking, and each biosynthetic process requires one or more enzymes to regulate turnover. Length, sulphation patterns, number and type of GAG chain present (e.g. CS vs. KS) can vary with the changing biological requirements and enzyme expression of the tissue. Translation of the core protein and N-linked oligosaccharide formation and attachment to the precursor protein proceeds in the ER lumen and continues after the protein is transported to the Golgi apparatus (Hassell *et al.*, 1986; Vertel *et al.*, 1993). The specific protein initiation sequence for N-linked oligosaccharide formation is Asn-x-Thr/Ser where x may be any amino acid except proline or aspartic acid and aromatic residues (e.g. phenylalanine) are located in close proximity to the attachment sequence (Dunlevy *et al.*, 1998). The majority of post-translational modifications however occur as processes of the medial- and trans- Golgi apparatus (Vertel *et al.*, 1993) where the protein precursor is converted into a proteoglycan. This process may involve the posttranslational modification of the core protein with N- or O- linked oligosaccharides to asparagine or serine / threonine, respectively. The N-linked oligosaccharides maybe further processed to more complex forms. There may also be possible removal of peptide portions of the core protein, see figure 1.9 (Hassell *et al.*, 1986).

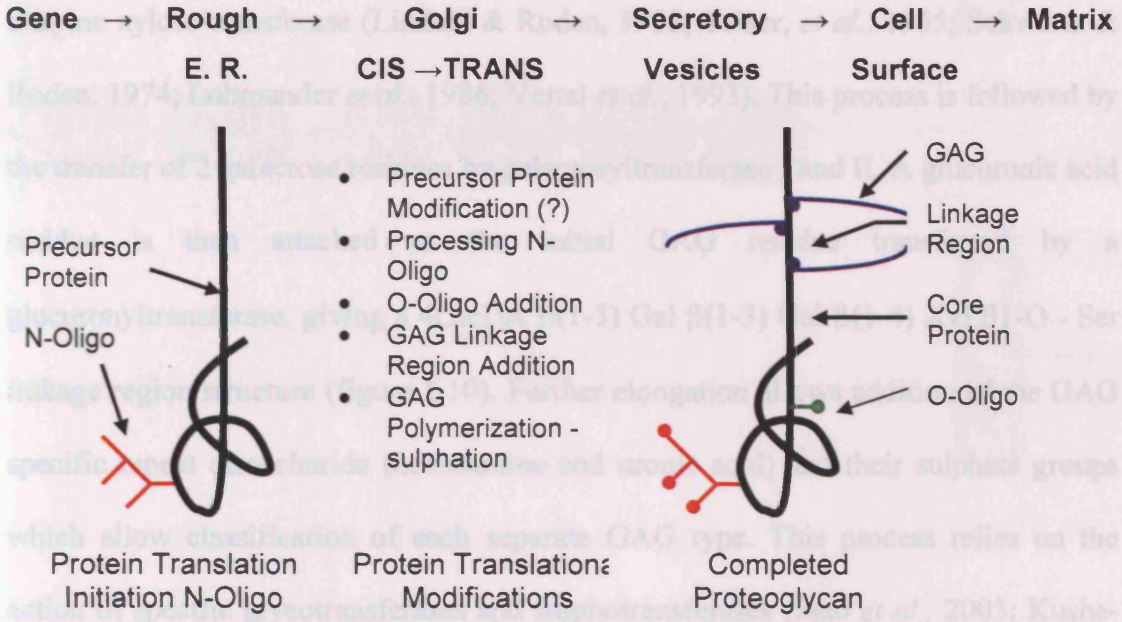

Figure 1.9 Proteoglycan biosynthesis - pathway through the cell to the ECM (adapted from Hassell *et al.*, 1986).

1.4.2. Uronic acid GAG biosynthesis

CS, DS HS (Hep) and HA are all GAGs that contain uronic acid as one component of their repeating disaccharide units. CS, DS and HS are all covalently bound through a tetra-saccharide linkage region [GlcUA-Gal-Gal-Xyl] to a serine within a consensus core protein sequence of Glu/Asp-x-Ser-Gly [figure 1.10] (Lindahl & Roden, 1965). Their biosynthesis begins with the transfer of xylose from UDP-Xylose to a hydroxyl group of a specific serine in a preformed protein late in the ER and in the Golgi by the enzyme xylose-transferase (Lindahl & Roden, 1965; Telser, *et al.*, 1965; Schwartz & Roden, 1974; Lohmander *et al.*, 1986; Vertel *et al.*, 1993). This process is followed by the transfer of 2 galactose residues by galactosyltransferase I and II. A glucuronic acid residue is then attached as the initial GAG residue transferred by a glucuronyltransferase, giving a 4GlcUA β(1-3) Gal β(1-3) Gal β(1-4) Xyl β1-O - Ser linkage region structure (figure 1.10). Further elongation allows addition of the GAG specific repeat disaccharide (hexosamine and uronic acid) and their sulphate groups which allow classification of each separate GAG type. This process relies on the action of specific glycotransferases and sulphotransferases (Sato *et al.*, 2003; Kushe-Gullberg & Kjellen, 2003). Because the linkage region tetra-saccharide is identical for all of the uronic acid type GAG chains, it is probable that the initiation enzyme for each GAG type compete for the tetra-saccharide substrate and may therefore play an important role in determining which GAG type will be produced on various PGs.

In contrast HA is synthesised at the plasma membrane (Prehm, 1984) by specific HA biosynthetic enzymes (HAS 1, HAS 2 and HAS 3). UDP-GlcNAc and UDP-GlcUA substrates are produced inside the cell and continuously transferred to the growing HA chain so that it is extruded into the extracellular space. Unlike the other uronic acid GAGs, its synthesis does not require a protein core for attachment.

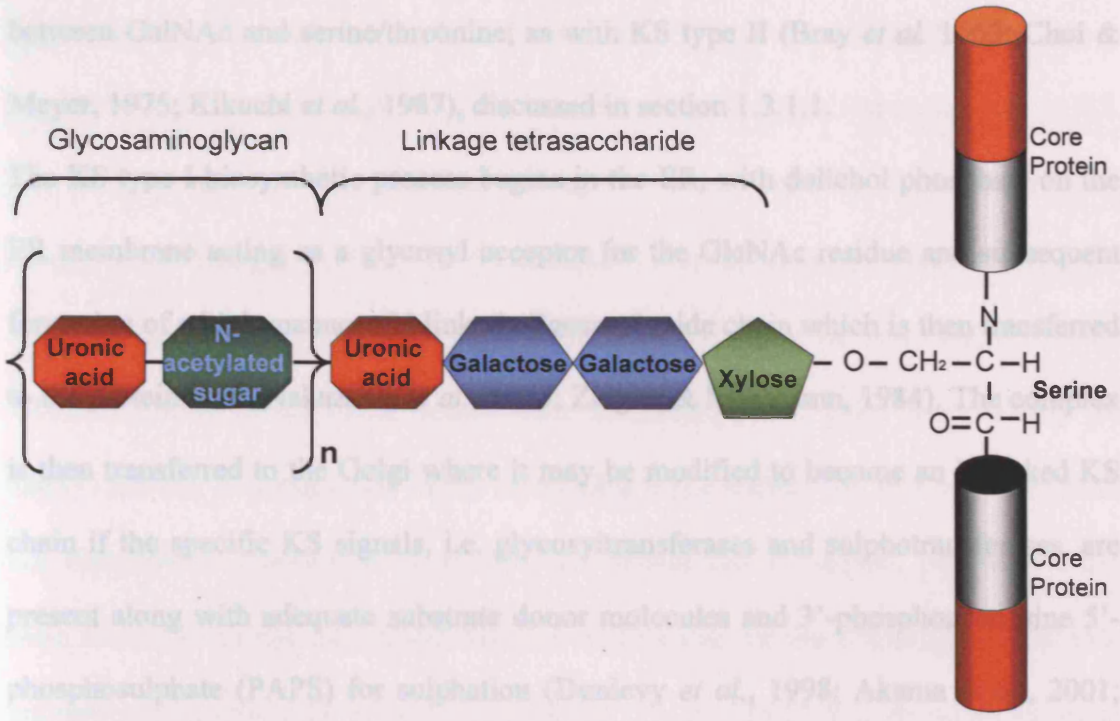

Figure 1.10 Structure of the linkage region of uronic acid containing GAGs which attach through O -glycosidic linkages to serine on the protein core, e.g. CS, DS, HS and Heparin (adapted from King, 1996).

1.4.3 KS GAG biosynthesis

KS biosynthesis differs from all other GAG synthesis as it may occur through either N-glycosidic linkages between GlcNAc and asparagine, as with KS type I (Seno *et al.*, 1965; Choi & Meyer, 1975; Plaas *et al.*, 1990), or through O-glycosidic linkages between GalNAc and serine/threonine, as with KS type II (Bray *et al.* 1967; Choi & Meyer, 1975; Kikuchi *et al.*, 1987), discussed in section 1.3.1.1.

The KS type I biosynthetic process begins in the ER, with dolichol phosphate on the ER membrane acting as a glycosyl acceptor for the GlcNAc residue and subsequent formation of a high mannose N-linked oligosaccharide chain which is then transferred to the protein core (Nakazawa *et al.*, 1983; Ziegler & Mersmann, 1984). The complex is then transferred to the Golgi where it may be modified to become an N-linked KS chain if the specific KS signals, i.e. glycosyltransferases and sulphotransferases, are present along with adequate substrate donor molecules and 3'-phosphoadenosine 5'-phosphosulphate (PAPS) for sulphation (Dunlevy *et al.*, 1998; Akama *et al.*, 2001; Kushe-Gullberg & Kjellen, 2003). If this pathway is not favoured the N-linked structure may be further processed to become a complex form N-linked oligosaccharide (Hassell *et al.*, 1986; Dunlevy *et al.*, 1998).

In contrast, KS type II linkage region biosynthesis and subsequent attachment of sugar units to the non-reducing end does not begin until the proteoglycan protein precursor reaches the Golgi apparatus (Hassell *et al.*, 1986). As with KS type I, chain elongation depends on the expression of glycosyltransferase and sulphotransferases and the availability of the UDP-sugar donors.

1.4.3.1 Glycosyltransferases and sulphotransferases

Galactosyltransferases:

Glycosyltransferases are responsible for the sequential addition of alternative Gal and GlcNAc monomers to the growing KS chain (reviewed by Funderburgh, 2000). So far, several families of galactosyltransferases (Gal-T) have been identified (Amado *et al.,* 1999) and two are important to the biosynthetic addition of Gal monomers to KS. β4 GalT-1 catalyses the UDP-Gal linkage to a non-reducing terminal GlcNAc acceptor, generating a β1-4 glycosidic linkage. It is involved in the production of non-sulphated poly-N-acetyllactosamine domains which comprise the basic unit of the KS molecule (Brew et al., 1968; Schanbacher & Ebner., 1970; Ujita *et al.*, 1999). β4 GalT-1 activity is upregulated in the developing chick cornea and this coincides with KS biosynthetic events (Cai *et al.*, 1996). Another Gal-T enzyme, β4 GalT-4, has been shown to be the only Gal-T enzyme responsible for the β linkage of Gal to a non-reducing terminal GlcNAc-6-sulphate (Seko *et al.*, 2003). It is therefore essential for the production of mono- and di-sulphated disaccharide KS domains.

N-acetylglucosaminyltransferases:

To date, seven different β1, 3-N-acetylglucosaminyltransferase (β3 Gn-T) enzymes have been identified (β3 Gn-T1, -T2, -T3, -T4, -T5, -T6 and -T7). They act by catalysing the addition of GlcNAc by β glycosidic linkages to the C-3 position of a non-reducing terminal Gal or GalNAc (Seko & Yamashita, 2004). A number of these are thought to influence KS biosynthesis. β3 GnT or iGnT is a polylactosamine producing enzyme has been cloned and its substrate specificity identified (Sasaki *et al.*, 1997; Zhou *et al.,* 1999; Shiraishi *et al.*, 2001). Until recently, it was unclear which of these enzymes was responsible for the addition of GlcNAc to sulphated

forms of KS. Seko & Yamashita, 2004, characterised the enzymatic activity of β3 GnT7. They found that it acts efficiently on Galβ1 - 4(SO_3^- - 6) GlcNAcβ1 - 3Galβ1 - 4(SO_3^- - 6) GlcNAc and Galβ1 - 4(SO_3^- - 6) GlcNAcβ1 - 3(SO_3^- - 6) Galβ1 – 4(SO_3^- - 6) GlcNAc, both of which are partial structures of KS, with 100% and 72% relative activity, respectively. β3 GnT7 had a much lower activity (5%) with substrates that lacked sulphation on the internal non-reducing end GlcNAc and where the non-reducing Gal was 6-sulphated reactivity was also reduced (3%) indicating that it catalyses the addition of GlcNAc to the non-reducing terminal of monosulphated disaccharides (Gal - 6SGlcNAc).

Sulphotransferases:

Sulphotransferase activity is responsible for the transfer of sulphate groups from 3'-phosphoadenosine 5'-phosphosulphate (PAPS) to position 6 of Gal or GlcNAc of KS. A number have so far been reported (Ruter & Kresse, 1984; Fukuta *et al.*, 1997; Uchimura *et al.*, 1998; Akama *et al.*, 2001). Two enzymes have been identified that are responsible for transferring sulphate groups specifically to KS. Gal-6-sulphotransferase (KSGal6ST) transfers sulphate groups to C6 of Gal and GlcNAc-6-sulphotransferase (GlcNAc6ST) transfers sulphate to the C6 of GlcNAc. Another enzyme (chondroitin sulphate sulphotransferase (C6ST)) catalyses the addition of a sulphate group to GalNAc of CS, but also to Gal of KS in both cartilage and cornea (Habuchi *et al.*, 1996). Five GlcNAc-6-sulphotransferase genes have been identified (Seko *et al.*, 2003). It is GlcNAc6ST-5 that is involved in the addition of sulphate to the non-reducing terminal GlcNAc of KS and this proceeds as the KS chain is being synthesised in both human (Akama *et al.*, 2001) and mouse tissues (Uchimura *et al.*, 1998).

Fukuta *et al.,* (1997), have cloned and characterised a Gal sulphotransferase enzyme (KSGal6ST), that catalyses the addition of sulphate to an internal Gal residue within the KS chain. It is specific for KS and comparison of the coding sequence of the two KS Gal sulphating enzymes KSGalST and C6ST (CS/KSGalT) reveals a 37% identity at the amino acid level (Fukuta *et al.*, 1997). Incorporation of sulphate groups into Gal of unsulphated disaccharides is much lower than that of disaccharides in which the GlcNAc is already sulphated, suggesting that GlcNAc sulphation precedes and may be a prerequisite for Gal sulphation during KS synthesis. The disulphated disaccharide unit of KS has been synthesised in vitro (Akama *et al.*, 2002) and sulphation of Gal residues is thought to signal an end to KS chain elongation (reviewed by Kushe-Gullberg & Kjellen, 2003). From the research described, it is apparent that KS is synthesised by the sequential actions of a number of KS specific enzymes β3GnT, GlcNAc6ST, β4GalT 4 and KSGal6ST. The proposed sequence of events is depicted in figure 1.11 (Seko & Yamashita., 2004).

1.4.4 Factors that effect GAG type generation – the role of enzymes and energy

There are a number of factors that are involved in selective biosynthesis of different glycosaminoglycans and what length of chains and sulphation patterns are produced by a cell of a particular tissue. These include UDP-xylose concentration of the cell and the NAD/NADH ratio (reviewed by Balduini *et al.*, 1989).

UDP-xylose is present in all connective tissues but at significantly different concentrations (Handley & Phelps, 1992) based on tissue specific factors. Xylose is required for the initial step in uronic acid type GAG linkage to serine residues on the core protein. In tissues where there is a high concentration of xylose-transferase, the UDP-molecule is moved to the protein core resulting in a subsequent decrease in free cytoplasmic UDP-xylose. High levels of cytoplasmic UDP-xylose act to block the

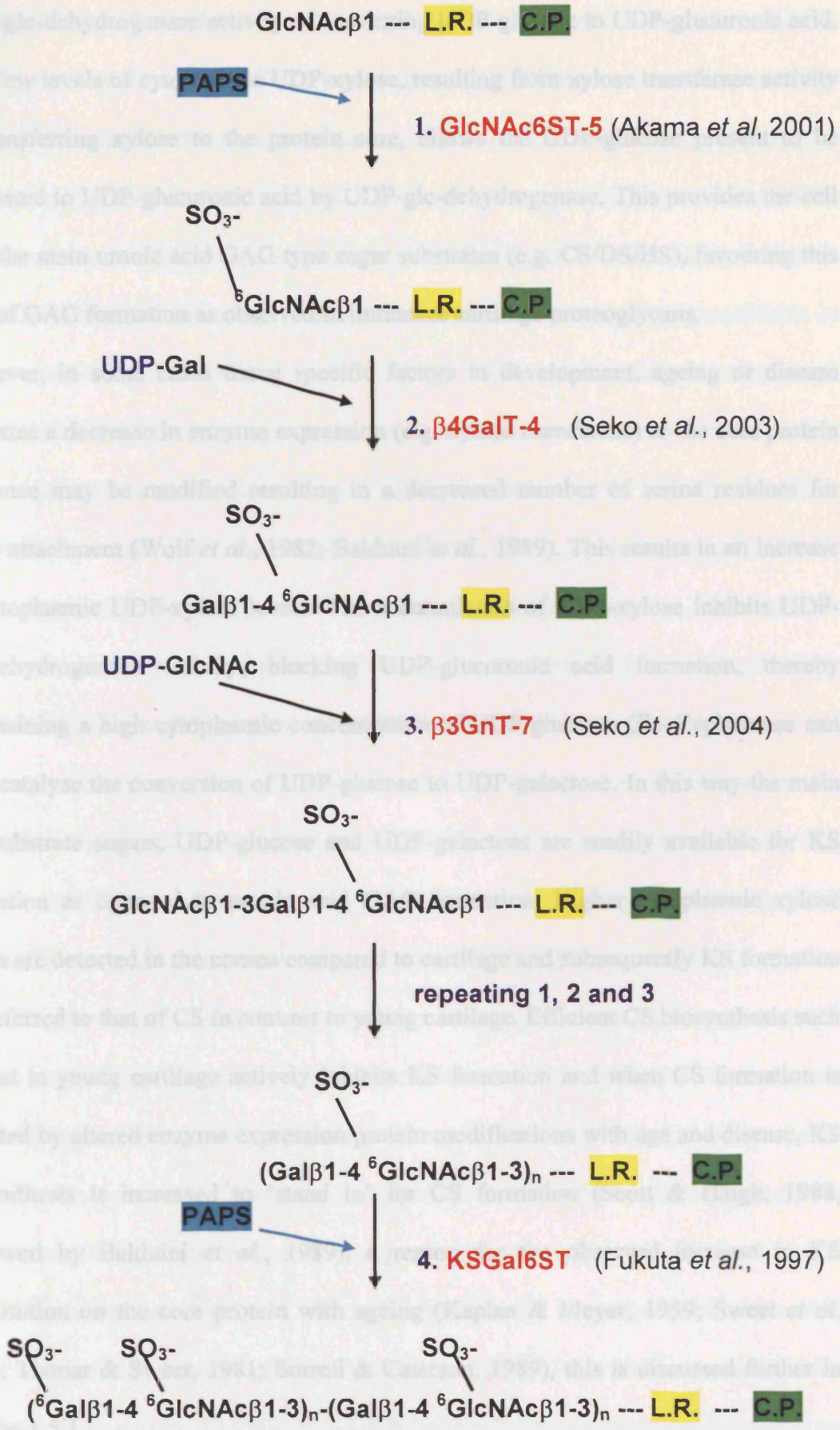

Figure 1.11 The proposed sequence of events in the KS biosynthetic pathway [L.R. =linkage region; C.P. = core protein] (Adapted from Seko *et al.*, 2004).

UDP-glc-dehydrogenase activity of converting UDP-glucose to UDP-glucuronic acid. And low levels of cytoplasmic UDP-xylose, resulting from xylose transferase activity of transferring xylose to the protein core, allows the UDP-glucose present to be converted to UDP-glucuronic acid by UDP-glc-dehydrogenase. This provides the cell with the main uronic acid GAG type sugar substrates (e.g. CS/DS/HS), favouring this type of GAG formation as observed in immature cartilage proteoglycans.

However, in some cases tissue specific factors in development, ageing or disease regulates a decrease in enzyme expression (e.g. xylose transferase) or the core protein sequence may be modified resulting in a decreased number of serine residues for GAG attachment (Wolf *et al.*, 1982; Balduini *et al.*, 1989). This results in an increase in cytoplasmic UDP-xylose levels. The accumulation of UDP-xylose inhibits UDP-glc-dehydrogenase activity, blocking UDP-glucuronic acid formation, thereby maintaining a high cytoplasmic concentration of UDP-glucose. Glc-4'epimerase can then catalyse the conversion of UDP-glucose to UDP-galactose. In this way the main KS substrate sugars, UDP-glucose and UDP-galactose are readily available for KS formation as opposed to uronic acid GAG formation. Higher cytoplasmic xylose levels are detected in the cornea compared to cartilage and subsequently KS formation is preferred to that of CS in contrast to young cartilage. Efficient CS biosynthesis such as that in young cartilage actively inhibits KS formation and when CS formation is effected by altered enzyme expression/protein modifications with age and disease, KS biosynthesis is increased to 'stand in' for CS formation (Scott & Haigh, 1988, reviewed by Balduini *et al.*, 1989), a reason for the observed increase in KS substitution on the core protein with ageing (Kaplan & Meyer, 1959; Sweet *et al*, 1979; Thonar & Sweet, 1981; Sorrell & Caterson, 1989), this is discussed further in section 1.5.1.

A second factor that affects selective GAG type biosynthesis in the cell is NAD / NADH concentrations. CS / DS is plentiful in many different tissues, however, KS concentrations increase in a range of tissues which are avascular in nature e.g. corneal stroma, ageing articular cartilage and IvD, where oxygen supply is acquired by diffusion from neighbouring tissues (Scott, 1994), this will be discussed further in sections 1.5 and 1.7. It is argued that KS is the choice 'reserve' polysaccharide in tissues where oxygen is lacking (Scott & Haigh, 1988) where it acts as a functional substitute for CS. This is because under aerobic conditions the ratio of NAD / NADH is plentiful in the cell and formation of UDP-glucuronic acid for CS, DS and HS is allowed to proceed under such conditions (Scott, 1991). Epimerisation of UDP-N-acetyl-glucosamine for KS formation is also readily allowed. However, as the specific uronic acid GAG sugar substrates are available the formation of such GAGs is possible and favoured depending on the availability of serine, xylose transferase and resulting cellular concentrations of UDP-xylose as described above. However, the UDP-glc-dehydrogenase step (UDP-Glc to UDP-GlcUA) is an oxidising reaction that requires NAD^+ as a substrate, releasing NADH and lowering cytoplasmic NAD levels. This step is sensitive to changes in NAD/NADH ratios of the cell. The anerobic glycolysis pathway is an alternative method for producing energy essential for cell survival in cases where oxygen levels are low. This pathway is dependent on NAD concentrations of the cell and so competes for NAD with CS biosynthesis. Therefore under anerobic conditions, tissues such as the cornea require any available cytoplasmic NAD concentrations for the production of energy essential for the basic metabolic processes of the cell. Its utilisation for CS formation under anaerobic conditions could jeopardise cell survival (Scott, 1991). Under similar conditions the epimerisation reaction of UDP-Glc to UDP-Gal for KS formation is not dependant on using up NAD stores. Therefore it has been suggested that under such anaerobic

conditions, familiar in cornea and ageing cartilage, KS formation is again favoured as a functional substitute for CS (Scott & Haigh, 1988; Scott, 1994). In this way the cells NAD supply is reserved for the more essential processes to the cells survival.

In full, the above factors, i.e. the protein core sequence, availability of initiating UDP-xylose, oxygen supply, expression of glycosyltransferase and sulphotransferase enzymes and subsequent UDP-sugar donor formation and sulphation, all contribute to the type of GAG modification which becomes substituted to the protein core precursor.

1.5. Cartilage ECM composition

Cartilage is commonly divided into fibrocartilage, elastic cartilage or hyaline cartilage based on its morphologic appearance and ECM composition. Fibrocartilage comprises of parallel bundles of collagen fibrils which provide this cartilage with its strength and rigidity and is the strongest of the three. Fibrocartilage interacts with dense fibrous tissues or hyaline cartilage e.g. intervertebral disc (IvD).

Elastic cartilage comprises proteoglycans collagen and elastic fibres. It is found in tissues requiring a great deal of flexibility where shape is important to its function e.g. the ear, the epiglottis and cuneiform of the larynx.

Hyaline cartilage is composed of chondrocytes housed in lacunae, proteoglycans and collagen. It is the most abundant cartilage in the body found predominantly at articular surfaces of movable joints where it is referred to as articular cartilage and is an important contributor to synovial joint function. It is also found in IvD (e.g. cartilage endplate), another load bearing tissue of the body (see section 1.6).

Articular cartilage is a wear resistant, load bearing surface tissue that protects bones at diarthrodal joints by transmitting applied loads at pressures that components of the joint can tolerate. It allows flexibility and support, absorbs shock by deforming under mechanical load and provides a smooth surface to permit low friction movement of the joint. It is composed mainly of a dense avascular, aneural, hypocellular ECM where 70% wet weight is composed of water, 7% of proteoglycans which are enmeshed in a rich collagen fibril network comprising 20% wet weight of the tissue (figure 1.12). Approximately 1% accounts for other matrix proteins. The overall composition does vary with species, developmental stage, age and pathology.

The chondrocytes are the only cell type present in articular cartilage and responsible for the production and maintenance of the ECM components. They make up less than 5% of the volume of adult articular cartilage. In healthy tissue, cartilage can be

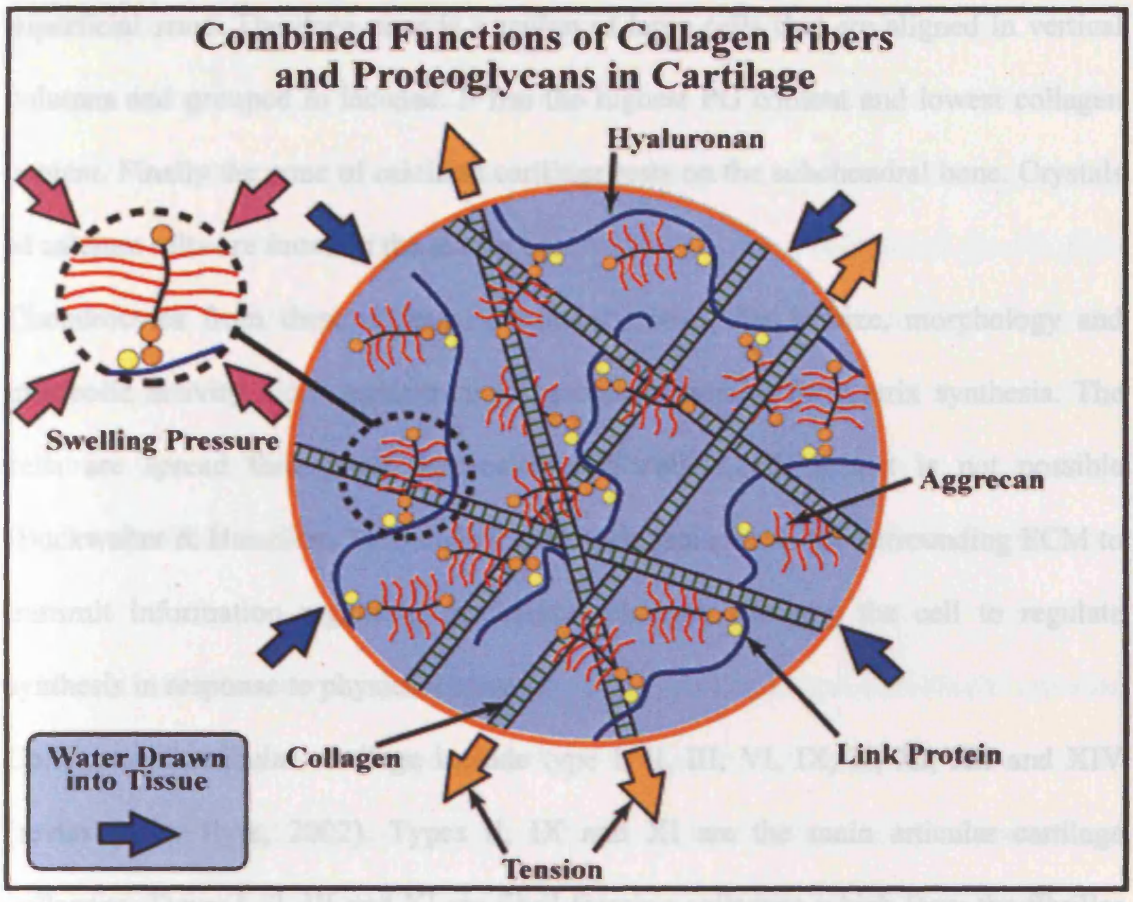

Figure 1.12 Aggrecan and collagen function in cartilage hydration. The load bearing properties of cartilage is provided by the tensile strength of the collagen fibre network and osmotic swelling pressure afforded by the high concentration of negatively charged aggrecan. The aggrecan is immobilised within the matrix by forming supramolecular aggregates with hyaluronic acid and link protein. (Hardingham 1998)

divided into four zones. The superficial zone is a layer of flattened cells and collagen found at the surface of cartilage giving it a greater tensile strength. The mid zone is a zone of randomly placed rounded cells. It has a much higher PG content than the superficial zone. The deep zone is a region of large cells that are aligned in vertical columns and grouped in lacunae. It has the highest PG content and lowest collagen content. Finally the zone of calcified cartilage rests on the subchondral bone. Crystals of calcium salts are found in the matrix here.

Chondrocytes from these different cartilage zones differ in size, morphology and metabolic activity. Each contains the organelles essential for matrix synthesis. The cells are spread throughout the matrix and cell - cell contact is not possible (Buckwalter & Hunziker, 1999). They must therefore rely on the surrounding ECM to transmit information regarding mechanical changes allowing the cell to regulate synthesis in response to physical changes.

Collagens of articular cartilage include type I, II, III, VI, IX, X, XI, XII and XIV (reviewed by Eyre, 2002). Types II, IX and XI are the main articular cartilage collagens. Types I, II, III and XI are fibril forming collagens which form the fibrillar meshwork that give the tissue its tensile properties. Non-fibrillar collagens include type X, a short chain network forming collagen associated with calcifying cartilage that is over expressed in OA and RA cartilage (Aigner *et al.*, 1993). Type VI collagen is usually found as a pericellular network surrounding the chondrocyte in lacunae. Fibril associated collagens of articular cartilage include type IX, XII and XIV (Robert *et al.*, 2001). Deletion of the Col 9a1 chain (Fassler *et al.*, 1994) has established type IX collagen as an important collagen of cartilage as mice developed degenerative joint disease within 4 months of age.

PGs including aggrecan, versican, decorin, biglycan, lumican and fibromodulin bind with or become sequestered in the rich collagen network of articular cartilage.

Together these molecules form a highly hydrated structure which can resist the compressive forces applied to it during movement (figure 1.12).

1.5.1 Changes in articular cartilage with development, ageing and disease

Developing cartilage is highly cellular compared to mature cartilage and retains the capacity to obtain nutrients and oxygen from the blood vessels of the underlying subchondral bone. On reaching early adulthood, bone growth ceases and growth plate closure results in the inability of cartilage chondrocytes to access nutrients from the subchondral bone. Diffusion via the synovial fluid from the blood vessels of the synovial capsule becomes the sole source of nutrients and oxygen to the cartilage chondrocytes and this diffusion is assisted by the action of compression and relaxation of the joint during movement.

During skeletal development and into maturity, the functions and activities of articular cartilage chondrocytes change. Growing chondrocytes produce new matrix components to build and remodel the articular surface. However, once mature and fully formed and when cartilage becomes damaged through use, chondrocytes no longer change the volume of the tissue but, instead, replace degraded matrix macromolecules, playing a role in remodelling the articular surface (Buckwalter, 1995). A decrease in chondrocyte metabolism occurs with increasing age.

Proteoglycan metabolism, expression and modifications vary greatly within cartilage during a lifetime. Genes are differentially expressed, for example aggrecan and biglycan become down regulated while decorin is upregulated with age (reviewed by Roughley & Lee, 1994; Melching *et al.,* 1997) and disease (Young *et al.,* 2005 A).

Post-translational modifications responsible for functional hydration and structural variability have been shown to alter greatly with age. During embryonic and early development, aggrecan core protein is highly substituted with C-4-S GAG chains.

However, during adulthood, C-4-S is largely replaced by sulphation at position 6 (Bayliss *et al.*, 1999; Calabro *et al.,* 2001). In addition, with age CS chain length and the number of attachments decrease (Sweet *et al.*, 1979; Thonar *et al.,* 1986). Concomitantly KS chain length and sulphation levels increase (Calabro *et al.,* 2001), as do the number of chain attachments through KS, CS I and CS II attachment regions of aggrecan (figure 1.13) where they possibly attach through O-linked oligosaccharides at CS attachment sites (Kaplan & Meyer, 1959; Sweet *et al*, 1979; Thonar & Sweet, 1981; Sorrell & Caterson, 1989). This replacement of CS with KS chains appears to occur in tissues where oxygen supply is reduced as tissues develop and enlarge and anaerobic glycolysis is required for energy production as described previously in section 1.4.4 (Scott, 1991, 1994; Scott & Haigh, 1988). This hypothesis is supported by the regional localization of KS containing proteoglycans. Articular cartilage and is an avascular tissue and ultrastructural examination has found that as it grows and enlarges, KS becomes more prevalent with increasing distance from the tissues oxygen supply. When the subchondral blood supply is cut off, as bone growth ceases, the KS content of cartilage in regions nearest the bone increases substantially (Stockwell, 1970). This may help to explain the increase observed in KS substitution with development and ageing, though the extent of its significance is still to be determined and heterogeneity observed in KS structure such as length and sulphation pattern structure may be due to expression differences of glycosyltransferases and sulphotransferases (see section 1.4).

Structural changes also occur in other proteoglycans with ageing and development. The GAG attachments on decorin and biglycan decrease in length and content of Iduronic acid increases (reviewed by Roughley & Lee, 1994). This may effect association capabilities with other molecules and hence the structural integrity of the cartilage ECM. ECM environment and cell behaviour trigger changes in expression of

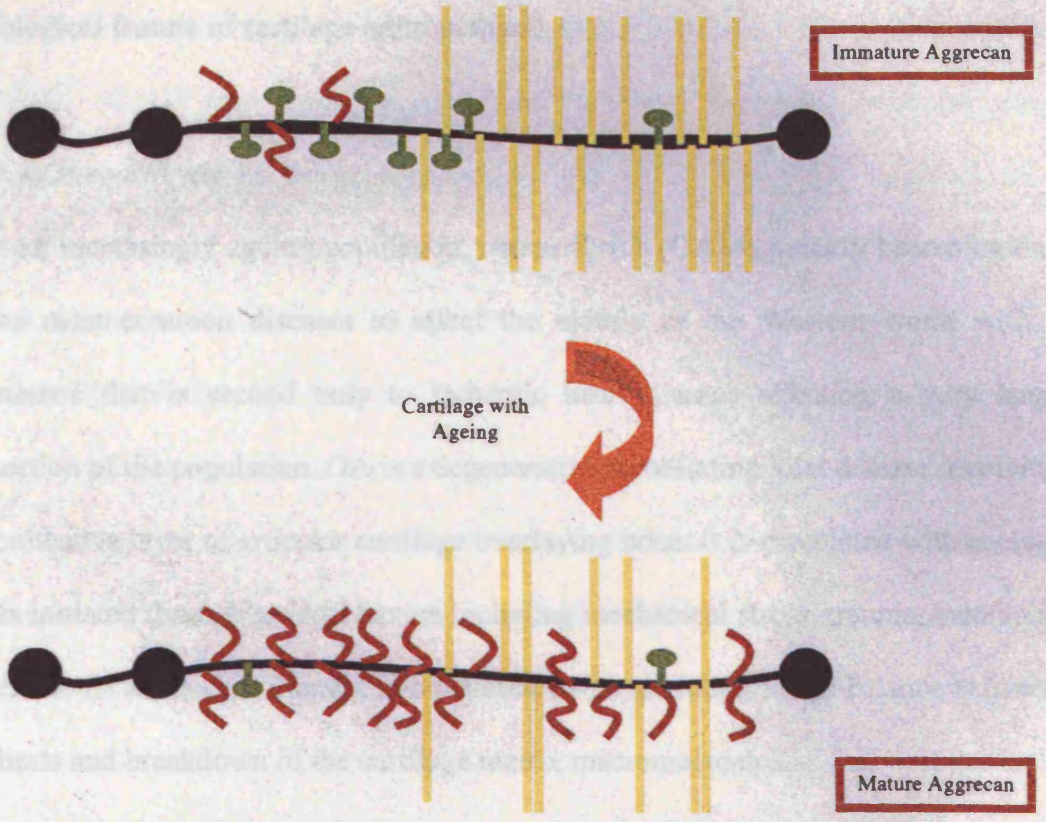

Figure 1.13 Increase in KS and decrease in CS substitution in cartilage aggrecan observed with increasing age and disease.

proteases and growth factors leading to degradation of the matrix structure, a common pathological feature of cartilage arthropathies.

1.5.1.1 Osteoarthritis

With an increasingly ageing population, osteoarthritis (OA) is quickly becoming one of the most common diseases to affect the elderly of the Western world with a prevalence that is second only to ischemic heart disease affecting a very large proportion of the population. OA is a degenerative, debilitating joint disease involving the protective layer of articular cartilage overlaying bone. It is associated with ageing, and is initiated through several factors including mechanical stress, trauma, metabolic or genetic factors and is thought to be caused by an alteration in the balance between synthesis and breakdown of the cartilage matrix macromolecules.

Articular cartilage degeneration progresses from early proteoglycan depletion in histologically intact tissue through to breakdown of collagen type II (Hollander *et al.*, 1995), fibrillation and finally late stage erosion of the tissue down to subchondral bone (Mankin *et al.*, 1971). OA is thought to progress as altered mechanical stresses transmit to the chondrocyte which cause them to produce inflammatory cytokines e.g. interleukin-1 (IL-1) and tumour necrosis factor-alpha (TNF-α). These cytokines then trigger further expression of matrix proteases which when secreted and activated act to hydrolyse proteoglycans and collagens of cartilage at specific peptide bonds resulting in degradation of the structural support system of the tissue (Caterson *et al.*, 2000). Cleavage of aggrecan results in a loss of the negatively charged GAGs into the synovial fluid which diminishes the water binding capability of the tissue and hence reduces the compressive protective function of the cartilage. Later stage cleavage of collagen causes fibrillation and the combined loss of these molecules is responsible for the exposure of bone at the surface and is thought to represent irreversible

cartilage damage. Bone surfaces are exposed resulting in outgrowths called osteophytes and thickening of the subcondral plate (Martel-Pelletier, 1999). For the individual all of this leads to clinically disabling symptoms of joint pain, inflammation and limited movement.

1.5.1.2. Rheumatoid arthritis

Rheumatoid arthritis (RA) is a systemic autoimmune, inflammatory disease. Infectious and genetic events are thought to be the initiating factors associated with RA. It occurs as a consequence of chronic inflammation of synovial joints (predominantly hands, wrists and feet) where blood specific inflammatory cells appear in the normally acellular synovial fluid and synovial membrane (reviewed by Feldmann *et al.*, 1996). This causes swelling, inflammation, and the characteristic pain associated with RA. Inflammatory cytokines cause activation of the matrix proteases responsible for matrix degradation leading to cartilage destruction (Chu *et al.*, 1992). In addition the cartilage becomes eroded and the synovial membrane thickens. Fibrous tissue then forms in the joint resulting in limited movement capabilities and crippling clinical symptoms associated with this disorder.

1.6 Intervertebral disc composition

Intervertebral disc (IvD) is a soft tissue that separates and cushions each vertebra from the next. Some of its component tissues resemble articular cartilage in both their biochemical composition and by having few blood vessels, nerves and cells. As with articular cartilage it also functions in mechanical loading. It allows flexibility associated with movement and therefore must be able to deal with compressive deformation caused by body weight and muscle activity, as does articular cartilage (reviewed by Urban & Roberts, 2003). The IvD consists of three distinct regions (figure 1.14), an inner highly hydrated region known as the nucleus pulposus, an outer collagenous anulous fibrosis consisting of 15-20 circular lamellae that surround the nucleus with elastic fibres which help the disc return to its original structure following movement. The disc region is separated from vertebrate bodies by a thin layer of hyaline cartilage called the cartilaginous endplate. Chondroycte like cells are responsible for synthesis of new matrix molecules to balance turnover caused by proteases such as matrix metalloproteinases (MMPs) and aggrecanases. The most important molecules of IvD include aggrecan and fibrillar collagens. Aggrecan attracts water into the matrix imparting a high osmotic pressure on the tissue and maintains a highly hydrated tissue as it does in articular cartilage. The nucleus has the highest concentration of aggrecan in the IvD and a lower concentration of collagen (figure 1.14). Type II collagen is the major collagen type found in the nucleus, while types I and II collagens are found in high levels in the annulus fibrosis (Eyre & Muir, 1977). Collagens afford tensile strength to the tissue. The nucleus also contains minor amounts of collagen types III, V, VI, IX, X, XI, XII and XIV as well as the SLRPs decorin, biglycan, lumican and fibromodulin which are thought to be involved in forming cross links with collagens (Cs-Sazbo, *et al.,* 2002; Strolovics *et al.,* 1999 A).

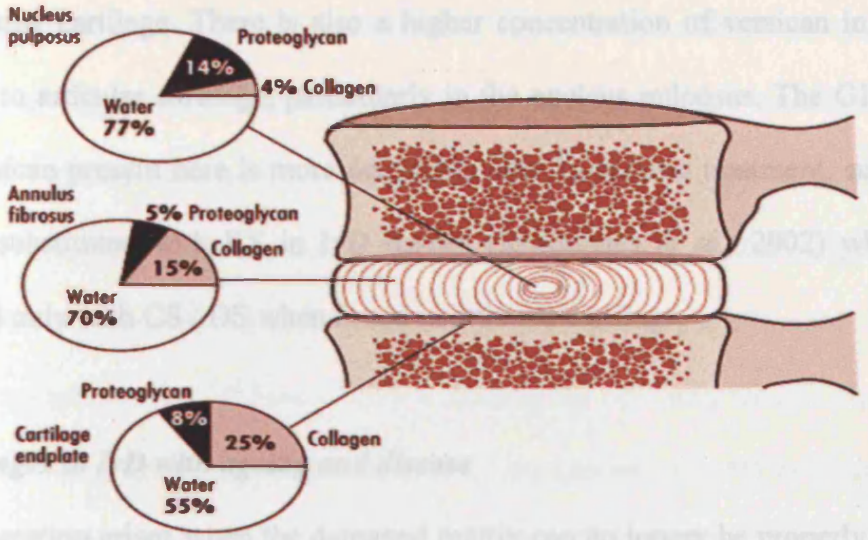

Figure 1.14 The IvD is a highly hydrated tissue that consists of three distinct regions, the nucleus pulposus, the anulous fibrosis and the cartilage endplate. The nucleus pulposus contains the highest concentration of proteoglycans and the lowest level of collagens (Roberts & Urban)

Other matrix proteins such as fibronectin are also present. Although IvD resembles cartilage in many ways, certain aspects of its composition is also unique to disc. For example, aggrecan of IvD is much more highly substituted with KS than aggrecan from articular cartilage. There is also a higher concentration of versican in the IvD compared to articular cartilage, particularly in the nucleus pulposus. The G1 domain of the versican present here is more detectable after keratanase treatment, suggesting that it is substituted with KS in IvD tissues (Sztrolovics *et al.,* 2002) while it is substituted only with CS / DS when found in articular cartilage.

1.6.1 Changes in IvD with ageing and disease

IvD degeneration arises when the damaged matrix can no longer be properly repaired or regenerated. IvD tissue has a very low cell composition, perhaps due to the avascular nature of the tissue. Because of this it may be more difficult for this tissue to synthesise new matrix molecules to balance turnover caused by the proteolytic activity of enzymes such as aggrecanases. Fibronectin levels are increased and it appears in fragmented form that is involved in the down-regulation of aggrecan synthesis and an up-regulation of MMPs (Johnson *et al.,* 2000). Therefore aggrecan and GAG content of the tissue decrease dramatically with age and disease and subsequently so does hydration and functional integrity of the tissue. Collagen levels increase and the tissue becomes more fibrotic. There is an increase in levels of decorin and biglycan in degenerate IvD (Inkinen *et al.,* 1998). Blood vessels and nerves appear more frequently with degeneration (reviewed by Urban & Roberts, 2003). Apoptosis increases significantly with 50% cell necrosis. Boundaries between the nucleus and annulus become less defined with age and degeneration. Discs tend to degenerate more quickly than other tissues and these degenerate discs inadequately carry load leading to chronic painful and disabling conditions.

1.7. Corneal ECM components

The biochemical composition and highly organised arrangement of the corneal stroma (500μm) provide corneal tissue with its essential physical property as the main refractive lens of the eye (Meek & Fullwood, 2001). It is an avascular transparent coat, with an appropriate curvature that helps with the initial transmission and focusing of light into the eye. It is composed of five main layers, the epithelium, Bowman's layer, stroma, Descemet's membrane and the endothelium (figure 1.15). The epithelium is the outer protective layer of the eye, consisting of several layers of cells that regenerate every 48 hours. After wounding the cells migrate quickly inwards to close the wound (reviewed by Steele, 1999). Lumican has recently been implicated in playing an important role in promoting this epithelial healing (Yeh *et al.*, 2005; Chakravarti *et al.*, 2005; Kao *et al.*, 2005).

The epithelium is anchored to the underlying Bowman's membrane by adhesion complexes called anchoring complexes (Linsenmayer *et al.*, 1986 review) involving collagen types IV, VI, VII and XVII. Evaporation of water from the surface of the epithelium allows for nutrient diffusion through the avascular stroma from the aqueous humour.

The Bowman's layer is an acellular matrix region that lays beside the basement membrane underlying the epithelium. The avian Bowman's layer has smaller collagen fibril diameters (18 – 22 nm) than those in the corneal stroma (Hay & Revel, 1969). It acts as a barrier to micro organisms and the corneal stroma.

The Stroma accounts for 90% of the corneal tissue (Maurice, 1957). Collagens present here are primarily types I and VI, and to a lesser extent types II, III, IV, V, VII, VIII, IX, XII and XVII (Newsome *et al.*, 1982). Type III collagen becomes more prevalent during inflammation and healing processes (reviewed by Robert *et al.*, 2001). The stroma of the cornea is rich in collagen VI (Zimmerman *et al.*, 1986) which becomes

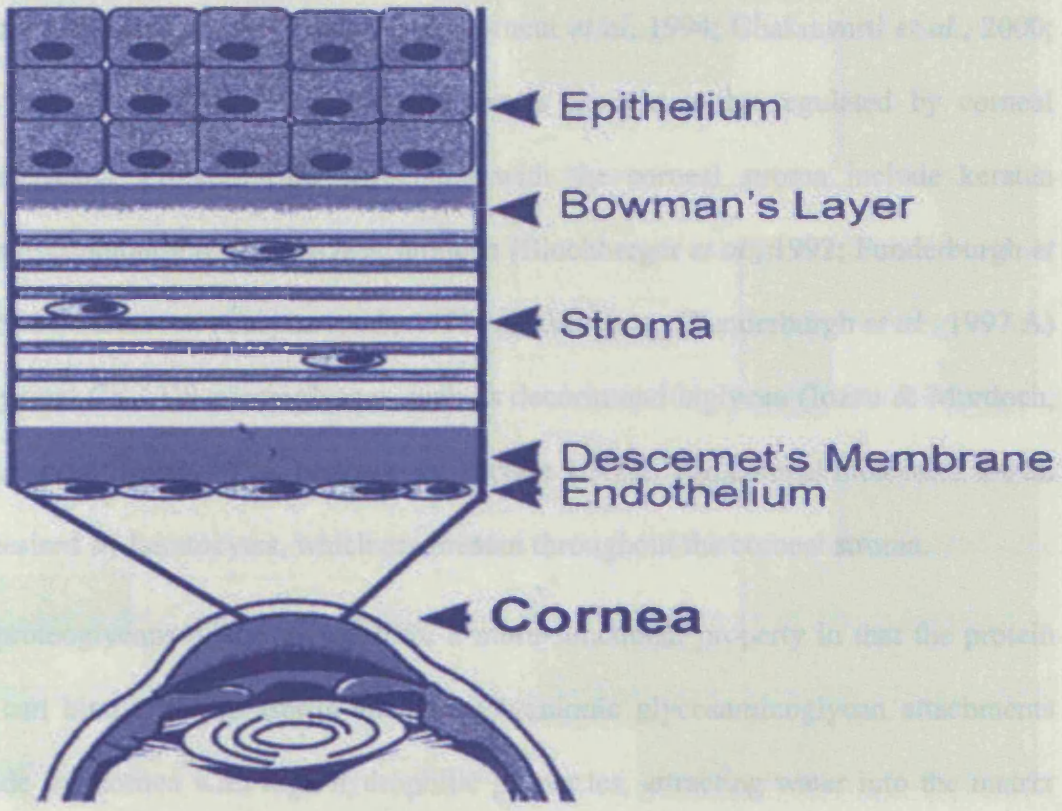

Figure 1.15 The cornea is a highly hydrated tissue that can be divided into 5 distinct regions, the outermost epithelium, the Bowman's layer, the stroma, Descemet's membrane and the inner endothelium.

detectible at the point of mesenchyme cell invasion (see section 1.7.1 below) of the primary stroma (Linsenmayer *et al*, 1986). The stroma also consists of a staggered collagen fibril assembly of type I and type V collagen of remarkably uniform diameter of 25 nm and intrafibrillar spacing of 66 nm (Birk *et al.*, 1990; Linesnmayer *et al.*, 1986). The uniform diameter and organised packing arrangement of the collagen fibrils have been shown to be essential to the refractive capabilities of the cornea (Scott & Bosworth, 1990; Scott, 1991; Corneut *et al*, 1994; Chakravarti *et al.*, 2000; Quantock *et al.*, 2001). This arrangement is thought to be regulated by corneal proteoglycans. Proteoglycans associated with the corneal stroma include keratan sulphate containing proteoglycans, lumican (Blochberger *et al.*, 1992; Funderburgh *et al.*, 1993), keratocan (Corpuz *et al.*, 1996) and mimecan (Funderburgh *et al.*, 1997 A) and typical CS / DS proteoglycans such as decorin and biglycan (Iozzo & Murdoch, 1996, review; Iozzo, 1998, review), see section 1.3.2.2. The corneal molecules are all synthesised by keratocytes, which are present throughout the corneal stroma.

The proteoglycans of the cornea have a multi-functional property in that the protein core can bind collagen fibrils and the polyanionic glycosaminoglycan attachments provide the cornea with high hydrophilic properties, attracting water into the matrix assembly allowing tissue swelling. This influences collagen fibril arrangement and light scattering allowing the maintenance of transparency, an essential property for normal visionary processing. The cornea is covered on the inner surface by Descemet's membrane and the endothelium which help maintain proper hydration of the tissue.

1.7.1. Changes in cornea with development, ageing and disease

The epithelium is responsible for initial synthesis and assembly of the primary corneal stroma in the embryonic chick, it is composed of heterotypic type I and II collagen

fibrils which are only one or two layers thick and FACIT collagen type IX. This primary stroma acts as a template for the mature version of the cornea, the secondary stroma (Linsenmayer *et al.*, 1986, review). Secondary stroma development is activated when the primary stroma becomes swollen and invaded by presumptive fibroblasts (Hay & Revel, 1969). The presence of HA is responsible for an osmotic pressure in the stroma that causes the transitional swelling associated with corneal developmental maturation. The swelling effect is thought to be triggered by cleavage or removal of FACIT collagen type IX from the primary stroma by type IX specific enzymes, as it inhibits swelling in the primary stroma by forming crosslinks with other collagen molecules and it has been observed to disappear rapidly after corneal swelling (Linsenmayer *et al.*, 1986). The invading mesenchyme cells differentiate into stromal fibroblasts and they begin to produce the specific corneal ECM components of the mature stroma (described in section 1.7). Finally, the secondary stroma becomes compact (Hay & Revel, 1969, review). Its thickness is halved and transparency develops which is thought to be a direct result of the appearance of sulphated KS and its affect on collagen fibrillogenesis (Corneut *et al.*, 1994; Chakravarti *et al.*, 2000; Dunlevy *et al.*, 2000).

Like cartilage and IVD, the cornea is another example of an avascular tissue that relies on receiving its oxygen and nutrient supply by diffusion from a different source, specifically the aqueous humour of the eye. The major proteoglycan of corneal stroma is the KSPG lumican whose KS content increases with increasing distance from the vascular supply (Scott & Haigh, 1988; reviewed by Scott, 1992; 1994). Interestingly, in mouse cornea where tissue is much thinner and consequently has a shorter diffusion distance from nutrient supplies than larger animals (e.g. rat and rabbit), the KS sulphation has been shown to be much lower based on light microscopy and electron microscopy (Scott & Haigh, 1988; Young *et al.*, 2005B). The ratio of KS to total

GAG appears to increase with increasing size of cornea from different species. DS to CS ratios are increased in mouse cornea, observed after its partial resistance to chondroitinase AC (Scott & Haigh, 1988). Their methods were sensitive but not quantitative, leaving the possibility for low levels of low sulphated KS to be present in mouse cornea which were below levels of immunochemical detection. However, the results emphasised the relationship between tissue thickness with increasing distances from oxygen supply and a concomitant increase in KS content that occurs during tissue development and expansion.

The generation and maintenance of the transparency of the corneal stroma, is a primary function of the SLRPs, namely decorin, biglycan, lumican, keratocan and mimecan (Corneut *et al.*, 1994; Dunlevy *et al.*, 2000) and is vitally important to the functioning of the whole eye. Dunlevy *et al.*, (2000) showed that expression of various SLRP mRNAs, especially lumican, and resulting production of KS-SLRP proteins with unsulphated KS post-translational modifications, was particularly high prior to key transparency development times during chick corneal development days 9-12. As transparency develops, in days 12-15, so to does the appearance of sulphated KS chains on the lumican core protein (Corneut *et al.*, 1994). Corneal stromal ECM development activates tissue specific factors, which signal for these post-translational modifications to occur to allow transparency to develop. As collagen fibril diameter is much the same in the partially transparent cornea with the poly-N-acetyl-lactosamine form of lumican in early developmental days 9-12, the lumican core protein is thought to regulate this fibril diameter. It is the accumulation of sulphated KS that brings organised spacing of the collagen fibrils which allows transparency to proceed in days 12-15 (Corneut *et al*, 1994). This indicates that the development of the sulphated form of KS on lumican is essential to visual function.

The above results have been supported by work carried out on KSPG knockout mouse models generated via gene targeting. Mice with lumican null mutations have been shown to have thicker collagen fibrils, a 40% reduction in stromal thickness and disordered fibril spacing (Chakravarti *et al.*, 2000). This is due to its lack of lumican core protein to regulate fibril thickness and a 25% reduction of KS content (Chakravarti, 2001 review) to keep stroma hydrated and thereby maintain thickness and keep an organised arrangement of collagen fibrils. These knockout (-/-) mice develop opaque corneas where the disorganised structure backscatters light by disrupting its passage through the cornea. This has been shown effectively to be the case with structural information obtained using X-ray diffraction studies (Quantock *et al.*, 2001), which allows fine detailed examination of corneal ultrastructure as near to the natural state as possible without the artefacts which can be caused by electron microscopy fixation methods.

A keratocan knockout mouse model has also been generated (Liu *et al.*, 2003). In humans, mutations of the keratocan gene cause cornea plana (CNA2) where the convex curvature of the cornea becomes flat. This affects the light refractive capabilities of the cornea and is associated with reduced visual activities, thinner and flatter cornea and corneal opacities (Liu *et al.,* 2003). Keratocan knockout mice revealed larger collagen fibril diameters and a reduction in organised packing; however this was not as severe as that observed in lumican knockout mice. Lumican, decorin, fibromodulin and mimecan expression were not affected by the knockout model.

Studies involving Mimecan knockout mice did not display a pathological phenotype compared to the wild type mice (Tasheva *et al.*, 2002). Corneal clarity and thickness also appeared to be unaffected. There was a reduction in skin tensile strength where 475g of force loaded caused rupture of skin samples in knockout mice compared to

741g in wild type mice. Ultrastructural EM examination of corneal fibrils revealed an increase in diameter in both corneal and dermal collagen fibril diameters (31.84 +/- 0.322 nm in knockout cornea compared to 22.4 +/- 0.269 nm in wild type cornea and 130.33 +/- 1.769 nm in knockout skin dermis samples compared to 78.82 +/- 1.157 nm in wild type skin dermis samples). In addition, fibrils were more loosely packed in knockout compared to wild type mice tissues indicating it has a role to play in collagen fibrillogenesis in vivo. Tasheva *et al.,* (2002) observed no significant abnormalities in bone structure in mutant mice by X-ray analysis.

CS/DS GAG also play an important role in corneal development and pathogenesis. C-0-S levels decline and C-4-S to C-6-S ratios increase significantly as corneal development proceeds, peaking on day 14 of avian corneal development at a key stage of the onset of transparency (Hart, 1976; Midura & Hascall, 1989). Hep/HS levels peak on day 5 of development prior to primary stromal swelling and fall to low levels by day 20 of development when transparency is complete. Studies focusing on the β-D-xylosidase disruption of the addition of xylose through O-glycosidic linkages to decorin in CS/DS PGs during chick corneal development revealed a disruption in lamellar organisation, while the collagen fibril diameters remained unaltered suggesting an important role for CS/DS PGs in intrafibrillar spacing during development (Hahn & Birk, 1992; reviewed by Michelacci, 2003). In macular corneal dystrophy, (see below) the structure of CS or DS changes. The chains become shorter (15 disaccharides compared to 40 disaccharides) and content of C-4-S to C-6-S increases indicating differences in efficiency of GAG chain substitution in such disorders (Plaas *et al.*, 2001).

Macular corneal dystrophies (MCD) are a group of autosomal recessive inherited disorders, which prove the critical role of sulphated forms of KS on KSPGs in vivo. They are reported to be a result of a systemic defect in KS sulphotransferases (Fukuta

et al., 1997; Akama *et al.*, 2001; Seko *et al.*, 2003; Seko & Yamashita, 2004) causing defective sulphated KS synthesis (Nakazawa *et al.*, 1984). This affects vision by altering the normal ordered structural arrangement of the cornea by disrupting the passage of light through the eye. Individuals who suffer from this disorder develop opaque corneas and progressive loss of vision during adolescence and can be blind by the age of 20 (Plaas *et al.*, 2001). Activity of both KS sulphotransferases (Gal6ST and GlcNAc6ST) has been measured in corneas from patients affected with macular corneal dystrophy, keratoconus and from normal human corneas (Hasegawa *et al.*, 2000). Gal6ST activity in MCD corneas was shown to be the same as that of keratoconus and normal corneas. However, GlcNAc6ST activity was much lower in MCD corneas than of normal or keratoconus corneas indicating that it is a defect in the transfer of sulphate to the GlcNAc residue of KS that results in low or unsulphated KS and corneal opacity associated with this disease. KS from MCD corneas are found mainly in an unsulphated form indicating that not only is sulphation of GlcNAc obstructed, but so too is sulphation of Gal, even though Gal6ST levels appear to be present at normal levels. This supports the idea that GlcNAc is sulphated first in the KS biosynthetic pathway (see section 1.4.3) and that sulphation of GlcNAc is required for Gal6ST sulphation of the KS Gal residue to proceed (Hasegawa *et al.*, 2000). KS from patients with MCD is also significantly shorter (3-4 disaccharides compared to ~14 disaccharides) than that of normal corneas (Plaas *et al.*, 2001).

MCD is not restricted to the cornea as it has been shown that sulphated KS is absent in serum from patients with MCD type I where it is found usually resulting from normal cartilage turnover (Thonar *et al.*, 1985). A mutation in the coding region of the CHST6 gene responsible for the GlcNAc6ST enzyme, causes MCD type I (Akama *et al.*, 2000). This may cause production of an inactive enzyme or mislocalisation of the enzyme that is produced.

In contrast, unsulphated KS is found in the corneal epithelium of MCD type II cases but normal sulphated KS is found in serum and corneal stroma of these patients. MCD type II patients show mutations in the upstream region of the same CHST6 gene coding for GlcNAc6ST (Akama *et al.*, 2000; Abbruzzese *et al.*, 2004). No significant difference in the in GlcNAc6ST activity in serum of normal human patients compared to MCD patients suggests that the GlcNAc6ST responsible for KS sulphation in cartilage of MCD type II patients may be different from that found in the corneal epithelium from the same patients (Hasegawa *et al.*, 1999), or that the upstream region of CHST6 affected by mutation may be a regulatory component which affects GlcNAc6ST expression only in corneal areas but not in cartilage (Akama *et al.*, 2000; Abbruzzese *et al.*, 2004).

Overall, the altering composition of synthesised GAG during corneal development has a direct affect on ensuing transparency in a number of ways. Firstly it provides the cornea with an osmotic pressure that attracts water into the stroma. It may also prevent vascularisation of the cornea and it regulates the fibrillogenesis, intrafibrillar spacing and architectural composition of the stroma, all essential qualities for normal corneal transparency (Hart, 1976).

1.8. Aims of this project

The aims of the project were:

- To produce mAbs that recognise keratanase or keratanase II generated neoepitope 'stubs' on corneal and skeletal KS.
- To characterise the epitopes and use these mAbs to investigate KS GAG structure.
- To produce mAbs to linear protein epitopes on corneal KSPGs.
- To investigate KSPG metabolism in "normal" and degenerate joint and intervertebral disc tissues.

Chapter 2 - Production and characterisation of monoclonal antibodies recognising keratanase-generated KS 'stub' neoepitopes

2.1 Introduction

Antibodies are immune system molecules which are produced in response to invasion by foreign antigens in the form of proteins, carbohydrates, glycolipids or nucleic acids. Foreign antigens are recognised by circulating macrophages which act with helper T cells to induce B lymphocytes to produce immunoglobulins (antibodies), with specific antigen (Ag) recognition capabilities. The antibody (Ab) binds to the invading antigen complex to mark it for destruction. One lymphocyte recognises and produces antibodies to one antigen and the immune system as a whole may respond specifically to millions of different molecules.

Although there are 5 different Immunoglobulin classes, Abs have the same basic primary structure, 2 identical heavy chains (~50 kDa) and 2 identical light chains (~25 kDa), which are bound together by disulphide bonds (figure 2.1). The basic structure of the Ab can be divided into 2 functional groups, the specificity function and the effector function. Papain digestion of an Ig cuts it into three parts. Two identical parts contain all of the light chain and part of the heavy chain with variable amino acid sequences at the N-terminal. These parts were shown to possess the Ag binding specificity function and are therefore known as the Fab region (Fragment – antigen binding). The antibody is therefore divalent. The remaining fragment is composed of the remaining heavy chains and is known as the Fc region (Fragment – crystalline) as it is easily crystallised. This region is responsible for effector function, where the binding of an Ig to an Ag allows the Fc region to mediate the hosts' immune response by marking the Ag and initiating its elimination.

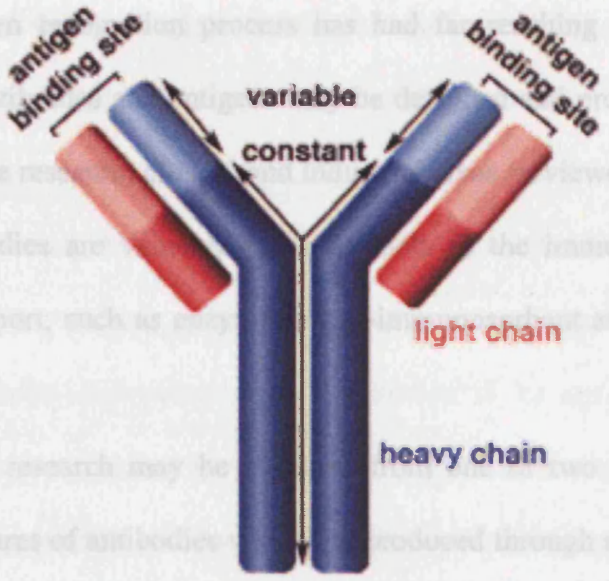

Figure 2.1 - Immunoglobulin structure

(http://www.biology.arizona.edu/immunology/tutorials/antibody/structure.html)

Differences in the sequence of the constant region of the heavy chains (C_H) code for five different Ig classes (IgG, IgA, IgD, IgE and IgM [table 2.1]). Small differences within the sequences of heavy chain of a single class results in different subclasses e.g. IgG_1, IgG_2, IgG_3, IgG_4 or subtypes, e.g. kappa light chains and lambda light chains. IgG, IgE, and IgD occur as monomers of the basic structural unit described and illustrated in figure 2.1, with two heavy chains and two light chains. IgA can occur as a dimer which is joined by a J chain. IgM occurs most commonly as a pentamer of 5 basic structural units joined together by a J chain.

Classes of Igs	Approximate molecular size	Heavy chain Isotype	Carbohydrate by weight (%)	Concentration in serum (mg per 100ml-1)
IgG	150,000	γ 53,000	2-3	600-1800
IgA	170,000-720,000	α 64,000	7-12	90-120
IgD	160,000	δ 58,000		0.3-40
IgE	190,000	ε 75,000	10-12	0.01-0.10
IgM	950,000	μ 70,000	10-12	50-190

Table 2.1 - Ig classification (Devlin, 1997)

The antibody-antigen recognition process has had far reaching implications in the scientific world. Antibodies and antigens may be designed and produced for a variety of applications in the research, clinical and industrial areas (reviewed by Jackson *et al.*, 1999). Such antibodies are valuable research tools in the immunodetection assays described in this report, such as enzyme linked-immunosorbant assays (ELISAs) and Western blotting.

Antibodies used in research may be obtained from one of two sources. Polyclonal antibodies are mixtures of antibodies which are produced through repeat immunisation of experimental animals with a selected antigen. The antibodies are produced in a variety of B-cells and are subsequently obtained from the blood of the animal. Large quantities of high affinity polyclonal antibodies (~10 mg/ml) may be produced from the blood serum. However, this method does not immortalise the antibody producing B-cells and therefore repeat immunisation of numerous animals are required to replenish stock of antibodies. In 1975 Kohler & Milstein succeeded in producing cell lines that were capable of producing a single antibody species – the monoclonal antibody (mAb), by fusing the specific harvested antibody producing B-cell with an immortal mouse myeloma cell line using polyethylene glycol (PEG). Utilising myeloma cells that had a defect in the salvage pathway for nucleic acid biosynthesis, hypoxanthine, aminopterin and thymidine (HAT) selection in specific growth medium ensured that only myeloma cells that had fused with B-cells survived. The myeloma cell line provided the properties essential for cell division, while the antibody-secreting cells provided the immunoglobulin secreting genes.

Supernatant from these fused hybridomas may be analysed by a variety of immunodetection methods, e.g. ELISA or SDS-PAGE and Western blotting, to determine if the resulting cell line contained the desired antibody specificity. Selected cell lines were then grown and cloned to limiting dilution to ensure that each mAb cell

line had been derived from a single cell. Monoclonal antibody stocks can be obtained from culture media of hybridoma cells. MAb hybridomas are advantageous over polyclonal Abs as, due to their unique specificity of binding and their immortal nature, they may be cryo-frozen, thawed and recultured in vitro allowing for a continuous, renewable source of the antibody, without the need to immunise more animals.

Many connective tissue molecules have been shown to be antigenic, and as such numerous monoclonal antibodies have been generated that are specific for antigenic determinants on many matrix molecules. They have proved to be invaluable tools in analysis of PG and GAG structure, abundance, sulphation patterns, and may be used as early markers of the degeneration of cartilage in arthritic disease amongst many other applications.

Immunisation using enzymatically generated neoepitope antigens from structures within the PG molecule, such as chondroitinase ABC digested aggrecan (Caterson *et al.*, 1985), have been used to cause pronounced antibody response in mice with resultant generation of monoclonal antibodies (table 2.2). These antibodies have been invaluable for studying PG distribution and structure within cartilage. By enzymatically removing the chondroitin sulphate (CS) chain, not only are the neoepitopes created, but this also removes the space filling CS chain, making the matrix more easily penetrated by antibodies. Antibodies have also been generated and characterised (table 2.2) to undigested full length KS and CS chains (Christner *et al.*, 1980; Caterson *et al.*, 1983; Couchman *et al.*, 1984; Mehmet *et al.*, 1986) and to protein core epitopes and protease-generated neoepitopes (Calabro *et al.*, 1992; Hughes *et al.*, 1995).

Antibody	Epitope recognised
2B6	Chondroitinase ABC and AC II generated chondroitin-4-sulphate (C-4-S) stubs and chondroitinase B-generated C-4-S in dermatan sulphate
3B3+	Chondroitinase ABC and AC II-generated chondroitin-6-sulphate (C-6-S) stubs
1B5	Chondroitinase ABC and AC II-generated chondroitin-0-sulphate (C-0-S) stubs
3B3-	Chondroitin-6-sulphate (C-0-6) at the non-reducing terminal
5D4	KS linear epitope – pentasulphated hexasaccharide
1B4	KS linear epitope – tetrasulphated hexasaccharide
4D1	Sulphated linear poly-N-acetyllactosamine epitope
2D3	Highly sulphated linear poly-N-acetyllactosamine epitope

Table 2.2 - Monoclonal antibodies and their epitopes (Christner *et al.*, 1980; Caterson *et al.*, 1983; Couchman *et al.*, 1984; Caterson *et al.*, 1985; Mehmet *et al.*, 1986).

The objective of the research described in this chapter was to develop a novel monoclonal antibody that would recognise a keratanase–generated neoepitope produced following exposure of KS GAG chains to the KS degrading enzyme keratanase from *Pseudomonas sp.* (EC 3.2.103). In order to produce the mAb, which could be used for studying KS substitution and sulphation patterns in a range of connective tissues, an antigen was required that would induce an immune response to raise the specific antibodies. In brief, trypsin generated bovine aggrecan KS-peptides (Heinegard & Axelsson, 1977) digested with keratanase (*Pseudomonas Sp*) were used in this study to induce antibody production in a mouse. For purposes of both immunisation and screening of subsequent hybridoma cell lines for antigen specificity, it was important that the antigen of interest was relatively pure and defined in form. Therefore, antigens were prepared by extraction of cartilage aggrecan from bovine nasal cartilage, and purification from other components in the connective tissue matrices through a series of density gradient centrifugation and chromatographic steps.

2.2 Materials

2.2.1 Stock solutions

Solutions and their components required for practical work are listed in table 2.3. Ethanol, acetic acid, hydrochloric acid, sodium hydroxide and methanol were all obtained from Fisher Scientific.

Buffer solution	**Components**
Dimethylmethylene Blue	32 mg DMMB; 1% (v/v) ethanol; 2.05% (v/v) 1 M NaOH; 0.35% (v/v) 98% formic acid; made up to 2 L Milli Q™ water.
TPCK-Trypsin buffer	0.1 M tris, pH 7.3, 0.1 M sodium acetate buffer
Keratanase buffer	10 mM tris-HCl, pH 7.4
Keratanase II buffer	10 mM sodium acetate, pH 6.8
Endo-β-galactosidase buffer	0.2 M sodium acetate, pH 5.8, containing 2 mg/ml BSA
Chondroitinase / keratanase / keratanase II buffer	0.1 M tris acetate, pH 6.8
2 x SDS PAGE sample buffer	0.125 M tris-HCl, pH 6.8, containing 4% (w/v) SDS; 20% (w/v) glycerol; 0.01% (w/v) bromophenol blue
SDS PAGE running buffer	25 mM trizma; pH 8.4 192 mM glycine; 0.01% (w/v) SDS.
SDS transfer buffer	25 mM trizma; pH 8.1-8.4; 192 mM glycine; 20% (v/v) methanol.
Tris buffered saline with azide (TSA)	50 mM trizma; pH 7.4 with HCl; 200 mM NaCl; 0.02% (v/w) NaN_3
Alkaline phosphatase substrate buffer (AP buffer)	100 mM trizma; pH 9.55; 100 mM NaCl; 5mM $MgCl_2$
NBT: nitro blue tetrazolium	50 mg/ml in 70 % dimethylformamide
BCIP: 5-bromo-4-chloro-3-indoylphosphate	50 mg/ml in dimethylamide
Lectin buffer	TSA, pH 7.5; 1 mM $MgCl_2$, 1 mM $MnCl_2$, 1 mM $CaCl_2$
Anion exchange chromatography equilibration buffer	0.05 M tris, pH 6.8
Anion exchange chromatography elution buffer	2 M NaCl, pH 6.8, 0.05 M Tris
Size exclusion chromatography equilibration buffer	0.1 M sodium sulphate, pH 6.5-7.5
ELISA coating buffer	20 mM sodium carbonate, pH 9.6
DEA substrate buffer	0.126 mM $MgCl_2$; pH to 9.8 with HCl; 48 ml Diethanolamine in 452 ml Milli Q™ water
Proteoglycan extraction buffer	4 M guanidine HCl, pH 5.8-6.8; 0.05 M sodium acetate, 10 mM Na_2EDTA, 0.1 M 6-amino hexanoic acid, 5 mM benzamidine, 0.5 mM PMSF

Table 2.3 Buffer solutions and their components

2.2.2 Dimethylmethylene Blue materials

Dimethylmethylene Blue (DMMB) dye (table 2.3) was used to measure sulphated glycosaminoglycan (S-GAG) in a sample. It works by binding to the negatively charged sulphate and carboxyl groups on the GAG chains forming a complex which produces a metachromatic shift in the absorbance maxima (Farndale *et al.,* 1986). The dye was made by dissolving 32 mg DMMB in 20 ml ethanol overnight with rotation at room temperature. 1.5 L Milli Q™ water was added to a 2 L cylinder along with 59 ml 1 M NaOH and 7 ml 98% formic acid. The dissolved DMMB solution was then added to this solution and made up to 2 L with Milli Q™ water and stirred for an additional 2 hours. The absorbance of the DMMB solution was checked against Milli Q™ water as a blank at 525 nm and 592 nm. This gave absorbance readings of approximately 0.3 and 1.4, respectively if sufficient dye was dissolved. The solution was stored in a light proof container.

Chondroitin sulphate C, sodium salt from shark cartilage was purchased from Sigma, a 0.5 mg/ml solution was routinely used to make a linear standard curve between 0 and 40 μg/ml GAG for DMMB analysis to calculate the concentration of sulphated GAG in unknown samples. 96 well flat bottom EIA microtitre plates were purchased from Elkay, UK. A labsystems multiscan MS plate reader was used to read the plates at a wavelength of 525 nm.

2.2.3 Keratan sulphate, chondroitin sulphate and protein degrading enzymes

L-(tosylamido-2-phenyl) ethyl chloromethyl ketone (TPCK) treated trypsin from bovine pancreas was purchased from Sigma. The keratan sulphate degrading enzymes, keratanase from *Pseudomonas sp* EC 3.2.103, keratanase II from *Bacillus sp* Ks 36 and endo-β-galactosidase from *Escherichia freundii*, were obtained from MP Biomedical. Chondroitinase ABC was obtained from Sigma-Aldrich, UK.

2.2.4 Immunisation, cell fusion and tissue culture materials

All monoclonal cell lines were cultured in RPMI-complete (RPMI-C) media consisting of RPMI 1640 media supplemented with 15% (v/v) foetal bovine serum, 2 mM L-glutamine, penicillin (100 U/ml), streptomycin (100 μg/ml), fungizone (0.25 μg/ml) and 0.5 mM β-mercaptoethanol. RPMI 1640 media, fetal bovine serum (FBS), PBS Dulbecco's, L-glutamine and penicillin streptomycin, fungizone (PSF) were all purchased from Gibco Brl (now Invitrogen). β-mercaptoethanol was from Sigma. All tissue culture and plastic plates were purchased from Corning Costar. 0.22 μm filter units were from Millipore. All complete culture media was filtered through the 0.22 μm filter units before use.

For immunisation and fusion, Freunds complete adjuvant and Freunds incomplete adjuvant were purchased from Gibco Brl (now Invitrogen). The X 63 Ag 8.563 (Ag8) myeloma cell line was obtained from stock cell lines frozen at -80 °C in the lab. 16 and 27.5 gauge needles were from Becton Dickenson. Polyethylene glycol (PEG), molecular weight 3,000 – 3,700, was from Sigma and hypoxanthine (100 μM), aminopterin (0.4 μm), thymidine (1.6 μm) [HAT] was purchased from Gibco Brl (now Invitrogen). 2 μM Hypoxanthine, 0.008 μM aminopterin and 0.032 μM thymidine were supplemented to RPMI-complete media (see above) for initial culture of newly fused monoclonal cell lines.

Cryoprotective media was made of 90% (v/v) fetal bovine serum, 10% (v/v) dimethyl sulphoxide (DMSO) [Hybri-Max obtained from Sigma-Aldrich, UK]. Cells were resuspended in this media and stocks maintained by freezing at –80 °C and in liquid nitrogen.

2.2.5 SDS-PAGE and Western blotting materials

4 - 12% and 4 - 20% pre-cast Tris glycine gradient gels were purchased from Invitrogen. Slab gels of required percentages (12% or 15%) were prepared using acrylagel and bisacrylagel from National Diagnostics. The electrophoresis tank was purchased from Invitrogen. Transfer tanks, power packs and molecular weight protein standards were all from Bio-Rad. β-mercaptoethanol was from Sigma-Aldrich. 0.22 μm Protran BA 83 nitrocellulose membrane designed for high binding capacity with low background interference was obtained from Schleicher & Schuell Bioscience. All of the monoclonal antibodies used in this investigation were obtained from stocks maintained in our laboratories. Antibody culture media was used at a 1:100 dilution and antibody ascities was used at a 1:5000 dilution. Anti-mouse IgG (H+L) alkaline phosphatase conjugated secondary antibody was from Promega, UK. Blots were developed in an alkaline phosphatase substrate made from 0.33 mg/ml nitro blue tetrazolium (NBT) and 0.165 mg/ml 5-bromo-4-chloro-3-indoylphosphate (BCIP) which were also purchased from Promega.

2.2.6 Lectin affinity blotting materials

A digoxigenin (DIG) glycan differentiation kit was obtained from Roche and was used in accordance with the manufacturers protocol. Lectins used include peanut agglutinin (PNA) which is specific for the core disaccharide Galβ(1-3)GalNAc present in O-linked oligosaccharides and galanthus nivalis agglutinin (GNA) specific for terminal mannose α(1-3), α(1-6) or α(1-2) linked to mannose, identifying high mannose N-linked oligosaccharides. These specific lectins were used to analyse for various oligosaccharides and different KS type I and II linkage regions exposed after enzymatic deglycosylation of the KS chain with various keratanases.

2.3 Methods

2.3.1 Deglycosylation (degradation) of keratan sulphate chains

Structural analysis of KS types I and II was aided by the use of different enzymes including keratanase purified from culture media of *Pseudomonas sp* EC 3.2.103, endo-β-galactosidase from *Escherichia freundii* and keratanase II from *Bacillus sp* Ks 36. Keratanase hydrolyses the internal β (1-4) galactosidic linkage between galactose and N-acetylglucosamine where the linking N-acetylglucosamine residue must be sulphated at position 6 and where the participating galactose residue remains unsulphated (Nakazawa *et al.*, 1975; Nakazawa & Suzuki, 1975; Nakazawa *et al.*, 1989; reviewed by Calabro *et al.*, 2001). Fucosylation at GlcNAc-6-S or proximate sialic acid groups can hamper the action of this enzyme.

Endo-β-galactosidase also specifically cleaves β (1-4) galactosidic linkages between galactose and N-acetylglucosamine (Fukuda & Matsumura, 1976). It favours digestion of KS GAG where the N-acetyl-lactosamine disaccharide is un-sulphated. However, it will cleave at the same monosulphated cleavage site as keratanase but at a much lower reaction rate, releasing oligosaccharides of various sizes (Fukuda & Matsumura, 1976). Keratanase II specifically cleaves the β (1-3) glucosaminidic linkage of N-acetylglucosamine-6-sulphate to galactose, irrespective of sulphation at galactose residues (Oguma *et al.*, 2001; Yamagishi *et al.*, 2003).

The cleavage sites of these enzymes on KS are as follows:

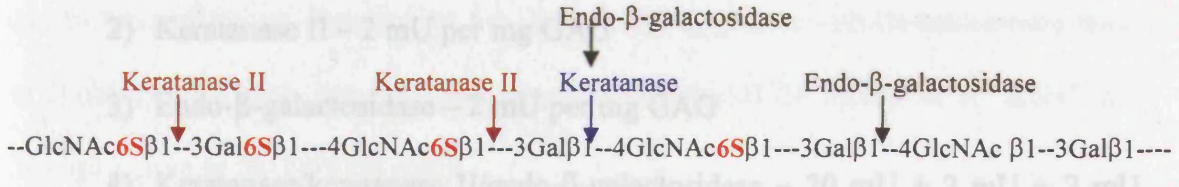

2.3.1.1 Quantification of GAG using the DMMB assay

GAG concentration of trypsin digested BNC A1D1 KS peptide fragments (provided by Professor Bruce Caterson, Cardiff University, see section 2.3.2 below) and bovine corneal KSPGs (purified as described in chapter 4) were determined using DMMB analysis. This assay works when the DMMB dye (section 2.2.2) binds to sulphate groups on GAG chains causing a shift in colour absorbance. 40 µl of a linear standard curve ranging from 0-40 µg/ml are applied to a 96 well multiplate along with 40 µl of appropriately diluted unknown samples. 200 µl of DMMB dye (section 2.2.2, table 2.3) was applied to each sample and standard and the absorbance read at 525 nm using a Lab Systems plate reader. All GAG quoted concentrations were calculated using this assay.

2.3.1.2 Determination of optimal enzyme conditions for keratanase, keratanase II and endo-β-galactosidase digestion

A volume equal to 400 µg GAG (as determined using the DMMB assay) of BNC A1D1 was digested using 100 mU of chondroitinase ABC per mg GAG for 24 hours at 37 °C, followed by dialysis to Milli Q™ water and lyophilisation. Four test aliquots containing 100 µg GAG were initially digested with keratanase, keratanase II or endo-β-galactosidase and a keratanase/keratanase II/endo-β-galactosidase mixture in their respective digestion buffers (see table 2.3) as follows:

1) Keratanase – 20 mU per mg GAG
2) Keratanase II – 2 mU per mg GAG
3) Endo-β-galactosidase – 2 mU per mg GAG
4) Keratanase/keratanase II/endo-β-galactosidase – 20 mU + 2 mU + 2 mU per mg GAG, respectively.

Samples were digested for 24 hours at 37 °C at which time an aliquot was taken for analysis using the DMMB assay. At 24 hours a further 20 mU of keratanase per mg GAG, 2 mU keratanase II per mg GAG, 2 mU endo-β-galactosidase per mg GAG and a mixture of 20 mU keratanase/2 mU keratanase II/2 mU endo-β-galactosidase II per mg GAG was added to each respective sample and digested for a further 24 hours at 37 °C followed by DMMB analysis. This process was repeated at 48, 72, 96 and 120 hours or until no further reduction in S-GAG could be detected by DMMB analysis.

The results for optimal enzyme conditions for corneal and skeletal KS (types I and II) has been summarised in tables 2.4 and 2.5, respectively. Optimal digestion of both corneal and skeletal KS with either keratanase, keratanase II or endo-β-galactosidase was accomplished after the addition of 80 mU, 6 mU and 8 mU of each enzyme, respectively per mg GAG for a minimum of 24 hours (figures 2.2 and 2.3; A, B & C, respectively). It was not possible to reduce S-GAG dye-binding by 100% using either keratanase or endo-β-galactosidase in either corneal or skeletal KS. This indicated that there were disulphated disaccharide domain motifs on KS towards the linkage region that could not be removed by keratanase or endo-β-galactosidase suggesting that disulphated disaccharide domains were found attached directly to the linkage region without any intermittent non- or mono-sulphated disaccharides (see chapter 3). 100% reduction in S-GAG was achieved in corneal KS with keratanase II as expected as it cleaves both mono- and di-sulphated disaccharides. However there was only a 60% reduction in S-GAG after keratanase II digestion in skeletal KS. This could possibly be due to incomplete pre-digestion of the BNC A1D1 aggrecan with chondroitinase ABC or contribution of the chondroitinase-generated sulphated CS disaccharide 'stubs' and linkage region to the DMMB assay.

Table 2.4 - % reduction in sulphated GAG in corneal KS (KS type I) determined by DMMB analysis

KS type I				%Reduction in S-GAG			
Time	**Total keratanase conc mU / mg GAG**	**Total keratanase II conc mU / mg GAG**	**Total endo-β-gal conc mU / mg GAG**	**Ker**	**Ker II**	**Endo -β-gal**	**Ker + ker II + endo-β–gal**
24hrs	20	2	2	28%	90%	1%	94%
48hrs	40	4	4	50%	96%	14%	99%
72hrs	60	6	6	50%	98%	28%	100%
96hrs	80	8	8	55%	99%	40%	100%
120hr	100	10	10	57%	99%	40%	100%

Table 2.5 - % reduction in sulphated GAG in skeletal KS (KS type II) determined by DMMB analysis

KS type II				%Reduction in S-GAG			
Time	**Total keratanase conc mU / mg GAG**	**Total keratanase II conc mU / mg GAG**	**Total endo-β-gal conc mU / mg GAG**	**Ker**	**Ker II**	**Endo -β-gal**	**Ker + Ker II + endo-β–gal**
24hrs	20	2	2	40%	62%	29%	51%
48hrs	40	4	4	44%	55%	25%	65%
72hrs	60	6	6	45%	61%	41%	64%
96hrs	80	8	8	50%	58%	55%	70%
120hr	100	10	10	51%	60%	56%	73%

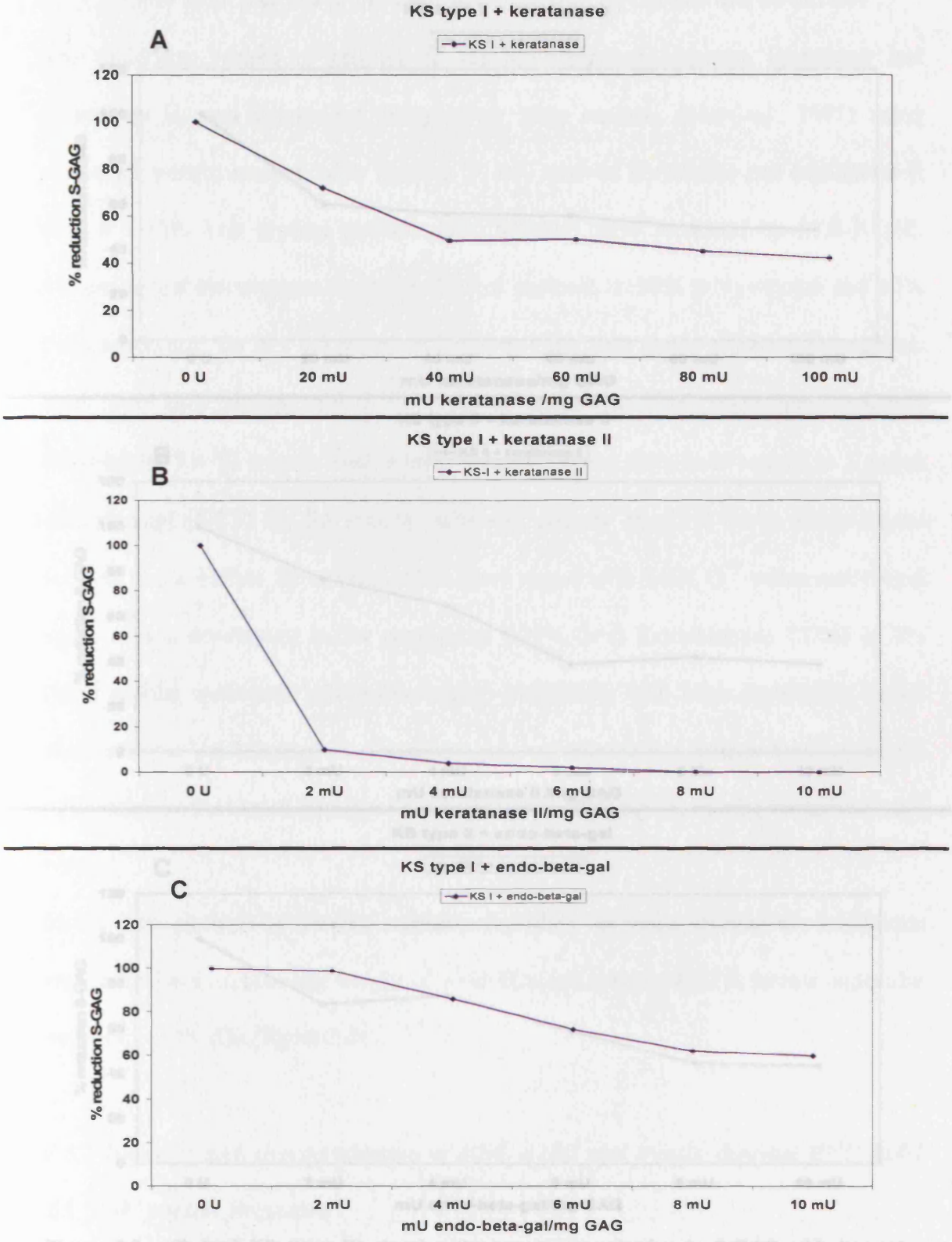

Figure 2.2 - Corneal KS (type I) - percentage reduction in S-GAG with increasing concentrations of keratanase (A. 80 mU/mg GAG of keratanase was required for optimal digestion of KSI), keratanase II (B. 6 mU/mg GAG of keratanase II was required for optimal digestion) or endo-β-galactosidase (C. 8 mU/mg GAG of endo-β-galactosidase was required for optimal digestion of KSI).

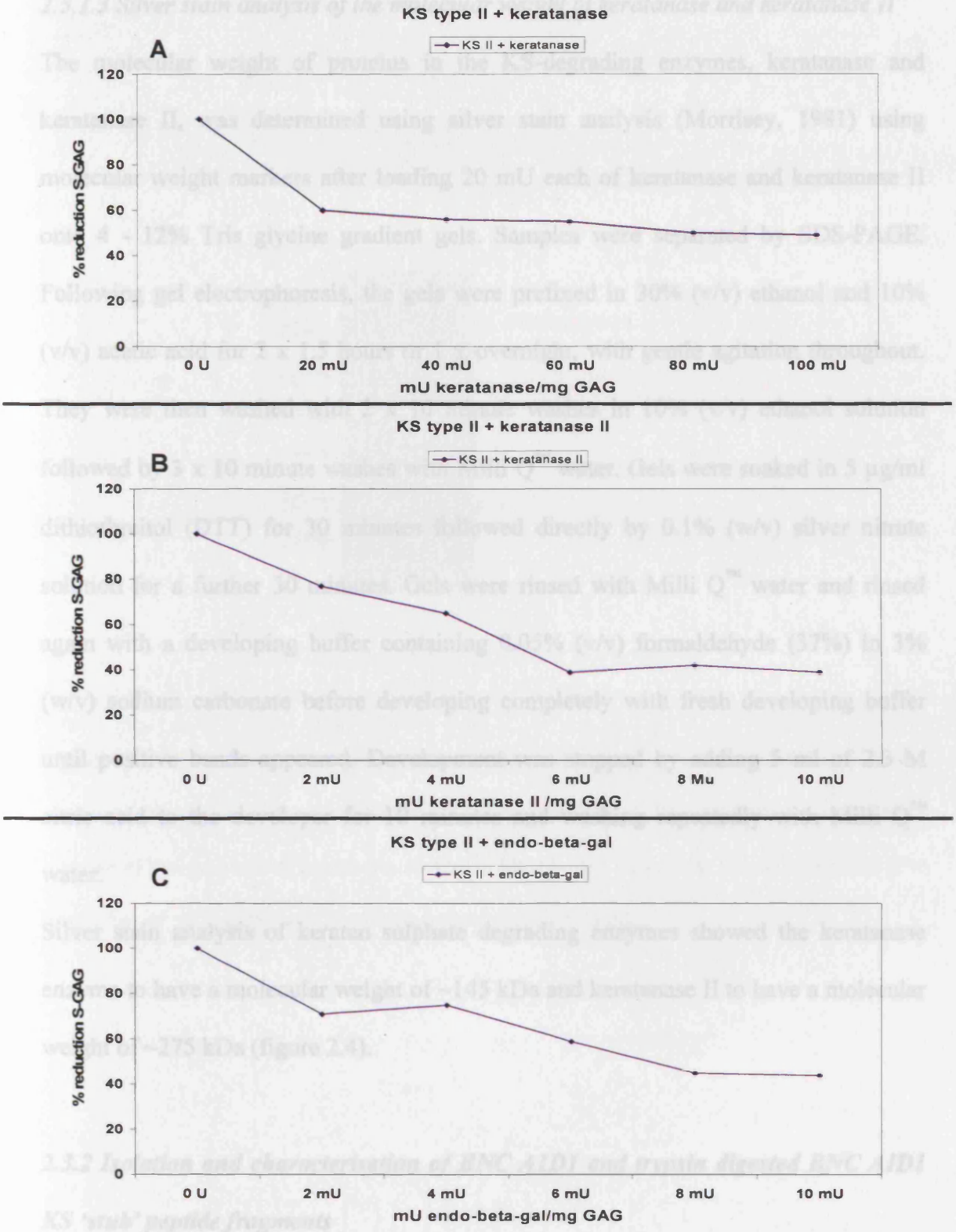

Figure 2.3 - Skeletal KS (type II) showing the percentage reduction in S-GAG with increasing concentrations of keratanase (A. 80 mU of keratanase per mg GAG was required for optimal digestion of KSII), keratanase II (B. 6 mU of keratanase II per mg GAG was required for optimal digestion of KSII) or endo-β-galactosidase (C. 8 mU of endo-β-galactosidase per mg GAG was required for optimal digestion).

2.3.1.3 Silver stain analysis of the molecular weight of keratanase and keratanase II

The molecular weight of proteins in the KS-degrading enzymes, keratanase and keratanase II, was determined using silver stain analysis (Morrisey, 1981) using molecular weight markers after loading 20 mU each of keratanase and keratanase II onto 4 - 12% Tris glycine gradient gels. Samples were separated by SDS-PAGE. Following gel electrophoresis, the gels were prefixed in 30% (v/v) ethanol and 10% (v/v) acetic acid for 2 x 1.5 hours or 1 x overnight, with gentle agitation throughout. They were then washed with 2 x 10 minute washes in 10% (v/v) ethanol solution followed by 3 x 10 minute washes with Milli Q™ water. Gels were soaked in 5 μg/ml dithiothreitol (DTT) for 30 minutes followed directly by 0.1% (w/v) silver nitrate solution for a further 30 minutes. Gels were rinsed with Milli Q™ water and rinsed again with a developing buffer containing 0.05% (v/v) formaldehyde (37%) in 3% (w/v) sodium carbonate before developing completely with fresh developing buffer until positive bands appeared. Development was stopped by adding 5 ml of 2.3 M citric acid to the developer for 10 minutes and washing repeatedly with Milli Q™ water.

Silver stain analysis of keratan sulphate degrading enzymes showed the keratanase enzyme to have a molecular weight of ~145 kDa and keratanase II to have a molecular weight of ~275 kDa (figure 2.4).

2.3.2 Isolation and characterisation of BNC A1D1 and trypsin digested BNC A1D1 KS 'stub' peptide fragments

The methods for the isolation of a keratanase-generated 'KS-stub'antigen are illustrated in figure 2.5. Expanded details are provided in the sections below.

Bovine nasal cartilage A1D1 aggrecan (A1D1 CsCl density gradient fraction) was provided by Professor Bruce Caterson, Cardiff University. Bovine cartilage aggrecan

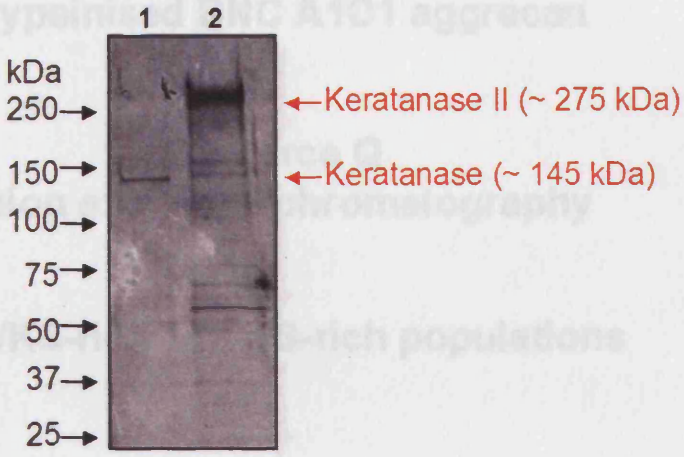

Figure 2.4 – Silver stain analysis of the keratan sulphate degrading enzymes. Enzymes were run alone under reducing conditions at a concentration of 20 milli units per lane. Silver staining of the gel showed keratanase to have a M_w of ~145 kDa (lane 1) and keratanase II to have a M_w of ~275 kDa (lane 2) with a number of smaller bands.

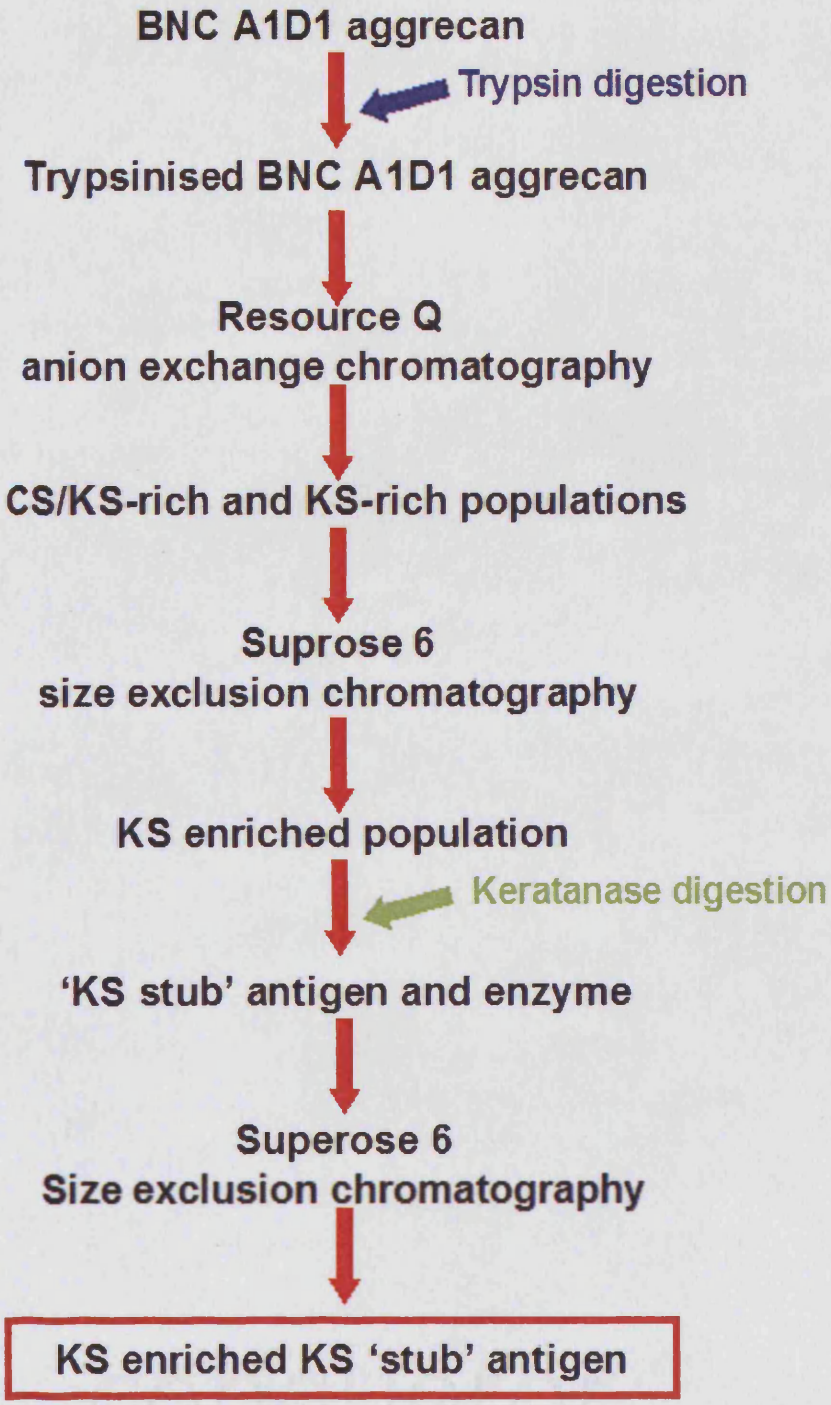

Figure 2.5- An overview of the procedures involved in production of the KS enriched 'stub' antigen used for immunization in mAb production.

was selected as starting material for the purification of KS rich peptide fragments (Heinegard & Axelsson, 1977) for use in immunisation for the production of keratanase generated KS 'stub' antibodies. Cartilage aggrecan A1D1 (410 mg dry weight) was previously prepared by extraction in 4 M guanidine HCl with a protease inhibitor cocktail (5 mM sodium acetate anhydrous, pH 5.8 – 6.8, 10 mM Na_2EDTA), 10 mM 6-aminohexanoic acid, 5 mM benzamidine-HCl, 0.5 mM PMSF, pH 5.8 - 6.8). The sample was then dialysed into 50 mM sodium acetate, pH 6.8 and partially purified under associative conditions by CsCl density gradient centrifugation. The aggrecan/link protein/HA complex (A1 fraction) was taken and solid Guanidine added to 4 M followed by subsequent CsCl density gradient separation under dissociative conditions. The dissociative density gradient was separated into three fractions (A1D1, A1D2 and A1D3) using methods described by Heinegard & Sommarin (1987). Bovine aggrecan monomers (A1D1) were obtained after dialysis against 0.15 M NaCl then water and freeze dried.

2.3.2.1 Characterisation of the macromolecular status of bovine A1D1 aggrecan by SDS-PAGE and Western blot analysis

DMMB analysis (see section 2.3.1.1) was carried out on appropriately diluted samples of the purified BNC A1D1 preparation. Subsequently 10 μg GAG was deglycosylated using 100 mU of chondroitinase ABC per mg GAG, 80 mU of keratanase per mg GAG and 6 mU of keratanase II per mg GAG (see section 2.3.1.2 above) and samples were lyophilised.

Equal amounts of the chondroitinase / keratanase digested BNC A1D1 samples were diluted in an appropriate volume of Milli Q™ water and further diluted 1:1 with 2x concentrated sample buffer (see table 2.3). The samples were reduced by adding 10% (v/v) β-mercaptoethanol and boiled for 5 minutes prior to separation by SDS-PAGE.

The samples were loaded onto 4 - 12% (or 4 - 20% Tris glycine gradient gels or slab gels of 12 or 15% depending on the molecule of interests predicted size) and separated under reducing conditions in SDS-running buffer (table 2.3) using a gel electrophoresis system at 150 volts for 90 minutes or until the bromophenol blue in the sample buffer reached the end of the gel cassette. Molecular weight of separated molecules were standardised utilizing a protein molecular weight standard from Bio-Rad. Samples were then electrophoretically transferred to nitrocellulose membranes using the SDS transfer buffer (table 2.3) in a transfer apparatus for 1 hour at 100 volts. For Western blot analysis, nitrocellulose membranes were blocked in 5% (w/v) BSA in TSA (see table 2.3) for a minimum of one hour at room temperature or overnight at 4 °C. Membranes were then probed with primary antibodies (see epitopes in table 2.2) 2B6 (hybridoma culture media 1:100 dilution), 3B3 (hybridoma culture media 1:100 dilution) and 1B5 (ascities 1:5000 dilution) in 1% BSA (w/v) in TSA overnight at room temperature. Blots were rinsed with 3 x 10 minute washes in TSA before incubation with an alkaline phosphatase conjugated goat anti-mouse secondary antibody at a dilution of 1:7500 in 1% (w/v) BSA in TSA for 1 hour at room temperature. After a further 3 x 10 minute washes in TSA, the immunoblots were incubated with an alkaline phosphatase substrate (see table 2.3 and section 2.2.5) for 10 - 50 minutes at room temperature or until optimal colour development of immunopositive bands was achieved. This analysis was used to determine the biochemical and macromolecular status of the BNC A1D1 aggrecan core protein.

Western blot analysis of the chondroitinase ABC and keratanase digested BNC A1D1 aggrecan using antibodies 2B6/3B3/1B5 recognising CS 'stub' epitopes on proteoglycan core proteins displayed staining of high molecular weight products (figure 2.6), indicating that the PG core protein was intact and suitable for digestion with TCPK – trypsin.

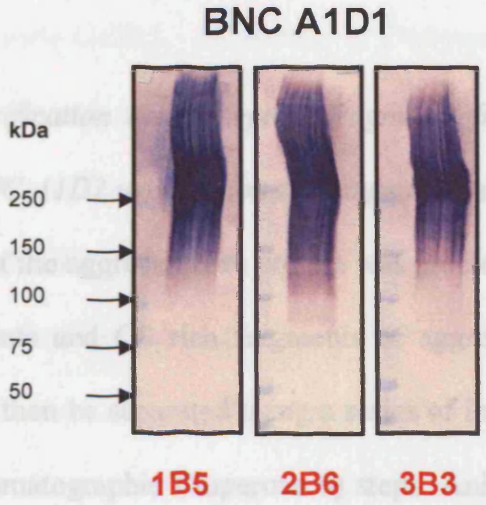

Figure 2.6 – Analysis of the macromolecular status of BNC A1D1. Chondroitinase ABC and keratanase digested bovine nasal cartilage aggrecan A1D1 was stained using CS isomer 'stub' mAbs 1B5, 2B6 and 3B3. Results demonstrate that the aggrecan core protein macromolecule was essentially intact with core protein metabolites ranging in molecular weight from 150 – 400 kDa as determined using Biorad molecular weight standards.

2.3.2.2 Trypsin digestion of BNC A1D1

400 mg dry weight of the BNC A1D1 sample was subjected to trypsin digestion using 2 μg TPCK treated trypsin per mg BNC A1D1 in a 0.1 M Tris, pH 7.3, 0.1 M Sodium acetate buffer (table 2.3), for 16 hours at 37 °C. The digest was then dialysed against Milli Q™ water and lyophilised (Heinegard & Axelsson, 1977).

2.3.2.3 Partial purification of KS-peptide fragments from CS-peptide fragments of trypsin digested BNC A1D1 using anion exchange chromatography

Trypsin digestion of the aggrecan core protein was predicted to result in the production of KS rich fragments and CS rich fragments of aggrecan (Heinegard & Axelsson, 1977) which could then be separated using a series of ion exchange (Resource Q) and size exclusion chromatographic (Superose 6) steps. Anion exchange chromatography was used as the initial separation procedure for the more highly charged CS peptide fragments which would elute at a higher molarity of NaCl (1M - 2M) from a population of lesser negatively charged KS peptide fragments predicted to elute at a lower molarity of NaCl (0.1 - 0.5 M). The freeze dried trypsin-digested aggrecan peptide preparation was reconstituted in 6 ml equilibration buffer (5 mM Tris, pH 6.8; see table 2.3) centrifuged at 1,500 rpm for 10 minutes and the supernatant passed through a 0.22 μm filter to remove remaining debris or air bubbles. The sample was then applied to a 6 ml Resource Q chromatography column equilibrated in 5 mM Tris, pH 6.8, at a flow rate of 4 ml/min. Bound material was sequentially eluted with a linear gradient of NaCl (0 M – 2 M) over 10 column volumes. 3 ml fractions were collected, dialysed against Milli Q™ water and analysed for glycosaminoglycans using the DMMB assay (section 2.3.1.1). SDS-PAGE and Western blot analysis (as section 2.3.2.1) was carried out on equal volumes of the GAG containing fractions after digestion with chondroitinase ABC (100 mU per mg GAG). The samples were

separated on 4 - 12% Tris-glycine gradient gels transferred onto nitrocellulose and analysed using Western blotting with mAbs 2B6/3B3 and 5D4 to determine the presence of any CS or KS GAG containing peptides, respectively.

In addition to Western blot analyses using antibodies, a set of membranes were also probed with the lectin peanut agglutinin – PNA (see section 2.2.6) recognising the core substituted disaccharide Galβ(1 - 3)GalNAc in O-glycan linked oligosaccharides that occur on the linkage region of O-linked skeletal KS. This KS-linkage region can become exposed after different keratanase treatments. It should be noted however, that this lectin (PNA) is not KS specific as it also identifies O-linked oligosaccharides aside from KS which are also located on the protein core of aggrecan and other molecules. Briefly, 40 µl samples were digested overnight at 37 °C using 80 mU of keratanase per mg of sulphated GAG measured using the DMMB assay. Digested samples were run on 4 - 12% SDS-PAGE gels and transferred to nitrocellulose using methods described in section 2.3.2.1. Lectin affinity analysis was carried out using a DIG glycan differentiation kit according to the manufacturer's protocol. Briefly, the nitrocellulose was blocked with 2 ml of blocking reagent (supplied with the kit) diluted 1:10 in TSA (see table 2.3) for a minimum of 1 hour at room temperature. Blots were rinsed 2 x 10 minutes with TSA and 1 x 10 minutes with TSA containing lectin buffer (table 2.3). Blots were then incubated with 100 µl PNA lectin in 10 ml lectin buffer for 1 hour at room temperature and rinsed again for 3 x 10 minutes with TSA before the addition of 10 µl polyclonal sheep anti-digoxigenin-AP (supplied with the kit) in 10 ml TSA for 1 hour at room temperature. Immunopositive staining was achieved after the addition of 10ml AP substrate buffer (table 2.3) containing NBT and BCIP (see section 2.2.5).

Figure 2.7 shows the Resource Q anion exchange chromatographic profiles detected using 214 nm (blue), 232 nm (pink) and 280 nm (green) wavelengths. Detection of

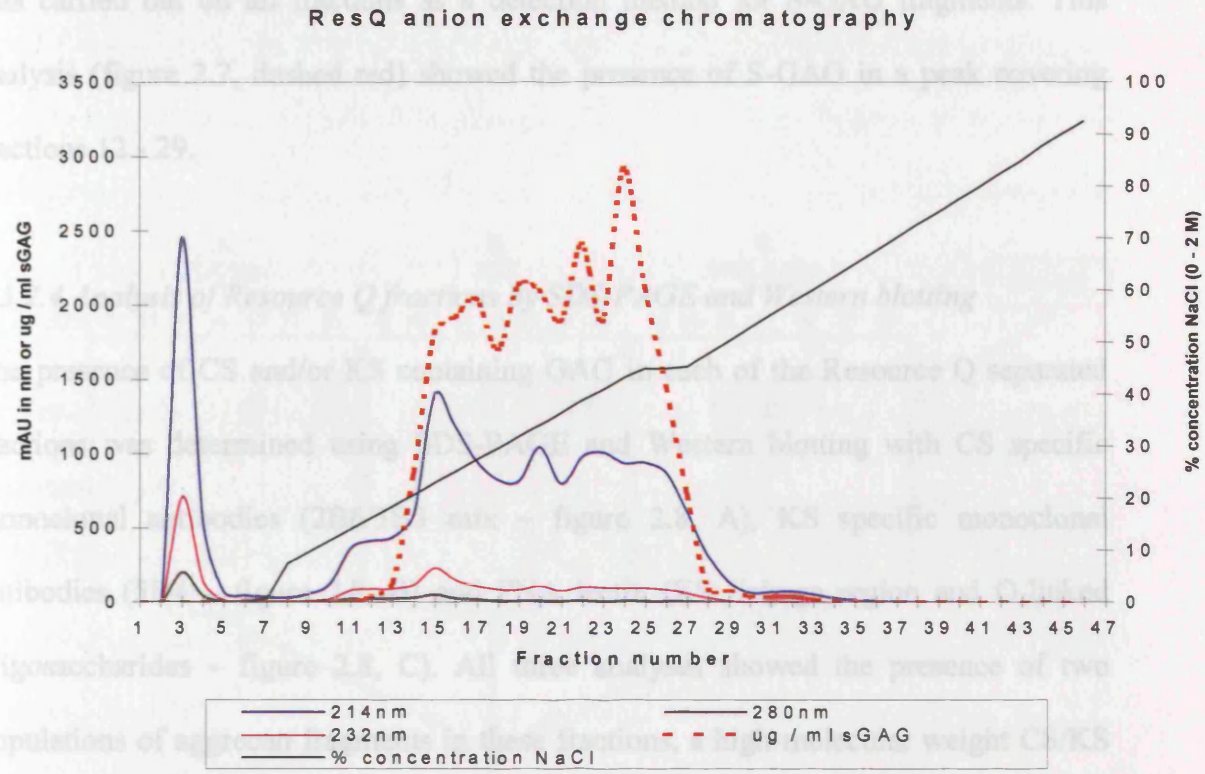

Figure 2.7 - Resource Q anion exchange chromatography profile (BNC-A1D1-trypsin), showing profiles detection using wavelengths of 280 nm (green ——), 232 nm (pink ——) and 214 nm (blue ——). DMMB analysis (red) of Resource Q fractions indicating quantities of sulphated GAG in each fraction. Sulphated GAG (red dashed line -----) was present in fractions 12 – 29.

carbohydrates [214 nm (blue) detects N-acetyl groups on GAG disaccharides] was high through fractions 10 – 30 representing a 0.2 – 1 M salt gradient. DMMB analysis was carried out on all fractions as a detection method for S-GAG fragments. This analysis (figure 2.7, dashed red) showed the presence of S-GAG in a peak covering fractions 12 - 29.

2.3.2.4 Analysis of Resource Q fractions by SDS-PAGE and Western blotting

The presence of CS and/or KS containing GAG in each of the Resource Q separated fractions was determined using SDS-PAGE and Western blotting with CS specific monoclonal antibodies (2B6/3B3 mix – figure 2.8, A), KS specific monoclonal antibodies (5D4 – figure 2.8, B) and PNA lectin (KS linkage region and O-linked oligosaccharides – figure 2.8, C). All three analyses showed the presence of two populations of aggrecan fragments in these fractions, a high molecular weight CS/KS containing population was identified in fractions 14-18 as well as 19 – 32 (data not shown). A low molecular weight population containing KS was identified in fractions 14-16.

2.3.2.5 Further purification of anion exchange purified KS- and KS/CS- peptide fragments using a Superose 6 size exclusion chromatography column

Fractions 14-16 from the Resource Q purification step, rich in low molecular weight 5D4 positive KS GAG-peptides and higher molecular weight 5D4 and 2B6/3B3 positive CS/KS GAG-peptides were pooled then dialysed against Milli Q™ water, lyophilised and reconstituted in size exclusion chromatography equilibration buffer (see table 2.3) and applied to a Superose 6 HR 10/30 size exclusion chromatography column equilibrated in 0.1 M sodium sulphate, pH 6.5–7.5. The sample was loaded (1.5 ml) and separated at a flow rate of 0.3 ml/min and 0.5 ml fractions were

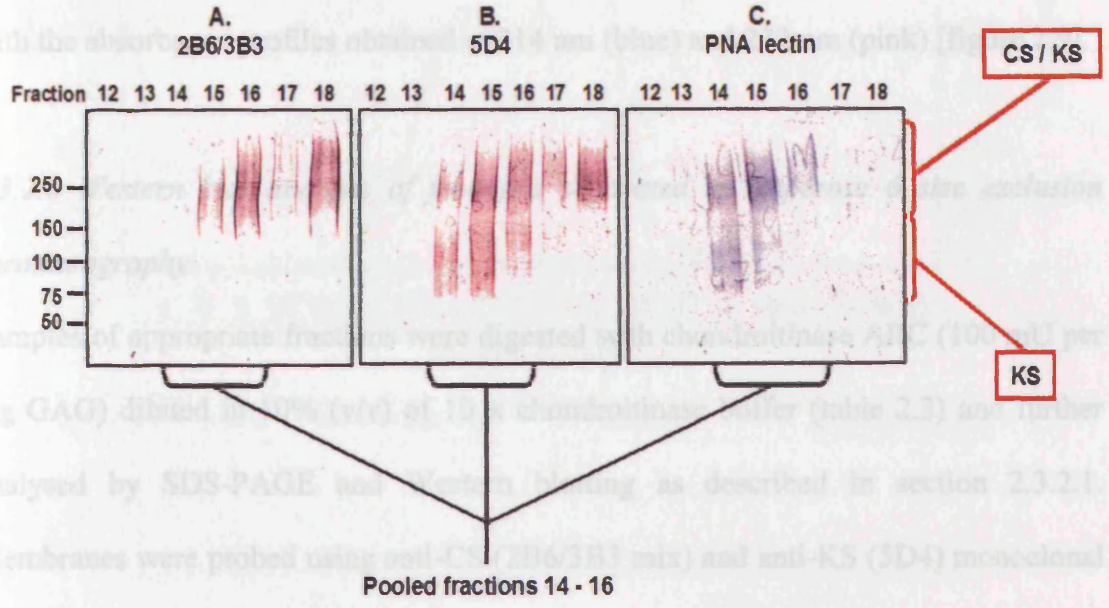

Figure 2.8 - SDS-PAGE and Western blot analysis of fractions after Resource Q anion exchange chromatography. Results revealed two subpopulations, one a high molecular weight CS/KS peptide fragment population and the other was a lower molecular weight KS peptide population present in fractions 14 - 16 as determined by 2B6/3B3 (A), 5D4 (B) and PNA lectin (C) analysis.

collected. Separation was monitored at wavelengths of 280 nm, 232 nm and 214 nm. UV absorbance at 214 nm (blue) showed two broad peaks in fractions 16-27 and 28-40 (figure 2.9). Peak fractions were dialysed against Milli Q™ water and analysed for GAG content using the DMMB assay (see section 2.3.1.1). DMMB analysis of all of the fractions revealed S-GAG to be present in fractions 15-40 (figure 2.9, red dashed line) falling into two broad peaks (fractions 15 - 27 and fractions 28 - 40), consistent with the absorbance profiles obtained at 214 nm (blue) and 232 nm (pink) [figure 2.9].

2.3.2.6 Western blot analysis of fractions separated by Superose 6 size exclusion chromatography

Samples of appropriate fractions were digested with chondroitinase ABC (100 mU per mg GAG) diluted in 10% (v/v) of 10 x chondroitinase buffer (table 2.3) and further analysed by SDS-PAGE and Western blotting as described in section 2.3.2.1. Membranes were probed using anti-CS (2B6/3B3 mix) and anti-KS (5D4) monoclonal antibodies. Western blot analysis of deglycosylated S-GAG positive fractions with KS specific mAb 5D4 (figure 2.10; A) and CS specific mAbs 2B6/3B3 (figure 2.10; B) indicated the presence of higher molecular weight CS/KS fragments in fractions 17-24, and lower molecular weight KS fragments in later fractions 25-29, (figure 2.10; A & B). Fractions 25-29 were subsequently pooled as a KS-peptide enriched fragment.

UNIVERSITY PRIFYSGOL CAERDYDD

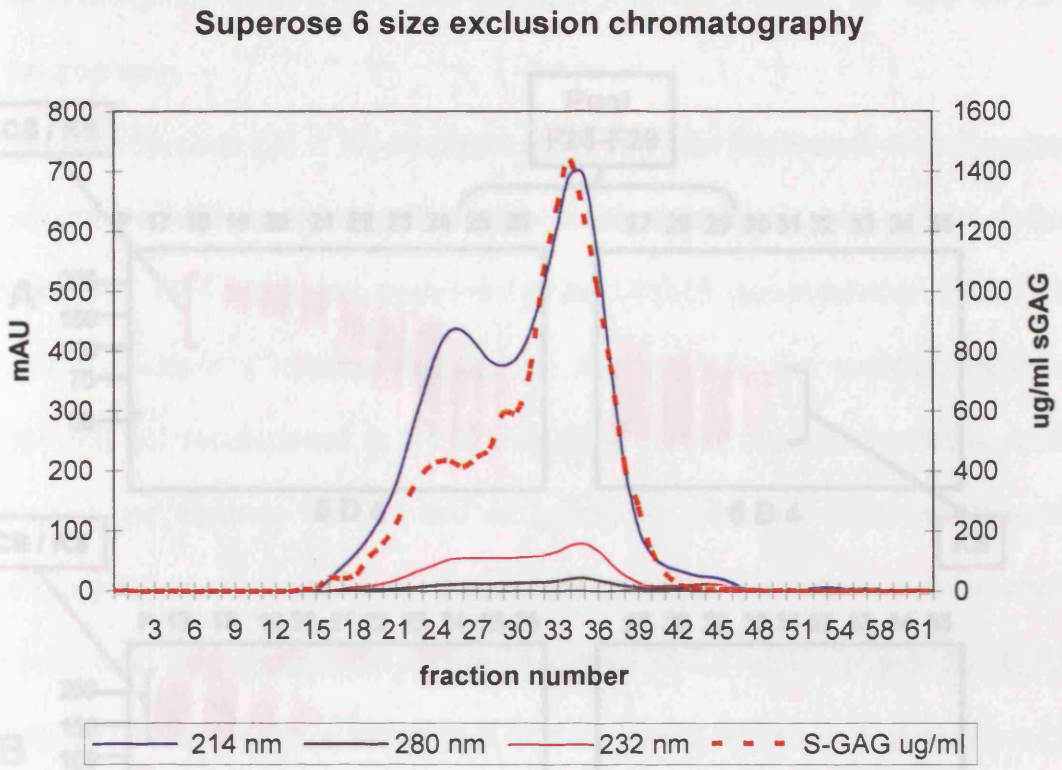

Figure 2.9 - Superose 6 size exclusion chromatography profile, with detection using 280 nm (green), 232 nm (pink) and 214 nm (blue). Two broad GAG (i.e. 214 nm absorbance) containing peaks (blue) separated in fractions 16-27 and 28-40. Sulphated GAG quantities are indicated by the red dashed profile and were determined by DMMB analysis. Fractions 15-40 contain the majority of sulphated GAG.

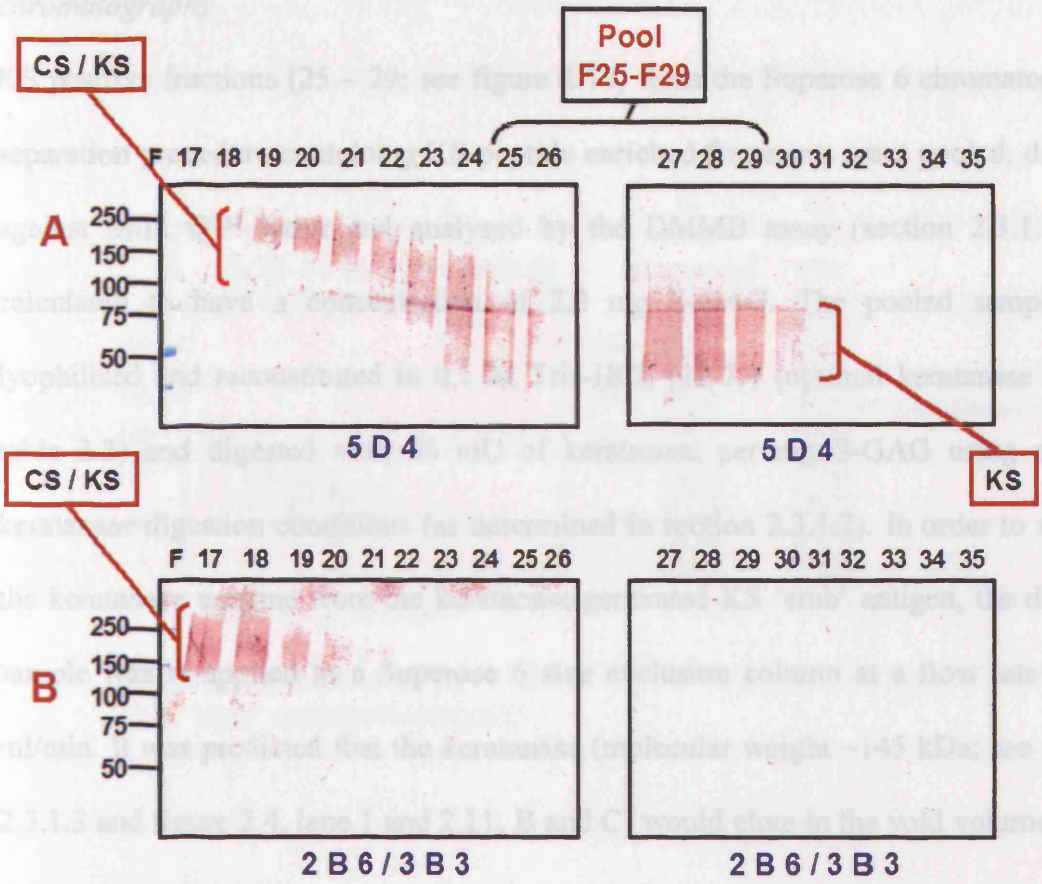

Figure 2.10 – Western blot analysis of fractions after Superose 6 size exclusion chromatography. Pooled fractions 14-16 from DEAE anion exchange chromatography containing KS- and KS/CS- peptide fragments were applied to a Superose 6 size exclusion chromatography column. Western blot analysis of the column eluate with mAbs 5D4 (panel A) and 2B6/3B3 mix (panel B) revealed that the CS/KS and KS populations had separated efficiently. Subsequently fractions 25-29 were pooled as a purified KS enriched peptide fragment preparation.

2.3.2.7 Digestion of purified KS-peptide fragments with keratanase and separation of contaminating keratanase from KS peptide fragment 'stubs' by size exclusion chromatography

KS positive fractions (25 – 29; see figure 2.10) from the Superose 6 chromatography separation procedure containing KS-peptide enriched fragments were pooled, dialysed against Milli Q™ water and analysed by the DMMB assay (section 2.3.1.1) and calculated to have a concentration of 2.2 mg S-GAG. The pooled sample was lyophilised and reconstituted in 0.1 M Tris-HCl, pH 7.4 (optimal keratanase buffer, table 2.3) and digested with 80 mU of keratanase per mg S-GAG using optimal keratanase digestion conditions (as determined in section 2.3.1.2). In order to remove the keratanase enzyme from the keratanase-generated KS 'stub' antigen, the digested sample was re-applied to a Superose 6 size exclusion column at a flow rate of 0.3 ml/min. It was predicted that the keratanase (molecular weight ~145 kDa; see section 2.3.1.3 and figure 2.4, lane 1 and 2.11, B and C) would elute in the void volume of the column. 0.5 ml fractions were collected and equal volumes (4 µl) were loaded onto 4 - 12% gradient gels in an appropriate sample buffer, electrophorised and transferred to nitrocellulose membrane (as described in section 2.3.2.1). Western blot analysis was carried out on all of the Superose 6 fractions using anti KS mAb 1B4 previously shown to recognise lower sulphated KS sulphation motifs still present after keratanase digestion (Mehmet *et al.*, 1986). Blots showed positive 1B4 staining for KS in fractions 22 - 28 (figure 2.11; A).

SDS-PAGE and silver stain analysis (see section 2.3.1.3) was also carried out on 4 µl volumes of all fractions collected after size exclusion chromatography to analyse separation of the keratanase enzyme from the KS 'stub' peptide fragment. This was to ensure that no antibodies would be generated to any contaminating keratanase enzyme. Silver stain analysis of the fraction revealed a ~145 kDa band in fraction

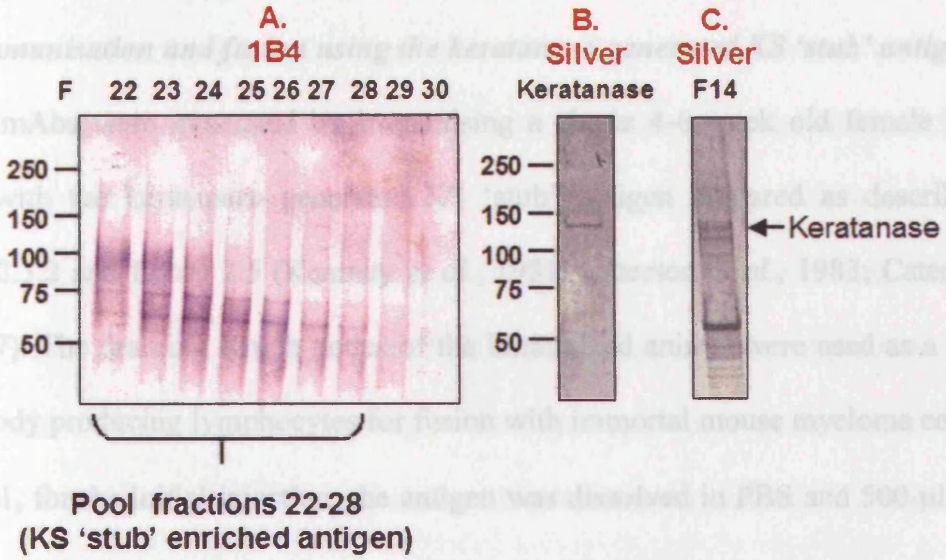

Figure 2.11 - Separation of lower molecular weight KS 'stub' peptides from higher molecular weight keratanase enzyme using size exclusion chromatography. Western blot analysis with mAb 1B4 revealed that KS 'stubs' eluted in fractions 22-28 (A). Silver stain analysis of fractions showed a band at ~145 kDa in fraction 14 (C). This was the same molecular weight as was previously observed for the keratanase enzyme control from the same keratanase batch (B).

14 (figure 2.11; C) that was similar in size to a silver stain of the enzyme alone (figure 2.4; lane 1 and figure 2.11, B). This data indicates that the keratanase enzyme had likely been separated in different fractions to the KS 'stub' peptide fragments (figure 2.11). Fractions 22 - 28 were pooled and selected as the immunising antigen.

2.3.3 Immunisation and fusion using the keratanase-generated KS 'stub' antigen

Murine mAbs were generated by immunising a single 4-6 week old female Balb/c mouse with the keratanase generated KS 'stub' antigen prepared as described in section 2.3.2 and figure 2.5 (Kearney *et al.*, 1981; Caterson *et al.*, 1983; Caterson *et al.*, 1987). The draining lymph nodes of the immunized animal were used as a source of antibody producing lymphocytes for fusion with immortal mouse myeloma cell line. On day 1, for the initial injection, the antigen was dissolved in PBS and 500 µl of the antigen solution was mixed with an equal volume of Freunds complete adjuvant. 10 - 50 µl was injected subcutaneously at 6 sites (2 at the hind footpads [10 - 20 µl each], 2 at lateral thoracic [50 µl each] and 2 at inguinal regions [50 µl each]). On day 3, the Ag was mixed with equal volumes Freunds incomplete adjuvant with similar volumes being injected at the same sites. The antigen was dissolved in saline for all subsequent immunisations with the same volumes at the same injection sites on days 6, 9 and 12.
On day 10 of the immunisation period an X 63 Ag 8.563 myeloma cell line, that does not express immunoglobulin heavy or light chains, was cultured in RPMI-C media in preparation for hybridoma fusion (Kearney *et al.*, 1979). Hybridoma fusion was carried out on day 14. The Ag 8 myeloma cells were harvested and washed twice with RPMI 1640 medium at 4 °C to remove FCS and other media components, resuspended in 20 ml RPMI-C and put on ice. The mouse was sacrificed by cervical dislocation and the draining lymph nodes nearest the sites of injection (axillary, brachial, inguinal and popliteal lymph nodes) were harvested under sterile conditions into ice cold (4 °C)

PBS, kept on ice and used as a source of activated lymphocytes for hybridoma production. The lymph nodes were teased apart to release the lymphocytes and passed through a 16 gauge needle, prior to filtering through a sterile glass wool pipette to separate the cells from connective tissues. To this cell suspension 14 ml of cold RPMI was gently added and the lymph cells and Ag 8 cells were spun at 1,500 rpm for 10 minutes at 4 °C. Media was aspirated off both cell pellets. The Ag 8s were resuspended in a known volume of cold RPMI and an appropriate volume representing a 2:1 Ag 8 to lymphocyte cell ratio was overlaid onto the lymphocyte pellet. This was spun at 4 °C for 10 minutes at 1,500 rpm. Media was aspirated from the tube and flicked to physically mix the two cell populations. 1 ml of poly ethylene glycol pre-warmed to 37 °C was added drop wise very slowly whilst shaking over a period of 1 minute. Following this, 10 ml of RPMI 1640 (room temperature) was added drop wise slowly whilst shaking the tube to slowly dilute out the PEG and promote cell fusion (Pontecorvo, 1975). A further 40 ml of warm RPMI 1640 was added slightly faster. This was then spun at 1,500 rpm for 10 minutes at 23 °C. Media was aspirated off and the cells resuspended in 200 ml of HAT supplemented RPMI-C culture media (see section 2.2.4). The media was also supplemented with macrophage feeder cells from a 3 ml peritoneal lavage of a Balb/c mouse. 1 ml per well of the fused cell media was applied to eight 24 well sterile Costar plates per fusion, and left at 37 °C for 2 weeks. Antibody producing hybridomas were generated from the fusion of mouse lymph node cells with the non Ig secreting Ag8 myeloma cell line (figure 2.12).

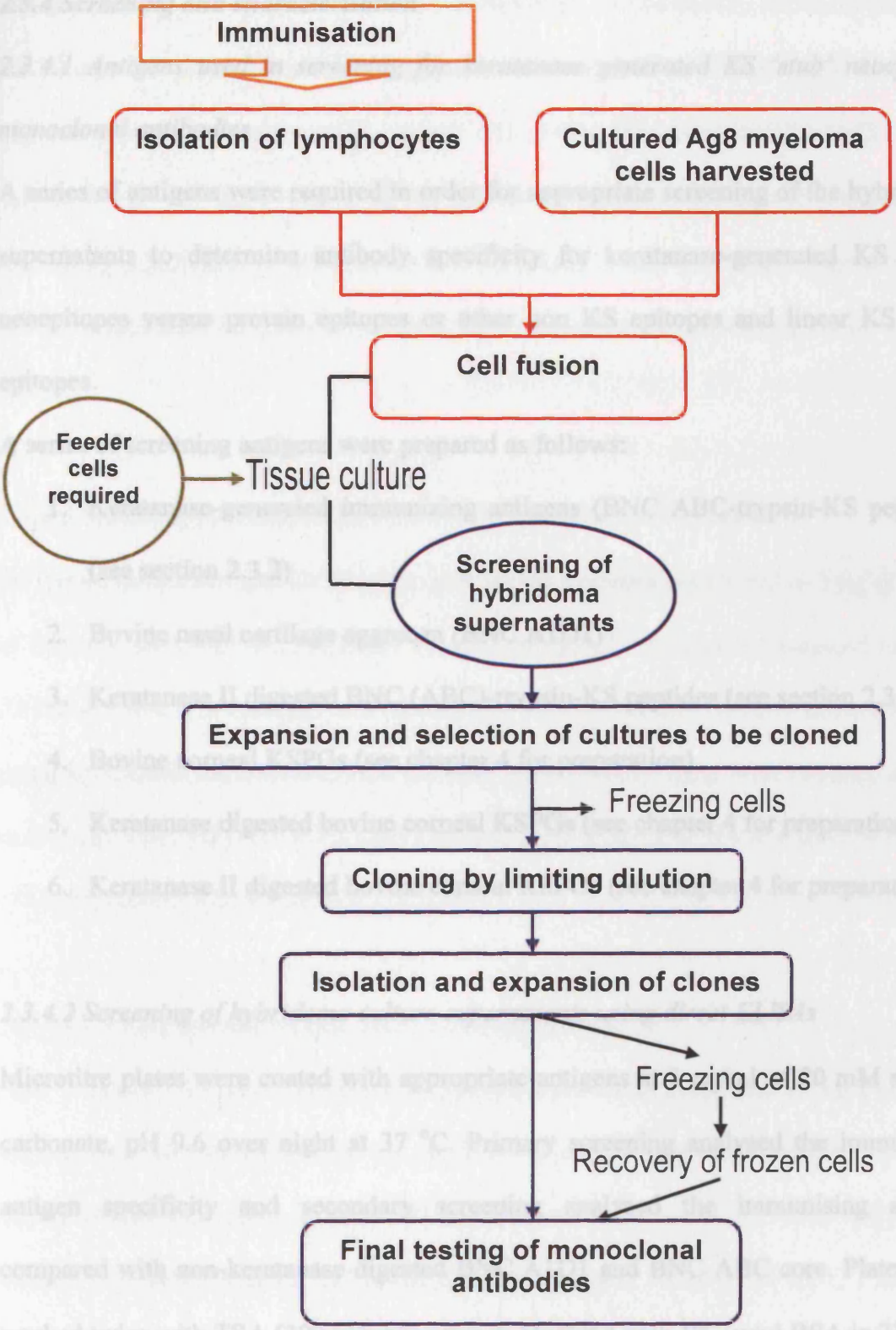

Figure 2.12 – General procedures for generating hybridomas which may permanently secrete monoclonal antibodies (adapted from: www.antibodyresources.com).

2.3.4 Screening and characterisation

2.3.4.1 Antigens used in screening for keratanase generated KS 'stub' neoepitope monoclonal antibodies

A series of antigens were required in order for appropriate screening of the hybridoma supernatants to determine antibody specificity for keratanase-generated KS 'stub' neoepitopes versus protein epitopes or other non KS epitopes and linear KS chain epitopes.

A series of screening antigens were prepared as follows:

1. Keratanase-generated immunizing antigens (BNC ABC-trypsin-KS peptides) (see section 2.3.2)
2. Bovine nasal cartilage aggrecan (BNC A1D1)
3. Keratanase II digested BNC (ABC)-trypsin-KS peptides (see section 2.3.2)
4. Bovine corneal KSPGs (see chapter 4 for preparation)
5. Keratanase digested bovine corneal KSPGs (see chapter 4 for preparation)
6. Keratanase II digested bovine corneal KSPGs (see chapter 4 for preparation)

2.3.4.2 Screening of hybridoma culture supernatants using direct ELISAs

Microtitre plates were coated with appropriate antigens at 5 μg/ml of 20 mM sodium carbonate, pH 9.6 over night at 37 °C. Primary screening analysed the immunising antigen specificity and secondary screening analysed the immunising antigen compared with non-keratanase digested BNC A1D1 and BNC ABC core. Plates were washed twice with TSA (300 μl/well) prior to blocking with 1% (w/v) BSA in TSA for a minimum of 1 hour at 37 °C. Plates were washed twice with TSA (300 μl/well) and 100 μl of culture supernatant from hybridoma wells was removed under laminar flow and added to appropriate microtitre plate wells and incubated for 2 hours at 37 °C. The plates were then washed three times with TSA prior to addition of an alkaline-

phosphatase (AP) conjugated secondary antibody (1:5000 dilution) incubated at 37 °C for 1 hour. The plates were washed again six times with TSA (300 µl/well). Finally an alkaline phosphatase substrate (1 mg/ml) was applied dissolved in DEA buffer (table 2.3) at 100 µl/well for 1 hour at 37 °C. The development of colour was observed and read using a Labsystems Multiscan MS plate reader at 405 nm. Positive development of colour indicated the presence of the sought monoclonal antibodies in the hybridoma media.

2.3.4.3 Screening for mAbs using SDS-PAGE and Western blot analysis

To further define the specificity of the new clones volumes equivalent to 5 µg of GAG, of the same antigens used in ELISA analysis (section 2.3.4.2), were separated on SDS-PAGE gradient gels and analysed by Western blotting (as described in section 2.3.2.1) using hybridoma supernatant from the new mAb clones, along with existing anti KS mAb (e.g. 5D4, 4D1, table 2.2) and lectin affinity blotting (PNA for skeletal KS and GNA for corneal KS, see section 2.3.2.3).

2.3.4.4 Cloning hybridoma cell lines to limiting dilution

New putative 'KS stub' antibody producing hybridoma cell lines of interest were expanded in 100 mm plates in 10 ml RPMI-C media (see section 2.2.4). A single confluent 100 mm plate of cells were re-suspended in 10 ml RPMI-C and further diluted 1:25000 by diluting 2µl of the cell suspension in 50 ml of RPMI-C 1 ml (tube 1). Tube 1 was further diluted 1:10 in RPMI-C in tube 2. 200 µl/well of each tube was plated into two sterile 96 well plates and left for 2 weeks at 37 °C. After 2 weeks hybridoma media from the wells of the 2 plates were screened by ELISA (as described above in section 2.3.4.2) using keratanase versus non-keratanase digested BNC (ABC) core (5 µg GAG / ml TSA) as coating antigens to re-screen for the keratanase 'stub'

mAbs. Positive subclones were culture expanded in several 100 mm plates and cells were preserved by re-suspending in a cryoprotective media [90% (v/v) fetal bovine serum, 10% (v/v) dimethyl sulphoxide (DMSO) see section 2.2.4] and frozen at –80 °C and in liquid nitrogen.

2.3.4.5 Identification of the Immunoglobulin class of the subclones

The immunoglobulin subclass of the monoclonal antibodies was determined using a clonotyping ELISA kit (Clonotyping system-AP; Southern Biotechnology Ass Inc.). A goat anti-mouse immunoglobulin capture antibody was coated at a concentration of 5 µg/ml in phosphate buffered saline (PBS) at 100 µl/well onto four 96 well microtitre plates and left overnight at 4 °C. After three washes with 300 µl TSA the plates were blocked with 200 µl/well 1% (w/v) BSA in TSA for a minimum of 1 hour at 37 °C. After a further three washes with TSA, 100 µl/well of the antibody hybridoma media was added and incubated for 1 hour at room temperature. Following four washes with TSA the plates were incubated with various alkaline phosphatase labelled secondary goat-anti mouse antibodies (IgM, IgA, IgG, IgG2a, IgG2b, IgG3) at a 1:500 dilution in 1% (w/v) BSA in TSA for 1 hour at room temperature. After a final six washes with TSA, 100 µl/well of AP substrate (table 2.3) was added and plates were read at 405 nm after 30 minutes and 60 minutes incubation at room temperature.

All new antibodies (BKS-1 and BKS-2) were identified as IgM, kappa light chain monoclonal antibodies.

2.3.4.6 Analysis of BKS-1 reactivity after removal of N-linked oligosaccharides from corneal and skeletal PG extracts

Eight volumes equivalent to 2 µg GAG of bovine corneal and cartilage PG extracts were digested with 80 mU of keratanase per mg GAG (see section 2.3.1.2) in 0.1 M

Tris acetate, pH 6.8 for 24 hours at 37 °C. After 24 hours, the samples were further digested with 6 mU of keratanase II per mg GAG and 8 mU endo-β-galactosidase per mg GAG of for 24 hours at 37 °C. Samples were further digested using enzymes from a protein deglycosylation kit obtained from Sigma-Aldrich according to the manufacturer's protocol. Briefly, the corneal and skeletal KS samples that had been pre-digested with keratanase followed by keratanase II and endo-β-galactosidase were lyophilised and reconstituted in 7.5 µl of Milli Q™ water. 2.5 µl of 5 x reaction buffer and 0.61 µl of denaturation solution (both supplied with the kit) were added and mixed gently. Samples were heated at 100 °C for 5 minutes. When cooled, 0.61 µl of TRITON X-100 solution (supplied with kit) was added and mixed gently. Each enzyme was diluted 10 x in 1 x reaction buffer and 1 µl of each added individually or sequentially in the following order following deglycosylation using the keratanase enzymes:

Experiment A:

1. PNGase F (from *cryseobacterium meningoseptium*),
2. O-glycosidase (from *streptococcous pneumonia*).

Experiment B:

1. β (1-4) - galactosidase (from *streptococcous pneumonia*),
2. β-N-acetyl glucosaminidase (from *streptococcus pneumonia*)
3. Neuraminidase / galactosiminidase / N-acetylglucosaminidase.

Samples were incubated overnight at 37 °C and run on 12% slab gels. Gels were transferred as described in section 2.3.2.1 and analysed by Western blotting using mAb BKS-1.

2.3.4.7 Analysis of BKS-1 reactivity with KSPGs isolated from different animal species

Tissues were obtained from bovine, porcine and human cornea and cartilage and from murine and avian cornea. These tissues were diced and extracted in 4 M guanidine HCl with protease inhibitors (table 2.3) as described in detail in chapter 4, section 4.3.1.1. Crude PG extracts were dialysed to Milli Q™ water and DMMB analysis carried out to ascertain GAG concentration of the samples. Volumes equivalent to 2 μg GAG were run undigested or digested with keratanase (80 mU/mg GAG, 24 hours at 37 °C) on 4 - 12% Tris glycine gradient gels prior to transfer onto nitrocellulose for BKS-1 analysis using Western blotting.

2.4 Results

2.4.1 Production and screening of novel keratanase-generated neoepitope mAbs, BKS-1 and BKS-2

2.4.1.1 ELISA analysis

Balb/c mice were immunised with the 'KS stub' peptide antigen and mAb hybridomas produced using procedures described in section 2.3.3. An initial screen of the 8 x 24 well plates by direct ELISA coating with the immunising antigen, revealed 4 potential hybridomas (well numbers 6A5, 1D4, 4B4, 5D3) selected on the bases of their higher optical density readings of 0.5 – 1.5 at 405 nm (data not shown). Positive wells were re-screened by direct ELISA using the 'KS stub' immunising peptide antigen, BNC (ABC) core and BNC A1D1 as coating antigens. This screen showed 2 of the positive clones (6A5 and 1D4; figure 2.13) to have little or no reactivity with BNC (ABC) core or with BNC A1D1 with optical density (OD) readings of < 0.5. However, strong reactivity was achieved using the immunising antigen KS 'stub' with an OD reading of > 3.0 (figure 2.13). In contrast, mAbs 5D3 and 4B4 showed positive reaction with the immunising antigen but also with BNC (ABC) core and BNC A1D1 suggesting that they may be antibodies to some other epitope common between all coating antigens, e.g. to a region of the protein core or an N- or O-linked oligosaccharide. Reactivity with 1B4 and 5D4 were used as positive and negative controls for binding of the coating antigens in these ELISAs (figure 2.13).

From these ELISA results 2 hybridoma cell lines, 6A5 and 1D4, were selected for further analysis and were designated BKS-1 and BKS-2, respectively. A third screening ELISA was carried out in which a keratanase generated 'KS stub' antigen was further digested with keratanase II. BKS-1 and BKS-2 immunoreactivity was shown to be greatly reduced with this coating antigen (results not shown). This indicated that the 2 antibodies were specifically recognising a keratanase-generated

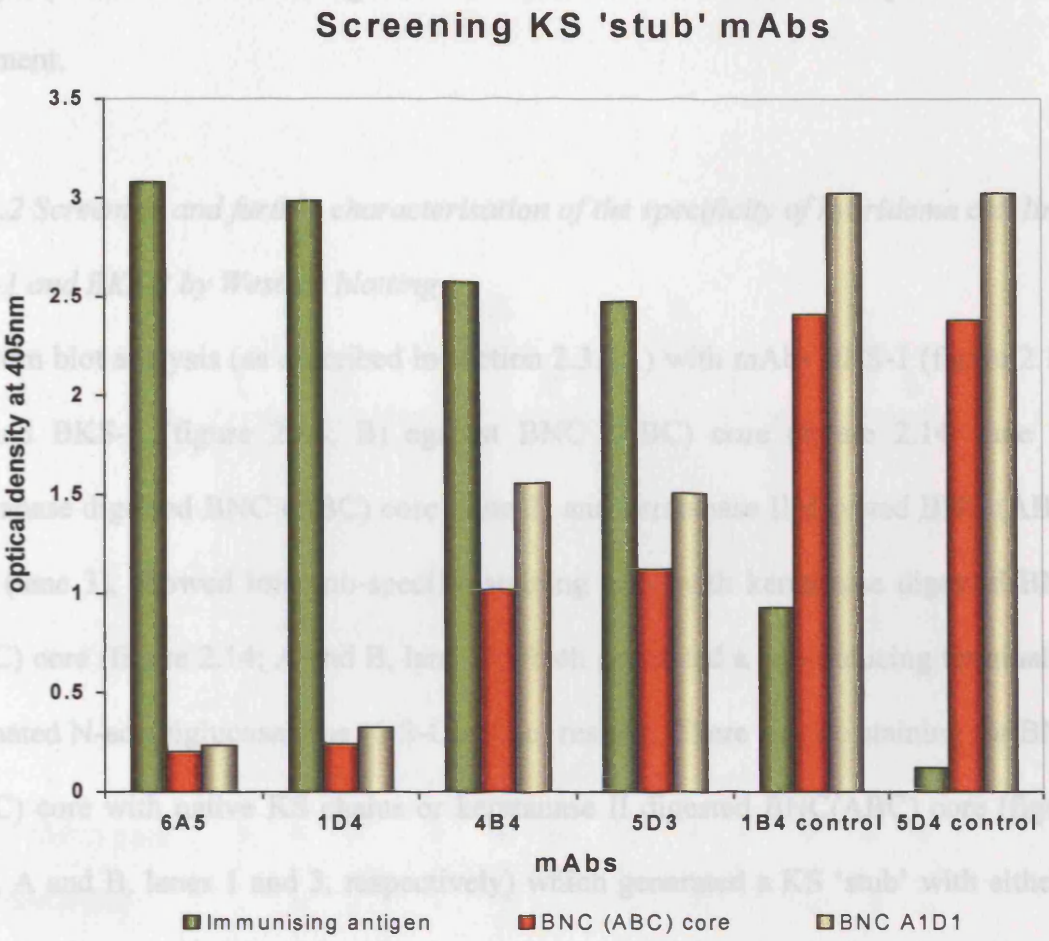

Figure 2.13 – Direct ELISA analysis of the positive hybridoma lines, i.e. 6A5, 1D4, 4B4 and 5D3 using the immunising antigen, BNC (ABC) core and bovine cartilage aggrecan (BNC A1D1) as coating antigens. Clones 6A5 and 1D4 were highly reactive with the keratanase digested immunising antigen and were not reactive with the undigested BNC (ABC) core or the BNC A1D1. Clones 4B4 and 5D3 were also positive with the immunising antigen; however, they also showed high reactivity with BNC ABC core and BNC A1D1. Anti-KS mAbs 1B4 and 5D4 were used as positive and negative controls for the coating antigens and showed reduced reactivity with the keratanase digested immunising antigen as expected.

neoepitope on the KS 'stub' region, which could be further removed by keratanase II treatment.

2.4.1.2 Screening and further characterisation of the specificity of hybridoma cell lines BKS-1 and BKS-2 by Western blotting

Western blot analysis (as described in section 2.3.2.1) with mAbs BKS-1 (figure 2.14; A) and BKS-2 (figure 2.14; B) against BNC (ABC) core (figure 2.14; lane 1), keratanase digested BNC (ABC) core (lane 2) and keratanase II digested BNC (ABC) core (lane 3), showed immuno-specific staining only with keratanase digested BNC (ABC) core (figure 2.14; A and B, lane 2) which generated a non-reducing terminal 6-sulphated N-acetylglucosamine (6-S-GlcNAc) residue. There was no staining for BNC (ABC) core with native KS chains or keratanase II digested BNC(ABC) core (figure 2.14; A and B, lanes 1 and 3, respectively) which generated a KS 'stub' with either a non-reducing terminal 6-sulphated galactose or an unsulphated galactose.

Controls for each of the antigens were run using anti–KS mAb 5D4 (figure 2.14; C) recognising linear sulphated poly-N-acetyl-lactosamine motifs (depicted in figure 2.16) and a PNA lectin (figure 2.14; D) recognising galactose-β-(1-3)-N-acetylgalactosamine on O-linked oligosaccharides (also depicted in figure 2.16). As expected 5D4 staining was strong before digestion of BNC (ABC) core with keratanase (figure 2.14; C; lane 1), was considerably reduced after keratanase and even more so after keratanase II digestion (figure 2.14; C; lanes 2 and 3). Conversely, staining for PNA lectin was limited before digestion of BNC (ABC) core (figure 2.14; D; lane 1) and was greatly increased after keratanase and keratanase II digestion (figure 2.14; D; lanes 2 and 3, respectively) as expected.

Further characterisation was carried out by Western blotting against a preparation of bovine corneal KSPGs with native KS chains (figure 2.15; A, B, C and D; lane 1),

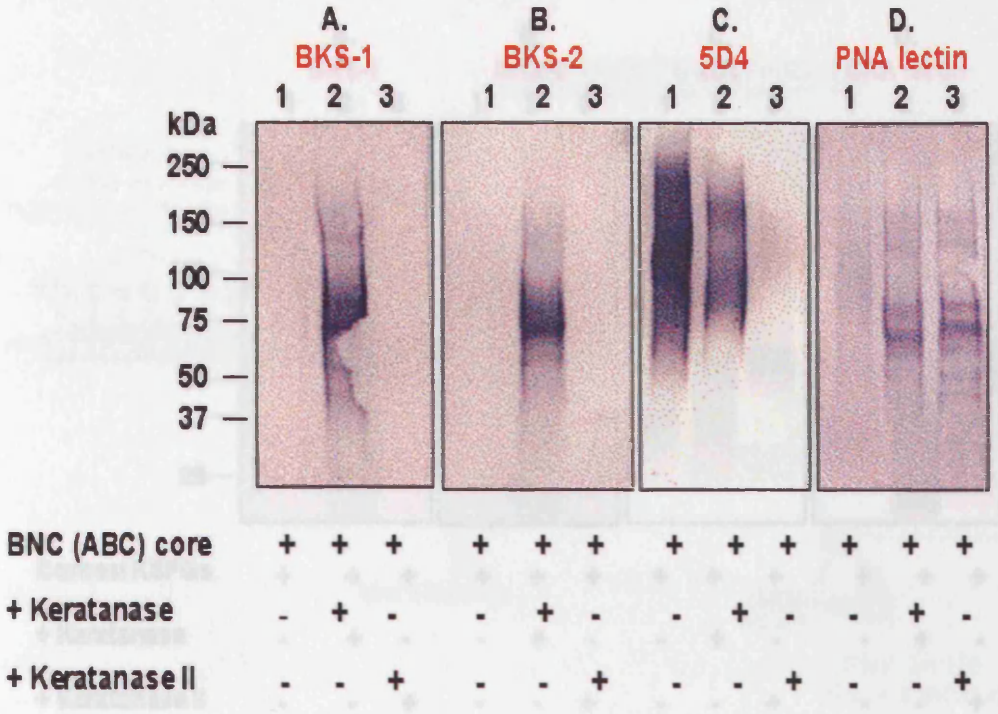

Figure 2.14 - Characterisation of mAbs against untreated BNC (ABC) core (lane 1), keratanase (lane 2) and keratanase II (lane 3) digested BNC (ABC) core. The new KS 'stub' mAbs ([**A**)]BKS-1 and [**B**] BKS-2) were specific only for keratanase digested BNC (ABC) core; [**C**] 5D4 control recognising the linear sulphated KS chain epitopes; [**D**] PNA lectin control recognising O-linked oligosaccharides similar to that remaining on KS after keratanase or keratanase II digestion.

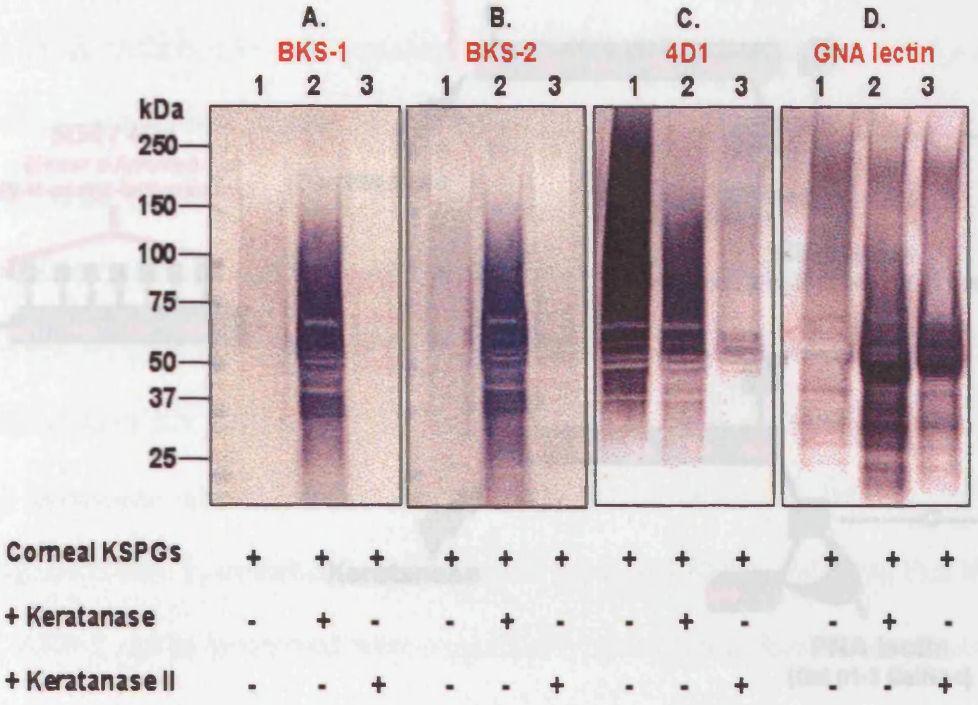

Figure 2.15 - Characterisation of mAbs against KS 'stubs' on corneal KSPGs. Corneal PGs (+/- keratanase or keratanase II) as screening antigens. The new KS 'stub' antibodies (**[A]** BKS-1 and **[B]** BKS-2) show specificity only for keratanase digested bovine corneal KSPGs (lane 2). **[C]** 4D1 control recognising linear sulphated KS chain epitopes showed reduced staining with digestion (lanes 2 & 3). **[D]** GNA lectin control to mannose of N-linked oligosaccharides similar to that remaining on KS after keratanase digestion. Lectin staining showed increased staining after both keratanase and keratanase II digestion of corneal KSPGs (D, lanes 2 & 3).

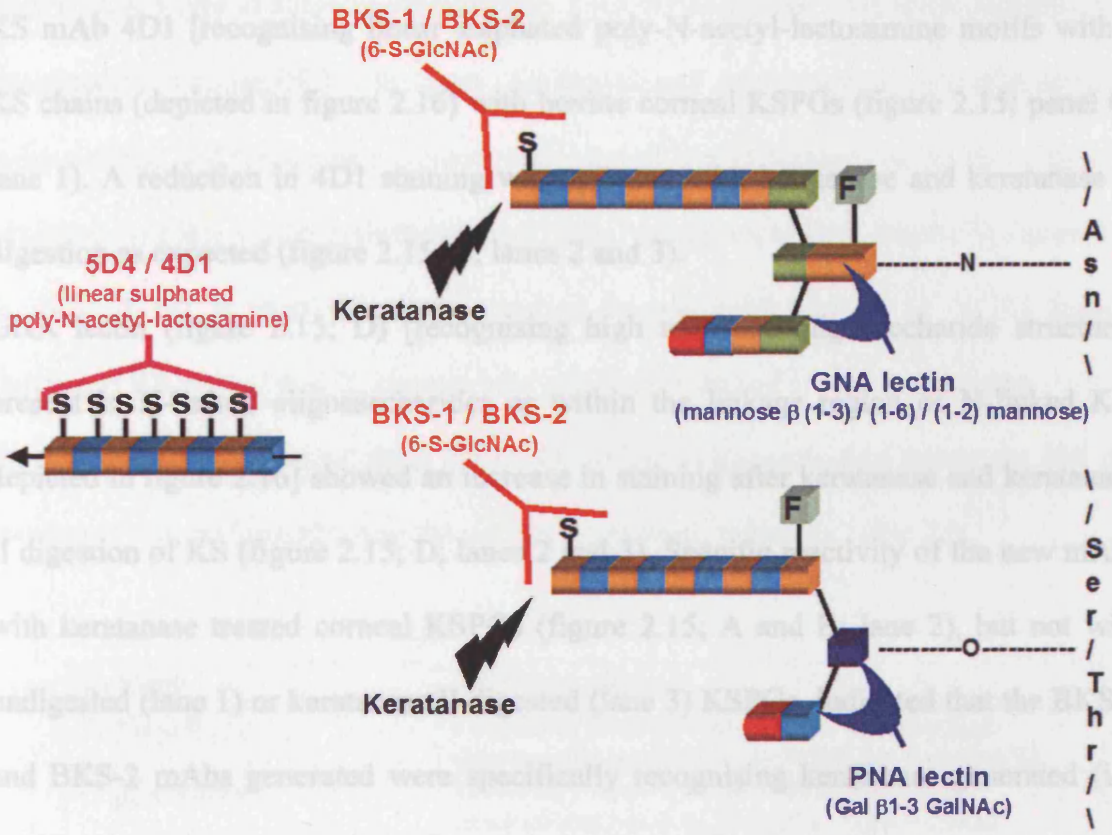

Figure 2.16 Predicted neoepitopes for KS 'stub' mAbs BKS-1 and BKS-2 at the non-reducing terminal 6-sulphated-N-acetylglucosamine residue (orange squares) of a keratanase digested KS chain (blue squares represent Gal residues; F represents fucose attachments and S represents sulphate groups). The diagram also shows the epitopes for the antibodies (5D4 & 4D1 in pink) and lectins (PNA & GNA in blue) used as controls for binding of coating antigens in direct ELISA screening analysis. 5D4 and 4D1 recognise linear sulphated poly-N-acetyl-lactosamine structures from within KS chains. PNA lectin recognises a Galβ1-3 GalNAc disaccharide from within the linkage region of KS type II or in O-linked oligosaccharides. GNA lectin recognises terminal mannose α(1-3), α(1-6) or α(1-2) linked to mannose, identifying high mannose N-linked oligosaccharides or KS type I linkage regions.

keratanase digested bovine corneal KSPGs (figure 2.15; A, B, C and D; lane 2) and keratanase II digested bovine corneal KSPGs (figure 2.15; A, B, C and D; lane 3) [generating the neoepitopes described above]. There was strong reactivity with anti-KS mAb 4D1 [recognising linear sulphated poly-N-acetyl-lactosamine motifs within KS chains (depicted in figure 2.16) with bovine corneal KSPGs (figure 2.15; panel C; lane 1). A reduction in 4D1 staining was apparent with keratanase and keratanase II digestion as expected (figure 2.15; C; lanes 2 and 3).

GNA lectin (figure 2.15; D) [recognising high mannose oligosaccharide structures present in N-linked oligosaccharides or within the linkage region of N-linked KS, depicted in figure 2.16] showed an increase in staining after keratanase and keratanase II digestion of KS (figure 2.15; D; lanes 2 and 3). Specific reactivity of the new mAbs with keratanase treated corneal KSPGs (figure 2.15; A and B; lane 2), but not with undigested (lane 1) or keratanase II digested (lane 3) KSPGs, indicated that the BKS-1 and BKS-2 mAbs generated were specifically recognising keratanase generated (i.e. not keratanase II generated) 'stub' structures in the KS chain. These analysis (figure 2.14, BNC (ABC) core and figure 2.15, corneal PGs) also indicate that the reactivity of the two new mAbs (BKS-1 and BKS-2) was not directed against a linkage region epitope, or amino acid sequence present on the core protein, as these differ between aggrecan and corneal KSPGs.

The results presented above strongly suggest that the new KS 'stub' mAbs, BKS-1 and BKS-2, were recognising the non-reducing terminal 6-sulphated-N- acetylglucosamine (6-S-GlcNAc) neoepitope that was generated as a direct result of keratanase cleavage of either KS type I or KS type II chains (depicted in figure 2.16).

2.4.1.3 Characterisation of BKS-1 epitopes

A series of digests were carried out to further establish the epitope of mAb BKS-1. Digests were carried out on PGs with KS type I substitutions isolated from cornea and PGs with KS type II substitutions isolated from cartilage that were both digested with keratanase to expose BKS-1 epitopes. Additional and subsequent digests with endo-β-galactosidase and keratanase II were also carried out to remove as much of the KS chains as possible whilst maintaining the BKS-1 neoepitopes (see chapter 3; figure 3.4; A, B, C & D). A short KS 'stub' attached through either the N- or O- KS linkage regions of KS types I and II, respectively remained attached to the protein core.

Further deglycosylation of these N- or O- linked oligosaccharide structures and KS structures was performed using the enzymes tabulated below in Table 2.6.

Enzyme	**Structure cleaved**
PNGase F	Completely removes Asp-N-linked complex high mannose oligosaccharides including asp-N-linked KS
O-glycosidase	Specifically cleaves serine or threonine linked unsubstituted Gal-β (1-3)-GalNAc from O-linked oligosaccharides, but not O-linked KS
α-2 (3,6,8,9) neuraminidase	Cleaves all non-reducing terminal Sialic acids
β (1-4) galactosidase	Specifically releases non-reducing terminal β(1-4) linked galactose residues
β-N-acetyl glucosaminidase	Cleaves non-reducing terminal β-linked N-acetylglucosamine residues

Table 2.6 – Deglycosylation enzymes and structures cleaved

This analysis was designed to demonstrate that BKS-1 specifically recognises the KS 'stub' structure generated as a result of keratanase digestion of KS GAGs which show no specificity for N- or O-linked oligosaccarides or to non-reducing terminal neuraminic acid, unsulphated galactose or N-acetylglucosamine. BKS-1 staining was present on both KS types I and II after digestion with keratanase followed by endo-β-galactosidase and keratanase II (figures 2.17; A and B, lane 1). This observation is discussed in more detail in chapter 3.

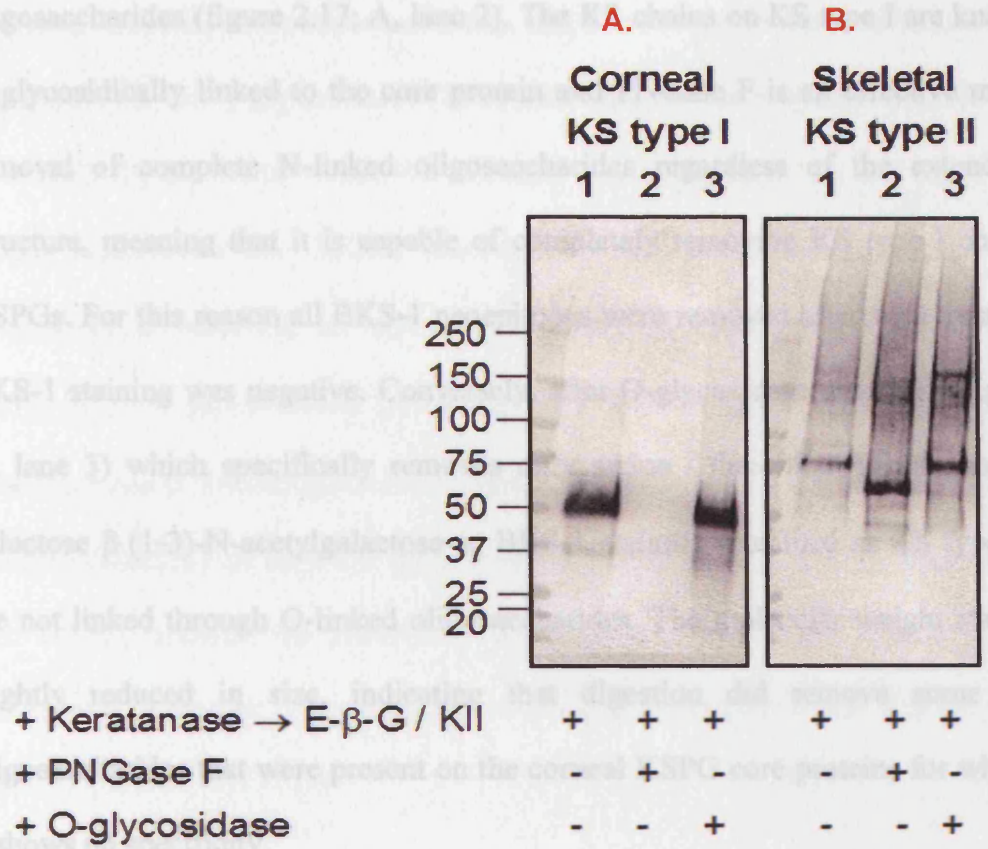

Figure 2.17 N- and O- glycosidase, digestion of KS types I (corneal KS - A) and II (skeletal KS - B) after keratanase followed by endo-β-galactosidase and keratanase II digestion (lane 1). PNGase F removed the BKS-1 KS 'stub' neoepitope on corneal KS type I which is linked through N-glycosidic linkages while staining remained on skeletal KS after removal of N-linked oligosaccharides (lane 2), indicating that BKS-1 was recognising a keratanase generated stub neoepitope and not an N-linked oligosaccharide. O-glycosidase removed O-linked oligosaccharides and demonstrated that BKS-1 was not recognising these structures (lane 3).

After PNGase F digestion of type I KS, BKS-1 positive immunostaining was abolished because there was cleavage of all asparagine N-linked complex mannose oligosaccharides (figure 2.17; A, lane 2). The KS chains on KS type I are known to be N-glycosidically linked to the core protein and PNGase F is an effective method for removal of complete N-linked oligosaccharides regardless of the extended chain structure, meaning that it is capable of completely removing KS type I chains from KSPGs. For this reason all BKS-1 neoepitopes were removed after such treatment and BKS-1 staining was negative. Conversely, after O-glycosidase treatment (figure 2.17; A, lane 3) which specifically removes only serine / threonine linked unsubstituted galactose β (1-3)-N-acetylgalactose-α, BKS-1 staining remained as KS type I chains are not linked through O-linked oligosaccharides. The molecular weight staining was slightly reduced in size, indicating that digestion did remove some O-linked oligosaccharides that were present on the corneal KSPG core proteins for which BKS-1 shows no specificity.

In bovine cartilage where skeletal KS type II KS is present the PG molecular weight was considerably reduced from 75 kDa to 60 kDa after PNGase F treatment (figure 2.17; B, lane 1 compared to lane 2) indicating their removal of N-linked oligosaccharides was accomplished. However, BKS-1 staining was not markedly affected by PNGase F treatment because KS type II is the major O-glycosidically linked KS GAG found on the core protein in cartilage aggrecan. The O-glycosidase used in this analysis requires that the O-linked oligosaccharide to be removed, have the exact structure of Galβ1---6GalNAc---O---S/T with no further substitutions (see table 2.6). However O-linked KS type II has got a complex extended structure and therefore cannot be removed using this enzyme. BKS-1 reactivity to the KS 'stub' neoepitope is still present after digestion using O-glycosidase (figure 2.17; B, lane 3) and removal of O-linked oligosaccharides. Even after the removal of the majority of the extended KS

portion of the chain using keratanase, endo-β-galactosidase and keratanase II treatment a range of structures still remain on the KS 'stub' (see chapter 3, section 3.3.2, figure 3.4) such as fucose and other attachments that would require removal before becoming a substrate for the O-glycosidase. The results reiterate the proposal that BKS-1 shows specificity for structures within the KS chain 'stub' (figure 2.16), and not to N- or O-linked oligosaccharides. BKS-1 staining was still present after α-2 (3, 6, 8, 9) neuraminidase [cleaving all non-reducing terminal branched or unbranched sialic acids], β (1-4) galactosidase [releasing only β (1-4) linked non-reducing terminal galactose] and β N-acetylglucosaminidase [cleaving all non-reducing terminal β-linked GlcNAc residues] on both KS types I and II (figure 2.18, lanes 1 – 4) demonstrating that BKS-1 showed no specificity for non-reducing terminal neuraminic acid, unsulphated galactose or unsulphated N-acetyl glucosamine which are all present on KS.

2.4.2 Western blot analysis examining species cross-reactivity of mAb BKS-1

BKS-1 immunoreactivity was analysed against cornea and cartilage proteoglycan extracts from a range of different animal species [bovine, human, chick, mouse and pig] (figure 2.19). BKS-1 showed a positive immunoreactivity with bovine, human and porcine cornea and cartilage, and weakly with avian and murine cornea after keratanase digestion.

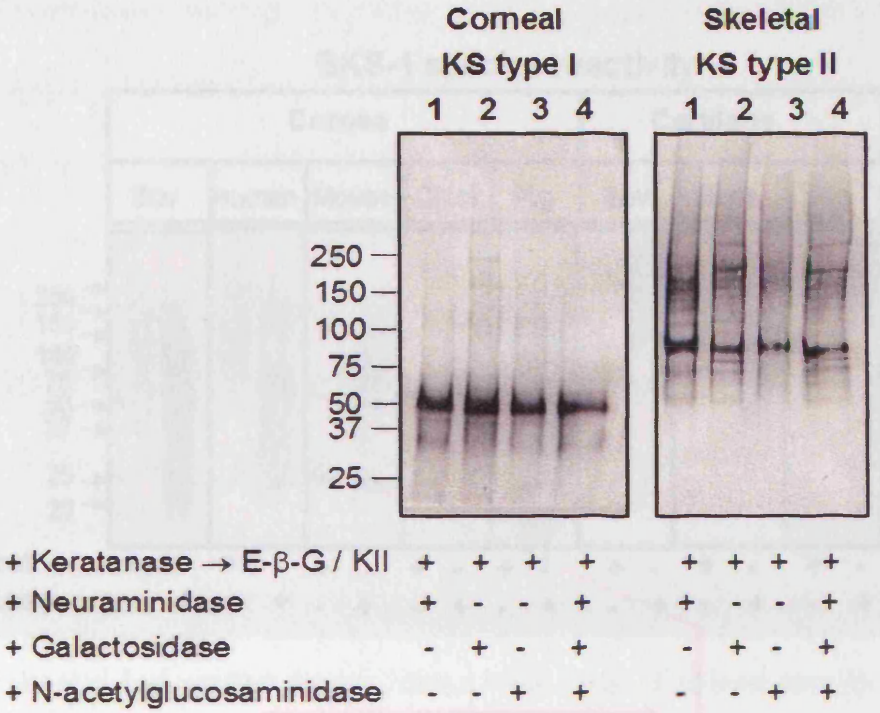

Figure 2.18 Neuraminidase, galactosidase and N-acetyl glucosaminidase digestion of KS types I (corneal) and II (skeletal) after keratanase followed by endo-β-galactosidase and keratanase II digestion. BKS-1 staining remained on both types I and II KS after treatment with each of these enzymes indicating that non-reducing terminal sailic acid, non-sulphated galactose or non-sulphated N-acetylglucosamine were not involved in the BKS-1 neoepitope.

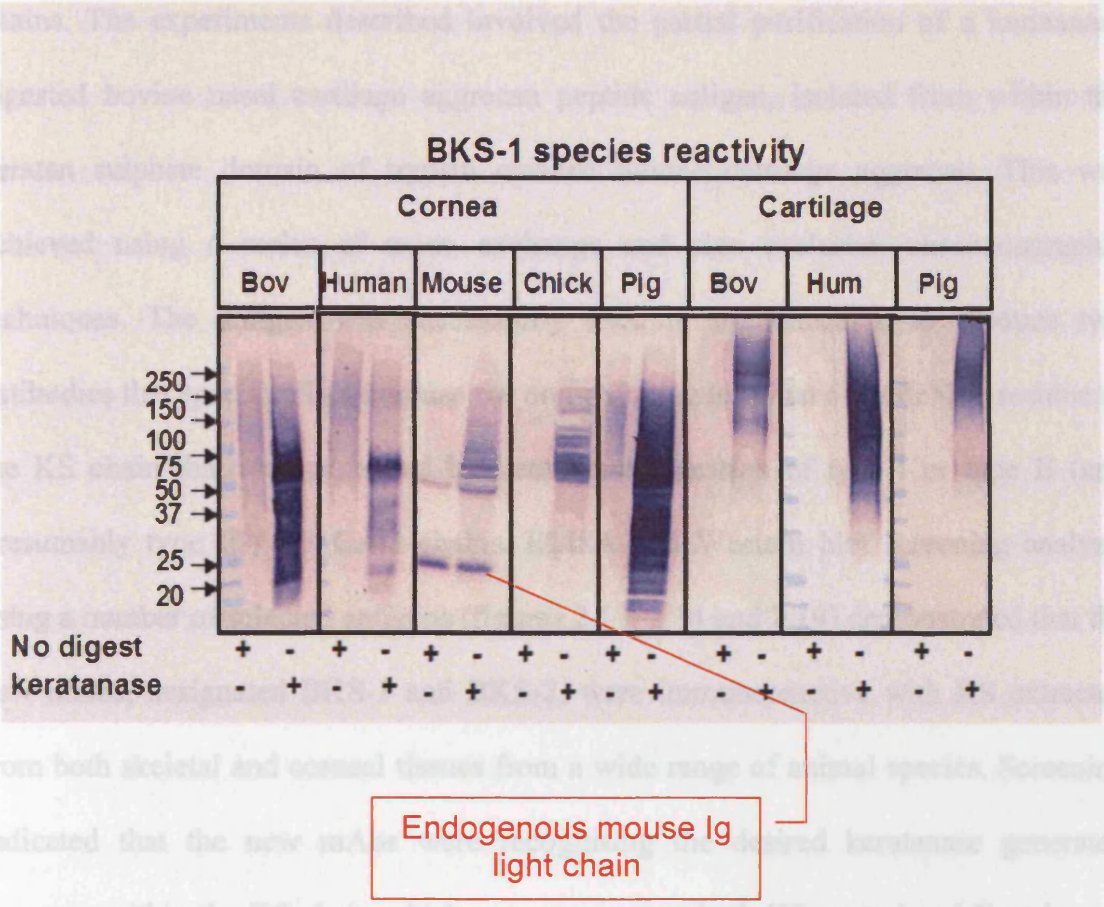

Figure 2.19 Animal species cross-reactivity of the KS 'stub' mAb BKS-1 before and after keratanase treatment.

2.5 Discussion

The aim of this chapter was to generate a novel monoclonal antibody probe which would recognise a keratanase-generated neoepitope at the non-reducing terminal of KS chains. The experiments described involved the partial purification of a keratanase digested bovine nasal cartilage aggrecan peptide antigen, isolated from within the keratan sulphate domain of trypsin cleaved bovine cartilage aggrecan. This was achieved using a series of anion exchange and size exclusion chromatographic techniques. The antigen was successfully used in immunisation to produce two antibodies that specifically recognise the non-reducing terminal 6-S-GlcNAc residue of the KS chain that was generated by keratanase digestion of type I or type II (and presumably type III) KS GAG chains. ELISA and Western blot screening analysis using a number of selected antigens (figures 2.13, 2.14 and 2.19) demonstrated that the new mAbs, designated BKS-1 and BKS-2, were immunoreactive with KS extracted from both skeletal and corneal tissues from a wide range of animal species. Screening indicated that the new mAbs were recognising the desired keratanase generated structure within the KS chain which was common to both KS types I and II and not a core protein or linkage region epitope as both of these latter structures differ between skeletal and corneal KS and KSPGs. These secondary screenings also demonstrated that the new Abs showed no specificity for the linear sulphated KS structure recognised by 5D4 and 4D1 as the tissue extracts required prior keratanase digestion to generate the antigen.

It was also shown that BKS-1 was not recognising N-linked oligosaccharides as digestion of corneal KSPGs (essentially all N-linked) with PNGase F abolished immunoreactivity with BKS-1. Similarly, PNGase F treatment of skeletal KSPGs did not remove BKS-1 reactivity as the majority of KS chains on cartilage aggrecan are attached to the core protein via an O-linked oligosaccharide. It was not possible to

demonstrate this using an O-glycosidase because this enzyme cannot remove O-linked KS type II from skeletal PG core proteins (table 2.6). In addition, further evidence for BKS-1 neoepitope to be a non-reducing terminal 6-S-GlcNAc residue was generated from a lack of reactivity for keratanase II digested KS types I or II.

It is known that keratanase hydrolyses the β (1-4) galactosidic linkage between galactose and N-acetylglucosamine where the linking galactose is unsulphated but the N-acetylglucosamine residue is sulphated at position 6 (Nakazawa *et al.*, 1975; Nakazawa & Suzuki, 1975) (see section 2.3.1) with a resulting 6-sulphated-N-acetylglucosamine remaining at the non-reducing terminal of the KS 'stub' on both skeletal and corneal KS after treatment. Based on the observations presented above it is proposed that BKS-1 specifically recognises the keratanase generated non-reducing terminal 6-S-GlcNAc residue that is generated after keratanase digestion of both KS types I and II (figure 2.16).

2.6 Chapter summary

- A keratanase digested bovine nasal cartilage aggrecan KS region peptide antigen was created and partially purified using anion exchange and size exclusion chromatography procedures.
- Two novel monoclonal antibodies were generated to the keratanase-generated 'KS stub' antigen and were called BKS-1 and BKS-2.
- The new antibodies were screened using ELISA and Western blotting techniques which demonstrated keratanase 'KS stub' specificity on both KS types I and II and presumably KS type III.
- BKS-1 was shown in Western blot analysis to cross react with keratanase-generated 'KS stub' neoepitopes in KS GAG for human, bovine, porcine, murine and avian cornea and cartilage tissues.
- The BKS-1 mAb specifically recognises a non-reducing terminal 6-sulphated N-acetyl glucosamine residue remaining on both KS types I and II after keratanase digestion. It shows no specificity for keratanase II digested KS.

Chapter 3 - Sulphation motif analysis of KS types I and II glycosaminoglycans.

3.1 Introduction

KS type I and KS type II are currently defined by their N- and O-linkages to a core protein, respectively rather than from their tissue source (e.g. corneal versus skeletal) because N- and O-linked KS post-translational modifications can occur either individually or collectively on a large number of matrix, cell surface and intracellular proteins (Funderburgh, 2000, review). The generally accepted structure for KS type I has been proposed to be composed of a pattern of non-sulphated N-acetyl-lactosamine disaccharides located next to the linkage region oligosaccharide, with mono-sulphated N-acetyl-lactosamine in the mid-regions of the KS GAG chain and disulphated N-acetyl-lactosamine disaccharides concentrated towards the non-reducing end of the KS GAG chain (Oeben *et al.,* 1987; Stuhlsatz *et al.,* 1989; see chapter 1 for review). The generic structure for KS type II has been reported to occur with a predominance of disulphated and occasional interdispersed monosulphate N-acetyl-lactosamine residues present throughout the KS glycosaminoglycan chain with some mono-sulphated N-acetyl-lactosamine residues present towards the non-reducing terminal of the KS glycosaminoglycan chain (Funderburgh, 2000 - see figure 1.3 chapter 1).

This chapter describes the use of the newly developed mAb, BKS-1 (see chapter 2), recognising keratanase generated KS 'stub' neoepitopes, in conjunction with other pre-existing anti-KS mAbs that recognise linear KS sulphation motifs (e.g. 5D4, Caterson *et al.*, 1983; Mehmet *et al.,* 1986), to examine KS disaccharide sulphation pattern motifs that occur on corneal (KS type I) and skeletal (KS type II) KSPGs after they have been subjected to sequential KS glycosaminoglycan degrading enzymes; i.e. keratanase, endo-β-galactosidase and keratanase II (see chapter 2, section 2.3.1 for further details).

3.2 Materials and Methods

3.2.1 Materials

All enzymes and related buffers were as described in chapter 2, sections 2.2 and table 2.3 and were used as detailed in section 2.3.1. All SDS-PAGE and Western blotting material were as described in section 2.2.5 and table 2.3 and methods as described in section 2.2.3.1. Bovine nasal cartilage aggrecan (ABC) core was obtained from stocks available in the lab (see chapter 2, section 2.3.1.1).

3.2.2 Analysis of deglycosylated KS chains using anti-KS mAbs (5D4, 4D1 and 1B4) and anti-KS 'stub' mAb BKS-1 recognising keratanase-generated KS 'stub' neoepitopes.

Partially purified bovine corneal KSPGs were used as a source of type I KS chains whilst bovine nasal cartilage aggrecan was used as a source of type II KS chains. Both preparations were either used undigested or subjected to a series of digests as follows:

1. No digestion
2. + keratanase
3. + keratanase II
4. + endo-β-galactosidase
5. sequential digest of keratanase → endo-β-galactosidase → keratanase II

Digests were carried out using optimal enzyme / substrate ratios as determined in chapter 2, section 2.3.1. Following digestion, samples were lyophilised and reconstituted in 1x SDS-sample buffer (table 2.3) prior to separation on 4-20% Tris glycine gradient gels. Gels were transferred to nitrocellulose membrane and subjected to Western blot analysis (see chapter 2, section 2.2.3.1) with a series of different KS

monoclonal antibodies recognising linear sulphation motif sequences within the KS chain, namely 5D4, 4D1, 1B4 [all at 1:100 dilution], (for epitopes see table 2.2) and with the new mAb BKS-1 recognising a keratanase-generated 'stub' neoepitope (hybridoma supernatant at a 1:100 dilution).

3.2.3 Sequential digestion of KS-rich PGs with specific KS degrading enzymes

Optimal KS enzyme digests (see chapter 2, section 2.3.1) were carried out with various sequences of enzymes for 24 hours each at 37 °C as follows:

Experiment 1:

A. No digest
B. + keratanase
C. + keratanase → endo-β-galactosidase
D. + keratanase → endo-β-galactosidase → keratanase II
E. + keratanase → keratanase II
F. + keratanase → keratanase II → endo-β-galactosidase

Experiment 2:

A. No digest
B. + endo-β-galactosidase
C. + endo-β-galactosidase → keratanase
D. + endo-β-galactosidase → keratanase → keratanase II
E. + endo-β-galactosidase → keratanase II
F. + endo-β-galactosidase → keratanase II → keratanase

Experiment 3:

A. No digest

B. + keratanase II

C. + keratanase II → keratanase

D. + keratanase II → keratanase → endo-β-galactosidase

E. + keratanase II → endo-β-galactosidase

F. + keratanase II → endo-β-galactosidase → keratanase

SDS-PAGE and Western blot analysis (as in chapter 2 section 2.3.2.1) was carried out on these digests with anti KS mAb 5D4 and anti KS 'stub' mAb BKS-1 to analyse the various KS chain structures remaining after such treatment.

3.3 Results

3.3.1 New sulphation pattern structures for KS - variations from the accepted generic structure proposed for KS

In order to determine the type of potential KS epitope structures that remain after different kinds of KS deglycosylation procedures, a series of digests were carried out as described in section 3.2.2 and were analysed on SDS-PAGE gels using Western blotting with KS specific mAbs. The results observed, showed positive immunoreactivity for all undigested KS type I chains (on corneal KSPGs) and KS type II chains (on nasal cartilage aggrecan) using existing mAbs 4D1, 1B4 (data not shown) and 5D4 (figure 3.1; A and B), which was consistent with previous observations (Caterson *et al.,* 1983; Mehmet *et al.*, 1986) that epitopes for these mAbs were all present on native KS GAG chains substituted on corneal KSPGs or nasal cartilage aggrecan.

Keratanase cleaves KS chains only between unsulphated Gal β1-4 GlcNAc-6S residues (Nakazawa *et al.*, 1975; Nakazawa & Suzuki, 1975) [illustrated in figure 3.2]. Because the action of this enzyme (and endo-β-galactosidase) is hampered by the presence of α (2 → 3) - linked fucose residues attached to the 6-S-GlcNAc of the disaccharide (Tai *et al.,* 1993), bovine nasal cartilage aggrecan was used as a source of KS type II B as it has been shown to be non-fucosylated whereas KS type II A from articular cartilage is fucosylated (Nieduszynski *et al.,* 1990 B).

Results of Western blot analysis of KS chains (digested with keratanase) that were substituted onto nasal cartilage aggrecan and corneal KSPGs showed for both samples a slight reduction in staining with all linear epitope anti-KS mAbs (5D4, 1B4 and 4D1 recognising linear sulphated poly-N-acetyl-lactosamine motifs) that were still present in the KS GAG chain. An example of this reduction in staining intensity is illustrated for mAb 5D4 in figure 3.1; A and B, lane 2. In addition, keratanase digestion

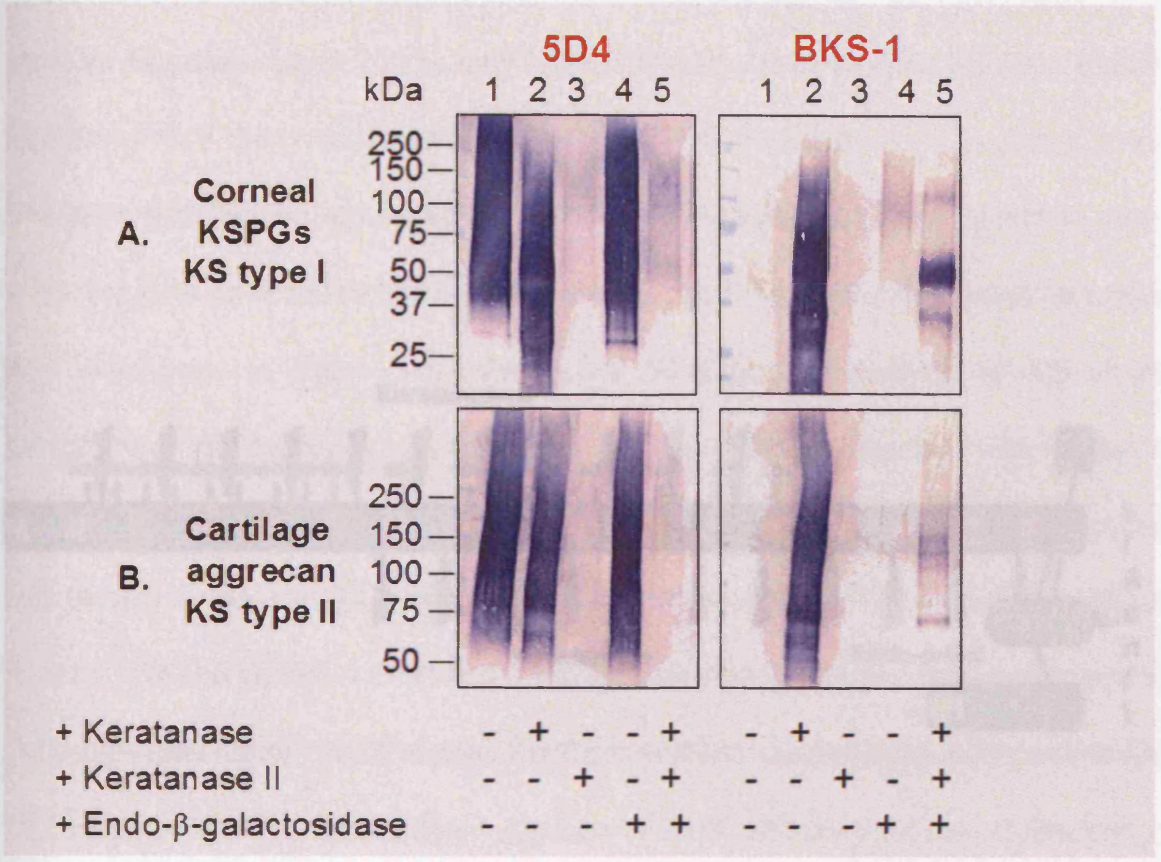

Figure 3.1 Antibody affinity blots resulting after no digest (lane 1), keratanase (lane 2), keratanase II (lane 3) or endo-β-galactosidase digests (lane 4), or a mixture of all 3 enzymes (lane 5) of bovine corneal KS type I (A) and bovine nasal cartilage KS type II (B) with detection using mAbs 5D4 and BKS-1.

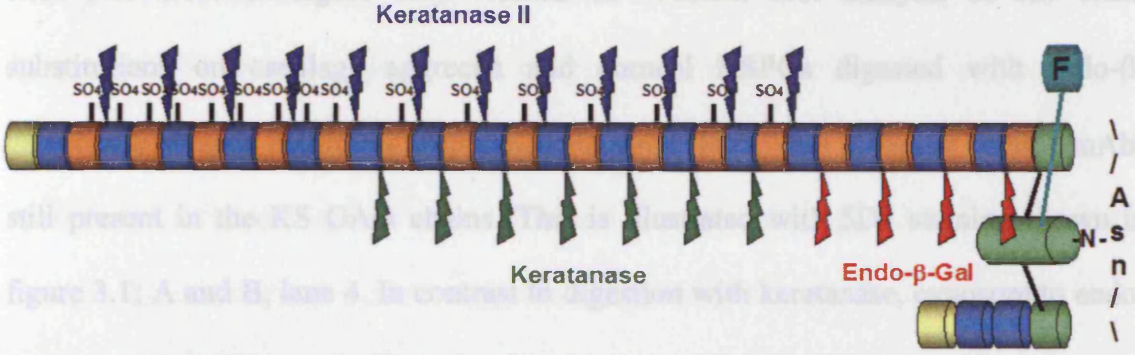

Figure 3.2 The generic structure of KS type I formed from repeating galactose (blue) and N-acetyl glucosamine (orange) showing sites of cleavage by keratanase, keratanase II or endo-β-galactosidase at di-, mono- and non-sulphated domains. The diagram shows a yellow symbol at the non-reducing terminal of the KS type I chain that may possess a range of monosaccharides (e.g. N-acetyl neuraminic acid, glycosyl neuraminic acid, galactose, N-acetyl galactose, N-acetyl glucose). The green symbols at the reducing end represent the linkage region mannose monosaccharides with fucose attachments (F).

of KSPGs isolated from cornea generated a shift in the migration of KS containing fragments form the 250 – 40 kDa range to a 100 – 20 kDa range. A similar shift in molecular weight products was not as markedly observed for KSPGs isolated from cartilage aggrecan, figure 3.1; B, lane 2, indicating that corneal KS contains a higher concentration of mono-sulphated disaccharides then skeletal KS.

Digestion with endo-β-galactosidase (Fukuda & Matsumura, 1976) cleaves at non-sulphated β1-4 galactosidic linkages, with weak reactivity at the keratanase cleavage sites (illustrated in figure 3.2). Results of Western blot analysis of KS chain substitutions on cartilage aggrecan and corneal KSPGs digested with endo-β-galactosidase again result in a slight reduction in staining with all linear epitope mAbs still present in the KS GAG chains. This is illustrated with 5D4 staining shown in figure 3.1; A and B, lane 4. In contrast to digestion with keratanase, exposure to endo-β-galactosidase did not significantly alter the molecular weight of products positive for 5D4 epitopes in either the cartilage aggrecan or the KSPG preparations. Collectively, this data indicates that only a small proportion of structural epitope for 5D4, namely linear pentasulphated hexasaccharide motifs (Mehmet *et al.*, 1986), are lost after digestion with either keratanase or endo-β-galactosidase resulting in decreased staining for each of the antibodies.

Keratanase II digestion, results in cleavage at β 1-3 glucosaminidic linkages in which the disaccharide structure may be either mono- or di- sulphated (Oguma *et al.*, 2001; Yamagishi *et al.*, 2003) [illustrated in figure 3.2]. Digestion of KS attached to cartilage or corneal KSPGs resulted in essentially a complete loss of staining for 5D4 in both corneal and skeletal KS (figure 3.1; A and B; lane 3), because keratanase II removes all linear mono- and di- sulphated poly-N-acetyl lactosamine epitopes required for 5D4 recognition. All 5D4 staining was lost as expected in both cartilage and corneal KSPGs

after sequential digestion of the extracts with keratanase followed by endo-β-galactosidase and keratanase II.

Conversely, after keratanase digestion of corneal and skeletal KS from corneal KSPGs and cartilage aggrecan, respectively, BKS-1 staining was positive as expected (figure 3.1; BKS-1; A and B, lane 2). However, after endo-β-galactosidase treatment, there was weak immunoreactivity (figure 3.1; BKS-1; A and B; lane 4), this staining was more pronounced in the corneal KSPG preparation. This weak BKS-1 reactivity may be explained by the ability of endo-β-galactosidase to less preferentially cleave at β (1-4) galactosidic linkages where the disaccharide structure is mono-sulphated (the keratanase cleavage site) at a much lower reaction rate to keratanase. In contrast, immunoreactivity was absent after keratanase II treatment (figure 3.1; BKS-1; A and B; lane 3). Interestingly, after sequential digestion with all three enzymes, in the sequence of an initial keratanase digestion followed by endo-β-galactosidase and then followed by keratanase II, immunostaining for BKS-1 was present as three distinct KSPG populations in both corneal KSPGs and skeletal aggrecan (figure 3.1; BKS-1; A and B; lane 5).

This data suggests that the proposed generic structure for KS chains (Oeben *et al.*, 1987; Stuhlsatz *et al.*, 1989) depicted in figure 3.2, is perhaps not fully validated. These researchers proposed a generic structure that constitutes a KS chain in which disulphated disaccharides occur towards the non-reducing end of the chain, with monosulphated disaccharides occurring towards the middle and non-sulphated disaccharides predominant towards the linkage region of the chain. Such a structure would suggest that keratanase digestion should result in a complete loss of 5D4 epitope and that the sequential digest (keratanase, endo-β-galactosidase then keratanase II) should result in a complete loss of BKS-1 epitope. However, the results presented above indicate that this was not the case and suggest that this structure

cannot be totally correct for all KS substitutions on corneal KSPGs or cartilage aggrecan. In fact these results indicate that there must be a number of variations of KS chain sulphation patterns present on proteoglycan molecules isolated from cornea and cartilage.

Figure 3.3 illustrates a range of new proposed KS chain structures, which have been deduced from Western blot analysis of digests involving deglycosylation of KS chains on corneal KSPGs and nasal cartilage aggrecan and Western blot analysis with new (BKS-1) and existing (5D4) KS mAbs. The proposed structures for KS chains include GAG chain variations where non- mono- or di- sulphated domain structures can occur attached directly adjacent to the core protein linkage region or can be located at various positions throughout the KS chain. Figure 3.3 also depicts the predicted range of KS 'stubs' remaining on each of the KS chain variations after digestion using different KS degrading enzymes.

3.3.2 Use of mAbs BKS-1 and 5D4 to verify proposed KS type I and KS type II structures

The analysis so far provided in this chapter indicates that both KS types I and II have complex patterns of sulphation motifs. We suggest that four basic types occur (figure 3.3; A). Analysis using BKS-1 and 5D4 support this conclusion and the rational for this is provided below.

Figure 3.4 A schematically illustrates the four predicted intact KS chain structures where different patterns of di-sulphated, mono-sulphated and non-sulphated KS chain disaccharide motifs occur before digestion with different glycosidases (figure 3.4 A; where red symbols represent 5D4 linear sulphated epitopes) and after digestion using keratanase, keratanase II and endo-β-galactosidase (figure 3.4 B, C and D; where green symbols represent predicted keratanase-generated BKS-1 neoepitopes with 6

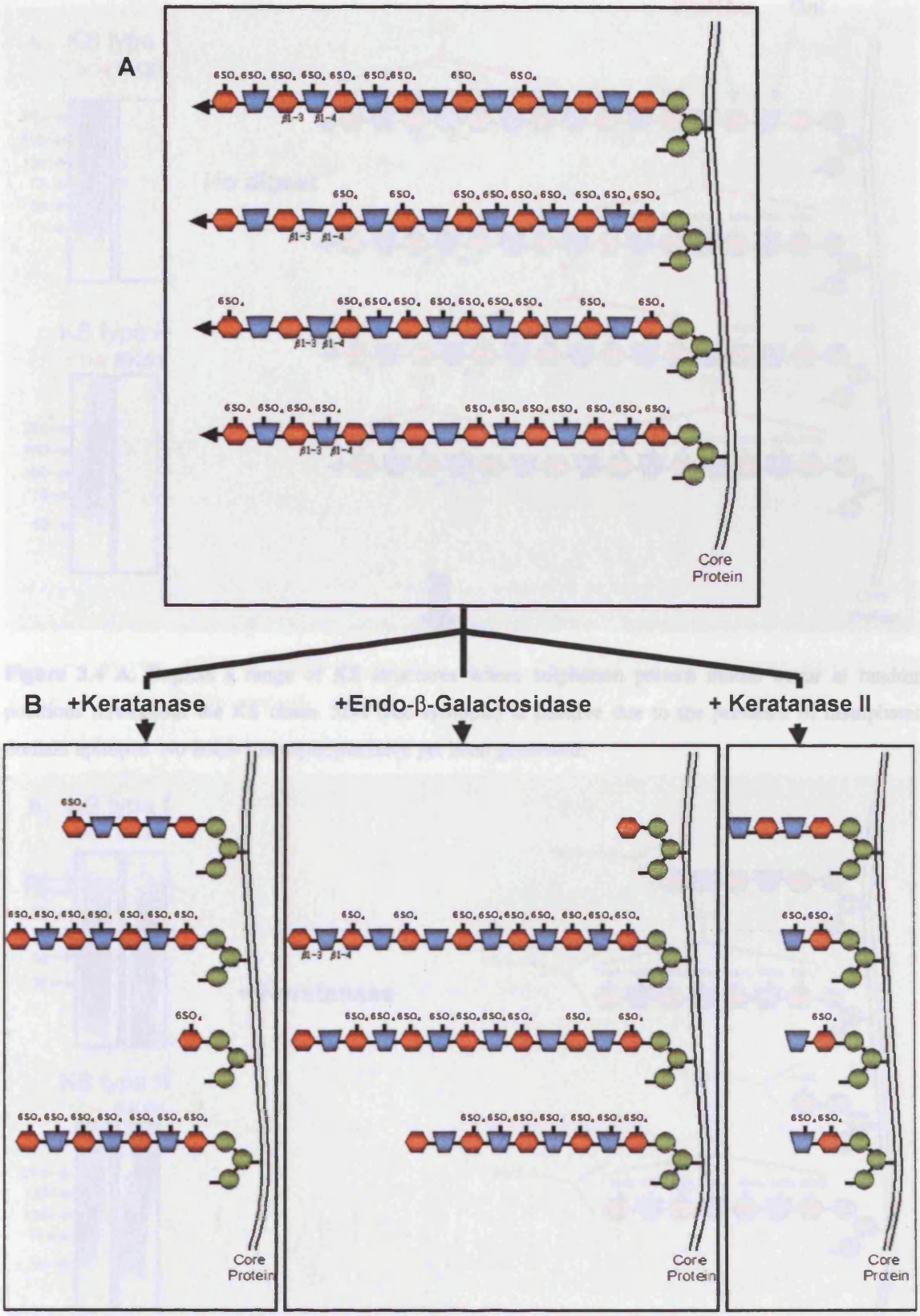

Figure 3.3 A. Predicted KS sulphation pattern variations which are in contrast to the generic structure proposed for KS (orange = GlcNAc, blue = Gal, green = linkage region). **B.** Cleavage by keratanase, keratanase II and endo-β- gal showing 'KS stubs' and linear sulphated 5D4 epitope remaining after digests of corneal or skeletal KS.

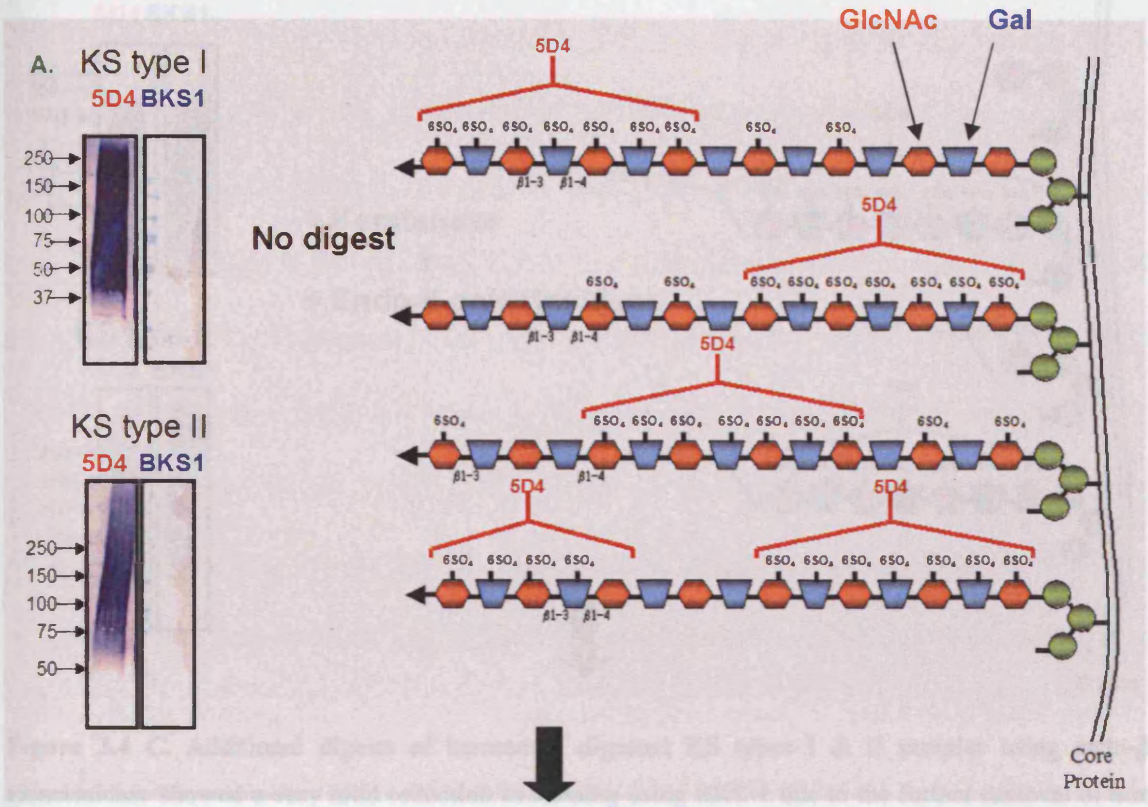

Figure 3.4 A. Depicts a range of KS structures where sulphation pattern motifs occur at random positions throughout the KS chain. 5D4 (red symbols) is positive due to the presence of disulphated domain epitopes. No BKS-1 neoepitopes have yet been generated.

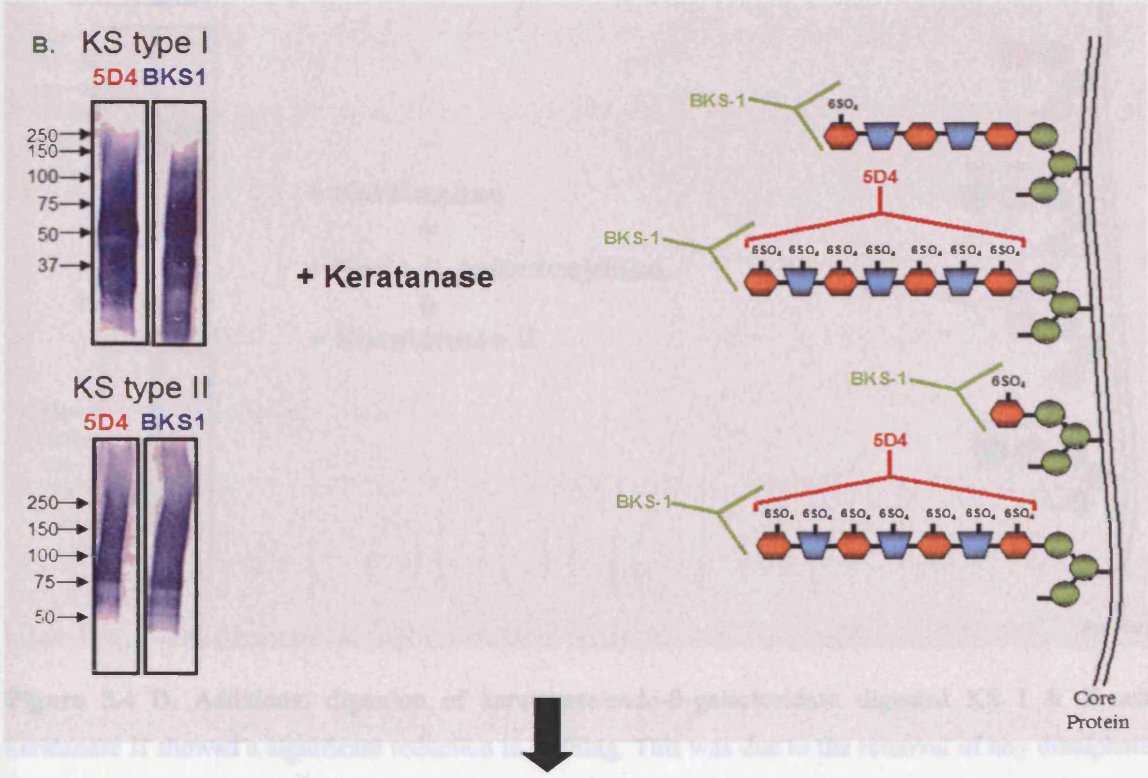

Figure 3.4 B Digestion with keratanase exposes a number of BKS-1 epitopes reflected by an increase in staining with BKS-1 compared to undigested KS (panel A). 5D4 staining was only slightly reduced indicating that there are disulphated domains remaining that cannot be removed by keratanase alone.

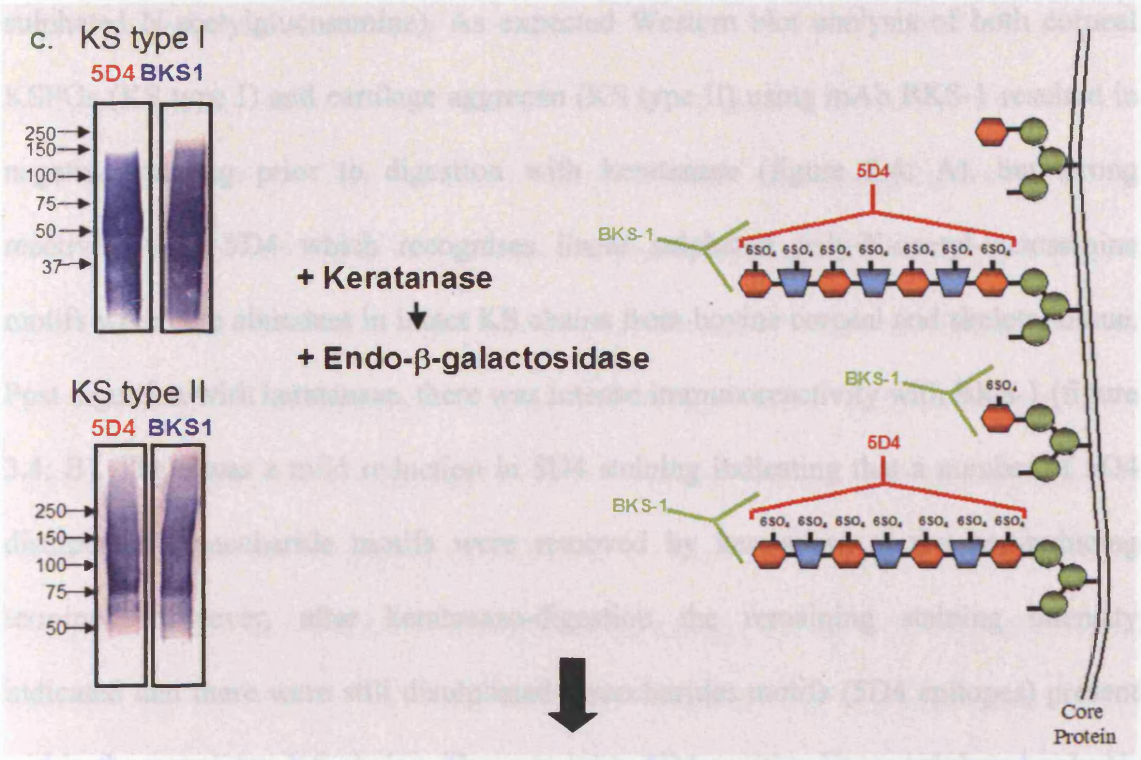

Figure 3.4 C. Additional digests of keratanase digested KS types I & II samples using endo-β-galactosidase showed a very mild reduction in staining using BKS-1 due to the further removal of non-sulphated domain structures which possessed a BKS-1 epitope at the non-reducing terminal. 5D4 staining was only slightly reduced.

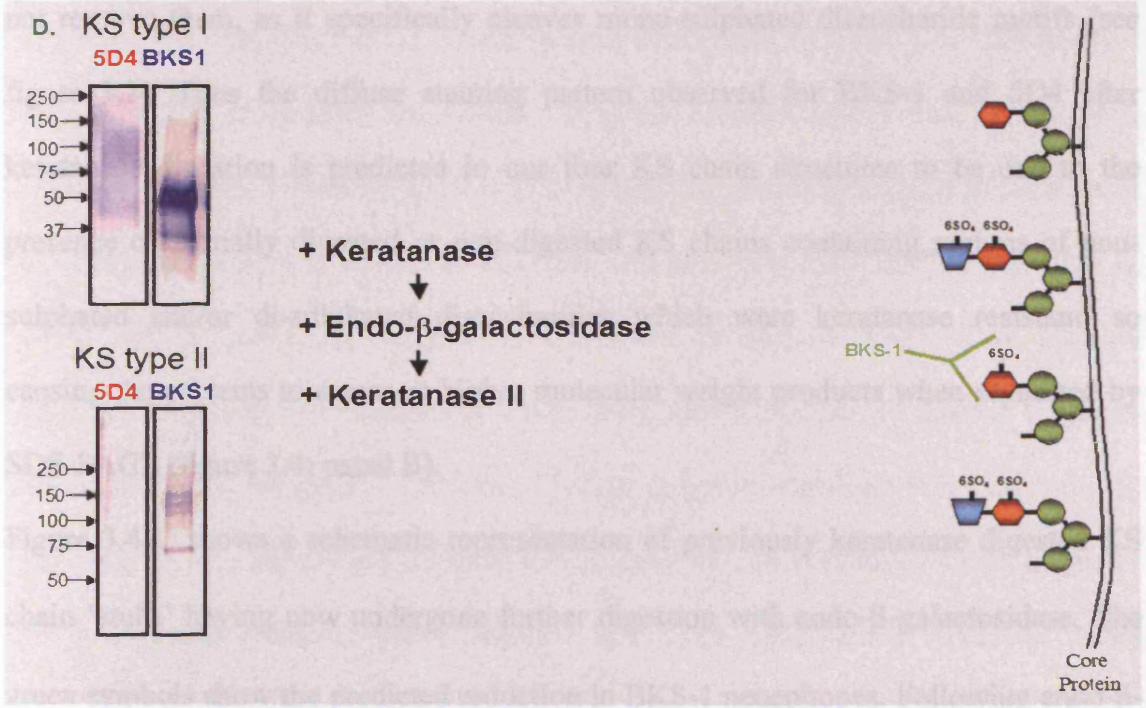

Figure 3.4 D. Additional digestion of keratanase/endo-β-galactosidase digested KS I & II with keratanase II showed a significant reduction in staining. This was due to the removal of any disulphated domain structures which are also 5D4 epitopes. Any remaining immunostaining was due to BKS-1 neoepitopes which could not be further cleaved by any of these three enzymes and indicated that 6-S-GlcNAc residues remained attached directly to the linkage region.

sulphated N-acetylglucosamine). As expected Western blot analysis of both corneal KSPGs (KS type I) and cartilage aggrecan (KS type II) using mAb BKS-1 resulted in negative staining prior to digestion with keratanase (figure 3.4; A), but strong reactivity with 5D4 which recognises linear sulphated poly-N-acetyl-lactosamine motifs which are abundant in intact KS chains from bovine corneal and skeletal tissue. Post digestion with keratanase, there was intense immunoreactivity with BKS-1 (figure 3.4; B). There was a mild reduction in 5D4 staining indicating that a number of 5D4 disulphated disaccharide motifs were removed by keratanase at the non-reducing terminal. However, after keratanase-digestion the remaining staining intensity indicated that there were still disulphated disaccharides motifs (5D4 epitopes) present within the remaining KS chains. The remaining 5D4 positive linear sulphated poly-N-acetyl lactosamine epitopes must either be attached directly to the linkage region or be attached through keratanase resistant non-sulphated domains where keratanase could not remove them, as it specifically cleaves mono-sulphated disaccharide motifs (see figure 3.2). Thus the diffuse staining pattern observed for BKS-1 and 5D4 after keratanase digestion is predicted in our four KS chain structures to be due to the presence of partially digested or non-digested KS chains containing regions of non-sulphated and/or di-sulphated disaccharides which were keratanase resistant, so causing the proteins to smear as higher molecular weight products when separated by SDS-PAGE (figure 3.4; panel B).

Figure 3.4 C shows a schematic representation of previously keratanase digested KS chain 'stubs' having now undergone further digestion with endo-β-galactosidase. The green symbols show the predicted reduction in BKS-1 neoepitopes. Following endo-β-galactosidase digestion, the BKS-1 staining was again partially reduced (figure 3.4; C) in both KS types I (from cornea) and II (from nasal cartilage aggrecan) compared to the keratanase digested KS chains (figure 3.4; B). This is predicted to be a result of the

endo-β-galactosidase specifically removing of a number of keratanase resistant non-sulphated domain 'stubs' described above to leave a number of unsulphated GlcNAc residues at the non-reducing end of the KS chain which were not recognised by BKS-1. However, diffuse staining still remained with BKS-1 and 5D4 indicating that there were still a number of long di-sulphated domain 'stubs' remaining on the keratanase/endo-β-galactosidase digested KS chains. These partially digested KS chains possess a keratanase-generated BKS-1 neoepitope at the non-reducing terminal (figure 3.4; C; BKS-1 neoepitopes indicated by the green symbol) and a region of disulphated disaccharides large enough to be recognised by 5D4 (figure 3.4; C, indicated by red 5D4 symbol) that were not substrates for the previously applied keratanase or endo-β-galactosidase enzymes.

Figure 3.4 D shows a schematic representation of the keratanase/endo-β-galactosidase digests of the four KS chain 'stub' structures followed by the predicted digestion products generated after further digestion with keratanase II (figure 3.4; D) where the reduced BKS-1 neoepitopes are indicated in green. Notably, after a final keratanase II digestion, the BKS-1 staining appears to have been significantly reduced to the form of two sharp bands of KSPGs at ~50 kDa and ~30 kDa in corneal KSPGs (KS type I), having similar molecular weights to a number of corneal KSPG core proteins (lumican, keratocan and mimecan). There were also a number of distinct aggrecan metabolite bands between ~ 150 and ~75 kDa in bovine cartilage PGs (KS type II). 5D4 staining was completely abolished, indicating that all remaining linear sulphated poly-N-acetyl-lactosamine repeat motifs had been successfully removed using keratanase II digestion. The sharp banding pattern observed using BKS-1 on the Western blots after deglycosylation using all three enzymes indicates that extensive deglycosylation of the KS chains on the core proteins of proteoglycan molecules had taken place leaving short disaccharide KS 'stub' linkage regions (figure 3.4; D). The

BKS-1 staining observed after such extensive deglycosylation, indicates that there were still a number of keratanase generated BKS-1 neoepitopes remaining which could not be further removed by either endo-β-galactosidase or keratanase II (figure 3.4; D). These neoepitope structures must therefore be on KS 'stub' structures that are attached directly to the KS linkage region, where there are no further di-, mono- or non-sulphated disaccharide substrates for further cleavage by any of these three enzymes. This suggests that the remaining low levels of BKS-1 staining results from non-reducing terminal 6-S-GlcNAc which may be attached to either the linkage region mannose of corneal KS, to the linkage region GalNAc of skeletal KS or to an adjacent Gal or 6-S-Gal. This data strongly indicates BKS-1 mAb specificity for a non-reducing terminal neoepitope containing 6-S-GlcNAc, regardless of the nature of the penultimate attaching sugar.

Essentially similar results were obtained if digest sequences were carried out as follows:

- Keratanase → keratanase II → endo-β-galactosidase
- Endo-β-galactosidase → keratanase → keratanase II.

3.3.3 Analysis of keratanase II → keratanase → endo-β-galactosidase sequential digests with 5D4 and BKS-1

Figure 3.5 A schematically illustrates the four predicted undigested KS structures from either cartilage aggrecan or corneal KS. Figure 3.5 B shows the predicted KS structures remaining after digestion with keratanase II. As expected, Western blot analysis showed no reactivity with BKS-1 either before or after keratanase II digestion because 6-S-GlcNAc epitopes for BKS-1 were not generated by keratanase II cleavage (figure 3.5; B). Also, 5D4 staining was completely abolished with keratanase II

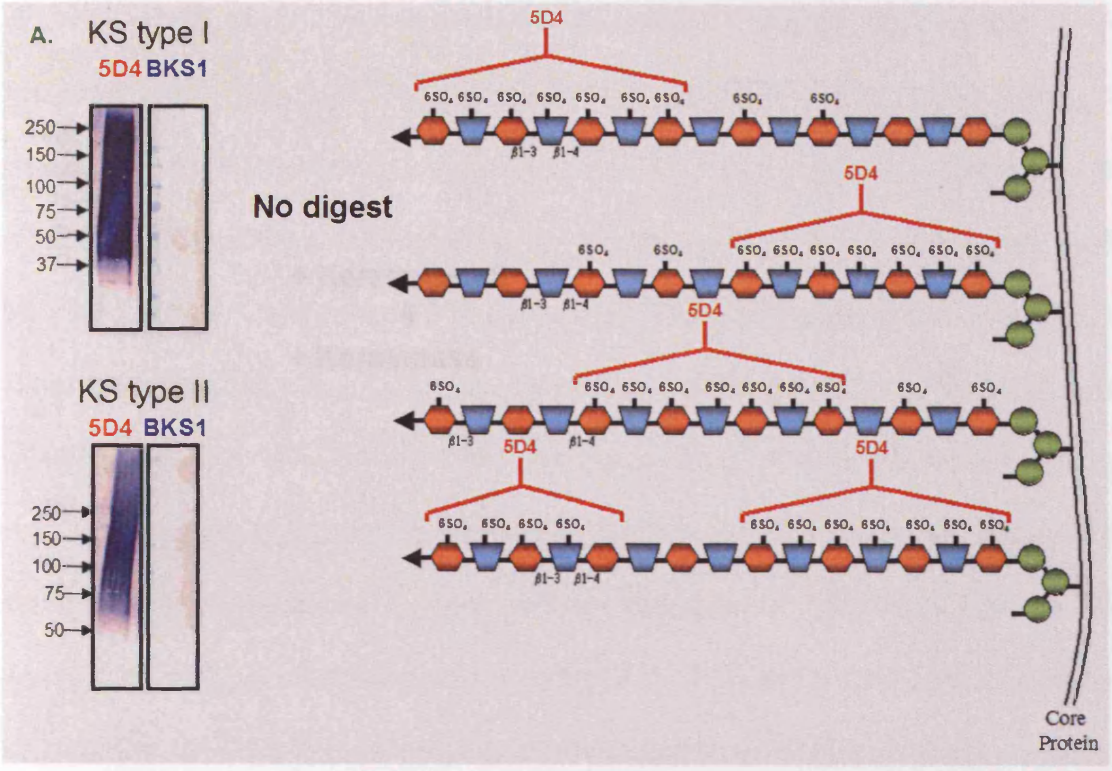

Figure 3.5 A. Depicts a range of KS structures where sulphation pattern motifs occur at random positions throughout the KS chain. 5D4 is positive due to the presence of disulphated domains, no BKS-1 neoepitopes have yet been generated.

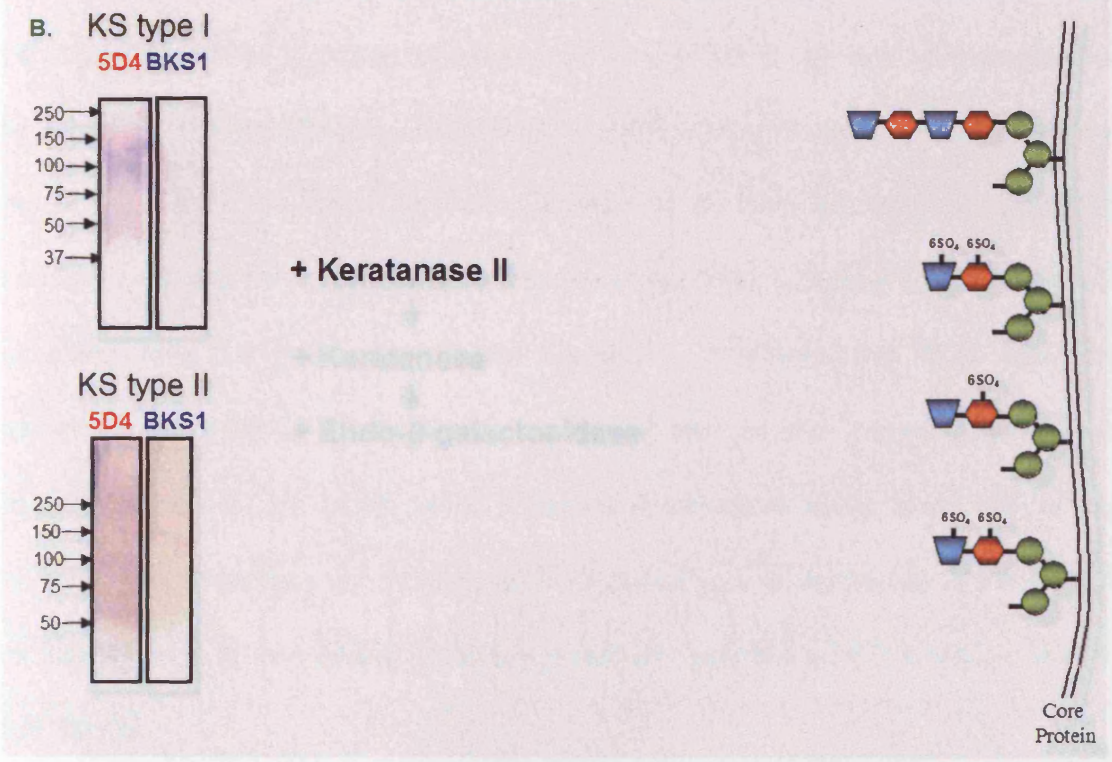

Figure 3.5 B Digestion with keratanase II removes all di- and mono- sulphated domain epitopes for 5D4. There are a number of non-reducing terminal 6-Gal or Gal residues which do not act as BKS-1 neoepitopes, therefore there is no BKS-1 staining.

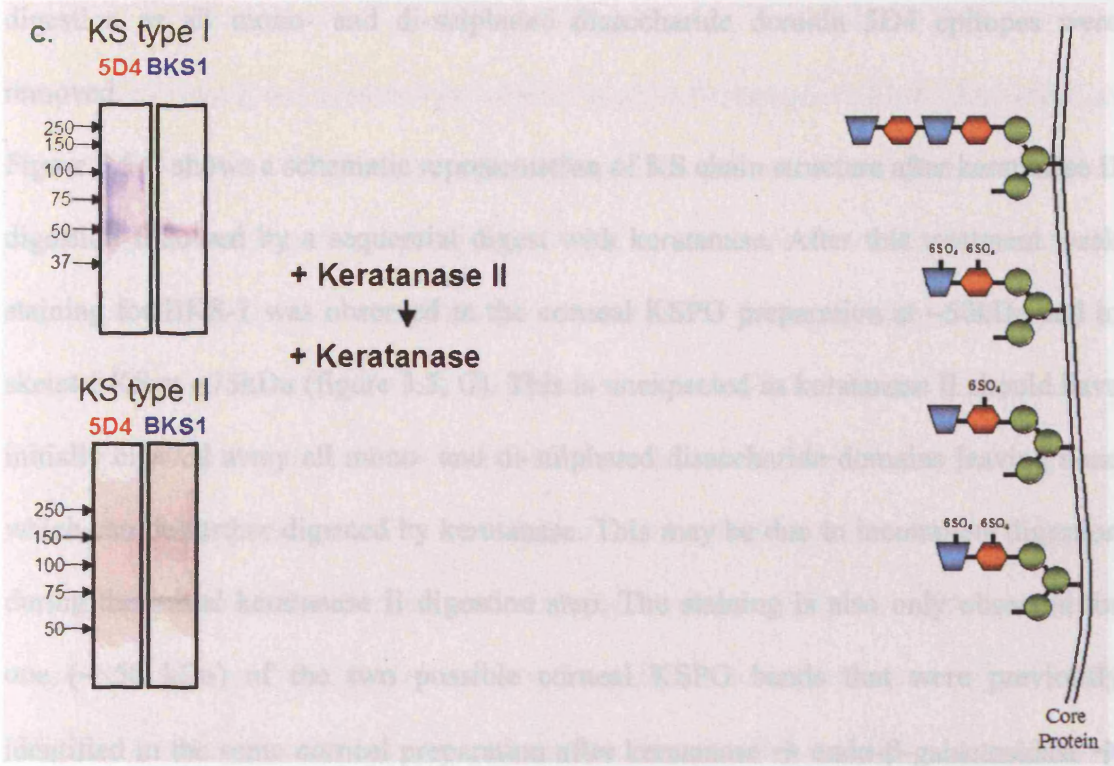

Figure 3.5 C Sequential digestion of KS I or II with keratanase II followed by keratanase was weakly positive for BKS-1. This was unexpected as all keratanase susceptible mono-sulphated domains were previously removed by keratanase II. 5D4 staining was again negative as in panel B above.

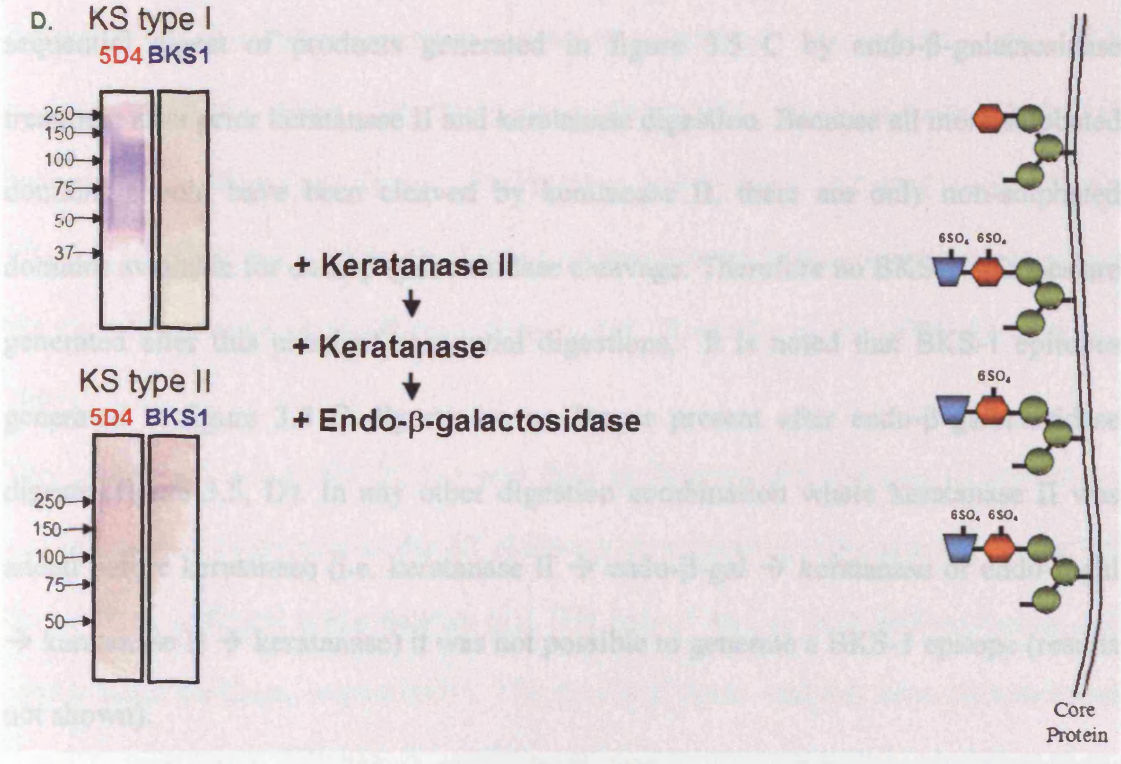

Figure 3.5 D No immunoreactivity was observed for either mAb after the addition of endo-β-galactosidase to the digested KS samples for similar reason to those given in panels B and C above.

digestion as all mono- and di-sulphated disaccharide domain 5D4 epitopes were removed.

Figure 3.5 C shows a schematic representation of KS chain structure after keratanase II digestion followed by a sequential digest with keratanase. After this treatment weak staining for BKS-1 was observed in the corneal KSPG preparation at ~50kDa and in skeletal KS at ~75kDa (figure 3.5, C). This is unexpected as keratanase II should have initially cleaved away all mono- and di-sulphated disaccharide domains leaving none which can be further digested by keratanase. This may be due to incomplete digestion during the initial keratanase II digestion step. The staining is also only observed for one (~ 50 kDa) of the two possible corneal KSPG bands that were previously identified in the same corneal preparation after keratanase → endo-β-galactosidase → keratanase II digestion illustrated in figure 3.4 D.

Finally, figure 3.5 D, depicts predicted KS chain structural domains following a sequential digest of products generated in figure 3.5 C by endo-β-galactosidase treatment after prior keratanase II and keratanase digestion. Because all monosulphated domains should have been cleaved by keratanase II, there are only non-sulphated domains available for endo-β-galactosidase cleavage. Therefore no BKS-1 epitopes are generated after this panel of sequential digestions. It is noted that BKS-1 epitopes generated in figure 3.5 C digests are no longer present after endo-β-galactosidase digests (figure 3.5, D). In any other digestion combination where keratanase II was added before keratanase (i.e. keratanase II → endo-β-gal → keratanase or endo-β-gal → keratanase II → keratanase) it was not possible to generate a BKS-1 epitope (results not shown).

3.4 Discussion

The currently accepted dogma from several studies (Oeben *et al.*, 1987; Stuhlsatz *et al*, 1989; Tai *et al.*, 1996, 1997; Funderburgh, 2000 review) have established generic structures for KS types I and II chains (see figure 1.2 and 1.3) derived from corneal and skeletal tissues, respectively. The distribution of unsulphated N-acetyl-lactosamine motifs, mono-sulphated disaccharides and di-sulphated disaccharides from the linkage region to the non-reducing termini between KS types I and II have been reported. They suggested that in corneal KS type I chains, non-sulphated N-acetyl-lactosamine disaccharides are found predominantly contiguous with the linkage region oligosaccharide, mono-sulphated N-acetyl-lactosamine occur in the mid-regions of the KS chain and disulphated N-acetyl-lactosamine disaccharides are clustered towards the non-reducing end of the KS glycosaminoglycan chain (Oeben *et al*, 1987; Funderburgh, 2000 review). In contrast, KS type II chain structures occur with a predominance of disulphated N-acetyl-lactosamine residues present throughout the KS glycosaminoglycan chain but with some intermittent mono-sulphated N-acetyl-lactosamine residues (see figure 1.3). Previous reports have indicated limited levels (Plaas *et al.,* 2001) or a complete absence of unsulphated N-acetyl-lactosamine within KS type II extended chain (Brown *et al.,* 1994; Huckerby *et al.,* 1994; Plaas *et al.*, 2001).

This study has used mAbs BKS-1 and 5D4 in Western blot analysis to investigate similarities and differences in the KS disaccharide sulphation motif patterns within KS chains from different tissue sources (i.e. KS types I and II from bovine cornea and bovine nasal cartilage, respectively). The results of these analyses have demonstrated that KS type I and KS type II chains both contain a combination of differentially sulphated (mono- versus di- versus unsulphated) N-acetyl-lactosamine domains on the different KSPG GAG chains. The resultant data suggests that in the bovine model

different tissue sources of KS most likely produce similar varieties of KS disaccharide structures, but that sulphation patterns are more randomly located along the KS chain than previously reported (Oeben *et al.,* 1987; Stuhlsatz *et al.,* 1989). The frequency of the regions containing di-sulphated disaccharide motifs appears to be greater in KS type II compared to KS type I. Also, there was no reactivity with BKS-1, recognising 6-sulphated N-acetylglucosamine residues, with native KS (i.e. before digestion with keratanase). This suggests that there are no 6-sulphated N-acetylglucosamine residues present as capping structures at the non-reducing terminal of KS as postulated previously by Huckerby *et al.,* 1995.

3.5 Chapter summary

- Monoclonal antibody BKS-1 was used in conjunction with mAb 5D4 in the analysis of KS sulphation motif patterns in KS types I and II from cornea and cartilage, respectively.
- Results demonstrated that, in contrast to the generic structure for KS proposed by Oeben *et al.,* 1987 and Stuhlsatz *et al.,* 1989 KS is more randomly substituted with sulphate groups than previously reported. It was found that non-, mono- and di-sulphated domain motifs were located at various linkage regions, mid regions and non-reducing terminal positions through both KS types I and II chains.
- KS type II appears to contain a larger portion of disulphated disaccharide motifs than KS type I.

Chapter 4 - Production and characterisation of two new mAbs to bovine corneal keratan sulphate proteoglycans.

4.1 Introduction

The cornea is a source particularly rich in KS containing proteoglycans where the KS is found primarily attached to one of 3 SLRPG core proteins; i.e. lumican (Blochberger *et al.,* 1992; Funderburgh *et al.,* 1993), keratocan (Corpuz *et al.,* 1996) or mimecan (Funderburgh *et al.,* 1997 A) [reviewed in chapter 1]. The enzymatic addition of sulphate groups to KS on KSPGs present in corneal tissues is thought to be essential for the proper interaction of corneal proteoglycans with collagen fibrils and in the regulation of collagen fibrillogenesis and the ultrastructural arrangement of the corneal extracellular matrix. The development of corneal transparency depends upon the proper interaction of these molecules (Scott & Haigh, 1988; Funderburgh *et al.,* 1991 A; Scott, 1992; Rada *et al.,* 1993; Cornuet *et al.,* 1994; Chakravarti *et al.,* 1998). Lumican has also recently been shown to have an important role in corneal wound healing by regulating polymorphonuclear (PMN) leukocyte infiltration in wounded corneas (Chakravarti *et al.,* 2005; Kao *et al.,* 2005; Yeh *et al.,* 2005).

These proteoglycans were selected as potential KS containing antigens for the production of mAbs to KS 'stub' epitopes generated after keratanase II digestion. Such immunisations could result in the production of antibodies recognising either a keratanase II generated KS 'stub' neoepitope containing a non-reducing terminal Gal or Gal-6-sulphate, or to SLRP protein core epitopes on lumican, keratocan or mimecan, all of which are currently not available in our lab but would be useful research tools.

4.2 Materials

4.2.1 Materials

All chemicals were of analytical grade and were purchased from Sigma-Aldrich unless otherwise stated. A comprehensive catalogue of materials and suppliers used throughout this project is listed in Appendix A.

All DMMB material (section 2.2.2), GAG degrading enzymes (section 2.2.3), immunisation and tissue culture material (section 2.2.4), SDS-PAGE and Western blotting material (section 2.2.5) and Lectin affinity material (section 2.2.6), were as described in chapter 2, section 2.2 and table 2.3. Bovine and porcine tissues were obtained from a local abattoir. Normal and pathological human cartilage was obtained as described in chapter 6, section 6.2.1.

4.2.2 Stock solutions

Solutions and their components required for practical work are listed in tables 2.3 and 4.1. Ethanol, acetic acid, hydrochloric acid, sodium hydroxide, methanol and urea were all obtained from Fisher Scientific.

Buffer solution	Components
Anion exchange chromatography equilibration buffer	6 M Urea, 0.05 M Tris, pH 6.8, containing 0.1% (w/v) chaps
Anion exchange chromatography elution buffer	6 M Urea, 2 M NaCl, 0.05 M Tris, pH 6.8, containing 0.1% (w/v) chaps
Proteoglycan extraction buffer	4 M Guanidine–HCl, 0.05 M Sodium acetate (anhydrous), 0.01 M Disodium EDTA, 0.1 M 6-amino hexanoic (caproic) acid, 5 mM Benzamidine-HCl, 0.5 mM phenyl methyl sulfonyl fluoride (PMSF), pH 5.8-6.8
Size exclusion chromatography equilibration buffer	0.1 M Sodium sulphate, pH 6.8

Table 4.1 Buffer solutions and their components

4.3 Methods

4.3.1 Preparation and purification of a keratanase II-generated bovine corneal KSPG antigen.

An overview of the keratanase II 'stub' KSPG antigen purification methods are illustrated in figure 4.1. Expanded details are provided in the sections below.

4.3.1.1 Proteoglycan extraction from bovine cornea

ECM molecules are firmly associated within their native tissues in a naturally occurring state. In order to isolate various proteoglycans they must be dissociated from their surrounding tissue. In cartilage, 4 M Guanidine HCl (a chaotrophic agent) acts to dissociate PG aggregates by breaking any non covalent bonds and removing them from their native environment into solution (Sajdera & Hascall, 1969; Heinegard & Sommarin, 1987). 4 M guanidine also facilitates extraction of SLRPs from corneal extracellular matrices (Corneut *et al.,* 1994).

20 bovine corneas were dissected, weighed and finely diced prior to extraction. The tissue was extracted in 10 ml 4 M Guanidine-HCl containing proteolytic inhibitors (table 4.1) per gram wet weight of tissue at 4 °C for 24 hours. Supernatants were collected and fresh extraction buffer was added to the tissue residue for a further 24 hours. Both supernatants were pooled.

4.3.1.2 Anion exchange chromatography of guanidine extracted corneal matrix molecules

The corneal PG extracts were pooled and dialysed against 6 M Urea; 50 mM Tris; pH 6.8, containing 0.1% (w/v) CHAPS (table 4.1). This crude PG extract was applied to a Resource Q anion exchange chromatography column (see chapter 2, section 2.3.2.3) which had been equilibrated in 6 M Urea; 50 mM Tris; pH 6.8, containing 0.1% (w/v)

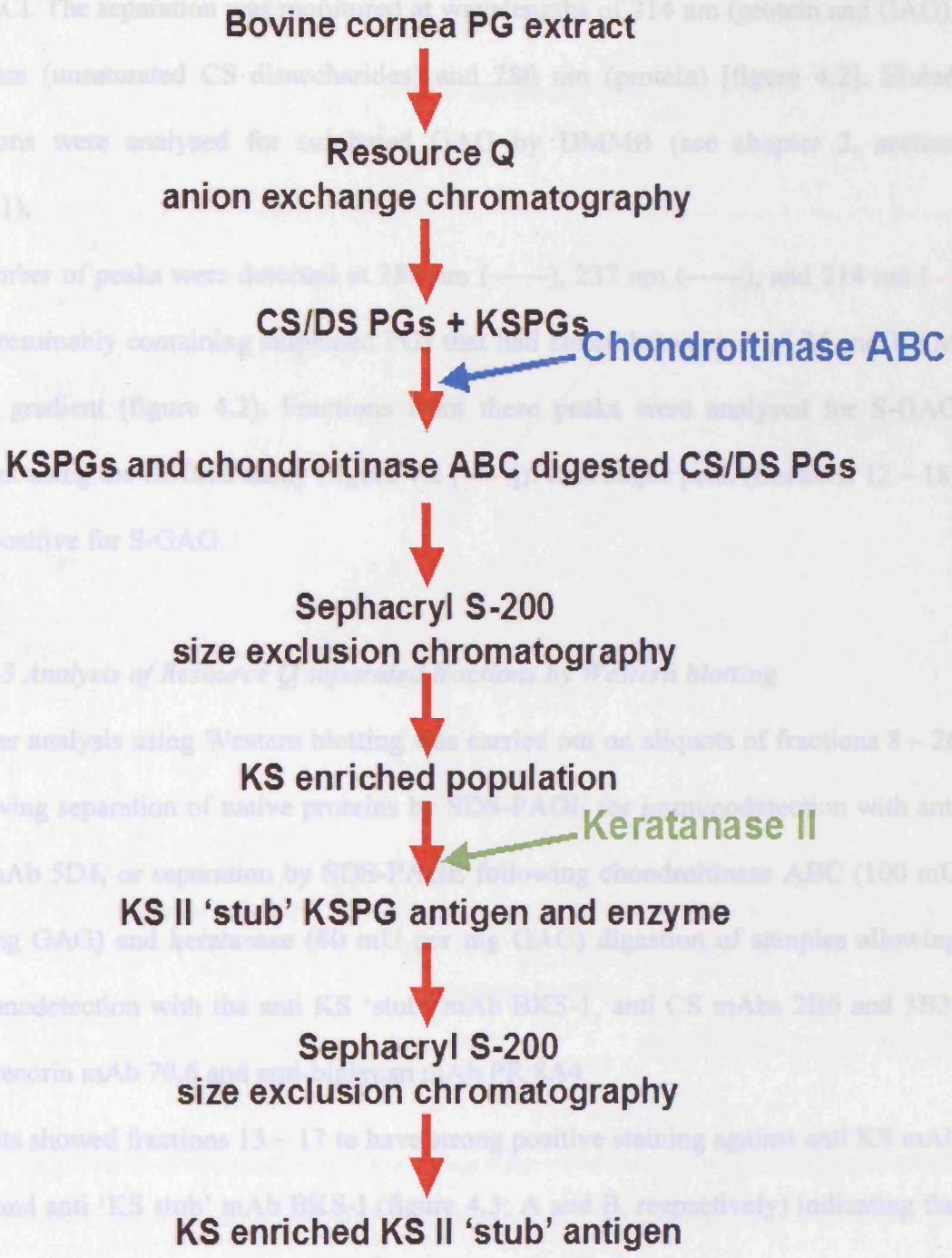

Figure 4.1 - An overview of the procedures involved in purification of a keratanase II-generated 'stub' KSPG antigen.

CHAPS (table 4.1), using a 50 ml superloop at a flow rate of 1 ml/min. Bound material was sequentially eluted into 1 ml fractions using a linear salt gradient of 0 – 2 M NaCl. The separation was monitored at wavelengths of 214 nm (protein and GAG), 232 nm (unsaturated CS disaccharides) and 280 nm (protein) [figure 4.2]. Eluted fractions were analysed for sulphated GAG by DMMB (see chapter 2, section 2.3.1.1).

A number of peaks were detected at 280 nm (——), 232 nm (——), and 214 nm (——) presumably containing sulphated PGs that had eluted between a 1.3 M and 1.6 M NaCl gradient (figure 4.2). Fractions from these peaks were analysed for S-GAG content using the DMMB assay (figure 4.2 [-----]). One major peak (fractions 12 – 18) was positive for S-GAG.

4.3.1.3 Analysis of Resource Q separated fractions by Western blotting

Further analysis using Western blotting was carried out on aliquots of fractions 8 – 26 following separation of native proteins by SDS-PAGE for immunodetection with anti KS mAb 5D4, or separation by SDS-PAGE following chondroitinase ABC (100 mU per mg GAG) and keratanase (80 mU per mg GAG) digestion of samples allowing immunodetection with the anti KS 'stub' mAb BKS-1, anti CS mAbs 2B6 and 3B3, anti decorin mAb 70.6 and anti-biglycan mAb PR 8A4.

Results showed fractions 13 – 17 to have strong positive staining against anti KS mAb 5D4 and anti 'KS stub' mAb BKS-I (figure 4.3; A and B, respectively) indicating the presence of a large amount of KS in these fractions. There was also positive immunoreactivity in these fractions for anti CS mAbs 2B6/3B3 at ~40, 30 and 17-20 kDa (figure 4.3, C), indicating that these fractions most likely contained a number of SLRPs such as decorin and biglycan that had CS / DS GAG attachments. There was also positive immunoreactivity for anti decorin protein epitope mAb 70.6 (figure 4.3;

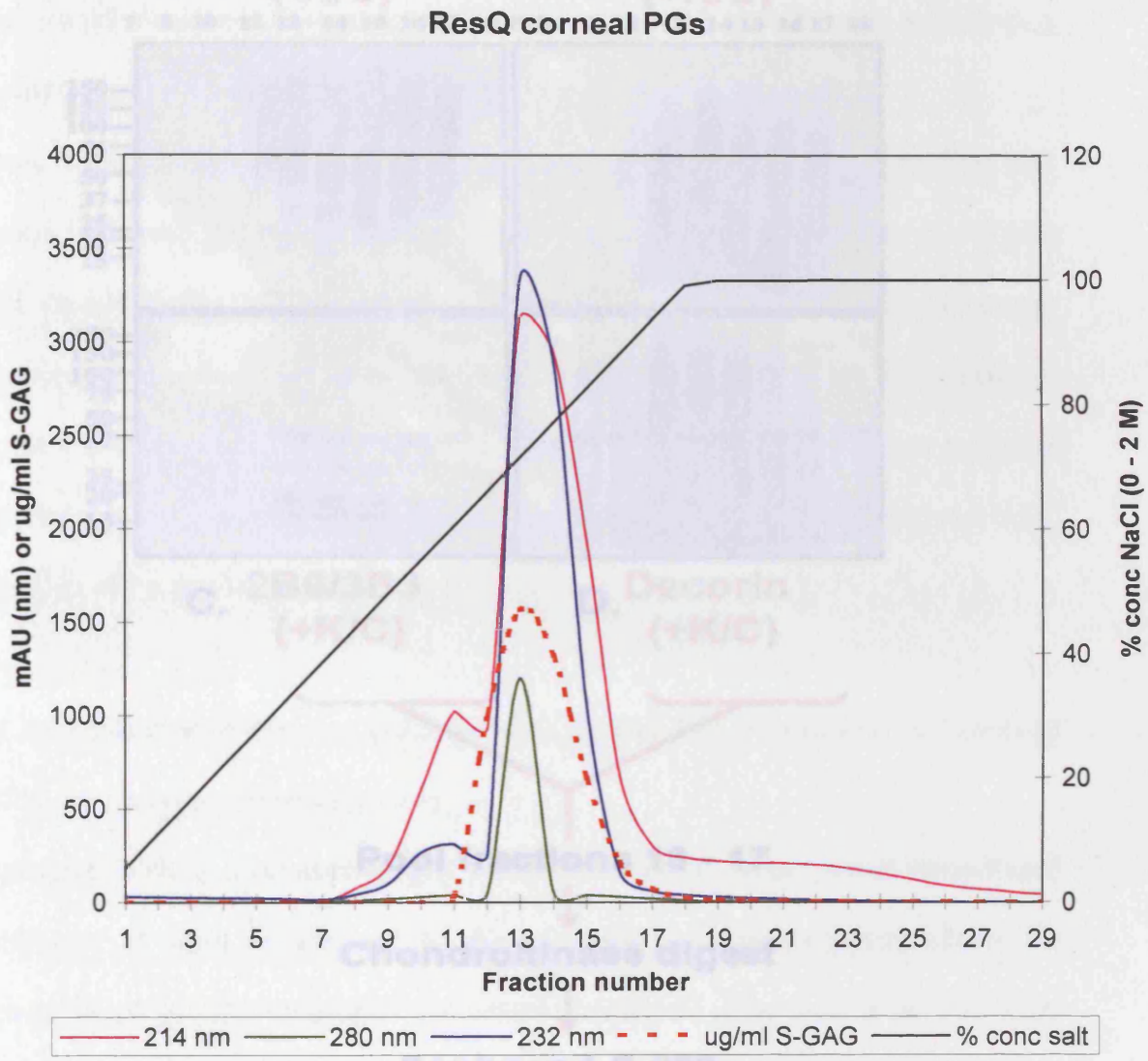

Figure 4.2 Resource Q anion exchange chromatography of bovine corneal proteoglycan extracts and DMMB analysis of separated fractions: pink – 214 nm (carbohydrate); blue – 232 nm (carbohydrate); green – 280 nm (protein) and dashed red – DMMB results (µg/ml S-GAG). All sulphated PGs eluted within a 1.3 – 1.6 M NaCl gradient (fractions 12-18).

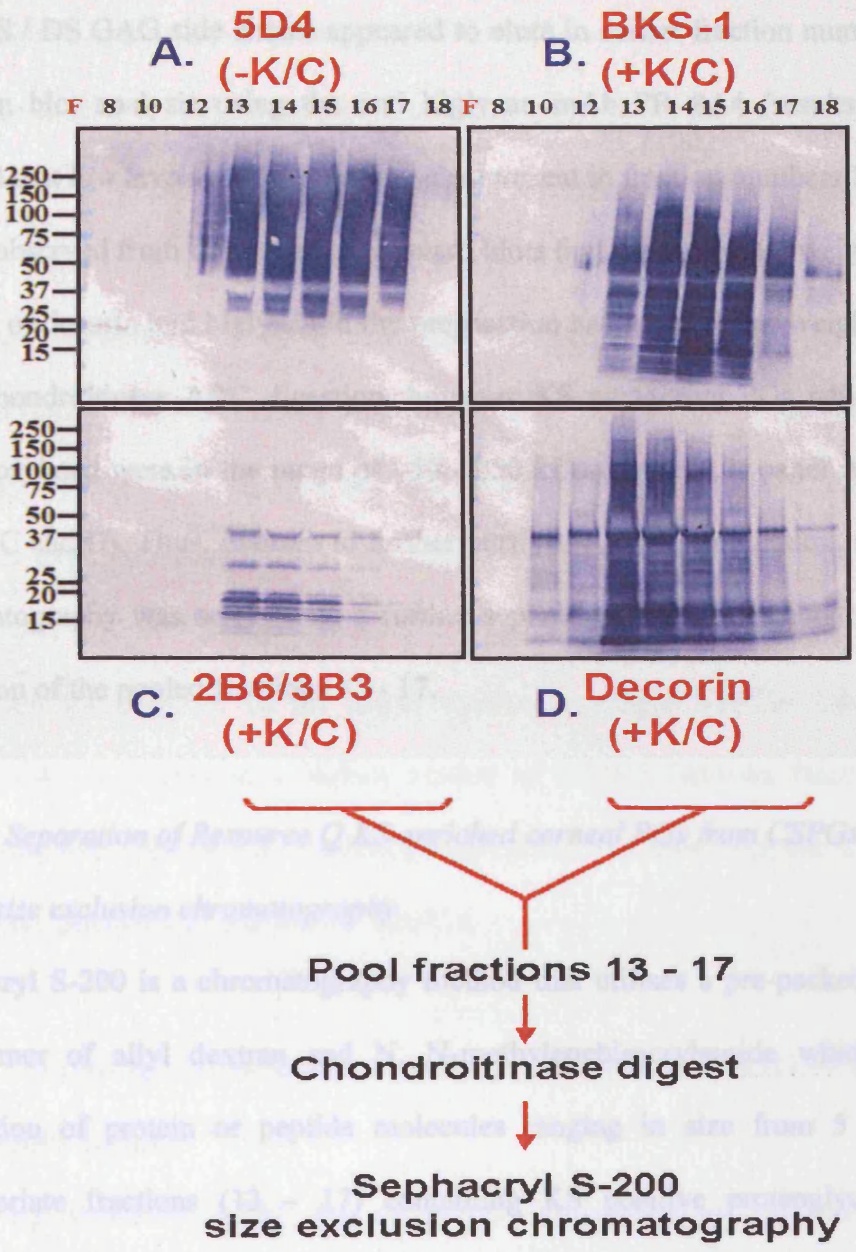

Figure 4.3 - Western blot results after Resource Q anion exchange chromatography. KSPGs and CS/DSPGs eluted in fractions 13 – 17 as shown by mAbs 5D4 & BKS-1 (A & B). Comparison of anti CS mAbs 2B6/3B3 (C), anti decorin mAb 70.6 (D) and 5D4 (B) blots depicted a difference in molecular weights of undigested KSPGs (~50 – 250 kDa) compared to chondroitinase ABC digested CS/DSPG (~40 kDa) indicating suitability of size exclusion chromatography as a further separation procedure.

D) in a larger range of fractions (10 – 18), where CS / DS substituted decorin had eluted in the same fractions as the KSPGs (13 – 17). Decorin that was not substituted with CS / DS GAG side chains appeared to elute in earlier fraction numbers 10 – 12. Western blot analysis using the anti biglycan mAb PR 8A4 (results not shown), showed that low levels of biglycan was also present in fraction numbers 13 – 17.

It was observed from this series of Western blots that the molecular weight of the core protein of decorin and biglycan in the preparation had a molecular weight of ~40 kDa after chondroitinase ABC digestion, however KS containing PGs which were non-deglycosylated were in the range of ~50 - 250 kDa (figure 4.3; panel A compared to panels C and D). Thus, in order to further purify the KSPG population, size exclusion chromatography was selected as a further separation step after chondroitinase ABC digestion of the pooled fractions 13 - 17.

4.3.1.4 Separation of Resource Q KS-enriched corneal PGs from CSPGs by Sephacryl S-200 size exclusion chromatography

Sephacryl S-200 is a chromatography method that utilises a pre-packed cross-linked copolymer of allyl dextran and N, N-methylenebisacrylamide which allows for separation of protein or peptide molecules ranging in size from 5 to 250 kDa. Appropriate fractions (13 – 17) containing KS positive proteoglycan from the Resource Q anion exchange chromatography step described above in section 4.3.1.2, were pooled and subjected to chondroitinase ABC digestion (100 mU per mg GAG) in a 0.1M Tris acetate buffer, pH 6.8 (see table 2.3) over night at 37 °C in order to remove the CS chains and allow for the separation of the core proteins of decorin and biglycan from native KS containing small PGs using size exclusion chromatography procedures. DMMB analysis was carried out before and after chondroitinase ABC digestion to determine GAG concentration. Total sulphated GAG (S-GAG) levels fell

from 4.7 mg to 2.7 mg after chondroitinase ABC digestion, indicating that approximately 2.7 mg of sulphated KS remained in the preparation. The sample was then dialysed against Milli Q™ water.

The chondroitinase ABC digested sample was lyophilised and reconstituted in 600 µl 0.1 M Na_2SO_4, pH 6.8 (table 4.1). 500 µl was applied to a HiPrep^R Sephacryl S-200 size exclusion chromatography column at a flow rate of 0.5 ml/min and 2 ml fractions collected. Separation was monitored at wavelengths of 214 nm (protein and GAG), 232 nm (unsaturated CS disaccharides) and 280 nm (protein). Eluted fractions were analysed by DMMB analysis (as described in section 2.3.1.1) and appropriate fractions selected for further analysis. A number of peaks resulted across fractions 20 – 65 (figure 4.4) with a large 214 nm (——) peak between fractions 20 – 35 predicted to contain the majority of the larger molecular weight KSPGs. DMMB analysis (figure 4.4; ----) revealed a higher content of S-GAG between fractions 20 – 33, concurring with the 214 nm chromatographic trace, and indicating that this was a peak of interest, predicted to contain the KSPGs.

4.3.1.5 Analysis of size exclusion chromatography separated fractions by SDS-PAGE and Western blotting

Following Sephacryl S-200 size exclusion chromatography and DMMB analysis (figure 4.4), fraction samples were further deglycosylated using keratanase where necessary and separated on 4 - 20% Tris glycine SDS-PAGE gradient gels and transferred for Western blotting using mAb probes 5D4 (anti-KS), 70.6 (anti-decorin), 2B6/3B3 and BKS-1 (requiring pre-digestion with keratanase at 80 mU per mg GAG). Western blot analysis of fractions 18 – 34 revealed that the majority of the KSPGs did separate in earlier fractions 20 - 26 (figure 4.5; A & C) and the deglycosylated CS/DS PGs in later fractions 28 - 34 (figure 4.5; B). From these results, fractions 20 - 26

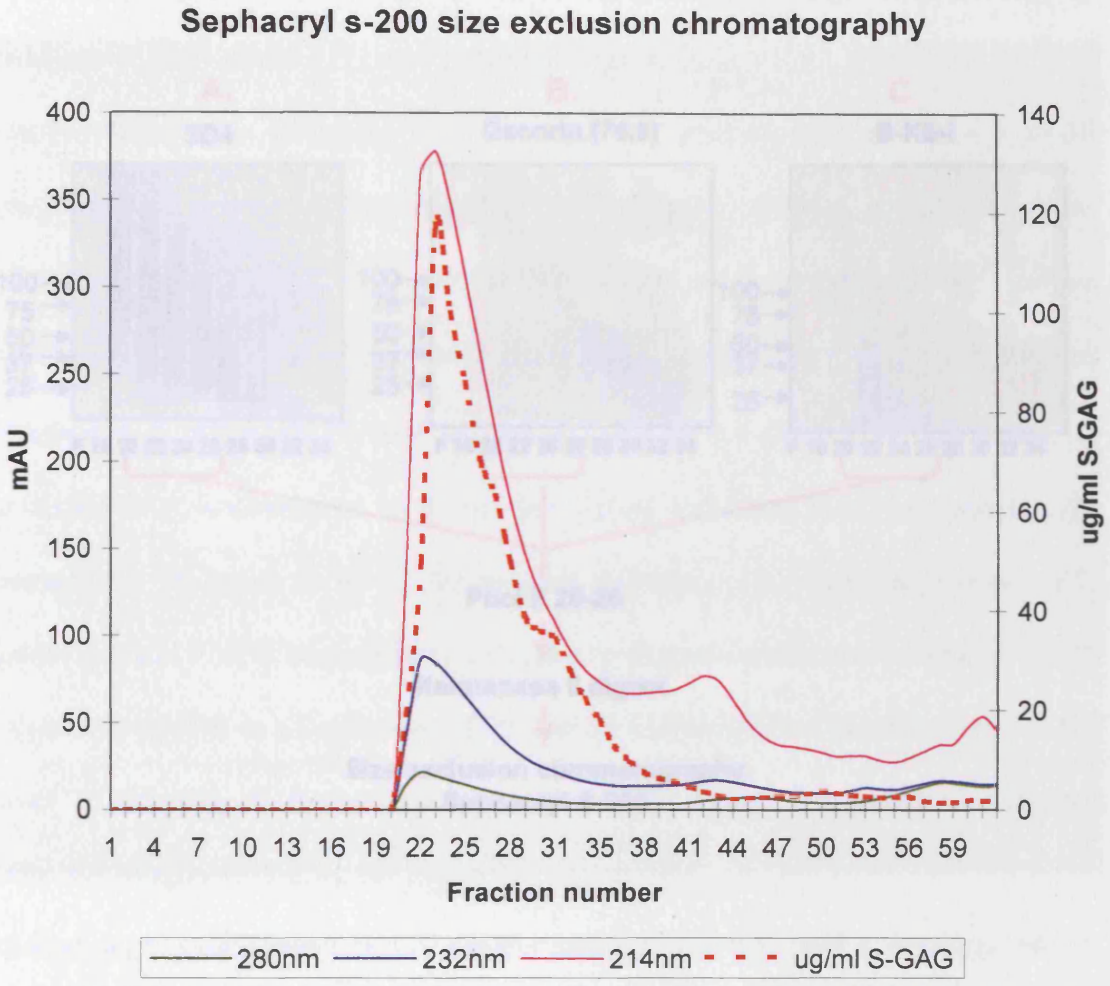

Figure 4.4 Sephacryl S-200 size exclusion chromatography separation of chondroitinase ABC digested CSPGs from undigested KSPGs: pink - 214 nm (protein and GAG); blue - 232 nm (carbohydrate); green - 280 nm (protein). The sulphated KSPGs detected using DMMB analysis (red dashed line) were present in fractions 20-33 where there was high absorbance at 214nm.

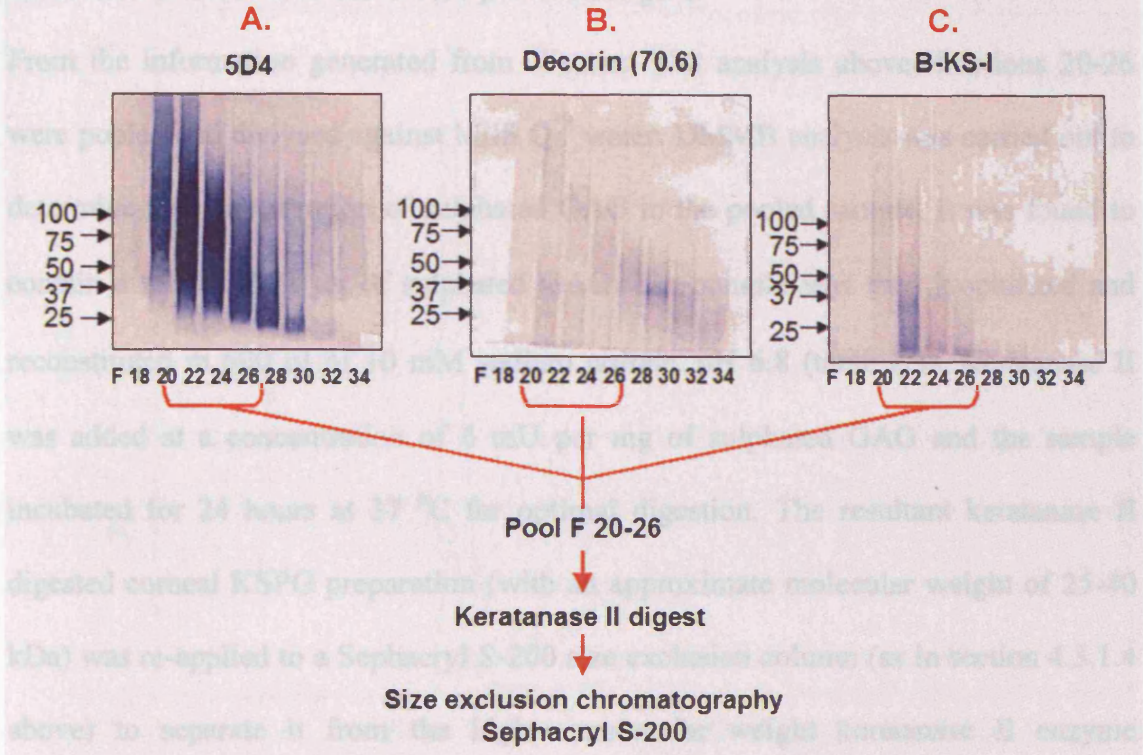

Figure 4.5 - Western blot results of fractions 18 – 34 after sephacryl S-200 size exclusion chromatography. Larger KSPGs separated in earlier fractions 20 – 26 (A and C) while smaller molecular weight decorin separated in later fractions 28 – 34 (B).

were pooled and dialysed against Milli Q™ water prior to further processing to generate keratanase II 'stub' and corneal KSPG antigens.

4.3.1.6 Keratanase II digestion of KS-enriched corneal PGs to generate a range of keratanase II 'stub' and KSPG core protein antigens

From the information generated from Western blot analysis above, fractions 20-26 were pooled and dialysed against Milli Q™ water. DMMB analysis was carried out to determine the concentration of sulphated GAG in the pooled sample. It was found to contain a total of 922 μg of sulphated GAG. The sample was then lyophilised and reconstituted in 600 μl of 10 mM sodium acetate, pH 6.8 (table 2.3). Keratanase II was added at a concentration of 6 mU per mg of sulphated GAG and the sample incubated for 24 hours at 37 °C for optimal digestion. The resultant keratanase II digested corneal KSPG preparation (with an approximate molecular weight of 25-40 kDa) was re-applied to a Sephacryl S-200 size exclusion column (as in section 4.3.1.4 above) to separate it from the higher molecular weight keratanase II enzyme (molecular weight ~275 kDa, see figure 2.4, chapter 2).

Fractions were pooled based on UV profile peaks (figure 4.6) pool 1: fractions 18-23, pool 2: fractions 24-30, pool 3: fractions 31-40. They were dialysed against Milli Q™ water, lyophilised and reconstituted in 2 ml Milli Q™ water.

4.3.1.7 Analysis of separation of keratanase II enzyme from keratanase II 'stub' KSPG antigen using Silver staining and Western blotting analysis

Silver stain analysis was used on 30 μl samples from each pool to determine where the keratanase II enzyme had been separated from the KSPGs with keratanase II generated 'KS stubs'. 30 μl samples were also used in SDS-PAGE and Western blot analysis using mAbs 2B6/3B3/1B5 (all at a 1:100 dilution) to analyse for the presence

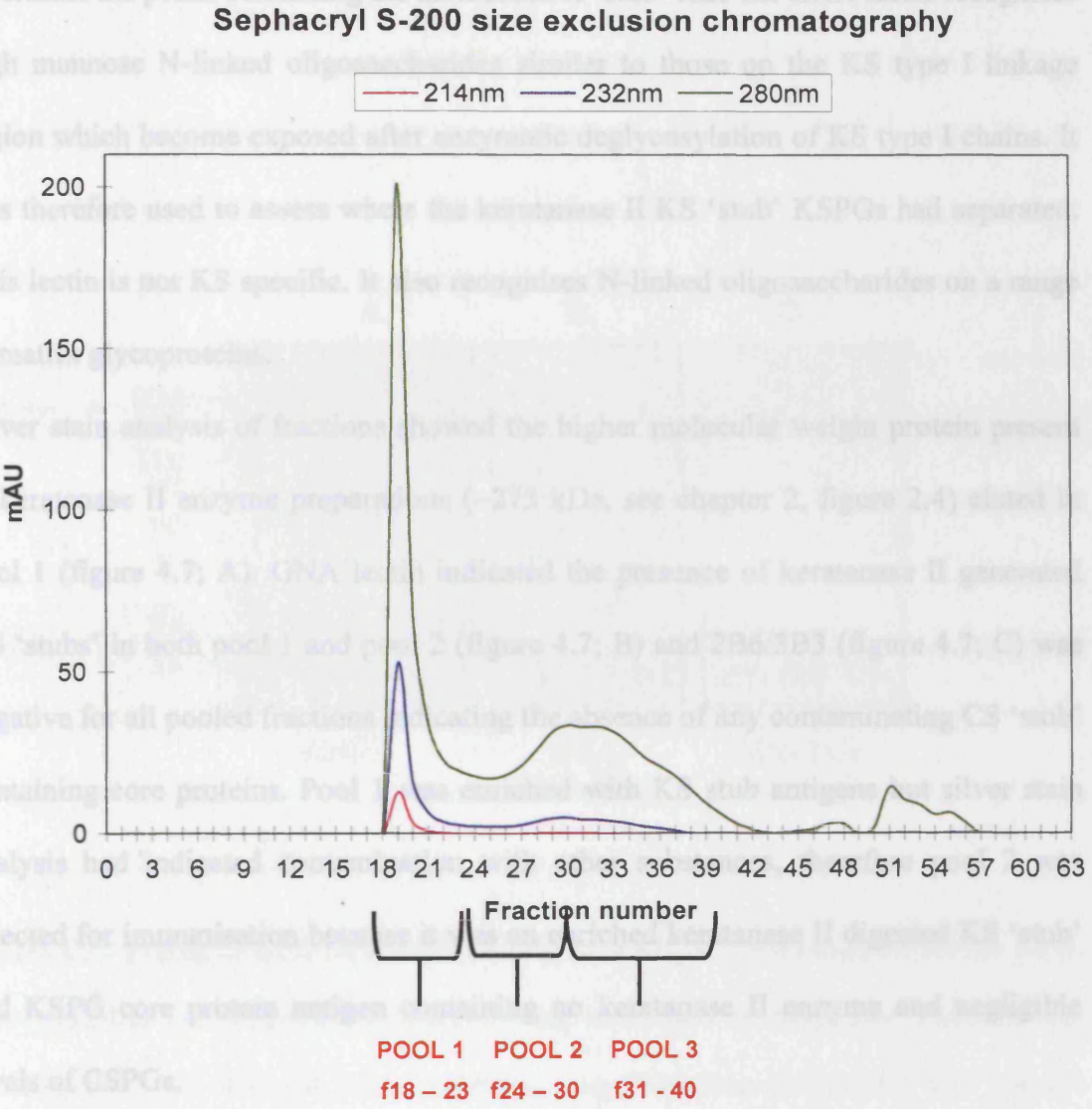

Figure 4.6 - Sephacryl S-200 size exclusion chromatography profile, separation of the keratanase II enzyme from the keratanase II digested KSPG 'stub' antigen. Showing detection at 280 nm (green), 232 nm (blue) and 214 nm (pink). Fractions were pooled based on peaks, pool 1: fractions 18 – 23, pool 2: fractions 24 – 30 and pool 3: fractions 31 – 40.

of any contaminating CS/DS and galanthus nivalis agglutinin (GNA) lectin (10 µl per 10 ml lectin buffer, see table 2.3 and similar to method described in section 2.3.2.3) to determine the peaks containing the keratanase II 'stub' KSPGs. GNA lectin recognises high mannose N-linked oligosaccharides similar to those on the KS type I linkage region which become exposed after enzymatic deglycosylation of KS type I chains. It was therefore used to assess where the keratanase II KS 'stub' KSPGs had separated. This lectin is not KS specific. It also recognises N-linked oligosaccharides on a range of matrix glycoproteins.

Silver stain analysis of fractions showed the higher molecular weight protein present in keratanase II enzyme preparations (~275 kDa, see chapter 2, figure 2.4) eluted in pool 1 (figure 4.7; A). GNA lectin indicated the presence of keratanase II generated KS 'stubs' in both pool 1 and pool 2 (figure 4.7; B) and 2B6/3B3 (figure 4.7; C) was negative for all pooled fractions indicating the absence of any contaminating CS 'stub' containing core proteins. Pool 1 was enriched with KS stub antigens but silver stain analysis had indicated contamination with other substances, therefore pool 2 was selected for immunisation because it was an enriched keratanase II digested KS 'stub' and KSPG core protein antigen containing no keratanase II enzyme and negligible levels of CSPGs.

4.3.2 Immunisation with a keratanase II-generated KSPG KS 'stub' antigen, fusion, cloning and screening of resulting hybridomas

Murine mAbs were generated again by immunising a single 4 - 6 week old female Balb/c mouse with the keratanase II KSPG 'stub' antigen, fusing resulting antibody producing lymphocytes with the mouse myeloma Ag 8 cell line and cloning resulting hybridomas of interest as described previously in chapter 2, section 2.3.3. Hybridoma culture media was screened using ELISA and Western blotting techniques using the

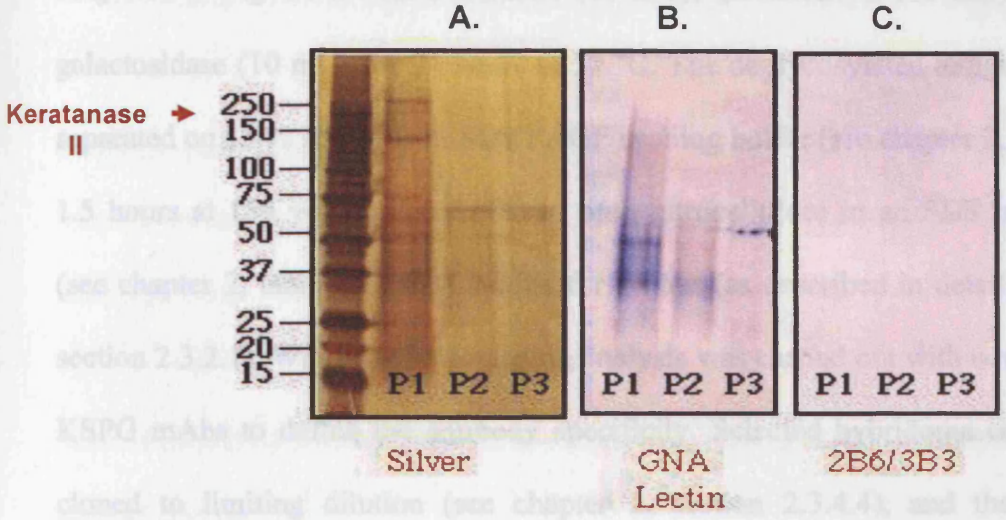

Figure 4.7 - Fractions from separation were pooled (P1, P2, P3) based on profile peaks (see figure 4.6). **(A)** Silver stain analysis showing which pool the keratanase II enzyme was present in (P1 ~ 275 kDa); **(B)** Western blotting using GNA lectin showing KS 'stub' positive samples; **(C)** Western blotting using mAbs 2B6/3B3 showing the absence of any contaminating CS.

keratanase II digested KS 'stub' immunising antigen prepared as described above in section 4.3.1 and the panel of antigens listed in chapter 2, section 2.3.4.1.

Further screening was carried out using purified bovine arterial lumican, bovine corneal extracts containing a lumican and mimecan mix, keratocan and lumican mix and bovine cartilage fibromodulin screening antigens were a gift from Professor James Funderburgh, University of Pittsburgh, USA. 5 μg samples of each were subjected to digestion with keratanase (10 mU), keratanase II (10 mU) and endo-β-galactosidase (10 mU) for 24 hours at 37 °C. The deglycosylated antigens were then separated on 15 % slab gels in SDS PAGE running buffer (see chapter 2, table 2.3) for 1.5 hours at 150 volts and transferred onto nitrocellulose in an SDS transfer buffer (see chapter 2, table 2.3) at 100 volts for 1 hour (as described in detail in chapter 2, section 2.3.2.1). Western blot screening analysis was carried out with newly generated KSPG mAbs to define the antibody specificity. Selected hybridoma cell lines were cloned to limiting dilution (see chapter 2, section 2.3.4.4), and the Ig subclass determined (see section 2.3.4.5).

The two new KSPG antibodies (LUM-1 and KER-1) were identified as IgM, kappa light chain monoclonal antibodies.

4.3.3 Analysis of mAb reactivity after removal of N- and O-linked oligosaccharides from corneal KSPG extracts

Eight volumes equivalent to 2 μg GAG of bovine corneal KSPG extracts were digested with 80 mU of keratanase per mg GAG, 6 mU of keratanase II per mg GAG and 8 mU of endo-β-galactosidase per mg GAG (see section 2.3.1.2) in 0.1 M Tris acetate, pH 6.8 for 24 hours at 37 °C. Samples were either left as such, or further digested using enzymes from a protein deglycosylation kit obtained from Sigma-Aldrich as described in chapter 2, section 2.3.4.6 where PNGase F or O-glycosidase

enzymes were either added individually or sequentially in the following order following deglycosylation using the keratanase enzymes:

1. KSPG + keratanase/keratanase II/endo-β-gal;
2. KSPG + keratanase/keratanase II/endo-β-gal + PNGase F;
3. KSPG + keratanase/keratanase II/endo-β-gal + O-glycosidase;
4. KSPG + keratanase/keratanase II/endo-β-gal + PNGase F + O-glycosidase.

Samples were incubated overnight at 37 °C and run on 12% slab gels. Gels were transferred as described in section 2.3.2.1 and analysed by Western blotting using the new KSPG mAbs.

4.3.4 Analysis of LUM-1 and KER-1 reactivity with KSPGs isolated from different animal species

Tissues were obtained from 18 moth old bovine cornea, cartilage and tendon, porcine cornea and cartilage, normal and OA human cartilage. These tissues were diced and extracted in 4 M guanidine HCl with protease inhibitors (table 2.3 and section 4.3.1.1). Crude PG extracts were dialysed to Milli Q™ water and DMMB analysis carried out to determine GAG concentration of the samples. Volumes equivalent to 6 μg GAG were digested with keratanase (80 mU per mg GAG) and keratanase II (6 mU per mg GAG,) and 3 μg GAG samples run on 4 - 20% Tris glycine gradient gels prior to transfer onto nitrocellulose for Western blot analysis with mAbs LUM-1 and KER-1.

4.4 Results

4.4.1 Screening of resulting hybridomas

4.4.1.1 Screening ELISAs

The primary screening of 8 x 24 well plates by direct ELISA against the keratanase II 'stub' immunising antigen revealed 4 possible wells containing antibody secreting hybridomas (2C6, 7C4, 11C4 and 1C3) with higher optical density readings (0.6 – 2.5) at 405 nm (figure 4.8). In addition, 2C6 and 7C4 were immunoreactive with keratanase II digested BNC (ABC) core, indicating that they were potential new keratanase II 'stub' mAbs. In contrast, mAbs 1C3 and 11C4 appeared to be reactive only with the keratanase II digested corneal KSPG immunising antigens, indicating potential new KSPG core protein mAbs.

A secondary screen by ELISA, coating with keratanase II digested BNC (ABC) core, keratanase digested bovine corneal KSPG and the keratanase II generated immunising antigen showed that two of the previously identified clones (2C6 and 7C4) were positive for the keratanase II generated 'stub' neoepitope as they had positive immunoreactivity with both of the keratanase II digested antigens (figure 4.9) but were negative for the keratanase digested KSPG antigen (figure 4.9), demonstrating that these two antibodies were specifically recognising keratanase II generated 'KS stub' neoepitopes containing either a non reducing terminal Gal-6-S or a Gal residue.

The other 2 clones (11C4 and 1C3) showed positive immunoreactivity with both keratanase II and keratanase digested bovine corneal KSPG antigens but not with the keratanase II digested BNC (ABC) core (figure 4.9). This indicated that the new mAbs 11C4 and 1C3 were in fact specific for corneal SLRP core protein epitopes.

Controls were carried out using 5D4, 4D1 and 1B4 monoclonal antibodies (recognising sulphated linear KS chain epitopes, see table 2.2) and results were as expected, with no immunoreactivity against keratanase II digested antigens and

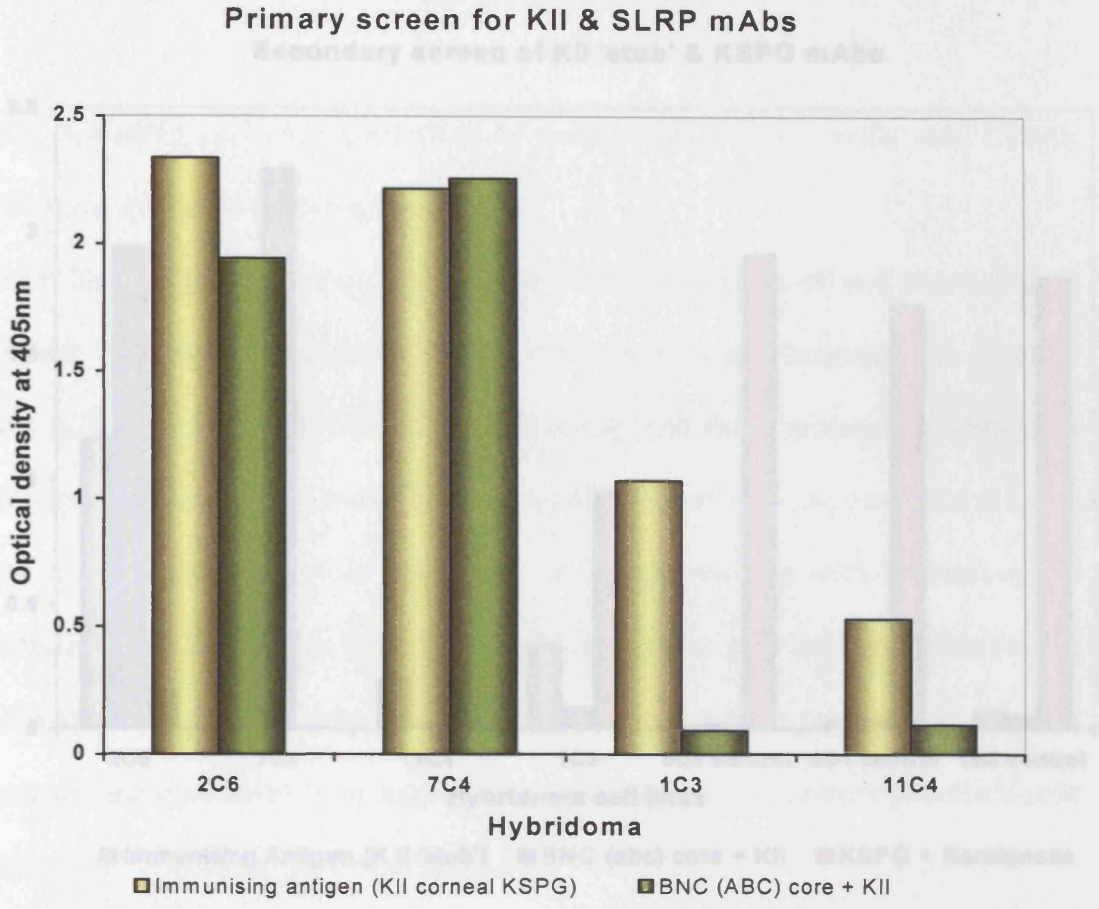

Figure 4.8 - Primary screen using ELISA against the keratanase II (KII) digested bovine corneal KSPG immunising antigen and a keratanase II digested bovine nasal cartilage ABC core antigen. 2C6 and 7C4 show strong immunoreactivity with both keratanase II digested bovine corneal KSPGs and keratanase II digested BNC ABC core suggesting that these are keratanase II generated 'KS stub' mAbs. However, 1C3 and 11C4 only show reactivity with keratanase II digested bovine corneal KSPGs, indicating that these may be KSPG core protein mAbs as opposed to GAG mAbs.

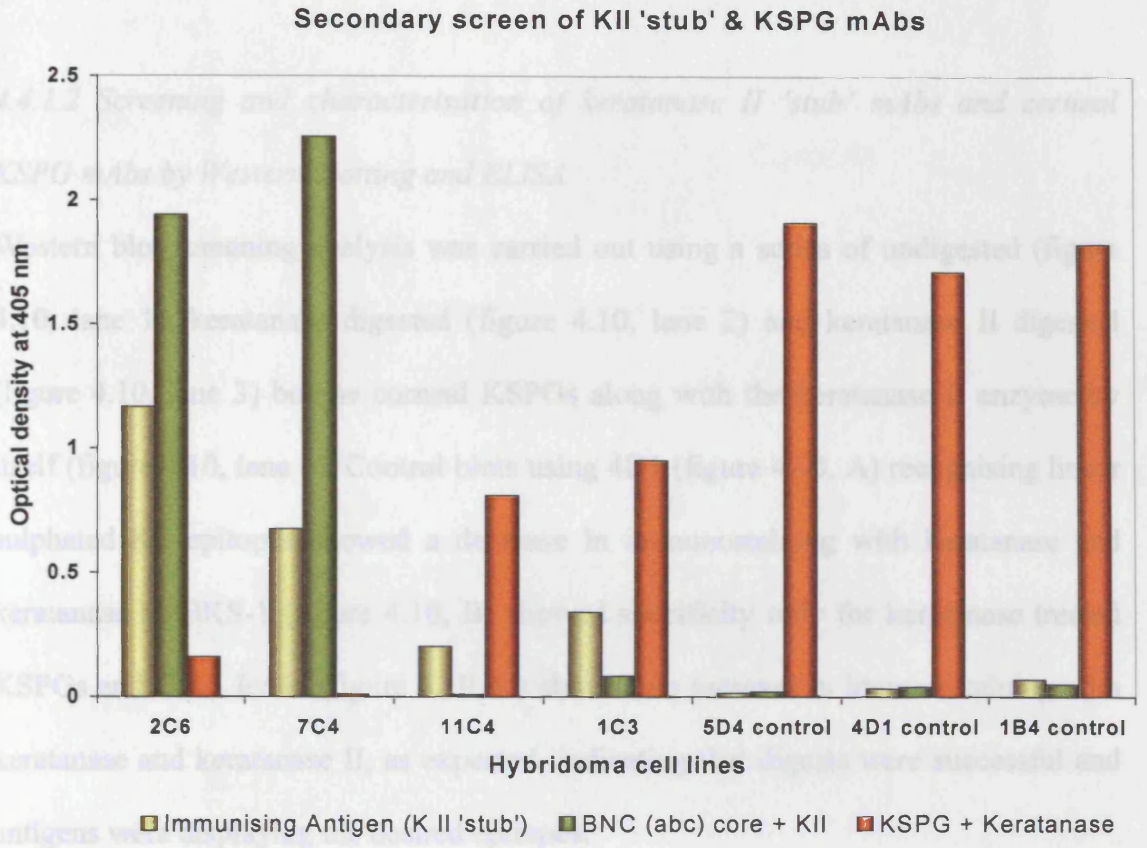

Figure 4.9 – Secondary screening using ELISA against keratanase II digested KSPGs, keratanase digested KSPGs and keratanase II digested BNC (ABC) core. 5D4, 4D1 and 1B4 were used as controls. 2C6 and 7C4 were specific for keratanase II generated 'KS stub' neoepitopes in both corneal and skeletal KS. 11C4 and 1C3 showed specific immunoreactivity with both keratanase and keratanase II digested bovine corneal PGs with no reactivity with BNC, indicating they were corneal KSPG core protein specific antibodies.

positive immunoreactivity remaining against keratanase digested antigens (figure 4.9). From these ELISA results 4 positive hybridomas (2C6, 7C4, 11C4 and 1C3) were selected and expanded for further analysis by Western blotting.

4.4.1.2 Screening and characterisation of keratanase II 'stub' mAbs and corneal KSPG mAbs by Western blotting and ELISA

Western blot screening analysis was carried out using a series of undigested (figure 4.10, lane 1), keratanase digested (figure 4.10, lane 2) and keratanase II digested (figure 4.10, lane 3) bovine corneal KSPGs along with the keratanase II enzyme by itself (figure 4.10, lane 4). Control blots using 4D1 (figure 4.10, A) recognising linear sulphated KS epitopes showed a decrease in immunostaining with keratanase and keratanase II, BKS-1 (figure 4.10, B) showed specificity only for keratanase treated KSPGs and GNA lectin (figure 4.10, C) showed an increase in immunostaining with keratanase and keratanase II, as expected, indicating that digests were successful and antigens were displaying the desired epitopes.

Western blot analysis using mAbs 11C4 and 1C3 (figure 4.10; D and E) on the partially purified corneal KSPGs, revealed staining of molecules with a molecular weight of ~60 – 100 kDa (lane 1; D and E). After keratanase digestion (figure 4.10, D and E, lane 2) these mAbs (11C4 and 1C3) were recognising molecules having molecular weights of 37 – 40 kDa and 50 – 60 kDa, respectively. After keratanase II digestion (figure 4.10, D and E, lane 3) the antibodies also recognised similarly sized products (11C4 recognising a 30 – 37 kDa molecule and 1C3 recognising a 45 – 55 kDa molecule). This data in conjunction with the ELISA data strongly suggests that these antibodies are recognising core protein epitopes within the KSPG populations present in corneal tissue and further more the two antibodies are recognising two different proteins. There was no immunoreactivity with the keratanase II enzyme ran

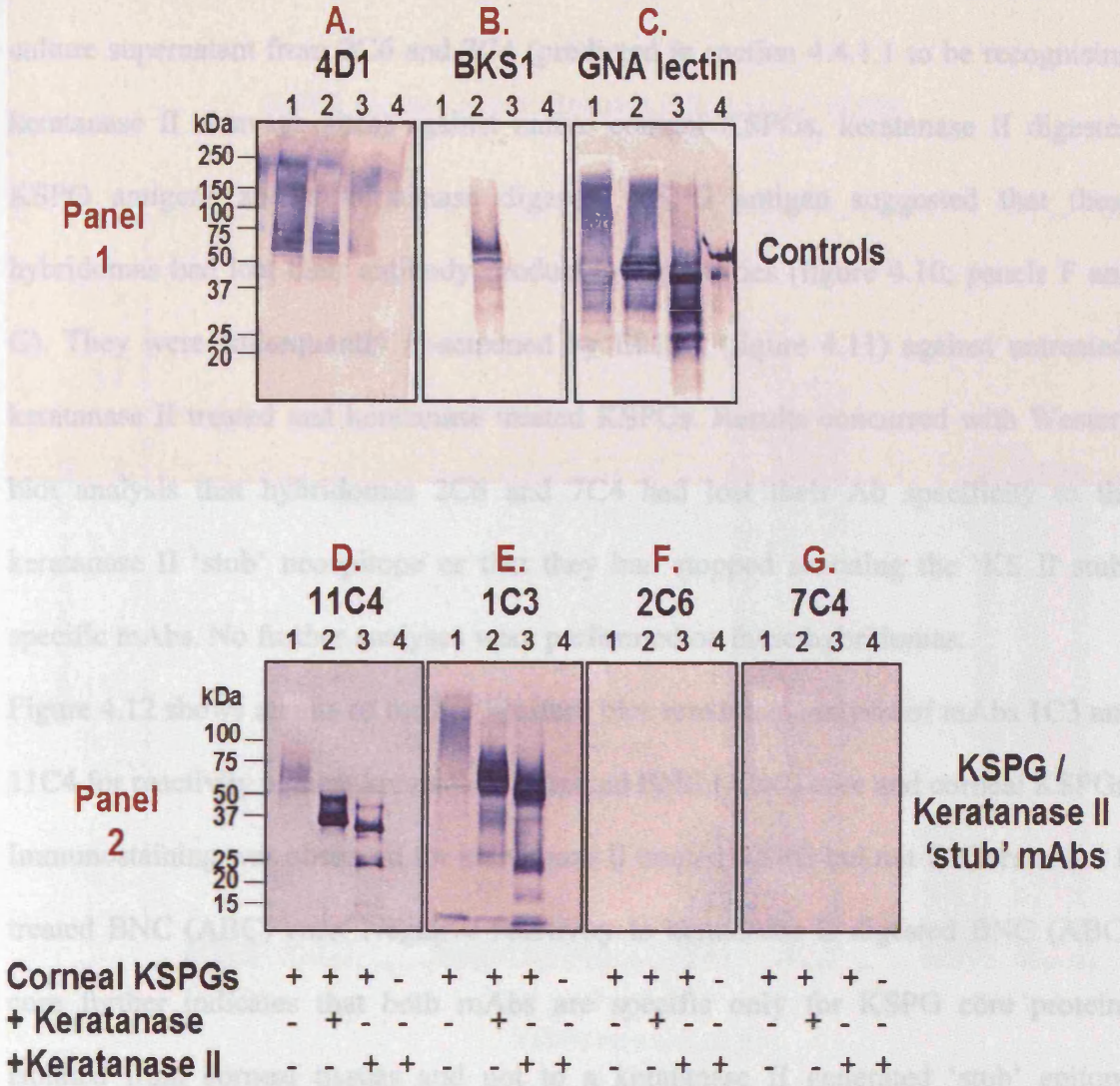

Figure 4.10 – Controls in panel 1 [4D1 (A), BKS1 (B) and GNA lectin (C)] show that the screening antigens have been digested appropriately (lane 1 = undigested corneal KSPGs, lane 2 = keratanase digested corneal KSPGs, lane 3 = keratanase II digested corneal KSPGs and lane 4 = keratanase II enzyme by itself). Panel 2, 11C4 and 1C3 (D and E) show positive immunoreactivity with both keratanase (lane 2) and keratanase II (lane 3) digested KSPGs at 2 different molecular weights (~37 kDa and ~50 kDa) indicating that they are recognising 2 distinct KSPG core proteins. 2C6 and 7C4 (F and G), the potential keratanase II 'KS stub' antibodies have lost reactivity for the epitope they were initially recognising in ELISA analysis.

on its own (figure 4.10, panel 2, D and E, lane 4).

Negative results obtained by Western blotting (figure 4.10; F and G) using hybridoma culture supernatant from 2C6 and 7C4 (predicted in section 4.4.1.1 to be recognising keratanase II cleavage sites) against native corneal KSPGs, keratanase II digested KSPG antigens and a keratanase digested KSPG antigen suggested that these hybridomas had lost their antibody producing capabilities (figure 4.10; panels F and G). They were subsequently re-screened by ELISA (figure 4.11) against untreated, keratanase II treated and keratanase treated KSPGs. Results concurred with Western blot analysis that hybridomas 2C6 and 7C4 had lost their Ab specificity to the keratanase II 'stub' neoepitope or that they had stopped secreting the 'KS II stub' specific mAbs. No further analyses were performed on these hybridomas.

Figure 4.12 shows results of further Western blot screening analysis of mAbs 1C3 and 11C4 for reactivity against keratanase II treated BNC (ABC) core and corneal KSPGs. Immunostaining was observed for keratanase II treated KSPG but not for keratanase II treated BNC (ABC) core. Negative reactivity to keratanase II digested BNC (ABC) core further indicates that both mAbs are specific only for KSPG core proteins isolated from corneal tissues and not to a keratanase II generated 'stub' epitope expected to also be present on aggrecan.

Preparations of purified bovine arterial lumican, bovine corneal lumican/mimecan, bovine corneal keratocan/lumican and bovine cartilage fibromodulin antigens, were obtained as a gift from Professor James Funderburgh, and used to definitively characterise 1C3 and 11C4 immunoreactivity to these specific KSPGs (figure 4.13). Samples were deglycosylated using a keratanase/keratanase II/endo-β-galactosidase mixture and 2μg loaded onto 15% slab gels for Western blot analysis with 1C3 and 11C4. 1C3 was shown to react with deglycosylated bovine arterial (figure 4.13, A, lane 1) and corneal lumican (figure 4.13, A, lanes 3 and 4) at ~50 kDa. 1C3 was

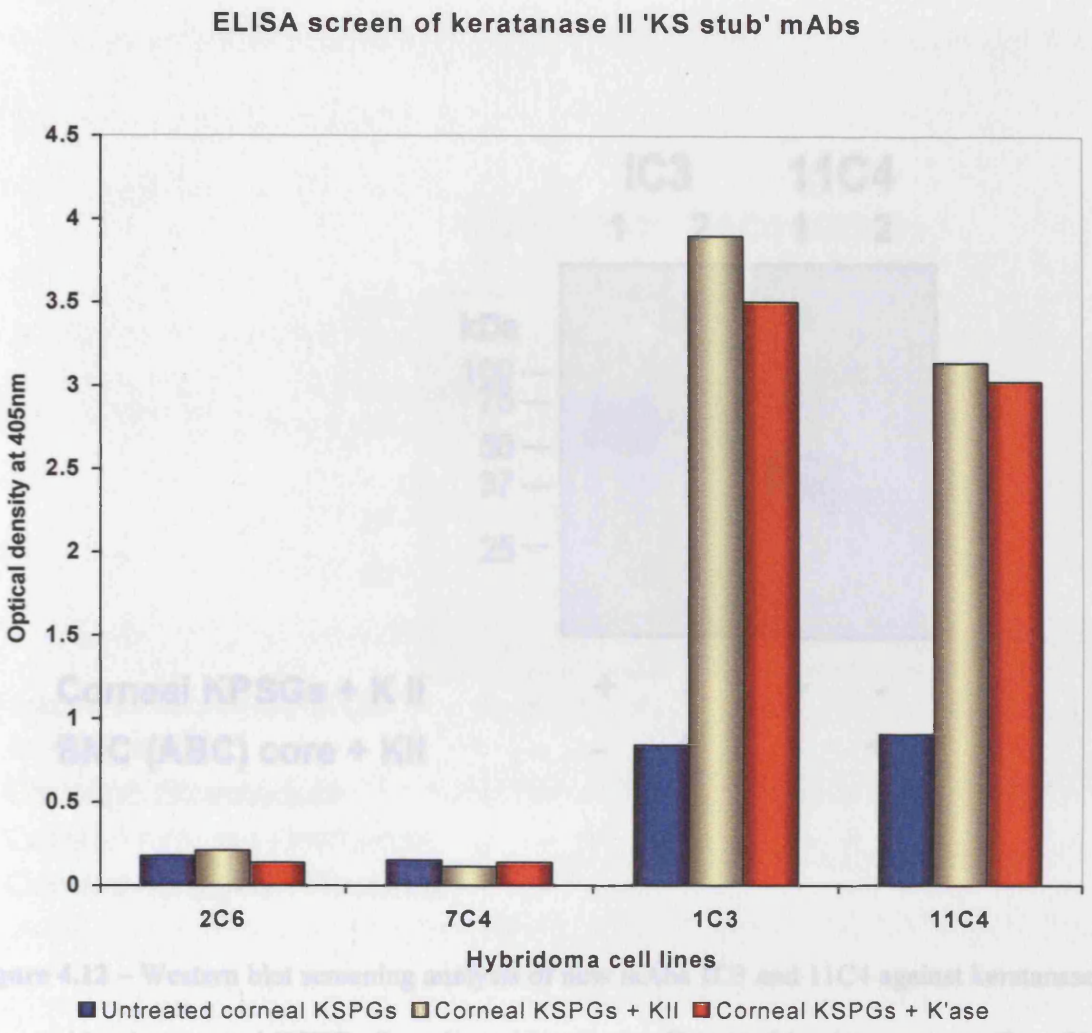

Figure 4.11 - Screen for keratanase II 'KS stub' mAbs against bovine corneal KSPGs, keratanase II digested bovine corneal KSPGs and keratanase digested bovine corneal KSPGs. Hybridomas from wells 2B6 and 7C4 appear to have lost their antibody producing capacity.

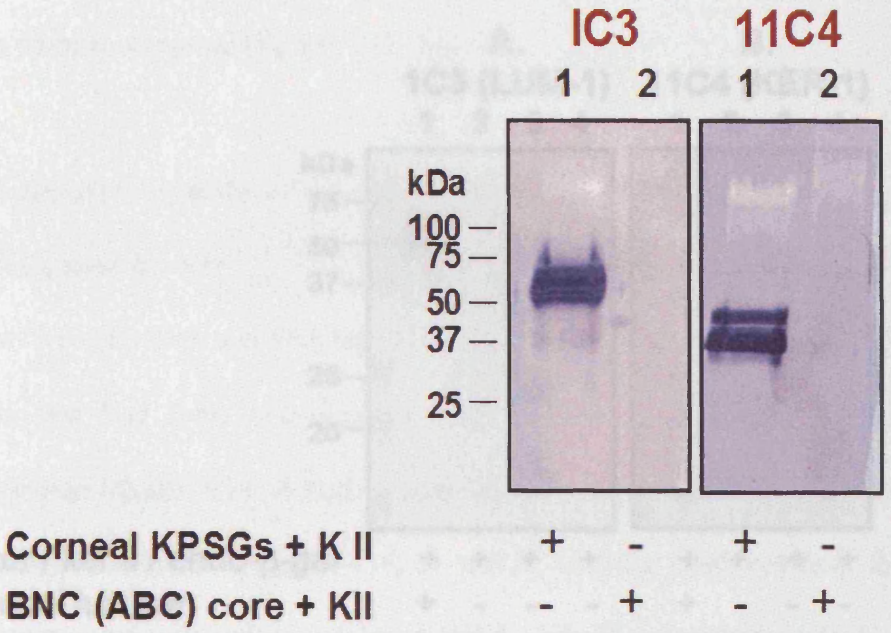

Figure 4.12 – Western blot screening analysis of new mAbs 1C3 and 11C4 against keratanase II treated bovine corneal KSPGs (lane 1) and keratanase II treated bovine aggrecan (lane 2). The results indicate that these mAbs are recognising corneal KSPG core protein epitopes and not a linear KS epitope or KS 'stub' neoepitope.

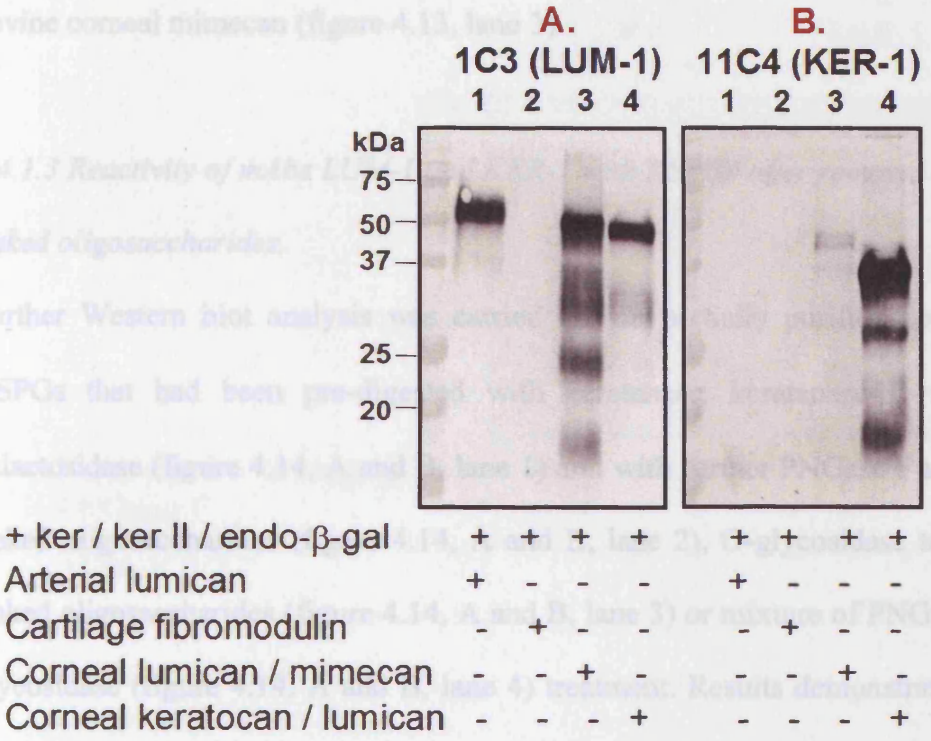

Figure 4.13 – Screening of LUM-1 and KER-1 using a range of KSPG antigens. LUM-1 was positive with bovine arterial lumican (A, lane 1), bovine corneal lumican / mimecan mix (A, lane 3) and with the bovine corneal keratocan / lumican mix (A, lane 4) at approximately 50 kDa. KER-1 was positive only with the bovine corneal keratocan / lumican mix (B, lane 4) at approximately 30 - 37 kDa. There was no immunoreactivity with either of the antibodies to bovine cartilage fibromodulin (A and B, lane 2).

subsequently named LUM-1 on account of its now defined specificity for lumican core protein. In contrast, 11C4 was shown to be specific for the deglycosylated bovine corneal keratocan at ~37 kDa (figure 4.13, B, lane 4). It was named KER-1 on account of its specific immunoreactivity with keratocan. There was no immunoreactivity with either antibody with bovine cartilage fibromodulin (figure 4.13, A and B, lane 2) or bovine corneal mimecan (figure 4.13, lane 3).

4.4.1.3 Reactivity of mAbs LUM-1 and KER-1 with KSPGs after removal of N- and O-linked oligosaccharides.

Further Western blot analysis was carried out on partially purified bovine corneal KSPGs that had been pre-digested with keratanase, keratanase II and endo-β-galactosidase (figure 4.14, A and B, lane 1) and with further PNGase F to remove N-linked oligosaccharides (figure 4.14, A and B, lane 2), O-glycosidase to remove O-linked oligosaccharides (figure 4.14, A and B, lane 3) or mixture of PNGase F and O-glycosidase (figure 4.14, A and B, lane 4) treatment. Results demonstrated that after removal of N- and O-linked oligosaccharides (A and B, lane 4) the LUM-1 and KER-1 mAbs were specifically recognising core protein epitopes, at molecular weights of ~37 kDa and ~30 kDa, respectively (Funderburgh & Conrad, 1990; Funderburgh *et al.,* 1993), and not keratanase II generated 'KS stub' linkage region neoepitopes or N- or O- linked oligosaccharides (figure 4.14).

4.4.1.4 Species cross-reactivity of mAbs KER-1 and LUM-1

LUM-1 and KER-1 were analysed for reactivity against cornea, cartilage and tendon proteoglycan extracts from a range of different species (bovine, human and pig) after keratanase and keratanase II digestion (figure 4.15). KER-1 showed strong reactivity with keratocan from bovine corneal tissue extracts and 18 month old bovine tensional

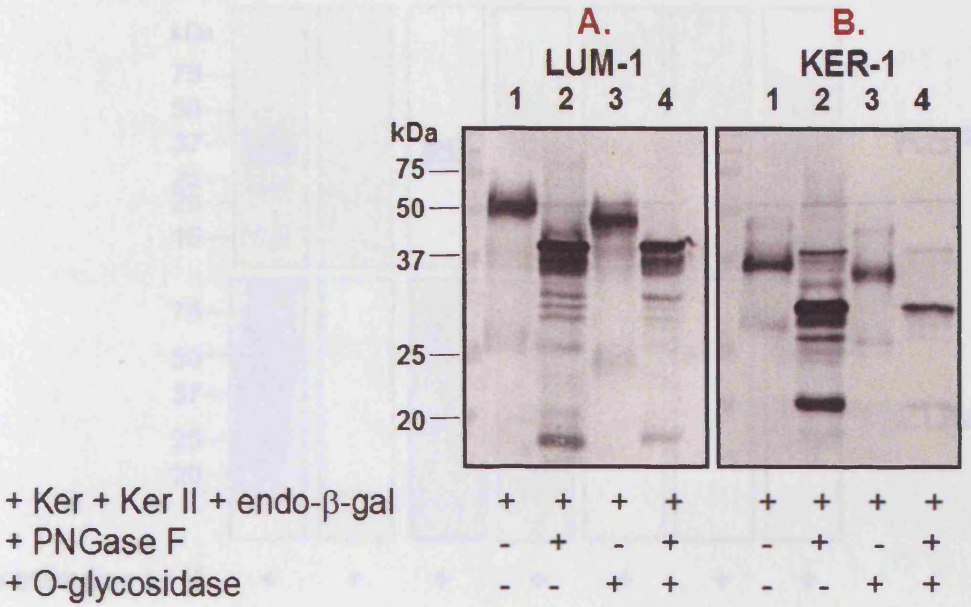

Figure 4.14 – Western blot analysis of LUM-1 and KER-1 reactivity and molecular weight shifts in lumican and keratocan after treatment with the three KS degrading enzymes alone (A and B, lane 1), with PNGase F to remove N-linked oligosaccharides (A and B, lane 2) with O-glycosidase (A and B, lane 3) and with a mixture of PNGase F and O-glycosidase (A and B, lane 4). The results conclusively demonstrate that mAbs LUM-1 and KER-1 are specific for lumican and keratocan core proteins and that they are not recognising any KS linkage region neoepitopes or N- or O- linked oligosaccharides. Core protein molecular weights of 37 kDa for lumican and 30 kDa for keratocan are in agreement with previously reported core protein sizes (Funderburgh & Conrad, 1990).

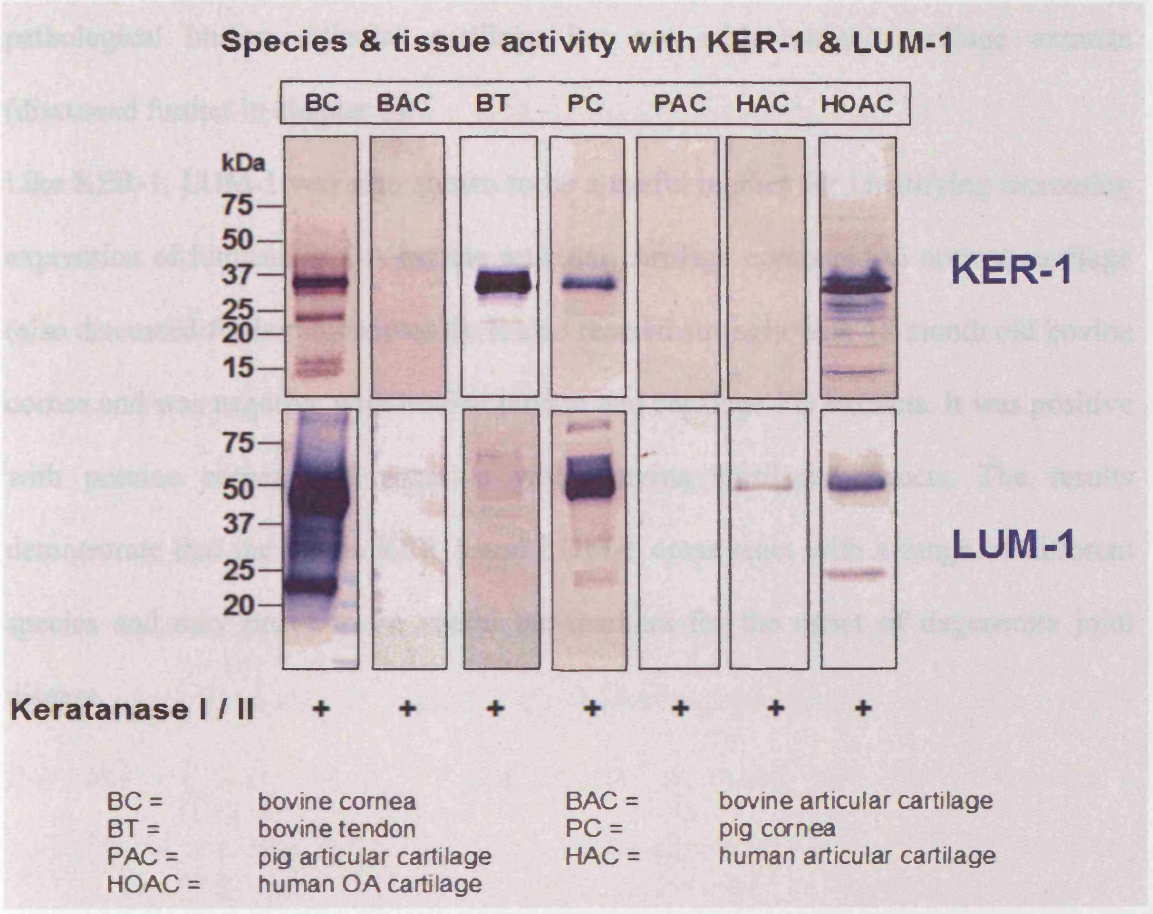

Figure 4.15 - Species reactivity of KER-1 and LUM-1 in Western blot analysis of KSPGs from bovine, porcine and human tissues. KER-1 reacted with keratocan present in bovine cornea and tendon, but not with bovine cartilage PG extracts. It also reacted with porcine cornea but not with porcine cartilage extracts. There was no reactivity with KER-1 in normal human articular cartilage, but it reacted strongly with osteoarthritic cartilage. LUM-1 only reacted with bovine cornea and was negative with tendon and cartilage PG extracts. It was positive with porcine cornea and negative with porcine cartilage extracts. There was weak LUM-1 reactivity with normal human articular cartilage and immunoreactivity was increased in OA cartilage.

tendon proteoglycan extracts, but was negative in extracts of 18 month old bovine cartilage. It reacted strongly with extracts of porcine cornea, but was negative in porcine cartilage. Interestingly it also reacted with keratocan extracted from pathological human articular cartilage but not with normal cartilage extracts (discussed further in chapter 6).

Like KER-1, LUM-1 was also shown to be a useful marker for identifying increasing expression of lumican in OA human articular cartilage compared to normal cartilage (also discussed further in chapter 6). It also reacted strongly with 18 month old bovine cornea and was negative with bovine tendon and cartilage PG extracts. It was positive with porcine cornea and negative with porcine cartilage extracts. The results demonstrate that the mAbs KER-1 and LUM-1 cross react with a range of different species and may prove to be useful bio-markers for the onset of degenerate joint disease.

4.5 Discussion

The aim of the work described in this chapter was to produce monoclonal antibodies to either the keratanase II generated 'KS stub' neoepitope on keratan sulphate chains or to KSPG core protein epitopes. Bovine corneas were used as a source of KS containing proteoglycans because they contained high levels of KSPGs and were therefore a rich source of KS chains. An antigen was therefore used that had potential to make a number of very useful monoclonal antibodies to both KSPG core protein epitopes and to keratanase II generated KS 'stub' neoepitopes. Keratanase II is a commercially available keratan sulphate degrading enzyme that cleaves the chain at β1-3 linkages between N-acetylglucosamine and galactose, where the disaccharide structure is either monosulphated on the N-acetylglucosamine or disulphated on both residues (see chapter 2, section 2.3.1; Oguma *et al*, 2001; Yamagishi *et al*, 2003). It would therefore remove all sulphated disaccharides from the KS chain, leaving only non-sulphated disaccharide domains on the remaining KS 'stubs', making a keratanase II generated KS 'stub' mAb a potentially important antibody for analysing KS sulphation patterns. The experiments described in this chapter detail the production of a number of antibodies by partially purifying a selected keratanase II digested bovine corneal KSPG antigen through a series of Resource Q anion exchange and Sephacryl S-200 size exclusion chromatographic steps and using the partially purified antigen for immunisation. This antigen preparation was also predicted to contain keratocan, lumican and mimecan core proteins. Resource Q anion exchange chromatography was used initially to separate the negatively charged corneal proteoglycans from other matrix proteins. Pooled sulphated PGs were then chondroitinase ABC digested to reduce the molecular weight of CS/DSPGs compared to native KSPGs. Size exclusion chromatography separated the CS/DSPGs core proteins from the high molecular weight KSPGs which were then keratanase II

digested. Size exclusion chromatography removed the keratanase II enzyme leaving a partially purified KSPG 'stub' antigen mixture. The antibodies produced to this antigen were characterised by ELISA and Western blot analysis (figures 4.8 – 4.15), which demonstrated that the experiments were successful in producing two antibodies to two different corneal KSPG core protein epitopes, lumican and keratocan. These antibodies were designated LUM-1 and KER-1, respectively. Removal of N- and O-linked oligosaccharides (figure 4.14) did not affect LUM-1 or KER-1 recognition capabilities, indicating that the antibodies were recognising KSPG core protein epitopes and not oligosaccharide side chain epitopes or a combination of both core protein and carbohydrate attachments. Keratan sulphate side chains would also have been removed by PNGase F in corneal KSPGs (see chapter 2, section 2.4.1.3, figure 2.17), therefore these monoclonal antibodies were not recognising a KS chain or KS linkage region epitope.

The procedure was also successful in producing two different mAbs (2C6 and 7C4) to a keratanase II generated non-reducing terminal Gal or Gal-6-S neoepitope. However, these cell lines were found to be unstable and failed to maintain antibody production. None-the-less, these antibodies did demonstrate that it was possible to generate such mAbs which could be useful tools in future analysis of KS structure.

4.6 Chapter summary

- An antigen was prepared using a keratanase II digested bovine corneal KSPG extract that was partially-purified using anion exchange and size exclusion chromatography.
- The antigen was used in immunisation to produce monoclonal antibodies to both the keratanase II generated 'stub' neoepitope, and to protein epitopes on corneal KSPG core proteins.
- Antibody specificity was determined by screening using a range of differentially deglycosylated KSPGs from cartilage and cornea.
- Keratanase II 'stub' mAb cell lines (2C6 and 7C4) were unstable and failed to maintain production of antibodies recognising the keratanase II generated 'KS stub' neoepitope.
- KSPG protein core mAbs were shown to be specific for lumican and keratocan, and were designated LUM-1 and KER-1, respectively.
- LUM-1 and KER-1 were shown to cross react with a number of different species.

Chapter 5 – Applications of BKS-1, LUM-1 and KER-1 monoclonal antibodies

5.1 Introduction

Chapters 2 and 3 detailed the production of three new mAbs, one that recognises a keratanase generated 'stub' neoepitope on KS (BKS-1) and two that recognise protein core epitopes on two of the KS-substituted small leucine rich proteoglycans (SLRPs) commonly found in cornea, lumican and keratocan (mAbs LUM-1 and KER-1, respectively). The aim of this chapter was to provide some examples of useful applications for mAbs BKS-1, LUM-1 and KER-1 in the analysis of KSPG metabolism in biological tissue samples.

5.2 Materials

All chemicals were of analytical grade and were purchased from Sigma-Aldrich unless otherwise stated. A comprehensive catalogue of materials and suppliers used throughout this project is listed in Appendix A. All enzymes and related buffers were as described in chapter 2, section 2.2.2 and table 2.3. SDS-PAGE and Western blotting material was the same as described in chapter 2, section 2.2.1 and table 2.3. Bovine corneas were obtained from a local abattoir. Normal and pathological human corneas were obtained from Dr Saeed Akthar, School of Ophthalmology and Vision Science, Cardiff University.

5.3 Methods

5.3.1 Analysis of KS substitution on lumican and keratocan from bovine cornea using BKS-1, LUM-1 and KER-1

50 μg GAG samples of partially purified bovine corneal PG extracts, prepared as described in chapter 4 section 4.2.2, were digested with 80 mU of keratanase per mg GAG (see section 2.3.1) in 0.1 M Tris acetate pH 6.8 for 24 hours at 37 ° C, followed by digestion using endo-β-galactosidase (8 mU per mg GAG) and keratanase II (6 mU per mg GAG). Equal GAG concentrations (3 μg – pre-digestion equivalent concentrations) of undigested and keratanase followed by endo-β-galactosidase and keratanase II digested bovine KSPGs were reduced using 10% (v/v) β-mercaptoethanol and loaded onto 12% slab gels as described previously in section 2.2.3.1. Gels were transferred and Western blot analysis carried out using mAbs LUM-1, KER-1 (see chapter 4), BKS-1 [recognising a keratanase generated KS 'stub' neoepitope] (see chapter 2) and 5D4 [recognising linear sulphated poly-N-acetyl-lactosamine motifs within KS chain structures] to analyse the level of KS substitution on keratocan and lumican in the bovine corneal PG extract.

5.3.2 Analysis of KS quantities in human cornea, limbus and sclera using mAb BKS-1 compared to mAb 5D4

Normal human cornea, limbus and sclera were obtained from Dr Saeed Akthar, Department of Opthamology and Vision Science, Cardiff University. The tissue sample was diced, extracted and partially purified as described for bovine cornea in chapter 4, section 4.2.2. Extracts were dialysed to Milli Q™ water and DMMB analysis carried out to determine GAG content. 3 μg GAG samples each of corneal, limbal and scleral extracts were left undigested for Western blot analysis with mAb 5D4 or digested with

80 mU of keratanase per mg GAG for Western blot analysis with mAb BKS-1. Samples were run on 4 – 20% Tris glycine gradient gels at 100 volts for 1.5 hours as described in section 2.2.3.1. Blots were transferred and probed with mAbs 5D4 and BKS-1 to analyse differential staining patterns of BKS-1 compared to 5D4.

5.3.3 Western blot analysis of normal versus pathological human cornea using mAbs BKS-1, 5D4, LUM-1 and KER-1

Pathological human cornea was obtained from Dr Saeed Akthar, Dept. of Ophthalmology and Vision Science, Cardiff University. Partially-purified corneal PGs were prepared for analysis as described in chapter 4, section 4.2.2 and DMMB analysis carried out to measure GAG content. 2 μg equivalent GAG samples of pathological human corneal PG extracts were analysed by SDS PAGE and Western blotting on 4 - 20% Tris glycine gradient gels, using mAbs LUM-1, KER-1, BKS-1 and 5D4 after deglycosylation using keratanase. 2 μg GAG samples of normal human corneal PG extracts were also analysed by Western blotting using these mAbs for comparison to the pathological human corneal extracts.

5.4 Results

5.4.1 BKS-1 – a useful monoclonal antibody for analysing variations in quantities of KS substitution on different proteoglycans from within a tissue extract

Western blot analysis of bovine corneal PG extracts demonstrated the presence of lumican at ~50 kDa and keratocan at ~30 kDa as expected after keratanase digestion followed by keratanase II and endo-β-galactosidase digestion and prior to the removal of N- or O-linked oligosaccharide side chains (figure 5.1). Interestingly, BKS-1 also showed a sharp band at ~50 kDa, corresponding to the same molecular weight as lumican (~50 kDa, see figure 5.1), indicating that lumican in this preparation was highly substituted with keratanase susceptible KS, i.e. a large proportion of mono-sulphated disaccharides. There was also very weak BKS-1 reactivity at corresponding molecular weight to keratocan, indicated at ~30 kDa in figure 5.1. This suggests that the keratocan in this particular preparation was either very mildly substituted with KS, or that any KS on that keratocan was largely di-sulphated or non-sulphated and therefore not initially keratanase susceptible.

5.4.2 BKS-1 – a useful monoclonal antibody for analysing variations in quantities of KS from different tissue extracts - a comparison to 5D4

Western blot analysis of PG extracts from normal human cornea, limbus and sclera from the eye demonstrated that BKS-1 was a more sensitive monoclonal antibody compared to 5D4 for analysis of KS quantities from different tissues. BKS-1 staining showed a much more subtle distribution of staining than 5D4 (figure 5.2). BKS-1 allows the observation that the cornea contains more KS than the sclera per 3μg GAG loaded, with lowest levels of KS present in the limbus. 5D4 showed a much more diffuse staining pattern, with little indication of differences in KS quantities within the cornea, limbus or sclera.

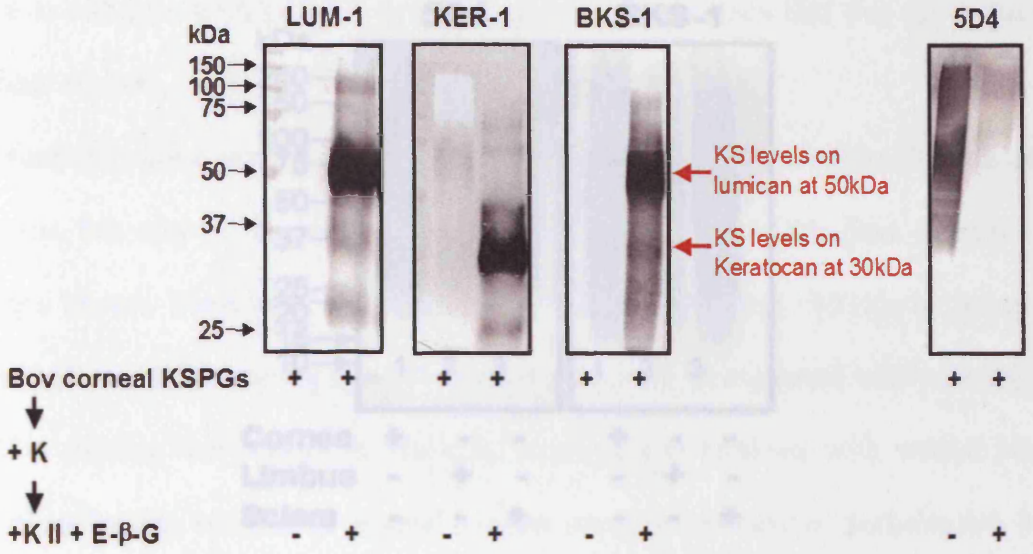

Figure 5.1 Western blot demonstration of the effectiveness of novel mAb BKS-1 in analysis of KS substitution and sulphation patterns on different KSPGs in bovine corneal PG extracts compared to 5D4 immunostaining.

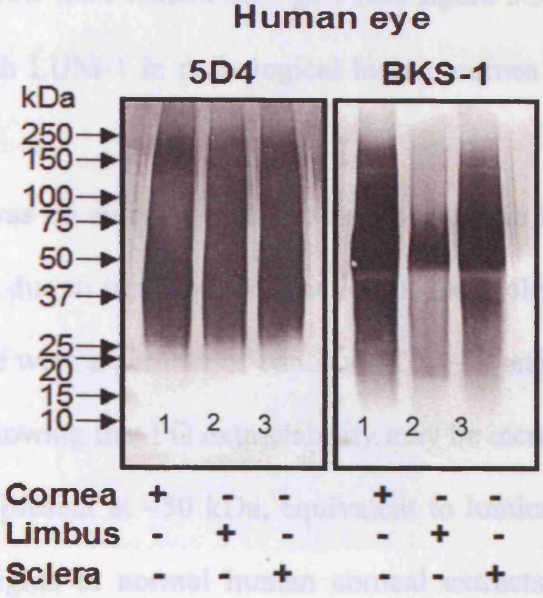

Figure 5.2 BKS-1 shows a more subtle distribution of staining in comparison to 5D4. It demonstrates differences in KS quantities within the cornea, limbus and sclera, whereas 5D4 does not.

5.4.3 LUM-1, KER-1 and BKS-1 analysis of normal versus pathological human cornea

The newly generated mAbs were also used in analysis of normal human corneal PG extracts compared to pathological human corneal PG extracts. Lumican levels were increased from normal to pathological human corneas at ~50 kDa when volumes equivalent to 2 μg GAG were loaded onto gels (see figure 5.3). There was also a weak band at ~25 kDa with LUM-1 in pathological human cornea that was not apparent in normal extracts.

Interestingly, there was no staining with the keratocan mAb in normal human corneal extracts, this may be due to inefficient extraction of the molecule from normal human corneal tissues. There were a number of bands at ~25, ~27 and ~30 kDa in pathological cornea (figure 5.3) showing that PG extractability may be increased with pathology.

BKS-1 staining was present at ~50 kDa, equivalent to lumican, with weaker bands at lower molecular weights in normal human corneal extracts. In pathological human corneal extracts BKS-1 staining was in the form of a diffuse band. One possible reason for such a diffuse smear here is that pathological human corneal KS may be much more highly sulphated towards the linkage region of the KS chain than normal human corneal KS, making it less keratanase susceptible at these di-sulphated domain regions therefore leaving larger 'stubs' on the KS chain from pathological tissue compared to normal tissue. This would the electrophoretic mobility of the pathological KSPG samples causing them to drag more into the gel causing the diffuse staining pattern observed in figure 5.3.

5D4 staining appeared as large molecular weight smear (37 – 300 kDa) in normal corneal extracts with a shift downwards in molecular weight (20 - 250 kDa) in pathological corneal tissue extracts, possibly due to the presence of KS on the proteoglycan breakdown products observed with LUM-1 and KER-1 immunostaining.

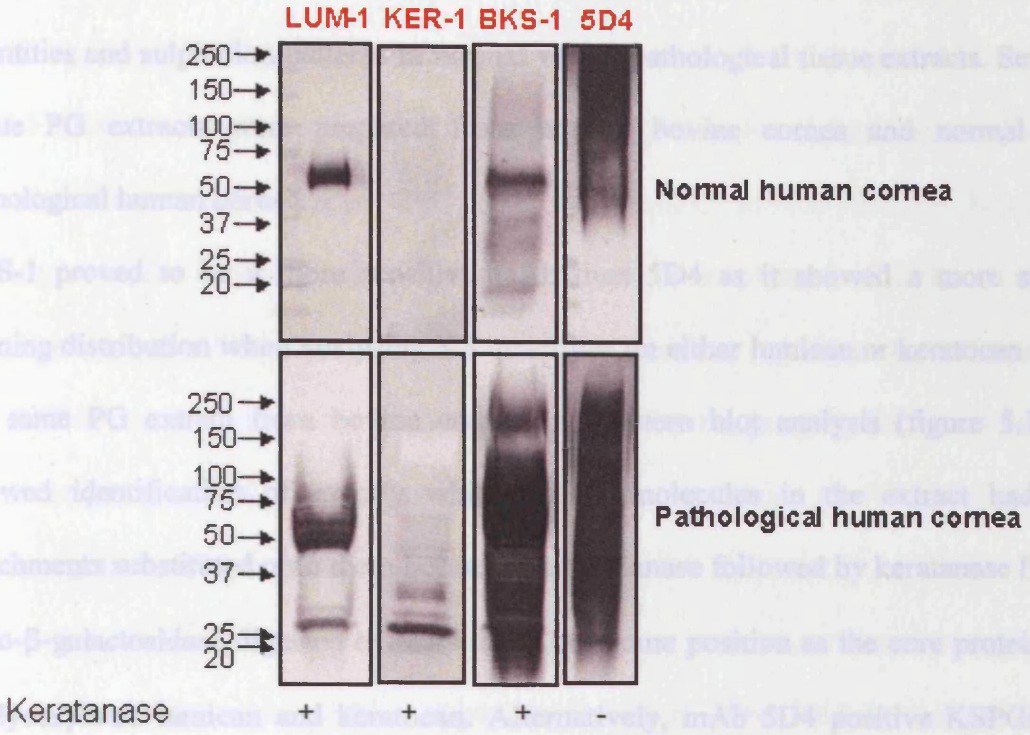

Figure 5.3 Lumican, keratocan and KS concentrations in normal versus pathological human corneal PG extracts.

5.5 Discussion

The aim of chapter 5 was to provide some examples of applications of all three newly generated mAbs (LUM-1, KER-1 and BKS-1), and to compare BKS-1 immunoreactivity to 5D4 reactivity in the analysis of variations in KSPG and KS quantities and sulphation patterns in normal versus pathological tissue extracts. Several tissue PG extracts were prepared from normal bovine cornea and normal and pathological human cornea.

BKS-1 proved to be a more sensitive mAb than 5D4 as it showed a more subtle staining distribution when analysing KS quantities on either lumican or keratocan from the same PG extract from bovine cornea in Western blot analysis (figure 5.1). It allowed identification of exactly which KSPG molecules in the extract had KS attachments substituted onto them because the keratanase followed by keratanase II and endo-β-galactosidase digested extracts ran to the same position as the core proteins of deglycosylated lumican and keratocan. Alternatively, mAb 5D4 positive KSPGs ran into the gel as a smear (before digestion) due to the presence of the large sulphated KS side chains recognised as strong 5D4 immunoreactivity. Also, 5D4 staining was abolished after deglycosylation using keratanase, endo-β-galactosidase and keratanase II, enzymes which facilitated mAb BKS-1 recognition and reduced the molecular heterogeneity of the KSPGs. MAb 5D4 did not allow for specific identification of which molecules contained KS GAGs. However, BKS-1 proved to be a more specific mAb for analysis of KS substitution on different KSPGs from the same tissue extract. The results show the importance of using BKS-1 as an antibody in analysis of differential KS substitution on different KSPGs and how this GAG substitution pattern may change with development, age and disease. These applications could also be utilised in analysis of tissues other than corneal KSPGs. For example, mAb BKS-1 can be used, in conjunction with the related CS 'stub' antibodies 2B6, 3B3 and 1B5, and N-

terminal sequence analysis of trypsin digested aggrecan core protein to determine the differential substitution of KS in different aged cartilage tissues. This analysis would help definitively identify the sites of KS substitution compared to the sites of CS substitution, and precisely how these substitutions change with age (reviewed in chapter 1, section 1.5.1) when there is an observed increase in KS compared to CS.

BKS-1 was also used to compare 5D4 staining in PG extracts from normal human cornea, sclera and limbus (figure 5.2). Again, this antibody proved BKS-1 to be a more specific mAb for identification of KS quantities in these extracts of different ocular tissues where mAb 5D4 staining did not show differences; i.e. these studies indicated that BKS-1 was shown to be a more sensitive antibody for gauging KS quantities in a tissue compared to 5D4 because it recognises just one neoepitope per KS chain whereas 5D4 recognises multiple epitopes on a single KS chain.

BKS-1 was also useful in the analysis of KS sulphation patterns in normal compared to pathological human corneal PG extracts compared to 5D4. BKS-1 staining in the normal human cornea showed that KS was substituted onto a molecule of about ~50 kDa, equivalent to the molecular weight of deglycosylated lumican. There was much weaker staining at ~20, ~30 and ~37 kDa. In pathological corneal extracts, BKS-1 staining formed a diffuse smear of between 20 – 200 kDa. This diffuse pattern may result from an increase in sulphation of KS chains towards the linkage region in pathological tissue making them less keratanase susceptible in these areas. This may help to explain the large smear observed after keratanase digestion due to the longer disulphated 'stub' regions remaining after such treatment. The positive 5D4 staining in pathological corneal extracts supports the hypothesis that these 'stub' structures are the result of sulphated domains opposed to non-sulphated domains as the 5D4 recognises linear sulphated poly-N-acetyl-lactosamine regions. The results show how BKS-1 can

be used in combination with 5D4 to give information on sulphation patterns within the KS chain in different tissues.

MAb LUM-1 showed that there was an increased level of lumican and a number of breakdown products in pathological compared to normal human corneas. KER-1 staining was negative in normal human corneal extracts. This may be due to problems with extracting this particular molecule from normal human cornea. KER-1 staining was positive at ~25, ~27 and ~30 kDa in pathological corneal extracts, indicating that keratocan extraction is allowed from this tissue.

5.6 Chapter summary

- Monoclonal antibodies BKS-1 and 5D4 were used in Western blot analysis of bovine corneal and human corneal, limbal and scleral PG extracts, to observe KS sulphation patterns and variations in levels of KS substituted onto the KSPG molecules in health and disease.
- BKS-1 immunostaining of bovine corneal PGs was able to distinguish that lumican, identified using mAb LUM-1, was more highly substituted with keratanase susceptible KS than keratocan, i.e. the KS present on the extracted lumican was largely mono-sulphated, whereas any KS present on the extracted keratocan may have been either largely di-sulphated or non-sulphated and therefore not susceptible to the initial keratanase digestion.
- BKS-1 staining showed a more subtle staining distribution in normal human corneal, limbal and scleral PG extracts compared to 5D4 where staining was more diffuse. BKS-1 allowed identification of variations in levels of KS substitution in different tissues.
- Lumican staining was increased in pathological compared to normal human corneas showing a number of lower molecular weight breakdown products.
- Extraction of keratocan from normal human cornea appeared to be inefficient and staining was negative with KER-1 in Western blotting.
- In contrast keratocan was extractable from pathological human corneas using the same extraction procedures where a number of bands were observed at ~25, ~27 and ~30 kDa.

Chapter 6 – Lumican and keratocan expression in normal and pathological human articular cartilage and intervertebral disc

6.1 Introduction

The functional stability of articular cartilage and intervertebral disc (IvD) tissues is sustained by the interactions of a large range of matrix molecules that are produced by the chondrocytes and disc tissue cells that are present there. These include collagens, proteoglycans and matrix proteins (reviewed in chapter 1). Whilst aggrecan provides a negatively charged environment through its CS and KS side chain attachments, that maintains a highly hydrated tissue, SLRPs such as decorin, biglycan, fibromodulin and lumican interact with each other and other matrix molecules to provide a stable structural environment where they are involved in collagen fibril assembly, cell adhesion and growth factor regulation (reviewed by Iozzo, 1999). Osteoarthritis is a disease that affects the functional capacity of cartilage primarily in hip and knee joints. It occurs as a result of biochemical abnormalities, inflammation and mechanical changes. During osteoarthritis and disc degeneration, changes in abundance and integrity of the matrix molecules cause the extracellular matrix to become disorganised and disrupted with increased water content (Buckwalter & Mankin, 1998). A range of proteases, which have not yet been fully identified, target the various matrix molecules present in the cartilage. Several enzymes have been identified that are responsible for degradation of aggrecan in these diseases; e.g. aggrecanases (ADAMTS-4 & -5) and MMPs; however, little is known about the roles of the KS SLRPs present there and any proteases responsible for their degradation in pathological conditions.

Lumican and keratocan are two small leucine rich keratan sulphate proteoglycans that are usually found in high levels in the cornea where they are thought to influence the regulation of collagen fibril diameter and interfibrillar spacing to endow an ordered and transparent corneal stromal structure that allows the passage of light through the

eye (reviewed in chapter 1). The presence of lumican has been previously reported in many tissues other than cornea such as cartilage, bone, aorta, sclera, IvD, skin, muscle, lung, amniotic membrane, kidney and teeth (Funderburgh *et al.,* 1987; Funderburgh & Conrad, 1989; Funderburgh *et al.,* 1991 B; Grover *et al.,* 1995; Cheng *et al.,* 1996; Cs-Szabo *et al.,* 1997; Chakravarti *et al.,* 1998; Knudson & Knudson, 2001, review; Raouf *et al.,* 2002; Chakravarti, 2003; Young *et al.,* 2005 A). An increased expression of lumican at the mRNA and protein level has been observed in pathological human articular cartilage compared to normal cartilage (Grover *et al.,* 1995; Cs-Szabo *et al.,* 1997) and in experimental animal models of OA (Young *et al.,* 2005 A). An increase in lumican protein levels has been demonstrated in the annulus fibrosis of human IvD with increasing age (Sztrolovics *et al.,* 1999 A). However, little is known about the molecular or proteomic changes in lumican expression that occur in human IvD degeneration (Urban & Roberts, 2003). In adult tissues keratocan expression has so far been reported as being largely "cornea specific" (Conrad & Conrad, 2003; Carlson *et al.,* 2005; Kawakita *et al.,* 2005) although expression has been demonstrated in the developing avian ocular tissues and nephrogenic mesenchymes where it has been proposed to have a role in embryonic cell migrations (Conrad & Conrad, 2003).

The aims of this chapter were to comprehensively examine the changes in expression of both lumican and keratocan, at the proteomic and molecular level, in human articular cartilage and intervertebral disc tissues in health and disease.

6.2 Materials

All chemicals were of analytical grade and were purchased from Sigma-Aldrich unless otherwise stated. A comprehensive catalogue of materials and suppliers used throughout this project is listed in Appendix A. All enzymes and related buffers were as described in chapter 2, section 2.2.3 and table 2.3. SDS-PAGE and Western blotting material was the same as that described in chapter 2, section 2.2.5 and table 2.3. All DMMB material was the same as that described in chapter 2, section 2.2.2 and table 2.3. A Bicinchoninic Acid (BCA) protein assay reagent kit was obtained from Pierce. Tri reagent and Chloroform ($CHCl_3$) were obtained from Sigma-Aldrich. RNeasy mini kit for isolation of RNA was obtained from Qiagen, UK. Oligonucleotide primers were from Invitrogen. RNA PCR kits containing GeneAmp, 10 x PCR buffer II (100 mM Tris-HCl pH 8.3; 500 mM KCl), $MgCl_2$ (25 mM solution), dNTPs (dATP, dCTP, dGTP, dTTP, all at a concentration of 10 mM), Rnase inhibitor, MuLV reverse transcriptase and oligo d(T) for RT-PCR reactions were all obtained from Applied Biosystems, UK. Taq DNA polymerase was from Promega. DNA molecular markers, 6x tracking dye and ethidium bromide were from Cambio, Cambridge, UK. Agarose (genetic technology grade) was from MP Biomedicals. QIA quick PCR purification kit for purification of PCR reaction products for sequencing was obtained from Qiagen, UK. Big dye terminator v1.1 cycle sequencing kit was from Applied Biosystems. Technegene thermal cycler for RT-PCR reactions was obtained from Techne, UK. An UltroSpec 2000 spectrophotometer was obtained from Amersham Pharmacia Biotech, UK.

6.2.1 Tissues for extraction of RNA and matrix proteoglycans

Normal human hip cartilage (n = 5) was obtained post operatively from the University Hospital of Wales, Cardiff within 5 hours of surgical procedures from patients

undergoing hip replacements due to hip fracture caused by osteoporosis. Osteoarthritic human hip cartilage (n = 7) and knee cartilage (n = 10) from similarly aged patients were obtained from Llandough Hospital, Cardiff within 5 hours of surgery from patients undergoing hip and knee replacement surgery. The degree of degeneration of the articular cartilage samples was graded at the hospitals based on methods previously described by Kellgren & Lawrence in 1957. OA grading was carried out by Dr Kedar Deogaonkar, Clinical Research Fellow, Dept of Orthopaedics, University Hospital of Wales, Cardiff, and was based as follows:

Grade 0: No features

Grade 1: Doubtful: minute osteophytes, doubtful significance and narrowing of the joint space, possible osteophytes lipping.

Grade 2: Minimal: definite osteophytes formation, unimpaired joint space and possible narrowing of joint space.

Grade 3: Moderate: moderate diminution of joint space, moderate multiple osteophytes formation, definite narrowing of joint space, some sclerosis and possible deformity of bone contour.

Grade 4: Severe: joint space greatly impaired, sclerosis of subchondral bone, large osteophytes formation, marked narrowing of joint space, severe sclerosis and definite deformity of bone contour.

(Kellgren & Lawrence, 1957).

Normal intervertebral discs from patients with Scoliosis (n = 2) and degenerate IvD (n = 5) from patients with different grades (I - V) of disc degeneration determined using a method described by Pfirrmann et al., (2001) were obtained from the University Hospital of Wales and Llandough Hospitals following surgical procedures. Samples

were graded from MRI scans again by Dr Kedar Deogaonkar, Clinical Research Fellow, Dept of Orthopaedics, University Hospital of Wales, as follows:

Grade I: Homogeneous in structure, bright white, distinction of nucleus and annulus is clear, signal intensity was hyperintense and isointense to cerebrospinal fluid, height of IvD is normal.

Grade II: Inhomogeneous in structure with or without horizontal bands, distinction of nucleus and annulus is clear, signal intensity was hyperintense and isointense to cerebrospinal fluid, height of IvD is normal.

Grade III: Inhomogeneous in structure, gray in colour, distinction of nucleus and annulus is not clear, signal intensity was intermediate, height of IvD is normal or slightly decreased.

Grade IV: Inhomogeneous in structure, gray to black in colour, distinction of nucleus and annulus is lost, signal intensity was intermediate to hypointense, height of IvD is normal or moderately decreased.

Grade V: Inhomogeneous in structure, black in colour, distinction of nucleus and annulus is completely lost, signal intensity was hypointense and IvD space is collapsed.

(Pfirrmann *et al.*, 2001).

All samples were collected with patient consent and ethical approval. Patient numbers, age, sex and grade of degeneration are listed in table 6.1.

Articular cartilage	Patient number	X-ray grading of OA	Age	Sex
Normal hip	1	0	83	F
	33	0	92	F
	34	0	81	F
	35	0	69	F
	36	0	89	F
OA hip	8	4	76	M
	9	3	73	M
	11	3	33	F
	12	4	75	F
	20	4	69	F
	23	4	83	M
	24	4	67	F
OA knee	3	4	80	F
	5	3	60	M
	6	3	79	M
	7	4	51	F
	10	4	82	M
	13	3	82	M
	14	3	76	M
	19	3	70	F
	21	4	84	M
	22	4	54	M
IvD	**Patient number**	**MRI grade of degeneration**	**Age**	**Sex**
Normal IvD	25	I	14	F
	26	I	13	F
Degenerate IvD	4	III	27	M
	15	IV	34	F
	16	IV	41	F
	17	V	54	F
	18	IV	43	M

Table 6.1 Normal and Osteoarthritic articular cartilage and normal and degenerate IvD samples collected for analysis by Western blotting and RT-PCR.

6.3 Methods

6.3.1 Lumican and keratocan mRNA expression in normal and OA human cartilage

6.3.1.1 RNA isolation

For the amplification of human complementary DNA (cDNA), total RNA was isolated from weight bearing areas of normal human hip (patient numbers: 1, 33, 34, 35 and 36, see table 6.1) and pathological (patient numbers: 3, 5, 6, 7, 8, 14, 19, 20, 21, 22, 23 and 24, see table 6.1) human hip and knee cartilage samples. Approximately 100 mg cartilage cuttings were initially weighed, snap frozen in liquid nitrogen and homogenised for 1 minute at 2,000 rpm in liquid nitrogen chilled Braun Mikro-Dismembrator Vessel (B.Braun Biotech International GmbH). 1 ml of Tri reagent per 100 mg tissue was added to the powdered cartilage. 200 µl of $CHCl_3$ was added and the mixture left to sit at room temperature for 15 minutes. Samples were then centrifuged at 13,200 rpm for 15 minutes in a U-32R centrifuge (Boeco, Germany). The upper aqueous phase was removed and mixed with an equal volume of 70% (v/v) ethanol. Qiagen RNeasy miniprep kit and reagents were used according to standard manufacturer's procedures to isolate total RNA from the sample. The minicolumns in the miniprep kit work by binding RNA to the silica-gel-based membrane allowing contaminants to be washed away by microspin technology. To remove DNA contaminants, the membranes were incubated with DNAse I (80 µl, Qiagen) during the wash steps. Purified RNA was subsequently eluted in 60 µl of sterile Milli Q™ water and the sample was then stored at –80 °C until used in RT-PCR analysis experiments. RNA concentrations and purity in each sample were measured using an Ultraspec 2000 (Pharmacia Biotech, UK) at 260 nm and 280 nm. RNA was also extracted from bovine cornea as a positive control for the human/bovine lumican and keratocan specific primers.

6.3.1.2 Reverse transcription of RNA (RT-PCR)

cDNA required for primer specific polymerase chain reaction amplification of a required target sequence was produced during the initial reverse transcription polymerase chain reaction (RT-PCR) procedure. RT-PCR required a concentration of either 50 or 500 ng of RNA for lumican or keratocan cDNA amplification respectively, in hip and knee articular cartilage, and also from the bovine corneal total RNA sample, with a final reaction volume of 20 µl (see table 6.2). The RT reaction mixture was gently mixed and incubated at room temperature for 10 minutes. It was then subjected to the following cycle: 42 °C for 30 minutes, 99 °C for 5 minutes and soaked at 4 °C.

RT mix	Volume
Mg free 10x PCR buffer II	2µl
25 mM $MgCl_2$	1.6 µl
2.5 mM dNTPs	1.6 µl
RNAse inhibitor	1 µl
Reverse transcriptase	1 µl
Oligo dT	1 µl
Milli Q™ water	11.8 µl – RNA volume
RNA sample	Volume = 50 – 500 ng

Table 6.2 RT-PCR reaction mixture

6.3.1.3 Primer design

For amplification of portions of lumican and keratocan cDNA, primers were designed using sequences of interest obtained from Genbank. They were designed using the Oligo 4.0s program for Macintosh. Primers were designed where sequences matched both bovine and human lumican and keratocan, so that bovine corneal RNA extracts could be used as positive controls for the lumican and keratocan primers. Primer sequences to lumican and keratocan are listed in table 6.3. A number of criteria had to be considered when designing the primers, these included:

1. primers should be between 20-25 nucleotides in length;
2. they should have an annealing temperatures of between 50 – 65°C;
3. they should have a GC content of between 40-60%;
4. self complementary sequences should be avoided to minimise primer dimer formation.

Human glyceraldehydes-3-phosphate dehydrogenase (GAPDH 1 and 2 [see table 6.3]) specific primers were also designed to be used as positive tissue controls in RT-PCR analysis of human cartilage tissues.

Primers	**Specificity**	**Sequence**	**Size of product**	**Annealing temp (°C)**
BCK 19 BCK 20	Human / bovine keratocan	5'CCTGATAGAAACCATTCCTGA 5'CTGCATTGTATTGGCTGGTAA	409 bp	52.1
BCK 21 BCK 22	Human / bovine lumican	5'ATGGTGCCTCCTGGAATCAAG 5'AGCTCAAGTCAAGGTATTCGA	391 bp	52.5
Hum GAPDH 1 Hum GAPDH 2	Human GAPDH	5'TGGTATCGTGGAAGGACTCAT 5'GTGGGTGTCGCTGTTGAAGTC	370 bp	58.1

Table 6.3 – Oligonucleotide primers used in RT-PCR amplification of human and bovine keratocan and lumican and human GAPDH positive control.

6.3.1.4 Polymerase chain reaction

Polymerase chain reactions (PCRs) were prepared as described in table 6.4, using 1 µl of the RT reaction mixture (see section 6.3.1.3 above) from each sample for lumican reactions and 2 µl of the RT reaction mixture for keratocan reactions. PCR reactions were processed in a Technegene thermal cycler. After an initial denaturation step at 95

°C for 60 seconds, the PCR reaction mixtures were amplified at 95 °C for 30 seconds, 45 seconds at the specified annealing temperature of the primers (52.1 °C for keratocan and 52.5 °C for lumican), 72 °C for 45 seconds and a final extension step of 5 minutes at 72 °C. Amplification was repeated 30 times for lumican and 40 times for keratocan. GAPDH housekeeping primers were run with an annealing temperature of 58.1 °C with each sample as a positive control.

PCR mix	Volume
Mg free 10x PCR buffer II	5 µl
25 mM $MgCl_2$	3 µl
2.5 mM dNTPs	4 µl
Primers (10 µM stock)	1 µl
Taq polymerase	0.3 µl
RT sample	1 – 5 µl
Milli Q™ water	34.7 - 30.7 µl

Table 6.4 - PCR reaction mixture

6.3.1.5 Agarose gel electrophoresis of PCR products

PCR reaction products were run for visualisation on 2 % (w/v) agarose gels made up in 30 ml Tris Borate EDTA buffer (Sigma T-3913). The solution was micro-waved to dissolve the agarose and allowed to cool from boiling to warm. 2 µl of a 10 mg/ml ethidium bromide solution was added to the gel. The gel was poured into a PCR cassette and allowed to set at room temperature for 10 minutes and at 4 °C for 10 minutes. A DNA ladder of standards was prepared by mixing 1 µl of dye solution (6x tracking dye Cambio BV-BT-10) with 2 µl of 1x PCR buffer and 3 µl of DNA ladder (LMV 50-1000 bp Cambio BV-1159-01). 5 µl of all PCR reaction products were mixed with 1 µl of tracking dye. 5 µl of the DNA ladder and 5 µl of all samples were loaded into wells in the gel and run at 120 volts in 0.5x TBE until the dye front

reached the bottom of the gel running cassette. Bands were visualised on a UV light box and pictures taken.

6.3.1.6 Sequence analysis of RT-PCR reactions

Samples from each set of RT-PCR reactions carried out were purified using a QIA quick PCR purification kit in order to purify single or double stranded DNA fragments from PCR reaction components such as primers, nucleotides, polymerases and salts. Briefly, 5 volumes of PB buffer from the kit were added to 1 volume of the PCR reaction. The sample was placed in a QIAquick spin column in a 2 ml collection tube and DNA was bound by spinning for 60 seconds at 13,200 rpm. The flow through was discarded and the spin column washed with 750 µl of PE buffer and spun again at 13,200 rpm for 1 minute. The flow through was discarded again and the column spun for a further 1 minute. The column was placed in a clean 1.5 ml microcentrifuge tube and 50 µl of EB buffer added to the centre of the membrane to elute the DNA by centrifuging at 13,200 rpm for 1 minute. Sequencing reactions using BigDye Terminator cycle sequencing kit (Applied Biosystems) were prepared as follows:

PCR sequencing mix	Volume
Big Dye	4 µl
5 µM forward primer	1 µl
Purified DNA	5 µl
H_2O	To 15 µl

Table 6.5 PCR sequencing reaction

The sequence reaction was gently mixed, spun and cycled as follows: 96 °C for 20 seconds; 50 °C for 10 seconds; 60 °C for 4 minutes °C and soaked at 4 °C. Amplification was repeated 26 times. 8 µl of Milli Q™ water; 2 µl of 3 M Sodium acetate, pH 5; and 50 µl of 100% ethanol were added to the PCR sequence reaction

product. This solution was mixed, spun and incubated at room temperature for 20 minutes and then centrifuged at maximum speed (13,200 rpm) for 20 minutes. The supernatant was removed and discarded and the DNA pellet washed with 250 µl of 70% (v/v) ethanol. The reaction mixture was centrifuged again at maximum speed for 5 minutes and the supernatant removed and discarded. The pellets were dried at 90 °C and brought to the sequencing department at Cardiff University for sequence analysis and verification of PCR products.

6.3.2 Preliminary SDS PAGE and Western blot analysis of lumican, keratocan and KS substitutions in normal and pathological human cartilage and IvD tissues

Preliminary studies were preformed on normal and OA human articular cartilage extract samples and pathological IvD tissue samples that were provided to our lab through ongoing collaboration with Dr Sally Roberts and Professor Stephen Eisenstein, Centre for Spinal Studies, RJAH, Orthopaedic Hospital, Oswestry. These samples were analysed by SDS PAGE and Western blot analysis using mAbs LUM-1 and KER-1 (see chapter 4 for characterisation). Volumes equivalent to 5 µg GAG were either left undigested or digested with keratanase (80 mU per mg GAG), keratanase II (6 mU per mg GAG) or endo-β-galactosidase (8 mU per mg GAG). Samples were loaded onto 4 – 20% Tris glycine gradient gels for SDS-PAGE and Western blot analysis as described previously in section 2.3.2.1. Blots were probed with mAbs LUM-1 and KER-1 to analyse the presence of corneal related KSPGs (lumican and keratocan) and the types of KS substitutions present on those KSPGs in normal versus pathological human articular cartilage and IvD.

6.3.3 KSPG protein levels in normal and OA human articular cartilage from hip and knee, analysis by Western blotting

Articular cartilage samples were harvested from weight bearing areas of all graded normal hip, OA hip and OA knee patient samples described above in table 6.1. These tissues were then finely diced and extracted in 4 M Guanidine HCl with a protease inhibitor cocktail as described previously (section 4.3.1.1). Crude 4M Guanidine HCl extracts were dialysed to 50 mM sodium acetate, pH 6.8 and DMMB analysis carried out to determine the sulphated GAG concentration of each sample. Protein concentrations were also determined for each sample using a Pierce Bicinchoninic Acid (BCA) protein assay kit. Briefly, a standard curve of 0, 20, 40, 60, 80, 100 and 200 μg/ml bovine serum albumin (BSA) was prepared in 50 mM sodium acetate, pH 6.8 and applied in triplicate to a 96 well microtitre plate. Samples were diluted 1:5, 1:10, 1:25 and 1:50 in 50 mM sodium acetate, pH 6.8 and applied in triplicate to the same 96 well micro titre plate. Working reagent was prepared according to the manufacturers protocol and 200 μl applied to each well and gently mixed. The plates were covered and incubated at 37 °C for 30 minutes. Plates were measured at and optical density of 575 nm on a labsystems multiscan MS plate reader and protein concentrations determined for all cartilage and IvD extract samples.

Further analysis was carried out on a range of normal hip and OA hip and knee PG extracts (table 6.1). 8 μg GAG per well and 25 μg protein per well of each of the samples were digested with keratanase, keratanase II and endo-β-galactosidase (as described in chapter 2, section 2.3.1.2) and were loaded onto 2 different 4 – 20% Tris glycine SDS-PAGE gradient gels and run as described previously in section 2.3.2.1. Blots were probed with mAbs LUM-1 and KER-1 to analyse the presence of corneal related KSPGs, lumican and keratocan, in normal versus OA human cartilage.

6.3.4 Lumican and keratocan mRNA expression in normal and degenerate human IvD

100 mg IvD tissue was removed from normal scoliosis patient samples (n = 2, patient sample numbers 25 and 26, see table 6.1), from grade III degenerate IvD samples (n = 1, patient sample 4), from grade IV degenerate IvD patient samples (n = 3, patient sample numbers 15, 16 and 18) and from grade V degenerate IvD patient samples (n = 1, patient sample number 17) and RNA extracted as described in section 6.3.1 above. RNA concentrations and purity in each sample were measured using an Ultraspec 2000 at 260 nm and 280 nm.

RT-PCR reactions were set up as described above in sections 6.3.1.2 – 6.3.1.4 (table 6.2). Volumes equivalent to 50 ng RNA were used for each sample to analyse lumican mRNA expression in normal compared to pathological human IvD using human lumican specific primers (BCK 21 and BCK 22) detailed in table 6.3. 1 µl of IvD RT cDNA was used in PCR reactions (table 6.4) with lumican specific primers.

Volumes equivalent to 215 ng RNA were used for each sample to analyse keratocan mRNA expression in normal compared to degenerate IvD. Human/bovine keratocan specific primers (BCK 19 and BCK 20) were designed (table 6.3) for amplification of keratocan message. 5 µl of IvD RT cDNA was used in PCR reactions (table 6.4) with the keratocan primers.

6.3.5 Analysis of lumican and keratocan protein levels in different grades of IvD degeneration

IvD samples were extracted in 1 ml 4 M Guanidine HCl with protease inhibitors per mg tissue as described previously in section 4.3.1.1. Samples were dialysed to 50 mM sodium acetate, pH 6.8 and DMMB (see section 2.3.1.1) and protein concentration analysis (see section 6.3.3) was carried out to determine sulphated GAG and protein

concentration, respectively. Volumes equivalent to 8 μg GAG and 25 μg protein were digested with a keratanase/keratanase II/endo-β-galactosidase mixture (section 2.3.1.2) and run on two different 4–20% Tris glycine gradient gels for electrophoresis as described in section 2.3.2.1. Western blot analysis was carried out using mAbs LUM-1 and KER-1, to analyse changes in protein expression of small leucine rich KSPG in degenerating human IvD PG extracts.

6.4 Results

6.4.1 Preliminary analysis of lumican, keratocan and KS substitutions in normal and pathological human cartilage and IvD tissues

Preliminary Western blot analysis of 5 μg GAG samples of undigested, keratanase digested (80 mU per mg GAG), keratanase II digested (6 mU per mg GAG) or endo-β-galactosidase digested (8 mU per mg GAG) PG extracts from normal and OA tissue samples and graded pathological IvD tissue extracts (grade I – IV) showed that lumican and keratocan levels were increased in pathological compared to normal tissues (figures 6.1 knee cartilage; A versus B; and figure 6.2 IvD samples, grade I, II, III and IV). This analysis also showed that digestion using keratanase or endo-β-galactosidase digestion of human articular cartilage and IvD lumican and keratocan resulted in a very slight decrease in molecular weight of the core protein by approximately 1 – 4 kDa (figures 6.1 and 6.2). Keratanase II digestion did not result in a shift in molecular weight of the core proteins of lumican or keratocan metabolites compared to undigested samples in cartilage or IvD tissues (figures 6.1 and 6.2). The results indicated that the KSPG molecules found in human articular cartilage and IvD tissues were substituted with very low molecular weight unsulphated or low- sulphated KS chains, and that there were no di-sulphated forms of KS attachments (figures 6.1 and 6.2). The results agreed with previously reported observations that the lumican found in human articular cartilage may possess either low or non-sulphated forms of KS (Melching & Roughley, 1999).

This preliminary analysis indicated that unlike the keratocan or lumican found in corneal tissues, both the keratocan and lumican present in normal or pathological cartilage and IvD did not necessarily require pre-digestion with any form of KS degrading enzyme to expose the core protein epitope recognised by LUM-1 or KER-1 because very little KS appeared to be present on these molecules.

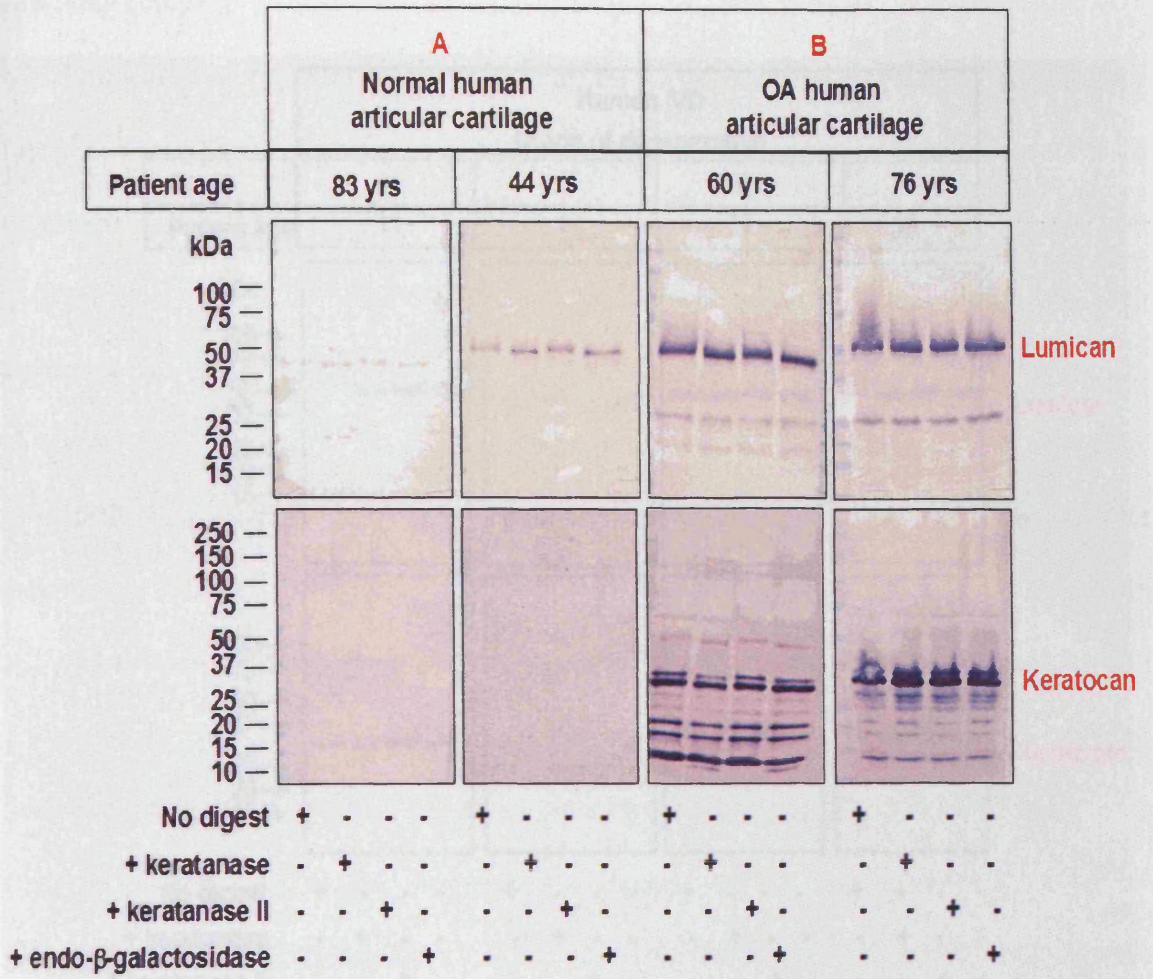

Figure 6.1 Preliminary Western blot analysis of normal human cartilage **(A)** compared to osteoarthritic human cartilage **(B)** using monoclonal antibodies to the small leucine rich PGs lumican (LUM-1, ~45–50 kDa) and keratocan (KER-1, ~30 kDa) show that expression of these molecules are increased in pathological human articular cartilage tissues compared to normal. There were also a number of smaller molecular weight breakdown products (10–20 kDa) of keratocan in pathological tissue. Keratanase and endo-β-galactosidase digestion decreased the molecular weights of both lumican and keratocan metabolites only slightly compared to that observed with corneal lumican and keratocan standards (see chapter 4, section 4.4.1.2; figure 4.10). Keratanase II did not affect the molecular weight of any of the KSPG molecules.

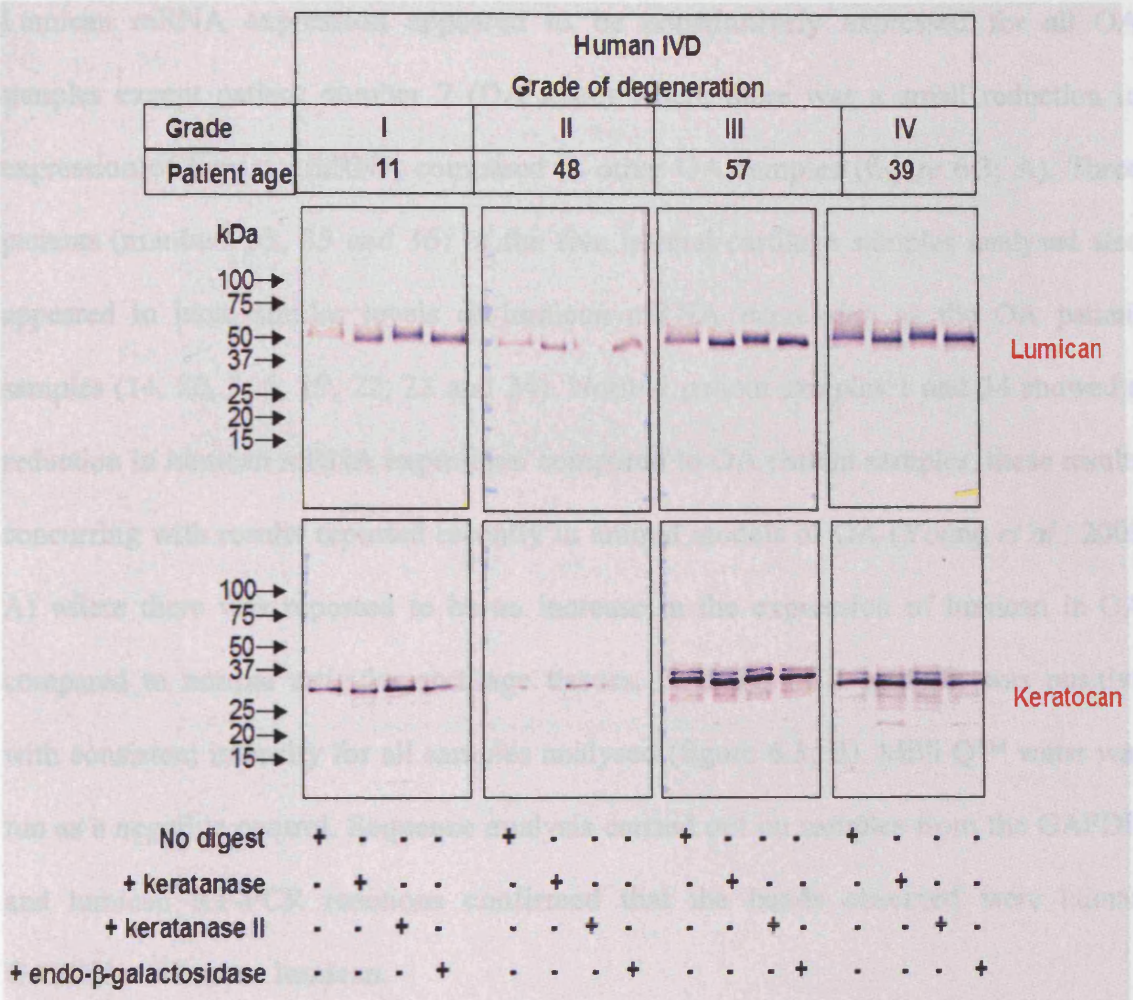

Figure 6.2 Western blot analysis of degenerate IvD tissues using mAbs LUM-1 to lumican (~45–50 kDa) and KER-1 to keratocan (~30 kDa) show that expression of these molecules are present in normal (grade I) and pathological (grades II, III, IV) IvD tissues at the protein level to different extents. Again keratanase and endo-β-galactosidase digestion caused a decrease in the molecular weights of both lumican and keratocan metabolites only slightly compared to that observed with bovine corneal lumican and keratocan standards (see chapter 4, section 4.4.1.2; figure 4.10). Keratanase II did not affect the molecular weight of the KSPG molecules.

6.4.2 Molecular and proteomic expression of lumican in normal versus OA human articular cartilage

Lumican mRNA expression appeared to be constitutively expressed for all OA samples except patient number 7 (OA knee) where there was a small reduction in expression of lumican mRNA compared to other OA samples (figure 6.3; A). Three patients (numbers 33, 35 and 36) of the five normal cartilage samples analysed also appeared to have similar levels of lumican mRNA expression as the OA patient samples (14, 20, 3, 5, 19, 22, 23 and 24). Normal patient samples 1 and 34 showed a reduction in lumican mRNA expression compared to OA patient samples, these results concurring with results reported recently in animal models of OA (Young *et al.,* 2005 A) where there was reported to be an increase in the expression of lumican in OA compared to normal articular cartilage tissues. GAPDH PCR analysis was positive with consistent intensity for all samples analysed (figure 6.3; B). Milli Q™ water was run as a negative control. Sequence analysis carried out on samples from the GAPDH and lumican RT-PCR reactions confirmed that the bands observed were human GAPDH and human lumican.

In contrast to the RT PCR analysis of normal patient samples 33, 35 and 36, and all OA patient samples, protein levels of lumican identified in Western blot analysis of extracts from the same patient samples using mAb LUM-1, showed an overall increase in protein expression of the lumican core protein (figure 6.3; C). This suggests that the increased lumican observed at the proteomic level in OA compared to normal cartilage may be due to an increase in lumican translation or a decrease in lumican breakdown and rather than an increase in lumican RNA synthesis.

Samples were loaded both on equal GAG (8 μg per well) and equal protein (25 μg per well) basis for SDS PAGE and Western blot analysis (figure 6.3, panels C and D, respectively). The same pattern was obtained where there was an increase in lumican

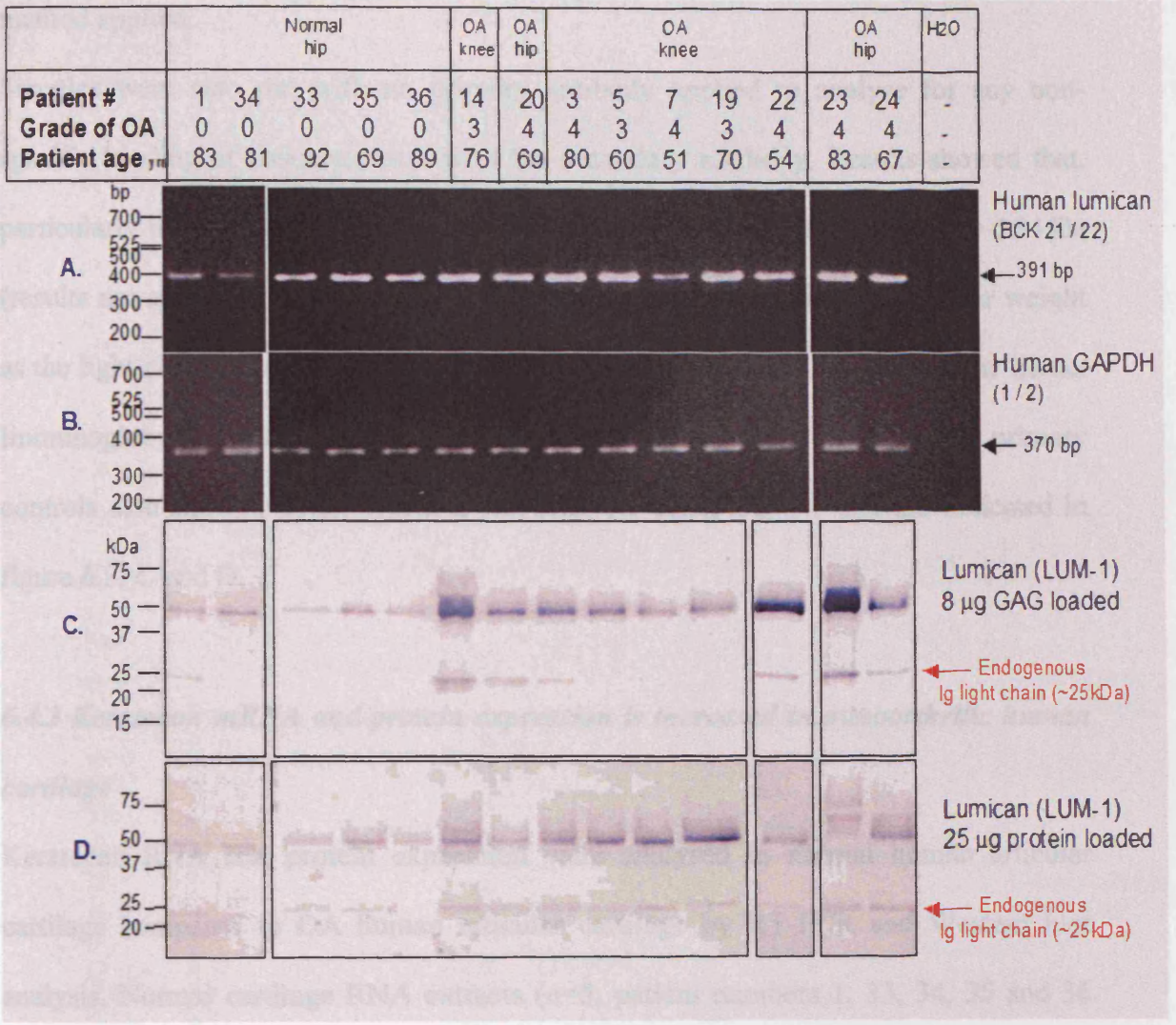

Figure 6.3 Lumican expression at the molecular (A) and proteomic (C and D) level observed in extracts from normal and pathological human articular cartilage obtained from hips and knees of patients undergoing joint replacement surgery. Panel A shows PCR analysis of RNA extracts from normal and OA patient tissues using lumican specific primers, Milli Q™ water was run as a negative control. Panel B shows GAPDH as a positive control for qualitative comparison of message levels. Panel C shows levels of lumican proteoglycan from the same normal and OA patient samples in SDS PAGE and Western blot analyses that had been loaded based on equal GAG concentrations. Panel D also shows lumican proteoglycan levels in Western blot analysis where patient samples had been loaded based on equal protein levels.

at the proteomic level in OA compared to normal cartilage regardless of loading method applied.

Samples were also run with no primary antibody applied to analyse for any non-specific binding of tissue extracts with the secondary antibody. Results showed that, particularly in pathological tissue samples, there was non-specific binding at ~25 kDa (results not shown). This molecular weight corresponds to the same molecular weight as the light chain of reduced endogenous human immunoglobulin present in the tissue. Immunoglobulin light chains identical to those that showed up in the no primary controls also showed up in Western blot analysis using LUM-1 and are indicated in figure 6.3; C and D.

6.4.3 Keratocan mRNA and protein expression is increased in osteoarthritic human cartilage

Keratocan RNA and protein expression were analysed in normal human articular cartilage compared to OA human articular cartilage by RT-PCR and Western blot analysis. Normal cartilage RNA extracts (n=5, patient numbers 1, 33, 34, 35 and 36 aged 83, 92, 81, 69, & 89 years, respectively) showed no expression of keratocan when 500 ng of RNA was used in RT PCR analysis (figure 6.4; A). In contrast, OA patient samples from a similar age range (n = 8, patient numbers 8, 20, 23, 3, 5, 7, 19 and 22 who were 76, 69, 83, 80, 60, 51, 70 and 54 year old patients, respectively) showed a large increase in expression of keratocan at the molecular level (figure 6.4; A). Milli Q™ water was run as a negative control and bovine cornea RNA RT-PCR was run as a positive control for keratocan expression. GAPDH was positive with consistent staining intensity for all cartilage samples. Sequence analysis of PCR products was carried out on samples from the GAPDH and keratocan RT-PCR reactions to confirm that the bands observed were human GAPDH and human keratocan.

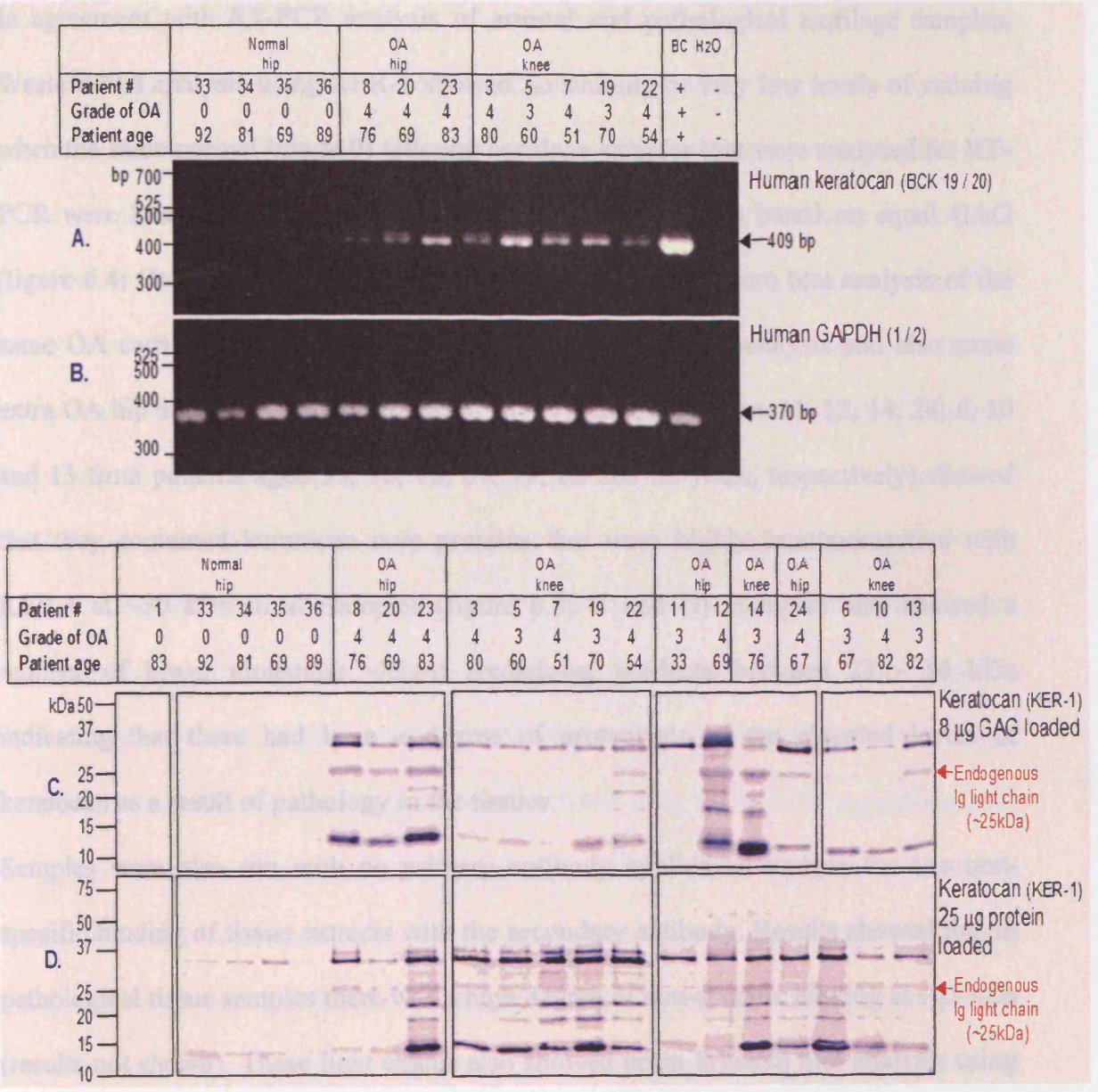

Figure 6.4 Keratocan expression at the molecular (A) and proteomic (C and D) level observed in normal and pathological human articular cartilage obtained from patients undergoing hip and knee joint replacement surgery. Panel A shows PCR analysis of RNA extracts from normal and OA patient tissues using keratocan specific primers. Panel B shows GAPDH as a positive control. BC = bovine corneal tissue run as a positive control. Milli Q™ water was run as a negative control. Panel C shows proteoglycan levels of keratocan from the same normal and OA patient samples in SDS PAGE and Western blot analyses using KER-1 that had been loaded based on equal GAG concentrations. Panel D also shows keratocan proteoglycan levels in Western blot analysis using KER-1 where samples had been loaded based on equal protein levels.

In agreement with RT-PCR analysis of normal and pathological cartilage samples, Western blot analysis using KER-1 showed no staining or very low levels of staining when the same normal (grade 0) articular cartilage samples that were analysed for RT-PCR were loaded for SDS PAGE and Western blot analysis based on equal GAG (figure 6.4; C) or protein (figure 6.4; D) concentrations. Western blot analysis of the same OA cartilage samples previously analysed in RT-PCR analysis and also some extra OA hip and knee samples collected (n = 7, patient numbers 11, 12, 14, 24, 6, 10 and 13 from patients aged 33, 75, 76, 67, 79, 82 and 82 years, respectively) showed that they contained keratocan core proteins that were highly immunoreactive with KER-1 at ~30 kDa in all samples (figure 6.4; C and D). Samples also showed a number of lower molecular weight breakdown products between 23 - 14 kDa indicating that there had been a degree of proteolysis of the elevated levels of keratocan as a result of pathology in the tissues.

Samples were also run with no primary antibody applied to analyse for any non-specific binding of tissue extracts with the secondary antibody. Results showed that in pathological tissue samples there was a high degree of non-specific binding at ~25 kDa (results not shown). These light chains also showed up in Western blot analysis using KER-1 and are indicated in figure 6.4; C and D.

6.4.4 Lumican expression is increased at the molecular and proteomic levels in grade I - V intervertebral disc degeneration

For this study, levels of expression of lumican in scoliosis patients were considered as non-degenerate; i.e. 'normal'. RT PCR analysis of tissue samples from scoliosis patients (n = 2, patient numbers 25 and 26, aged 13 and 14 years, respectively), grade III IvD degeneration (n = 1, patient number 4, aged 27 years), grade IV IvD degeneration (n = 3, patient numbers 15, 16 and 18, aged 34, 41 and 54, respectively)

and grade V IvD degeneration (n = 1, patient number 17, aged 43) showed very low levels of lumican expression in 'normal' scoliosis patients and in one of the grade IV patients (figure 6.5; A). In all other patients with different grades of degenerate disc lumican expression was greatly increased (figure 6.5; A). Milli Q™ water was run as a negative control and bovine cornea RNA RT-PCR run as a positive control. GAPDH was positive with consistent staining intensity for all IvD patient samples. Sequence analysis was carried out on samples from the GAPDH and lumican RT-PCR reactions and confirmed that the bands observed were human GAPDH and human lumican.

SDS-PAGE and Western blot analysis of extracts from patients with grade I – V IvD degeneration (grading methods determined by Pfirrmann *et al.,* 2001) demonstrated an apparent up-regulation of lumican in pathological disc tissues (figure 6.5; C and D). Lumican was present in low levels in one of the non-degenerate scoliosis patients (patient number 25) and appeared to be absent when 8 μg GAG or 25 μg protein were loaded for Western blot analysis of the second normal patient (patient number 26). Lumican levels were increased in all other pathological disc tissues, with the occurrence of breakdown product visible at ~30 kDa in extracts from patient number 15 where there was no apparent expression of lumican at the molecular level when 50 ng RNA were used in analysis (figure 6.5; A, C and D). Again the same increasing pattern of lumican expression was observed when samples were loaded for analysis based on GAG or protein concentrations. No primary antibody controls were run for the same tissue extracts and again showed the presence of non-specific binding at ~25 kDa in grade III and IV degenerate discs (results not shown). Identical non-specific binding was also present in Western blot analysis of samples with LUM-1 mAb and are indicated in figure 6.5, C and D.

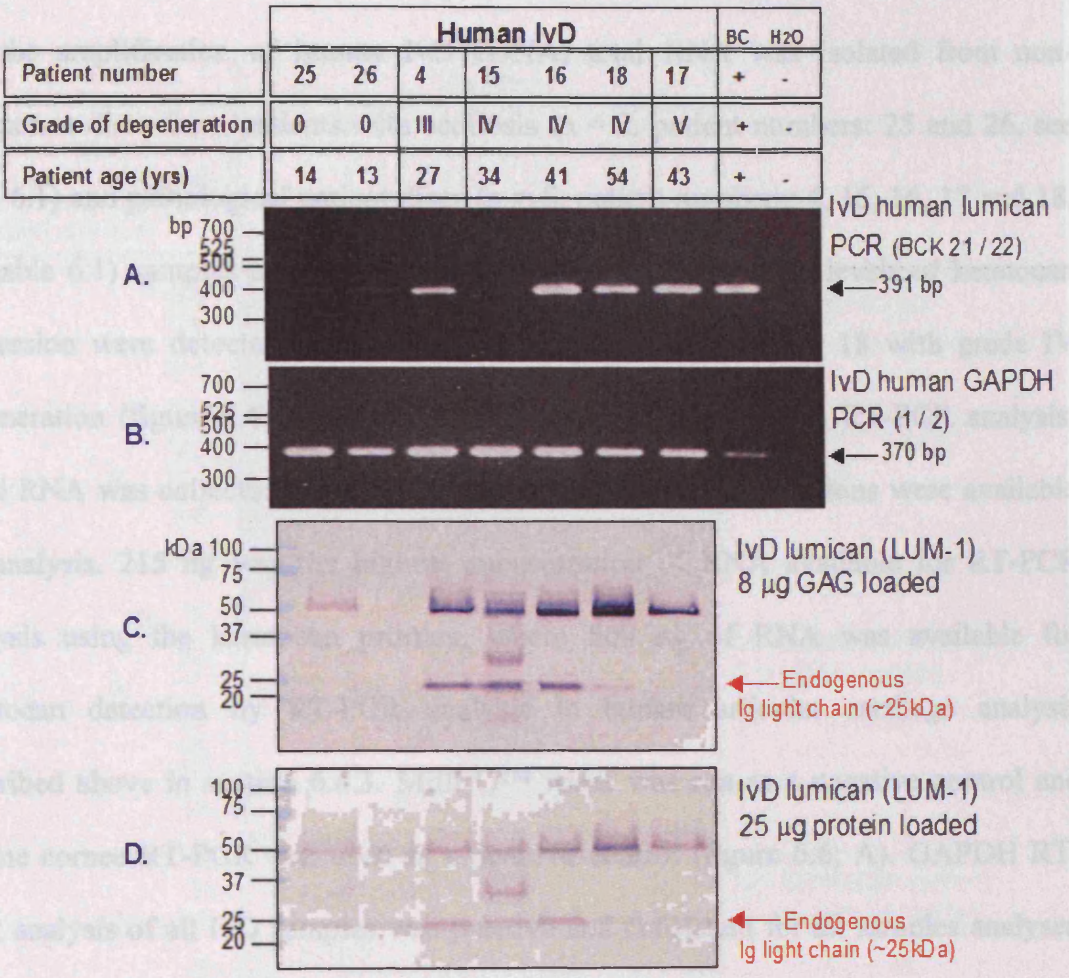

Figure 6.5 Lumican expression at the molecular and proteomic level observed in non-degenerate and pathological human intervertebral disc. Panel A shows PCR analysis of RNA extracts from non-degenerate and degenerate tissues using lumican specific primers (BCK 21 / 22). Panel B shows GAPDH as a positive control using human GAPDH specific primers (1 / 2). BC = bovine corneal tissue run as a positive control. Milli Q™ water was run as a negative control. Panel C shows levels of lumican protein from the same non-degenerate and degenerate IvD tissue samples in SDS PAGE and Western blot analysis using LUM-1 that had been loaded based on equal GAG concentrations. Panel D also shows lumican levels in Western blot analysis using LUM-1 where samples had been loaded based on equal protein levels.

6.4.5 Keratocan mRNA and protein expression in normal and degenerate IvD

For the amplification of human IvD cDNA, total RNA was isolated from non-degenerate discs from patients with scoliosis (n = 2, patient numbers: 25 and 26, see table 6.1) and pathological patient discs (n = 5, patient numbers: 4, 15, 16, 17 and 18, see table 6.1) samples as described in section 6.3.1 above. Low levels of keratocan expression were detected for all patients except patient number 18 with grade IV degeneration (figure 6.6; A) when 215 ng of RNA were used in RT-PCR analysis. Total RNA was collected from IvD tissues and limited concentrations were available for analysis. 215 ng was the highest concentration of RNA available for RT-PCR analysis using the keratocan primers, where 500 ng of RNA was available for keratocan detection by RT-PCR analysis in human articular cartilage analysis described above in section 6.4.3. Milli Q™ water was run as a negative control and bovine cornea RT-PCR was used as a positive control (figure 6.6; A). GAPDH RT-PCR analysis of all IvD samples was positive and consistent for all samples analysed (figure 6.6; B). Sequence analysis was carried out on samples from the GAPDH and keratocan RT-PCR reactions and results confirmed that the bands observed were human GAPDH and human keratocan.

Western blot analysis using mAb KER-1 demonstrated that keratocan core protein was present in non-degenerate and degenerate IvD tissues when samples were loaded based on equal GAG or equal protein concentrations (figure 6.6; C and D). Extracts from patient numbers 4 (grade III), 15 (grade IV) and 16 (grade IV) showed lower levels of keratocan at ~30 kDa and higher levels of keratocan breakdown products at ~13 kDa compared to other samples (figure 6.6; C and D). These patients (4, 15 and 16) also showed higher levels of non-specific binding of endogenous immunoglobulin at ~25 kDa (figure 6.6; C and D).

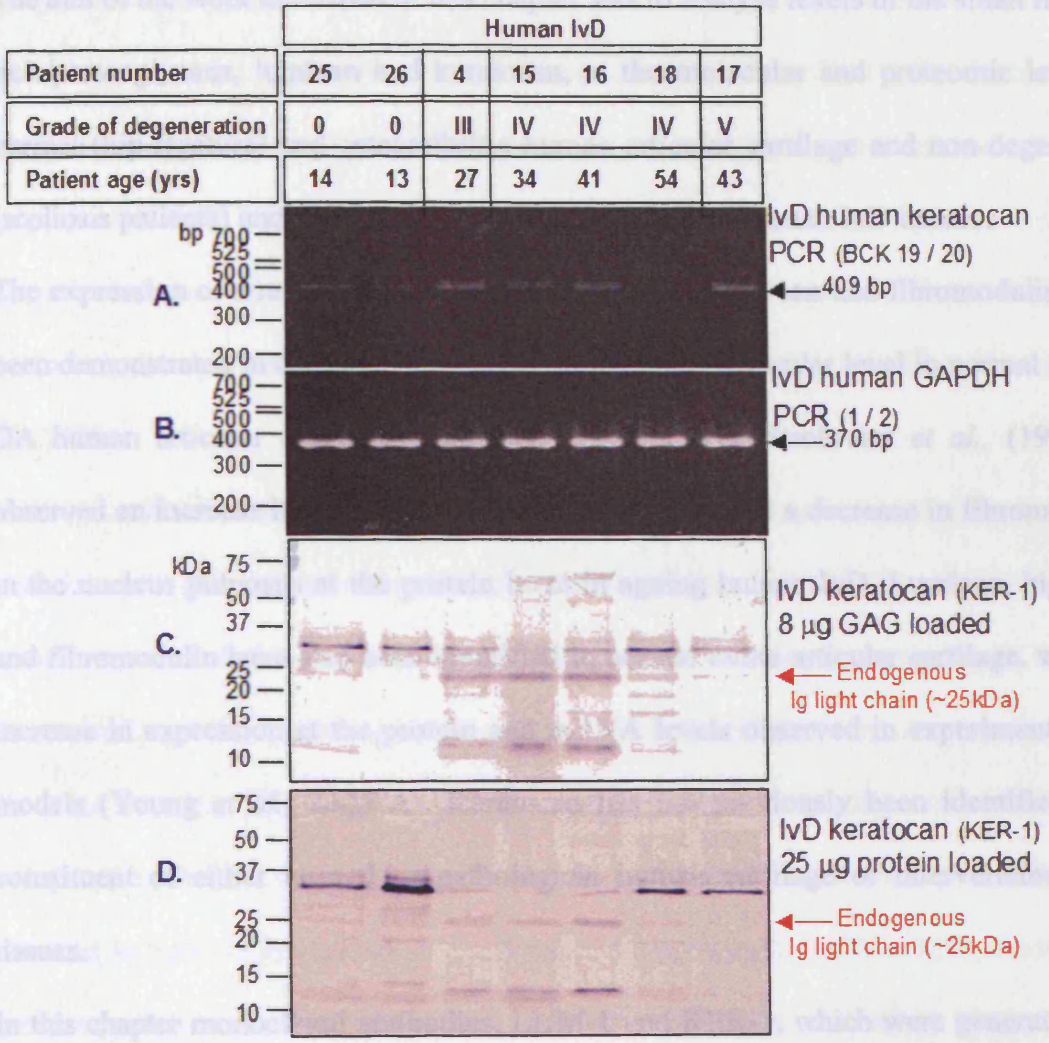

Figure 6.6 Keratocan expression at the molecular (A) and proteomic (C and D) levels observed in non-degenerate and pathological human intervertebral disc. Panel A shows PCR analysis of RNA extracts from non-degenerate and degenerate tissues using keratocan specific primers (BCK 19 / 20). Panel B shows GAPDH as a positive control using human GAPDH specific primers (1 / 2). Panel C shows levels of keratocan from the same non-degenerate and degenerate IvD tissue samples in SDS PAGE and Western blot analysis using KER-1 that had been loaded based on equal GAG concentrations. Panel D also shows keratocan levels in Western blot analysis using KER-1 where samples had been loaded based on equal protein levels.

6.5 Discussion

The aim of the work described in this chapter was to analyse levels of the small leucine rich proteoglycans, lumican and keratocan, at the molecular and proteomic level in normal (hip fracture) and osteoarthritic human articular cartilage and non-degenerate (scoliosis patients) and differentially graded pathological human IvD tissues.

The expression of a range of SLRPs such as lumican, biglycan and fibromodulin have been demonstrated in cartilage at both the protein and molecular level in normal versus OA human articular cartilage (Cs-Szabo *et al.,* 1997). Strolovics *et al.,* (1999 A) observed an increase in lumican in the annulus fibrosis and a decrease in fibromodulin in the nucleus pulposus at the protein level in ageing human IvD. Lumican, biglycan and fibromodulin have also been identified in normal ovine articular cartilage, with an increase in expression at the protein and mRNA levels observed in experimental OA models (Young *et al.,* 2005 A). Keratocan has not previously been identified as a constituent of either normal or pathological human cartilage or intervertebral disc tissues.

In this chapter monoclonal antibodies, LUM-1 and KER-1, which were generated and characterised as described in chapter 4, were used in the analysis of lumican and keratocan protein levels in normal compared to OA human cartilage and in normal compared to pathological human IvD by SDS PAGE and Western blot analyses. RT-PCR analysis was also carried out on RNA extracts from the same samples where possible, using human/bovine keratocan and human/bovine lumican specific primers.

Western blot and PCR analysis of tissue and total RNA extracts from normal and OA human articular cartilage have demonstrated an increased expression of keratocan at both proteomic and molecular levels in pathological cartilage. A number of smaller molecular weight breakdown products were observed for keratocan PGs in OA tissue compared to normal tissue. Similar analysis of differentially graded pathological IvD

extracts showed that keratocan was expressed at the molecular level in low amounts in all grades of disc degeneration when 215 ng of RNA were used in RT-PCR analysis. Keratocan was also expressed at the proteomic level in all grades of disc degeneration but with a larger degree of proteolysis in grades III and IV degraded tissues compared to grades I and V. These grades (III and IV) also showed an increased presence of non-specific binding of endogenous immunoglobulin. This molecule (keratocan) was previously thought to be largely 'corneal specific' (Carlson *et al.*, 2005; Kawakita *et al.*, 2005).

Lumican mRNA was also present in three of the normal articular cartilage samples with the same intensity as nine of the OA cartilage samples, but at a reduced intensity in two normal samples compared to the OA samples. Lumican was shown to increase dramatically at the protein level in osteoarthritic cartilage compared to all normal cartilage samples. This suggests that the increased lumican protein expression in OA compared to normal cartilage may be due to an increase in lumican translation or a decrease in lumican breakdown and not due to an increase in lumican RNA synthesis. Lumican mRNA was not expressed in normal human IvD tissues when 50 ng of RNA were used in analysis. Expression was greatly increased when the same concentration of RNA was analysed in pathological IvD tissues. Lumican protein levels were absent or extremely low in non-degenerate IvD extracts and protein expression was also dramatically increased in pathological tissue.

Analysis of undigested, keratanase, keratanase II and endo-β-galactosidase digested extracts of keratocan and lumican from both articular cartilage and IvD tissues demonstrated that in contrast to the keratocan and lumican found in corneal tissue the keratocan and lumican present here was substituted with small molecular weight (approximately 1 – 4 kDa) low- or non-sulphated KS chains.

The new mAbs (LUM-1 and KER-1) have proved to be useful tools in identification of low and increased levels of corneal associated KSPGs in irregular tissue locations with pathology. It is still not clear whether the increase in expression observed for these SLRPs is an attempt to repair damage caused by losses due to aggrecan degradation or whether it actually causes more damage to the tissue extracellular matrix structure. The observed up-regulation of lumican and keratocan synthesis in cartilage and IvD by chondrocytes and disc cells, along with other generally non-cartilage associated molecules, such as collagen I (Young *et al.*, 2005 A), may reflect an attempt to compensate for the damage caused by aggrecan degradation or an attempt to produce the fibrocartilage scar tissue associated with OA and degenerative disc tissue.

6.6 Chapter summary

- RNA message for lumican is constitutively expressed in normal human and OA cartilage. However, lumican protein is increased in its expression with the onset of OA, a finding similar to that described by Cs-Szabo *et al.,* 1997.
- A novel finding was that RNA message for lumican is also expressed in human IvD tissues and this expression increases with the progression of disc pathology; i.e. expression patterns for lumican appear to be different with the onset of cartilage and disc degeneration. An additional novel finding was that lumican protein is also increased with the progression of IvD degeneration.
- A novel finding was the induction of RNA expression for keratocan in normal versus OA cartilage. Thus, lumican and keratocan expression patterns differ in normal and OA cartilage.
- In addition, keratocan expression at the protein level also occurs with the onset of degenerate joint disease.
- A novel finding was that keratocan is also expressed at the RNA and protein levels in IvD tissues. RNA expression appears to increase with pathology but this may not be reflected at the protein level.

Chapter 7 - General Discussion

In the early 1980s the challenge of connective tissue research was assisted with the emergence of a range of novel monoclonal antibodies recognising various matrix proteoglycans (Funderburgh *et al.,* 1983; Hughes *et al.,* 1995) and carbohydrate side chains present on proteoglycans (Christner *et al.,* 1980; Conrad *et al.,* 1982; Caterson *et al.,* 1983; Couchman *et al.*, 1984; Caterson *et al.,* 1985). Matrix molecules were emerging as being important structural and functional entities of connective tissues. The availability of antibodies allowed for the elucidation of the distribution and structures of these molecules and for a better understanding of pathological conditions associated with them as they could be used to analyse the structural and metabolic changes that occur during development, in ageing and with the onset of disease.

The Caterson laboratory was the first lab to generate monoclonal antibodies such as 5D4 (Caterson *et al.,* 1983) and 1B4 (Caterson *et al.,* 1985), recognising linear sulphated poly-N-acetyl-lactosamine epitopes on KS. These mAbs have been shown to recognise subtle differences in sulphation patterns of the linear poly-N-acetyl-lactosamine epitopes that they recognise (Mehmet *et al.,* 1986; Caterson *et al.,* 1987). Mehmet *et al.,* (1986) demonstrated that the epitopes recognised by 5D4 contain a minimum penta-sulphated hexasaccharide structure, whereas 1B4 recognised a minimum tetra-sulphated hexasaccharide. Caterson *et al.,* (1987) demonstrated through the use of competitive radioimmunoassays that 5D4 epitope is equally represented on both skeletal and corneal KS, whilst there appeared to be seven times more IB4 epitope on corneal KS than on skeletal KS indicating that there were differences in sulphation patterns within these KS chains and that they could be investigated using antibodies such as these. Antibodies have also been generated to native CS (e.g. 6C3 and 7D4)

and also to chondroitinase generated 'CS stub' neoepitopes (e.g. 2B6, 3B3, 1B5) that have been well characterised (Caterson *et al.,* 1985; Caterson *et al.,* 1990). Together these and other similar antibodies have helped to identify matrix molecules that have CS or KS side chain attachments in a wide range of tissues besides cartilage or cornea (Caterson *et al.,* 1987; Sorrell *et al.,* 1990; Shiozawa *et al.,* 1991; Meyer-Puttlitz *et al.,* 1995; Fischer et al., 1996; Takagi *et al.,* 1996; Hamanaka *et al.,* 1997; Inkinen *et al.,* 1998; Akama *et al.,* 2001; Papageorgakopoulou *et al.*, 2002). They have also been important for the identification of subtle changes in sulphation patterns in different tissues (Sorrell *et al.,* 1988; Sharif *et al.,* 1996; Takagi *et al.,* 1996; Inkinen *et al.,* 1998; Plaas *et al.*, 1998; Bayliss *et al.,* 1999; Young *et al.,* 2005 B). In recent times, a large proportion of the analysis of KS structural composition has also been carried out using nuclear magnetic resonance (NMR) spectroscopy (Thornton *et al.,* 1989; Nieduszynski *et al.,* 1990; Brown *et al.,* 1994 & 1998; Lauder *et al.,* 1997; Huckerby *et al.,* 1998 & 1999).

The aims of this study were to (i) develop and characterise a range of novel keratanase or keratanase II generated 'KS stub' monoclonal antibodies, (ii) to use any newly generated 'KS stub' mAbs in conjunction with existing anti KS mAbs such as 5D4 to analyse variations in KS types I and II sulphation patterns from the generally accepted opinion, (iii) to generate monoclonal antibodies to KS SLRPs such as lumican and keratocan, and then (iv) to investigate the expression of lumican and keratocan at the RNA and protein expression levels in musculoskeletal connective tissues.

Initially the investigation resulted in the production and characterisation of two novel keratanase generated 'KS stub' monoclonal antibodies (BKS-1 and BKS-2; see chapter 2). Characterisation of the new antibodies demonstrated that they showed specificity for the non-reducing terminal 6-sulphated-N-acetyl-glucosamine neoepitope, on both

KS type I and KS type II (and presumably type KS III), generated as a direct result of keratanase digestion.

The novel anti 'KS stub' mAb BKS-1, was used in conjunction with existing anti KS mAb 5D4 to facilitate a new approach to the analysis of subtle differences in sulphation patterns on KS derived from bovine cornea and nasal cartilage aggrecan after the application of different sequences of three KS degrading enzymes (see chapter 3). To date structural analysis of KS from a number of studies have found two essentially different sulphation patterns for KS type I and KS type II (see chapter 1, figures 1.2 - 1.4). Both corneal and skeletal KS are composed of repeating units of galactose and N-acetyl glucosamine disaccharide structures linked through an N- or O-linked oligosaccharide to the core protein, respectively. Oeben *et al.,* (1987) have proposed that in corneal KS type I, di-sulphated N-acetyl-lactosamine disaccharides are concentrated towards the non-reducing terminal of the chain, with mono-sulphated N-acetyl-lactosamine disaccharides found in the mid regions and non-sulphated N-acetyl-lactosamine disaccharides at the linkage region of the chain. This reasoning was based on a combination of their analysis of the disaccharide composition of four peptidokeratan sulphate preparations from porcine cornea, and on their assumption that during KS biosynthesis, as chain elongation proceeded, an associated increase in sulphotransferase activity also occurred resulting in the addition of two sulphate groups per disaccharide [β1 - 4(SO_3^--6)GlcNAcβ1 - 3(SO_3^--6)Galβ1] towards the non-reducing end of the chain. For the same reason when the KS chain was shorter at the beginning of elongation, sulphotransferase activity was low and this resulted in either low-sulphated [β1 - 4(SO_3^--6)GlcNAcβ1 - 3Galβ1] or non-sulphated [β1 - 4GlcNAcβ1 - 3Galβ1] regions being positioned closer to the linkage region. It is now somewhat clearer that KS chain elongation and sulphation takes place in two independent steps

(see chapter 1, section 1.4.3.1; Seko & Yamashita, 2004). First the KS chain is extended through the action of a number of glycosyltransferases that add GlcNAc and Gal to the non-reducing end of the growing chain (Brew *et al.,* 1968; Schanbacher & Ebner., 1970; Sasaki *et al.*, 1997; Ujita *et al.*, 1999; Zhou *et al.,* 1999; Shiraishi *et al.*, 2001). At the same time an N-acetylglucosamine sulphotransferase enzyme catalyses the addition of a sulphate group to C-6 of GlcNAc creating mono-sulphated disaccharides as the chain elongates (Uchimura *et al.*, 1998; Akama *et al.*, 2001). Once the mono-sulphated version of the KS chain is formed a Gal sulphotransferase enzyme catalyses the addition of sulphate groups to internal Gal residues within the KS chain (Fukuta *et al.,* 1997). This suggests that the degree of sulphation does not rely on the chain length as suggested and may be regulated by something else.

Other studies (Stuhlsatz *et al.,* 1989) have reported skeletal KS type II to have varying degrees of sulphation where KS from the KS domain of aggrecan was more highly sulphated (5 – 7 di-sulphated disaccharide repeats with 1 – 3 mono-sulphated disaccharide repeats) compared to KS from the CS I and II domains of aggrecan (1 – 4 di-sulphated disaccharide repeats with larger [2 – 6] mono-sulphated disaccharide regions). Stuhlsatz *et al.,* (1989) also postulated a KS type II structural pattern similar to that proposed for KS type I with non-sulphated disaccharide motifs concentrated at the linkage region, mono-sulphated disaccharide motifs at the mid regions and di-sulphated disaccharide motifs concentrated towards the non-reducing terminal of the chain. Skeletal KS has also been reported to be composed of predominantly disulphated disaccharide motifs with occasional monosulphated disaccharides in which the participating galactose is sulphated with very low or no non-sulphated disaccharide structures (Brown *et al.,* 1994; Funderburgh, 2000 review).

A number of other studies (Dickenson *et al.,* 1990; Block *et al.,* 1992; Huckerby *et al.,* 1998) have identified anomalies to the generic structure described for KS. In 1998

Huckerby *et al.*, analysed endo-β-galactosidase derived bovine corneal KS type I oligosaccharides using ^{1}H-NMR spectroscopy. They reported evidence for unsulphated N-acetylglucosamine residues within the "sulphated" region of the KS type I chain indicating that non-sulphated disaccharides were located at regions other than being concentrated towards the linkage region of the chain as previously postulated for porcine corneal KS type I by Oeben *et al.*, (1987). Also, bovine IvD KS type II has been shown to contain a 6-S-GlcNAc residue attached directly to the linkage region GalNAc (Dickenson *et al.*, 1990) where Oeben *et al.*, (1987) and Stuhlsatz *et al.*, (1989) had predicted only non-sulphated disaccharide domains to be. The results obtained in chapter 3 using mAbs 5D4 and BKS-1 to analyse KS sulphation patterns in bovine corneal and bovine nasal cartilage aggrecan KS support these observations. Both KS types I and II showed a partial insensitivity to keratanase digestion which was supported by the appearance of a large 5D4 positive smear (only mildly reduced in comparison to undigested samples) in Western blot analysis of keratanase digested samples. The results indicated that there were variations in sulphation patterns within KS chains as keratanase is known to cleave at monosulphated disaccharides where GlcNAc is sulphated and Gal is unsulphated. The results demonstrated that, after keratanase digestion, there were regions that remained attached towards the reducing terminal that were keratanase resistant with over sulphated (recognised by 5D4) and non-sulphated domains (figure 7.1). By using bovine nasal cartilage aggrecan as a source of KS type II, that has been shown to be devoid of fucose attachments compared to articular cartilage aggrecan KS type IIA (Nieduszynski *et al.*, 1990 B), the presence of regions of mono-sulphated fucosylated disaccharides that would be resistant to keratanase digestion (Tai *et al.*, 1993) could be ruled out. The results were supported by analysis of further digestion using endo-β-galactosidase, which

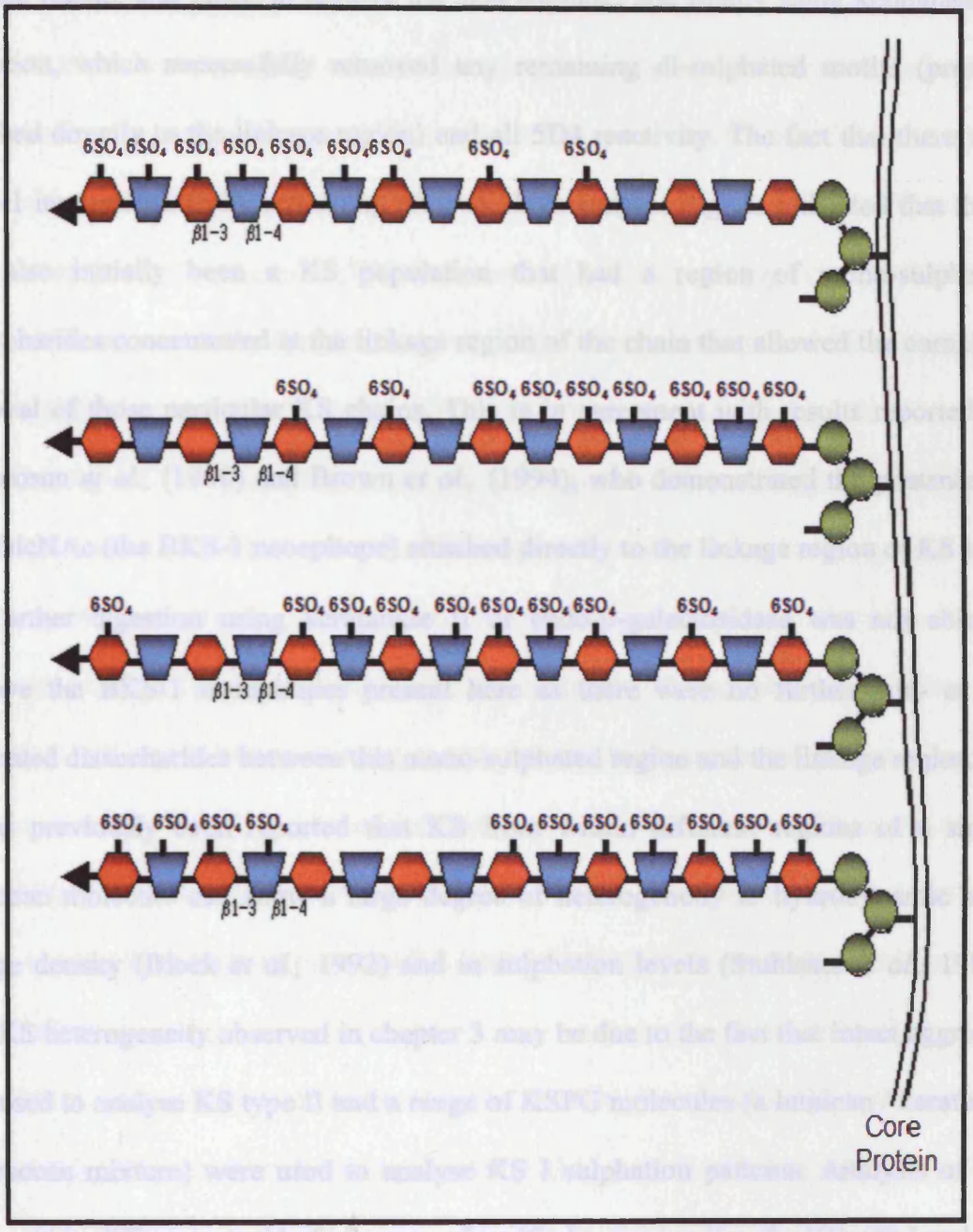

Figure 7.1 Heterogeneity in the sulphation patterns of KS with non-, mono- or di-sulphated domains occurring attached directly to the linkage region.

successfully removed any remaining undersulphated motifs present towards the linkage region, and failed to remove the 5D4 staining, and finally using keratanase II digestion, which successfully removed any remaining di-sulphated motifs (present attached directly to the linkage region) and all 5D4 reactivity. The fact that there was BKS-1 immunoreactivity remaining after all three enzyme digests indicated that there had also initially been a KS population that had a region of mono-sulphated disaccharides concentrated at the linkage region of the chain that allowed the complete removal of those particular KS chains. This is in agreement with results reported by Dickenson *et al.,* (1990) and Brown *et al.,* (1994), who demonstrated the presence of 6-S-GlcNAc (the BKS-1 neoepitope) attached directly to the linkage region of KS type II. Further digestion using keratanase II or endo-β-galactosidase was not able to remove the BKS-1 neoepitopes present here as there were no further non- or di-sulphated disaccharides between this mono-sulphated region and the linkage region.

It has previously been reported that KS from within different regions of a single aggrecan molecule can show a large degree of heterogeneity in hydrodynamic size, charge density (Block *et al.,* 1992) and in sulphation levels (Stuhlsatz *et al.,* 1989). The KS heterogeneity observed in chapter 3 may be due to the fact that intact aggrecan was used to analyse KS type II and a range of KSPG molecules (a lumican / keratocan / mimecan mixture) were used to analyse KS I sulphation patterns. Analysis of KS from within different peptide fragments of purified aggrecan (i.e. the KS, CS I and CS II domains) or from purified lumican, keratocan or mimecan, would help to determine if particular populations of KS (e.g. figure 7.1) exist on specific regions of aggrecan or on particular KSPGs that specifically have non-, mono- or di-sulphated disaccharide domain patterns attached directly to the linkage region of the KS chains.

An increase of KS GAG substitutions compared to CS substitutions on the KS, CS I and CS II domains of cartilage aggrecan with age has been well documented (Mourao

et al., 1976; Heinegard & Axelsson, 1977; Thonar & Sweet, 1981; Inerot & Heinegard, 1983; Thonar *et al.*, 1986; Bayliss, 1990; Barry *et al.*, 1995; Pratta *et al.*, 2000). However the exact sites of KS substitution along these regions are less well defined by consensus sequence assignment. The new 'KS stub' mAbs (BKS-1 or BKS-2) generated and characterised as described in chapter 2, could be used in the future for analysis of purified aggrecan A1D1 from bovine articular cartilage of different aged animals (foetal, newborn, 1yr, 2yr and 7yr old), to determine sites of KS substitution which remain common or change during development and ageing. To allow for identification of the sites of KS substitution, trypsin digested aggrecan could be separated into KS, CS/KS and CS rich fragments using anion exchange and size exclusion chromatography. After deglycosylation using keratanase and chondroitinase ABC, mAb affinity purification of fragments containing KS and CS 'stubs' identified by SDS PAGE and Western blotting, samples could be subjected to N-terminal amino acid sequencing to identify the site for attachment of KS chains on PG core proteins. Competitive ELISAs can be set up using mAb BKS-1 in conjunction with anti CS 'stub' mAbs to quantify changes in KS and CS substitutions on aggrecan identified with ageing.

Attempts to also produce an antibody to a non-reducing terminal 6-sulphated-galactose or an unsulphated galactose neoepitope, generated as a result of keratanase II digestion of KS chains, resulted in the production of two such novel monoclonal antibodies. The hybridoma cell lines failed to maintain production of keratanase II-generated 'KS stub' epitope mAbs. However, the work demonstrated that it was possible to generate such mAbs; i.e. proof of principle.

As a by-product of the attempts to generate the keratanase II 'KS stub' mAbs, two monoclonal antibodies to SLRPs lumican and keratocan were generated. The new mAbs (LUM-1 and KER-1) have proved to be useful tools in identification of low and

increased levels of corneal associated KSPGs in musculoskeletal tissue locations with pathology (chapter 6). It is still not clear whether the increase in expression observed for these SLRPs is an attempt to repair damage caused by losses due to aggrecan degradation or whether it actually causes more damage to the matrix structure. The observed up-regulation of lumican and keratocan synthesis in cartilage and IvD by chondrocytes and IvD cells, along with other generally non-cartilage associated molecules, such as collagen I (Young *et al.,* 2005 A), may reflect an attempt to repair the cartilage damage caused by the proteolytic degradation of aggrecan due to the action of MMPs and aggrecanases or an attempt to produce the fibrocartilage scar tissue associated with OA.

In the cornea, lumican containing the non-sulphated polylactosamine form of KS, similar to the form that has been identified in chapter 6 as being present in pathological cartilage and IvD, has been shown to be involved in the infiltration of macrophages in corneal wounds through interaction with lumican receptors (Funderburgh *et al.,* 1997 B). Molecules such as lumican have also been implicated in regulating corneal wound healing and inflammatory responses (Yeh *et al.,* 2005; Vij *et al.,* 2005 A; Chakravarti *et al.,* 2005; Kao *et al.,* 2005). Lumican knockout models have demonstrated its importance as an up-regulator of Fas-Fas Ligand (FasL) signalling and induction of pro-inflammatory cytokines in corneal inflammatory responses during wound healing (Vij *et al.,* 2005 A & 2005 B; Chakravarti *et al.,* 2005). Lumican is thought to have a role in binding FasL and in presenting it to Fas or to stabilise the Fas-FasL complex and help mediate signalling (Vij *et al.,* 2005 B). The Fas-FasL signalling pathway has been implicated in many inflammatory diseases including osteoarthritis and rheumatoid arthritis. Fas-FasL has been shown to have two major functions. Firstly it activates apoptotic pathways to regulate cell turnover and maintain a balance between synthesis and degradation. OA tenocytes have been shown to undergo spontaneous

apoptosis and to be much more susceptible to the higher levels of FasL than tenocytes from normal tissues (Machner *et al.,* 2003). It has also been shown to have pro-inflammatory functions through its chemotactic properties towards neutrophilic polymorphonuclear (PMNs) leukocytes. Very low levels of Fas-FasL have been shown to attract large numbers of inflammatory cells into the tissue (Ottonello *et al.,* 1999; O'Connell, 2001). They induce the infiltrated neutrophils and other cells to produce cytokines such as IL-1 β, which is a neutrophil chemotactant itself, thus amplifying the infiltration process and maintaining inflammatory responses. Infiltration of PMNs in corneal healing after epithelium debridement has been shown to be slowed from 24 hours in wild type mouse models to 48 hours in lumican knock out models and induction of inflammatory cytokines was reduced in lumican -/- models indicating lumican as an important modulator of the inflammatory response in corneal wound healing (Chakravarti *et al.,* 2005; Kao *et al.,* 2005).

In cartilage, pro-inflammatory cytokines such as IL-1, which are produced by inflammatory cells that have been attracted through the Fas-FasL signalling pathway, have been shown to be primarily responsible for inducing protease synthesis such as matrix metalloproteinases (MMPs) and aggrecanases, and subsequent cartilage matrix catabolism associated with OA. Therefore the up-regulation of non- or low-sulphated forms of lumican in arthritic diseases may directly contribute to the production of the cytokines and proteases responsible for cartilage degradation.

Lumican has also recently been shown to regulate keratocan gene expression in the mouse cornea (Carlson *et al.,* 2005). Over expression of lumican resulted in an increased expression of keratocan at both the protein and mRNA levels. Analysis of lumican knockout models also demonstrated a decreased expression of keratocan compared to wild type mice (Carlson *et al.,* 2005). These results demonstrated that lumican regulates keratocan expression at the transcriptional level. Perhaps this

regulatory transcriptional role is also active in articular cartilage and the increased expression of lumican with pathology results in a comparable increase in keratocan expression.

The work carried out as part of this thesis has resulted in the generation of a range of useful monoclonal antibodies recognising novel KS 'stub' neoepitopes and lumican and keratocan core protein epitopes. They have proved to be important tools in the elucidation of the structural variations and the distribution of various matrix molecules in different connective tissues. Collectively, the data in this thesis provides new and confirmatory information regarding the heterogeneous nature of KS sulphation motif structure and new information about lumican and keratocan expression at the molecular and proteomic levels in musculoskeletal tissue. The generic structure for KS has been challenged and is proposed to be composed of a range of KS chain structures that are more heterogeneous in nature, even from within the same tissue, than previously thought (Oeben *et al.*, 1987; Stuhlsatz *et al.*, 1989). The work also suggests that the expression of the small leucine rich PGs, lumican and keratocan, may be useful biomarkers to detect cellular changes in metabolism that lead to the onset of degenerative joint disease.

References

- Abbruzzese C., Kuhn U., Molina F., Rama P. & DeLuca M. (2004) Novel mutations in the CHST6 gene causing macular corneal dystrophy. *Clinical Genetics.* **65:** 120 – 125.
- Abramson S.R. & Woessner J.F. Jr. (1992) cDNA sequence for rat dermatan sulfate proteoglycan-II (decorin). *Biochim Biophys Acta.* **1132(2):** 225-227.
- Aigner T., Bertling W., Stoss H., Weseloh G. & von der Mark K. (1993) Independent expression of fibril-forming collagens I, II and III in chondrocytes of human osteoarthritic cartilage. *Journal of Clinical Investigation.* **91**: 829-837.
- Akama T.O., Nishida K., Nakayama J., Watanabe H., Ozaki K., Nakamura T., Dota A., Kawasaki S., Inoue Y., Maeda N., Yamamoto S., Fujiwara T., Thonar E.J., Shimomura Y., Kinoshita S., Tanigami A. & Fukuda M.N. (2000) Macular corneal dystrophy type I and type II are caused by distinct mutations in a new sulphotransferase gene. *Nature Genetics.* **26(2):** 237-41.
- Akama T.O., Nakayama J., Nishida K., Hiraoka N., Suzuki M., McAuliffe J., Hindsgaul O., Fukuda M. & Fukuda M. (2001) Human corneal GlcNAc 6-0-sulphotransferase and mouse intestinal GlcNAc 6-0-sulphotransferase both produce keratan sulphate. *The Journal of Biological Chemistry.* **276 (19):** 16271 – 16278.
- Akama T.O., Misra A.K., Hindsgaul O. & Fukuda M.N. (2002) Enzyme synthesis in vitro of the disulphated disaccharide unit of corneal keratan sulphate. *The Journal of Biological Chemistry.* **277 (45):** 42505 – 42513.

- Akimoto Y., Yamakawa N., Furukawa K., Kimata K., Kawakami H. & Hirano H. (2002) Changes in distribution of the long form of type XII collagen during chicken corneal development. *The Journal of Histochemistry and Cytochemistry.* **50:** 851 – 862. et al 2002
- Amado M., Almeida R., Schwientek T. & Clausen H. (1999) Identification and characterization of large galactosyltransferase gene families: galactosyltransferases for all functions. *Biochim Biophys Acta.* **1473(1):** 35-53. Review
- Antonsson P., Heinegard D. & Oldberg A. (1989) The keratan sulphate enriched region of bovine cartilage proteoglycans consists of a consecutively repeated hexapeptide motif. *The Journal of Biological Chemistry.* **264:** 16170-16173.
- Antonsson P., Heinegard D. & Oldberg A. (1991) Posttranslational modifications of fibromodulin. *The Journal of Biological Chemistry.* **266:** 16859-16861.
- Antonsson P., Heinegard D. & Oldberg A. (1993) Structure and deduced amino acid sequence of the human fibromodulin gene. *Biochim Biophys Acta.* **1174(2):** 204-6.
- Aspberg A., Miura R., Bourdoulous S., Shimonaka M., Heinegard D., Schachner M., Ruoslahti E. & Yamaguchi Y. (1997) The C-type lectin domains of lecticans, a family of aggregating chondroitin sulphate proteoglycans, bind tenascin-R by protein-protein interactions independent of carbohydrate moiety. *Proceeding of the National Academy of Science, USA.* **94:** 10116 – 10121.
- Baker J.R., Cifonelli J.A. & Roden L. (1969) The linkage of corneal keratosulphate to protein. *Biochemical Journal.* **115**: 11.

- Baker J.R., Cifonelli J.A. & Roden L. (1975) The linkage of corneal keratan sulfate to protein. *Connect Tissue Research.* **3**: 149-56.
- Baker J.R. & Caterson B. (1979). The isolation and characterization of the link proteins from proteoglycan aggregates of bovine nasal cartilage. *The Journal of Biological Chemistry.* **254:** 2387-2393.
- Balduini C., De Luca G. & Castellani A.A. (1989). Biosynthesis of skeletal and corneal keratan sulphate. *Keratan Sulphate: Biology, Chemistry, Chemical Pathology.* Greiling H and Scott JE, Editors. The Biochemical Society, London. Pages 53 – 65.
- Barry F.P., Neame P.J., Sasse J. & Pearson D. (1994) Length variation in keratan sulphate domain of mammalian aggrecan. *Matrix Biology.* **14**: 323-328.
- Barry F.P., Rosebberg L.C., Gaw J.U., Gaw J.U., Koob T.J. & Neame P.J. (1995) N- and O-Linked keratan sulphate on hyaluronan binding region of aggrecan from mature and immature bovine cartilage. *The Journal of Biological Chemistry.* **270**: 20516-20524.
- Bayliss M.T. (1990) Proteoglycan structure and metabolism during maturation and ageing of human articular cartilage. *Biochemical Society Transactions.* **18:** 799 – 802.
- Bayliss M.T., Osborne D., Woodhouse S. & Davidson C. (1999). Sulfation of chondroitin sulfate in human articular cartilage. The effect of age, topographical position, and zone of cartilage on tissue composition. *The Journal of Biological Chemistry.* **274:** 15892-900.
- BenEzra D. & Foidart J.M. (1981) Collagens and non collagenous proteins in the human eye. I. Corneal stroma in vivo and keratocyte production in vitro. *Current Eye Research.* **1**: 101-10.

- Bidanset D.J., Guidry C., Rosenberg L.C., Choi H.U., Timpl R. & Hook M. (1992) Binding of the proteoglycan decorin to collagen type VI. *The Journal of Biological Chemistry.* **267:** 5250-5256.
- Birk D.E., Fitch J.M., Babiarz J.P. & Linsenmayer T.F. (1988) Collagen type I and type V are present in the same fibril in the avian corneal stroma. *Journal of Cell Biology.* **106**: 999-1008.
- Birk D.E., Fitch J.M., Babiarz J.P., Doane K.J. & Linsenmayer T.F. (1990) Collagen fibrillogenesis in vitro: interaction of types I and V collagen regulates fibril diameter. *Journal of Cell Science.* **95:** 649-57.
- Bishop P.N., Crossman M.V., McLeod D. & Ayad S. (1994) Extraction and characterization of the tissue forms of collagen types II and IX from bovine vitreous. *Biochemical Journal.* **299(Pt 2):** 497-505.
- Blaschke U.K., Eikenberry E.F., Hulmes D.J., Galla H.J. & Bruckner P. (2000) Collagen XI nucleates self-assembly and limits lateral growth of cartilage fibrils. *The Journal of Biological Chemistry.* **275(14):**10370-8.
- Blochberger T.C., Vergnes J.P., Hempel J. & Hassell J.R. (1992) cDNA to chick lumican (corneal keratan sulphate proteoglycan) reveals homology to the small interstitial proteoglycan gene family and expression in muscle and intestine. *The Journal of Biochemistry.* **267:** 347 – 352.
- Block J.A., Inerot S.E. & Kimura J.H. (1992) Heterogeneity of keratan sulphate substituted on human chondrocytic large proteoglycans. *The Journal of Biological Chemistry.* **267**: 7245-7252.
- Bode-Lesniewska B., Dours-Zimmermann M.T., Odermatt B.F., Briner J., Heitz P.U. & Zimmermann D.T. (1996) Distribution of the large aggregating

proteoglycan versican in adult human tissues. *The Journal of Histochemistry and Cytochemistry.* **44:** 303 – 312.

- Boot-Handford R.P., Tuckwell D.S., Plumb D.A., Farrington C. & Poulson R. (2003) A novel and highly conserved collagen (proα1(XXVII)) with unique expression pattern and unusual molecular characteristics establishes a new clade within the vertebrate fibrillar collagen family. *The Journal of Biological Chemistry.* **278:** 31067 – 31077.
- Bovolenta P. & Fernaud-Espinosa I. (2000) Nervous system proteoglycans as modulators of neurite outgrowth. *Progress in Neurobiology.* **61**: 113-32.
- Bray B.A., Lieberman R. & Meyer K. (1967) Structure of human skeletal keratosulfate. The linkage region. *The Journal of Biological Chemistry.* **25**: 3373-80.
- Brew K., Vanaman T.C. & Hill R.L. (1968) The role of alpha-lactalbumin and the A protein in lactose synthetase: a unique mechanism for the control of a biological reaction. *Proceedings of the National Academy of Science, USA.* **59(2):** 491-7.
- Brown G.M., Huckerby T.N., Morris H.G., Abram B.L. & Nieduszynski I.A. (1994) Oligosaccharides derived from bovine articular cartilage keratan sulphates after keratanase II digestion: Implications for keratan sulphate structural fingerprinting. *Biochemistry* **33:** 4836 – 4836.
- Brown G.M., Huckerby T.N., Abram B.L. & Nieduszynski I.A. (1996) Characterization of a non-reducing terminal fragment from bovine articular cartilage keratan sulphates containing alpha(2-3)-linked sialic acid and alpha(1-3)-linked fucose. A sulphated variant of the VIM-2 epitope. *Biochemical Journal.* **319 (Pt 1):** 137-41.

- Brown G.M., Huckerby T.N., Bayliss M.T. & Nieduszynski I.A. (1998). Human aggrecan KS undergoes structural changes during adolescent development. *The Journal of Biological Chemistry.* **273**: 26408-26416.
- Buckwalter J.A., Rosenberg L.C. & Tang L.H. (1984) The effect of link protein on proteoglycan aggregate structure. An electron microscopic study of the molecular architecture and dimensions of proteoglycan monomers and link proteins of bovine fetal epiphyseal cartilage. *The Journal of Biological Chemistry.* **259**: 5361-5363.
- Buckwalter J.A. (1995) Osteoarthritis and articular cartilage use, disuse, and abuse: experimental studies. *Journal of Rheumatology. Supplement* **43:** 13-5.
- Buckwalter J.A. & Hunziker E.B. (1996) Orthopaedics. Healing of bones, cartilages, tendons, and ligaments: a new era. *Lancet.* **348 Suppl 2:** sII18.
- Buckwalter J.A. & Mankin H.J. (1998) Articular cartilage: tissue design and chondrocyte-matrix interactions. *Instr Course Lect.* **47:** 477-486. Review.
- Cai C.X., Gibney E., Gordon M.K., Marchant J.K., Birk D.E. & Linsenmayer T.F. (1996) Characterization and developmental regulation of avian corneal beta-1,4-galactosyltransferase mRNA. *Experimental Eye Research.* **63(2):** 193-200.
- Calabro A., Hascall V.C. & Caterson B. (1992) Monoclonal antibodies directed against epitopes within the core protein structure of the large aggregating proteoglycan (Aggrecan) from the swarm rat chondrosarcoma. *Arch Biochem Biophys.* **298**: 349-360.
- Calabro A., Midura R., Wang A., West L., Plaas A. & Hascall V.C. (2001) Fluorophore-assisted carbohydrate electrophoresis (FACE) of glycosaminoglycans. *Osteoarthritis and Cartilage.* **9 (A):** S16 – S22.

- Carlson E.C., Liu C.Y., Chikama T., Hayashi Y., Kao C.W., Birk D.E., Funderburgh J.L., Jester J.V. & Kao W.W. (2005) Keratocan, a cornea-specific keratan sulfate proteoglycan, is regulated by lumican. The Journal of Biological Chemistry. **280(27):** 25541-7.
- Caterson B., Christner J.E. & Baker J.R. (1983). Identification of a monoclonal antibody that specifically recognises corneal and skeletal keratan sulphate. *Journal of Biological Chemistry.* **258**: 8848-8854.
- Caterson B., Christner J.E., Baker J.R. & Couchman J.R. (1985). Production and characterisation of monoclonal antibodies directed against connective tissue proteoglycans. *Federation of American Societies of Experimental Biology.* **44**: 386-393.
- Caterson B., Calabro T. & Hampton A. (1987) Monoclonal antibodies as probes for elucidating proteoglycan structure and function. In *Biology of proteoglycans.* Wright T.N. & Mecham R.P., Editors. Academic Press Inc. Orlando, San Diego, New York, Austin, Boston, London, Sydney, Tokyo, Toronto. Pages: 1 – 25.
- Caterson B., Mahmoodian F., Sorrell J.M., Hardingham T.E., Bayliss M.T., Carney S.L., Ratcliffe A. & Muir H. (1990) Modulation of native chondroitin sulphate structure in tissue development and in disease. *Journal of Cell Science.* **97(Pt 3):** 411-7.
- Caterson B., Flannery C.R., Hughes C.E. & Little C.B. (2000) Mechanisms involved in cartilage proteoglycan catabolism. *Matrix Biology.* **19:** 333 – 344.
- Chakravarti S., Magnuson T., Lass J.H., Jepsen K.J., LaMantia C. & Carroll H. (1998). Lumican regulates collagen fibril assembly: skin fragility and corneal opacity in the absence of lumican. *Journal of Cell Biology.* **141**: 1277-1286.

- Chakravarti S., Petroll W.M., Hassell J.R., Jester J.V., Lass J.H., Paul J. & Birk D.E. (2000). Corneal opacity in lumican-null mice: defects in collagen fibril structure and packing in the posterior stroma. *Investigative Ophthalmology and Vision Science.* **41**: 3365-3373.
- Chakravarti S. (2001) The cornea through the eyes of knockout mice. *Experimental Eye Research.* **73:** 411 – 419.
- Chakravarti S. (2003) Functions of lumican and fibromodulin: lessons from knockout mice. *Glycoconjugate Journal.* **19:** 287 – 293.
- Chakravarti S., Vij N., Roberts L., Wu F. & Savino L. (2005) Lumican regulates wound healing and innate immune responses in cornea. *The Association for Research in Vision and Ophthalmology.* **Program number 2129.**
- Chang J. & Poole C.A. (1996) Sequestration of type VI collagen in the pericellular microenvironment of adult chondrocytes cultured in agarose. *Osteoarthritis & cartilage.* **4**: 275-285.
- Cheng H., Caterson B., Neame P.J., Lester G.E. & Yamauchi M. (1996) Differential distribution of lumican and fibromodulin in tooth cementum. *Connect Tissue Research.* 34(2):87-96.
- Choi H.U. & Meyer K. (1975). The structure of keratan sulphates from various sources. *Biochemical Journal.* **151**: 543-553.
- Christner J.E., Caterson B. & Baker J.R. (1980). Immunological determinants of proteoglycans. Antibodies against the unsaturated oligosaccharide products of chondroitinase ABC-digested cartilage proteoglycans. *The Journal of Biological Chemistry.* **255**: 7102-5.

- Chu C.Q., Field M., Allard S., Abney E., Feldmann M. & Maini R.N. (1992). Detection of cytokines at the cartilage/pannus junction in patients with rheumatoid arthritis: implications for the role of cytokines in cartilage destruction and repair. *British Journal of Rheumatology.* **31**: 653-61.
- Cintron C., Hong B.S., Covington H.I. & Macarak E.J. (1988) Heterogeneity of collagens in rabbit cornea: type III collagen. *Investigative Ophthalmology and Vision Science.* **29**: 767-775.
- Cole G.J. & McCabe C.F. (1991) Identification of a developmentally regulated keratan sulfate proteoglycan that inhibits cell adhesion and neurite outgrowth. *Neuron.* **7**: 1007-1018.
- Conrad G.W., Ager-Johnson P. & Woo M-L. (1982) Antibodies against the predominant glycosaminoglycan of the mammalian cornea, keratan sulphate-1. *Journal of Biological Chemistry.* **257:** 464 – 471.
- Conrad E. (1997) Commentary on heparin-like glycosaminoglycans. *Angiogenesis.* **1 (1):** 16 – 19.
- Conrad A.H. & Conrad G.W. (2003) The keratocan gene is expressed in both ocular and non-ocular tissues during early chick development. *Matrix Biology.* **22(4):** 323-37.
- Cornuet P.K., Blochberger T.C. & Hassell J.R. (1994) Molecular polymorphism of lumican during corneal development. *Investigative Ophthalmology and Vision Science.* **35**: 870-877.
- Corpuz L.M., Funderburgh J.L., Funderburgh M.L., Bottomley G.S., Prakash S. & Conrad G.W. (1996) Molecular cloning and tissue distribution of keratocan. *The Journal of Biological Chemistry.* **271**: 9759-9763.

- Couchman J.R., Caterson B., Christner J.E. & Baker J.R. (1984) Mapping by monoclonal antibody detection of glycosaminoglycans in connective tissues. *Nature.* **307**: 650-652.
- Cs-Szabo G., Melching L.I., Roughley P.J. & Glant T.T. (1997) Changes in mRNA and protein levels of proteoglycans and link protein in human OA cartilage samples. *Arthritis and Rheumatism.* **40 (6):** 1037 – 1045.
- Cs-Szabo G., Ragasa-San Juan D., Turumella V., Masuda K., Thonar E.J. & An H.S. (2002) Changes in mRNA and protein levels of proteoglycans of the anulus fibrosus and nucleus pulposus during intervertebral disc degeneration. *Spine.* 27(20): 2212-2219
- Danielson K.G., Fazzio A., Cohen I., Cannizzaro L.A., Eichstetter I. & Iozzo R.V. (1993). The human decorin gene: intron-exon organization, discovery of two alternatively spliced exons in the 5' untranslated region, and mapping of the gene to chromosome 12q23. *Genomics.* **15**: 146-160.
- Dickenson J.M., Huckerby T.N. & Nieduszynski I.A. (1990) Two linkage region fragments isolated from skeletal KS contain a sulphated N-acetylglucosamine residue. *Biochemical Journal* **269:** 55 – 60.
- Doege K., Sasaki M., Horigan E., Hassell J.R. & Yamada Y. (1987) Complete primary structure of the rat cartilage proteoglycan core protein deduced from cDNA clones. *The Journal of Biological Chemistry.* **262:** 17757 – 17767.
- Doege K.J., Sasaki M., Kimura T. & Yamada Y. (1991) Complete coding sequence and deduced primary structure of the human cartilage large aggregating proteoglycan, aggrecan. Human-specific repeats, and additional alternatively spliced forms. *The Journal of Biological Chemistry.* **266(2):** 894-902.

- Duance V.C. (1983). Surface of articular cartilage: immunohistochemical studies. *Cell Biochemistry and Function.* **1**: 143-144.
- Dunlevy J.R., Neame P.J., Vergness J.P. and Hassell J.R. (1998) Identification of the N-linked oligosaccharide sites in chick corneal lumican and keratocan that receive keratan sulphate. *The Journal of Biological Chemistry.* **273:** 9615 – 9621.
- Dunlevy J.R., Beales M.P., Berryhill B.L., Cornuet P.K. & Hassell J.R. (2000) Expression of the keratan sulphate proteoglycans lumican, keratocan and osteoglycin/mimican during chick corneal development. *Experimental Eye Research.* **70**: 349-362.
- Eronen I., Mononen T. & Mononen I. (1985) Isolation and partial characterization of keratan sulphate from human brain. *Biochimica et Biophysica Acta.* **843:** 155 – 158.
- Eyre D.R. & Muir H (1977) Quantitative analysis of types I and II collagens in the human intervertebral disc at various ages. *Biochimica et Biophysica Acta.* **492:** 29 – 42.
- Eyre D.R. (2002) Collagen of articular cartilage. *Arthritis Research.* **4**:.30-35.
- Farndale R.W., Buttle D.J. & Barrett A.J. (1986) Improved quantitation and discrimination of sulphated glycosaminoglycans by use of dimethylmethylene blue. *Biochemica et Biophysica Acta.* **883**: 173-177.
- Fassler R., Schnegelsberg P.N.J., Dausman J., Shinya T., Muragaki Y., McCarthy M.T., Olsen B. & Jaenisch R. (1994) Mice lacking α1(IX) collagen develop noninflammatory degenerative joint disease. *Proceeding of the National Academy of Science, USA.* **91:** 5070 – 5074.

- Feldmann M., Brennan F.M. & Maini R.N. (1996) Rheumatoid Arthritis. *Cell.* **85**: 307-310.
- Fisher L.W., Termine J.D. & Young M.F. (1989) Deduced protein sequence of bone small proteoglycan I (biglycan) shows homology with proteoglycan II (decorin) and several nonconnective tissue proteins in a variety of species. *The Journal of Biological Chemistry.* **264**: 4571-4576.
- Fisher L.W., Heegaard A.M., Vetter U., Vogel W., Just W., Termine J.D. & Young M.F. (1991). Human biglycan gene. Putative promoter, intron-exon junctions, and chromosomal localization. *The Journal of Biological Chemistry.* **266**: 14371-14377.
- Fischer D.C., Henning A., Winkler M., Rath W., Haubeck H.D. & Greiling H. (1996) Evidence for the presence of a large keratan sulphate proteoglycan in the human uterine cervix. *Biochemical Journal.* **320 (Pt 2):** 393-9.
- Fitch J.M., Mentzer A., Mayne R. & Linsenmayer T.F. (1988) Acquisition of type IX collagen by the developing avian primary corneal stroma and vitreous. *Developmental Biology.* **128**: 396-405.
- Fitzgerald J. & Bateman J.F. (2001) A new FACIT of the collagen family: COL21A1. *Federation of European Biochemical Society Letters.* **505**: 275-280.
- Folkman J. & Shing Y. (1992) Control of angiogenesis by heparin and other sulfated polysaccharides. *Advances in Experimental Medicine and Biology.* **313:** 355-364.
- Frielander D.R., Milev P., Karthikeyan L., Margolis R.K., Margolis R.U. & Grumet M. (1994) The neuronal chondroitin sulphate proteoglycan neurocan binds to the neural cell adhesion molecules Ng-CAM/L1/NILE and N-CAM,

and inhibits neuronal adhesion and neurite outgrowth. *The Journal of Biological Chemistry.* **125**: 669-680.

- Fukuda M.N. & Matsumura G. (1976) Endo-β-galactosidase of Escherichia freundii. Purification and endoglycosidic action on keratan sulfates, oligosaccharides, and blood group active glycoprotein. *The Journal of Biological Chemistry.* **251**: 6218-6225.
- Fukuta M., Inazawa J., Torii T., Tsuzuki K., Shimada E. & Habuchi O. (1997) Molecular cloning and characterization of human keratan sulphate Gal-6-Sulphotransferase. *The Journal of Biological Chemistry.* **272 (51):** 32321 – 32328.
- Funderburgh J.L., Stenzel-Johnson P.R., Chandler J.W. (1983) Monoclonal antibodies to rabbit corneal keratan sulphate proteoglycan. *Current eye Research* **2:** 769 – 776.
- Funderburgh J.L., Caterson B. & Conrad G. (1987) Distribution of proteoglycans antigenically related to corneal keratan sulphate proteoglycan. *The Journal of Biological Chemistry.* **262:** 11634 – 11640.
- Funderburgh J.L. & Conrad G.W. (1989) Detection and purification of corneal keratan sulphate proteoglycans from non-corneal tissues. In *Keratan sulphate: Chemistry, Biology and Chemical Pathology.* Greiling H. & Scott J.E., Editors. The Biochemical Society, London. Pages: 39 – 49.
- Funderburgh J.L. & Conrad G.W. (1990) Isoforms of corneal keratan sulphate proteoglycan. *The Journal of Biological Chemistry.* **265**: 8297-8303.
- Funderburgh J.L., Funderburgh M.L., Mann M.M. & Conrad G.W. (1991 A). Physical and biological properties of keratan sulphate proteoglycan. *Biochemical Society Transactions.* **19**: 871-876.

- Funderburgh J.L., Funderburgh M.L., Mann M.M. & Conrad G.W. (1991 B). Arterial lumican: properties of a corneal-type keratan sulphate proteoglycan from bovine aorta. *The Journal of Biological Chemistry.* **266:** 24773 – 24777.
- Funderburgh J.L., Funderburgh M.L., Brown S.J., Vergnes J.P., Hassell J.R., Mann M.M. & Conrad G.W. (1993) Sequence and structural implications of a bovine corneal keratan sulphate proteoglycan core protein. Protein 37B represents bovine lumican and proteins 37A and 25 are unique. *The Journal of Biological Chemistry.* **268**: 11874-11880.
- Funderburgh J.L., Corpuz L.M., Roth M.R., Funderburgh M.L., Tasheva E.S. & Conrad G.W. (1997 A) Mimican, the 25 kDa corneal keratan sulphate proteoglycan, is a product of the gene producing osteoglycin. *The Journal of Biological Chemistry.* **272**: 28089-28095.
- Funderburgh J.L., Mitschler R.L., Funderburgh M.L., Roth M.R., Chapes S.K. & Conrad G.W. (1997 B) Macrophage receptors for lumican. A corneal keratan sulfate proteoglycan. *Investigative Ophthalmology & Vision Science.* **38:** 1159-1167.
- Funderburgh J.L. (2000) Keratan Sulphate: structure, biosynthesis and function. *Glycobiology.* **10**: 951-958.
- Gelse K., Poschl E. & Aigner T. (2003). Collagens-structure, function, and biosynthesis. *Advanced Drug Delivery Reviews.* **28**: 1531-1546.
- Gill M.R., Oldberg A. & Reinholt F.P. (2002) Fibromodulin-null murine knee joints display increased incidences of osteoarthritis and alterations in tissue biochemistry. *Osteoarthritis & Cartilage.* **10:** 751 – 757.

- Gillard G.C., Caterson B. & Lowther D.A. (1975) The synthesis of hyaluronic acid by sheep and rabbit articular cartilage in vitro. *Biochemical Journal.* **145(2):**209-13.
- Grover J., Chen X.N., Korenberg J.R. & Roughley P.J. (1995) The human lumican gene. Organization, chromosomal location, and expression in articular cartilage. *The Journal of Biological Chemistry.* **270(37):** 21942-9.
- Habuchi O., Hirahara Y., Uchimura K. & Fukuta M. (1996) Enzymatic sulfation of galactose residue of keratan sulfate by chondroitin 6-sulfotransferase. *Glycobiology.* **6(1):** 51-57.
- Hahn R.A. & Birk D.E. (1992). β-D xyloside alters dermatan sulfate proteoglycan synthesis and the organization of the developing avian corneal stroma. *Development.* 115: 383-393.
- Halberg D.F., Proulx G., Doege K., Yamanda Y. & Drickamer K. (1988). A Segment of the cartilage proteoglycan core protein has lectin-like activity. *The Journal of Biological Chemistry.* **263**: 9486-9490.
- Hamanaka H., Maeda N. & Noda M. (1997) Spatially and temporally regulated modification of the receptor-like protein tyrosine phosphatase zeta/beta isoforms with keratan sulphate in the developing chick brain. *European Journal of Neuroscience.* **9(11):** 2297-308.
- Handley C.J. & Phelps C.F. (1972) The concentrations of sugar nucleotides in bovine corneal epithelium and endothelium. *Biochemical Journal.* **127**: 911-912.
- Hardingham T.E. & Muir H. (1974) Hyaluronic acid in cartilage and proteoglycan aggregation. *Biochemical Journal.* **139**: 565-581.

- Hardingham T.E. & Fosang A.J. (1992) Proteoglycans: many forms and many functions. *The Federation of American Societies for Experimental Biology Journal.* **6**: 861-869.
- Hardingham T. (1995) Changes in chondroitin sulphate structure induced by joint disease. *Acta Orthopaedica Scandinavica (Suppl 266).* **66**: 107-110.
- Hardingham T. (1998) Cartilage: aggrecan–link protein–hyaluronan aggregate URL http://www.glycoforum.gr.jp/science/hyaluronan/HA05/HA05E.html. Accessed September 2002.
- Hart G.W. (1976) Biosynthesis of glycosaminolgycans during corneal development. *The Journal of Biological Chemistry.* **251(21):** 6513-21.
- Hascall V.C. & Heinegard D. (1974) Aggregation of cartilage proteoglycans. I. The role of hyaluronic acid. *The Journal of Biological Chemistry.* **249**: 4232-4241.
- Hasegawa N., Torii T., Nagaoka I., Nakayasu K., Miyajima H. & Habuchi O. (1999) Measurment of activities of human serum sulfotransferases which transfer sulphate to the galactose residues of keratan sulphate and to the nonreducing end N-acetylglucosamine residues of N-acetyllactosamine trisaccharide: comparison between normal controls and patients with macular corneal dystrophy. *Journal of Biochemistry.* **125:** 245 – 252.
- Hasegawa N., Torii T., Kato T., Miyajima H., Furuhata A., Nakayasu K., Kanai A. & Habuchi O. (2000) Decreased GlcNAc 6-O-sulfotransferase activity with macular corneal dystrophy. *Investigative Ophthalmology and Vision Science.* **41:** 3670 – 3677.
- Hashimoto T., Wakabayashi T., Watanabe A., Kowa H., Hosoda R., Nakamura A., Kanazawa I., Arai T., Takio K., Mann D.M. & Iwatsubo T. (2002) CLAC: a

novel Alzheimer amyloid plaque component derived from a transmembrane precursor, CLAC-P/collagen type XXV. *European Molecular Biology Organization Journal.* **21**: 1524-1534.

- Hassell J.R., Kimura J.H. & Hascall V.C. (1986). Proteoglycan core protein families. *Annual Review of Biochemistry.* **55**: 539-567.
- Hedbom E. & Heinegard D. (1989) Interactions of a 50kDa connective tissue matrix protein with collagen I and collagen II. *The Journal of Biological Chemistry.* **264**: 6898-6905.
- Heinegard D. & Hascall V.C. (1974) Aggregation of cartilage proteoglycans: characteristics of the proteins isolated from trypsin digests of aggregates. *The Journal of Biological Chemistry.* **249 (13):** 4250-4256.
- Heinegard D. & Axelsson I. (1977). Distribution of keratan sulphate in cartilage proteoglycans. *The Journal of Biological Chemistry.* **252**: 1971-1979.
- Heinegard D. & Sommarin Y. (1987). Isolation and characterization of proteoglycans. *Methods in Enzymology.* **144**: 319-372.
- Hemming F.J. & Saxod R. (1998). Regulated expression of keratan sulphate and peanut agglutinin binding sites during organogenesis in the developing chick. *Histochemistry and Cell Biology.* **110**: 189-200.
- Hering T.M., Kollar J. & Huynh T.D. (1997) Complete coding sequence of bovine aggrecan: Comparative structural analysis. *Archives of Biochemistry and Biophysics.* **345**: 259-270.
- Hildebrand A., Romaris M., Rasmussen L.M., Heinegard D., Twardzik D.R., Border W.A. & Ruoslahti E. (1994). Interaction of the small interstitial proteoglycans biglycan, decorin and fibromodulin with transforming growth factor beta. *Biochemical Journal.* **302**: 527-34.

- Hollander A.P., Pidoux I., Reiner A., Rorabeck C., Bourne R. & Poole A.R. (1995) Damage to type II collagen in aging and osteoarthritis starts at the articular surface, originates around chondrocytes, and extends into the cartilage with progressive degeneration. *The Journal of Clinical Investigation.* **96(6):** 2859-69.
- Huckerby T.N., Brown G.M, Dickenson J.M. & Nieduszynski I.A. (1994) Spectroscopic characterisation of disaccharides derived from keratan sulfates. *European Journal of Biochemistry.* **229:** 119 – 131.
- Huckerby T.N., Brown G.M., Dickenson J. M. & Nieduszynski I. (1995) Spectroscopic characterisation of disaccharides derived from keratan sulphates. *European Journal of Biochemistry* **229:** 119 – 131.
- Huckerby T.N., Tai G.U. & Nieduszynski I. (1998) Oligosaccharides derived by endo-β-galactosidase digestion of bovine corneal keratan sulphate. Characterisation of tetrasaccharides with incomplete sulphation and containing unsulphated N-acetylglucosamine residues. *European Journal of Biochemistry.* **253:** 499 – 506.
- Huckerby T.N., Nieduszynski I.A., Bayliss M.T. & Brown G.M. (1999) 600 MHz NMR studies of human articular cartilage keratan sulfates. *European Journal of Biochemistry.* **266:** 1174 – 1183.
- Hughes C.E., Caterson B., Fosang A.J., Roughley P.J. & Mort J.S. (1995). Monoclonal antibodies that specifically recognize neoepitope sequences generated by 'aggrecanase' and matrix metalloproteinase cleavage of aggrecan: application to catabolism in situ and in vitro. *Biochemical Journal.* **305**: 799-804.

- Imamura T. & Mitsui Y. (1987). Heparan sulfate and heparin as a potentiator or a suppressor of growth of normal and transformed vascular endothelial cells. *Experimental Cell Research.* **172**: 92-100.
- Inerot S. & Heinegard D. (1983) Bovine tracheal cartilage proteoglycans. Variations in structure and composition with age. *Collagen and Related Research.* **3**: 245-262.
- Inkinen R.I., Lammi M.J., Lehmonen S., Puustjarvi K., Kappa E. & Tammi M.I. (1998) Relative increase of biglycan and decorin and altered chondroitin sulphate epitopes in degenerating human intervertebral disc. *Journal of Rheumatology.* **25:** 506 – 514.
- Iozzo R.V. & Murdoch A.D. (1996). Proteoglycans of the extracellular environment: clues from the gene and protein side offer novel perspectives in molecular diversity and function. *The Federation of American Society for Experimental Biology Journal.* **10**: 598-614.
- Iozzo R.V. (1998). Matrix proteoglycans: from molecular design to cellular function. *Annual Review of Biochemistry.* **67**: 609-652.
- Iozzo R.V. (1999). The biology of the small leucine-rich proteoglycans. *Journal of Biological Chemistry.* **274**: 18843-18846.
- Jackson L.R., Trudel L.J. & Lipman N.S. (1999) Small-Scale Monoclonal Antibody Production In Vitro: Methods and Resources. *Lab Animal.* **28 (3):** 38 – 50.
- Jonhson S.L., Aguiar D.J. & Ogilvie J.W. (2000) Fibronectin and its fragments increase with degeneration in the human intervertebral disc. *Spine.* **25:** 2741 – 2747.

- Kadler K.E., Holmes D.F., Trotter J.A. & Chapman J.A. (1996). Collagen fibril formation. *Biochemical Journal.* **316**:1-11.
- Kao C., Chikama T.I., Lui C.Y., Harvey S.A.K., Funderburgh M.L., Funderburgh J.L. & Kao W.W. (2005) Lumican serves as a substratum for PMN formation and migration during myelopoiesis and corneal wound healing. *The Association for Research in Vision and Ophthalmology.* **Program number 2130.**
- Kao W.W. & Liu C.Y. (2003) Roles of lumican and keratocan on corneal transparency. *Glycoconugate Journal.* 19: 275-285.
- Kaplan D. & Meyer K. (1959) Ageing of human cartilage. *Nature.* **183**: 1267-1268.
- Kawakita T., Espana E.M., He H., Hornia A., Yeh L.K., Ouyang J., Liu C.Y. & Tseng S.C. (2005) Keratocan expression of murine keratocytes is maintained on amniotic membrane by down-regulating transforming growth factor-beta signaling. The Journal of Biological Chemistry. **280(29):** 27085-92.
- Kearney J.F., Radbruch A., Liesegang B. & Rajewsky K. (1979). A new mouse myeloma cell line that has lost immunoglobulin expression but permits the construction of antibody-secreting hybrid cell lines. *Journal of Immunology.* **123**: 1548-1550.
- Kearney J.F., Barletta R., Quan Z.S. & Quintans J. (1981). Monoclonal vs. heterogeneous anti-H-8 antibodies in the analysis of the anti-phosphorylcholine response in BALB/c mice. *European Journal of Immunology.* **11(11):** 877-883.
- Kikuchi Y., Yasumoto K. & Meyer K. (1987) Amino acid sequence of a peptide from keratan sulphate II-core protein linkage region. *Journal of Biochemistry.* **102**: 1519-1524.

- Kellgren J.H. & Lawrence J.S. (1957) Radiological assessment of osteo-arthrosis. *Annals of the Rheumatic Diseases.* **16 (4):** 494-502.
- King M.W. (1996) The medical biochemistry page. URL http://www.indstate.edu/thcme/mwking/glycans.html. Accessed September 2002.
- Knudson C.B. & Knudson W. (2001) Cartilage proteoglycans. *Seminars in Cell and Developmental Biology.* **12(2):** 69-78.
- Koch M., Foley J.E., Hahn R., Zhou P., Burgeson R.E., Gerecke D.R. & Gordon MK. (2001). Alpha 1(Xx) collagen, a new member of the collagen subfamily, fibril-associated collagens with interrupted triple helices. *The Journal of Biological Chemistry.* **276**: 23120-23126.
- Koch M., Laub F., Zhou P., Hahn R.A., Tanaka S., Burgeson R.E., Gerecke D.R., Ramirez F. & Gordon M.K. (2003). Collagen XXIV, a vertebrate fibrillar collagen with structural features of invertebrate collagens: selective expression in developing cornea and bone. *The Journal of Biological Chemistry.* **278**: 43236-43244.
- Kohler G. & Milstein C. (1975) Continuous cultures of fused cells secreting antibody of predefined specificity. *Nature.* **256(5517):** 495-7.
- Korenberg J.R., Chen X.N., Doege K., Grover J. & Roughley P.J. (1993) Assignment of the human aggrecan gene (AGC1) to 15q26 using fluorescence in situ hybridization analysis. *Genomics.* **16(2):** 546-548.
- Krusius T., Finne J., Margolis R.K. & Margolis R.U. (1986) Identification of an O-glycosidic mannose-linked sialylated tetrasaccharide and keratan sulfate oligosaccharides in the chondroitin sulfate proteoglycan of brain. *The Journal of Biological Chemistry.* **261**: 8237-8242.

- Krusius T. & Ruoslahti E. (1986) Primary structure of an extracellular matrix proteoglycan core protein deduced from cloned cDNA. *Proceedings of the National Academy of Science, USA.* **83(20):** 7683-7.
- Krusius T., Gehlsen K.R. & Rouslahti E. (1987) A fibroblast chondroitin sulphate proteoglycan core protein contains lectin-like growth factor-like sequences. *The Journal of Biological Chemistry.* **262:** 13120 – 13125
- Kuivaniemi H., Tromp G. & Prockop D.J. (1997) Mutations in fibrillar collagens (types I, II, III, and XI), fibril-associated collagen (type IX), and network-forming collagen (type X) cause a spectrum of diseases of bone, cartilage, and blood vessels. *Human Mutation.* **9**: 300-15.
- Kushe-Gullberg M. & Kjellen, (2003) Sulphotransferases in glycosaminoglycan biosynthesis. *Current Opinion in Structural Biology.* **13:** 605 – 611.
- Lauder R.M., Huckerby T.N., Nieduszynski I.A. & Plaas A.H. (1998). Age-related changes in the structure of the keratan sulphate chains attached to fibromodulin isolated from articular cartilage. *Biochemistry Journal.* **330**: 753-757.
- Lauder R.M., Huckerby T.N., Brown G.M., Bayliss M.T. & Niedusynski I.A. (2001). Age-related changes in the sulphation of chondroitin sulphate from human articular cartilage aggrecan. *Biochemical Journal.* **358**: 523-528.
- Leroux J.Y., Guerassimov A., Cartman A., Delaunay N. Webber C., Rosenberg L.C., Banerjee S. & Poole A.R. (1996). Immunity to the G1 globular domain of the cartilage proteoglycan aggrecan can induce inflammatory erosive polyarthritis and spondylitis in BALB/c mice but immunity to G1 is inhibited

by covalently bound keratan sulfate in vitro and in vivo. *Journal of Clinical Investigation.* **97**: 621-632.

- Li S.W., Prockop D.J., Helminen H., Fassler R., Lapvetelainen T., Kiraly K., Peltarri A., Arokoski J., Lui H., Arita M., et al. (1995) Transgenic mice with targeted inactivation of the Col2 alpha 1 gene for collagen II develop a skeleton with membranous and periosteal bone but no endochondral bone. *Genes and Development.* **9(22):** 2821-2830.
- Lindahl U. & Roden L. (1965) The chondroitin 4-sulphate protein linkage. *The Journal of Biological Chemistry.* **241 (9):** 2113 – 2119.
- Linsenmayer T.F., Bruns R.R., Mentzer A. & Mayne R. (1986) Type VI collagen: immunohistochemical identification as a filamentous component of the extracellular matrix of the developing avian corneal stroma. *Developmental Biology.* **118(2):** 425-431.
- Little C.B., Hughes C.E., Curtis C.L., Janusz M.J., Bohne R., Wang-Weigand S., Taiwo Y.O., Mitchell P.G., Otterness I.G., Flannery C.R. & Caterson B. (2002). Matrrix metalloproteinases are involved in C-terminal and interglobular domain processing of cartilage aggrecan in late stage cartilage degradation. *Matrix Biology.* **21**: 271-288.
- Liu C.Y., Birk D.E., Hassell J.R., Kane B. & Kao W.W. (2003). Keratocan-deficient mice display alterations in corneal structure. *The Journal of Biological Chemistry.* **278**: 21672-21677.
- Lohmander L.S., CeLuca S., Nilsson B., Hascall V.C., Caputo C.B., Kimura J.H. & Heinegard D. (1980). Oligosaccharides on proteoglycans from the swarm rat chondrosarcoma. *The Journal of Biological Chemistry.* **255**: 6084-6091.

- Lohmander L.S., Hascall V.C., Yanagishita M., Keuttner K.E. & Kimura J.H. (1986). Post-translational events in proteoglycan synthesis: kinetics of synthesis of chondroitin sulphate and oligosaccharides on the core protein. *Archives of Biochemistry and Biophysics.* **250**: 211-227.
- Luckman S.P., Rees E. & Kwan A.P. (2003) Partial characterisation of cell-type X collagen interactions. *Biochemical Journal.* **372:** 485 – 493.
- Mc Cormick D., van der Rest M., Goodship J., Lozano G., Ninomiya Y. & Olsen B.R. (1987) Structure of the glycosaminoglycan domain in the type IX collagen-proteoglycan. *Proceedings of the National Academy of Science, USA.* **12:** 4044-4048.
- Machner A., Baier A., Wille A., Drynda S., Pap G., Drynda A., Mawrin C., Buhling F., Gay S., Neumann W. & Pap T. (2003) Higher susceptibility to Fas ligand induced apoptosis and altered modulation of cell death by tumor necrosis factor-alpha in periarticular tenocytes from patients with knee joint osteoarthritis. *Arthritis Research and Therapy.* **5(5):** R253-61.
- Malmstrom A. & Aberg L. (1982) Biosynthesis of dermatan sulphate. Assay and properties of the uronosyl C-5 epimerase. *Biochemical Journal.* **201 (3):** 489-493.
- Mankin H.J., Dorfman H., Lippiello L. & Zarins A. (1971) Biochemical and metabolic abnormalities in articular cartilage from osteo-arthritic human hips. II. Correlation of morphology with biochemical and metabolic data. *Journal of Bone and Joint Surgery American volume.* **53 (3):** 523-537.
- Margolis R.K. & Margolis R.U. (1993) Nervous tissue proteoglycans. *Experientia.* **49(5):** 429-446.

- Martel-Pelletier J. (1999) Pathophysiology of osteoarthritis. *Osteoarthritis and Cartilage.* **7**: 371-373.
- Mathews M.B. & Cifonelli J.A. (1965) Comparative biochemistry of keratosulfates. *The Journal of Biological Chemistry.* **240 (11):** 4140-5.
- Maurice D.M. (1957) The Structure and transparency of the corneal stroma. *Journal of Physiology.* **136**: 263-286.
- Meek K.M. & Fullwood N.J. (2001) Corneal and scleral collagens – a microscopist's perspective. *Micron.* **32:** 261-272.
- Mehmet H., Scudder P., Tang P.W., Hounsell E.F., Caterson B. & Feizi T. (1986) The antigenic determinants recognized by three monoclonal antibodies to keratan sulphate involve sulphated hepta- or larger oligosaccharides of the poly (N-acetlyllactosamine) series. *European Journal of Biochemistry.* **57**: 385-391.
- Melching L.I., Cs-Szabo G. & Roughley P.J. (1997) Analysis of proteoglycan messages in human articular cartilage by a competitive PCR technique. *Matrix Biology.* **16(1):** 1-11.
- Melching L.I. & Roughley P.J. (1999) Modulation of keratan sulfate synthesis on lumican by the action of cytokines on human articular chondrocytes. *Matrix Biology.* **18(4):** 381-90.
- Mendler M., Eich-Bender S.G., Vaughan L., Winterhalter K.H. & Bruckner P. (1989) Cartilage contains mixed fibrils of collagen types II, IX, and XI. *Journal of Cell Biology.* **108:**191-197.
- Meyer K., Linker A., Davidson E.A. & Weissmann B. (1953) The mucopolysaccharides of bovine cornea. *The Journal of Biological Chemistry.* **205:** 611-616.

- Meyer K., Davidson E., Linker A. & Hoffman P. (1956) The acid mucopolysaccharides of connective tissue. *Biochimica et Biophysica Acta.* **21:** 506-518.
- Meyer-Puttlitz B., Milev P., Junker E., Zimmer I., Margolis R.U. & Margolis R.K. (1995) Chondroitin sulfate and chondroitin/keratan sulfate proteoglycans of nervous tissue: developmental changes of neurocan and phosphacan. *Journal of Neurochemistry.* **65(5):** 2327-2337.
- Michelacci Y.M. (2003). Collagens and proteoglycans of the corneal extracellular matrix. *Brazilian Journal of Medical and Biological Research.* **36 (8):** 1037-1046.
- Midura R.J. & Hascall V.C. (1989) Analysis of the proteoglycans synthesized by corneal explants from embryonic chicken. II. Structural characterization of the keratan sulfate and dermatan sulfate proteoglycans from corneal stroma. *The Journal of Biological Chemistry.* **264(3):** 1423-30.
- Miura R., Aspberg A., Ethell I.M., Hagihara K., Schnaar R.L., Ruoslahti E. & Yamaguchi Y. (1999) The proteoglycan lectin domain binds sulphated cell surface glycolipids and promotes cell adhesion. *The Journal of Biological Chemistry.* **274:** 11431 – 11438.
- Mochizuki Y., Shinomura T. & Kimata K. (1998) Leucine rich proteoglycans. URL http://www.glycoforum.gr.jp/science/word/proteoglycan/PGA04E.html. Accessed September 2002.
- Mourao P.A., Rozenfeld S., Laredo J. & Dietrich C.P. (1976) The distribution of chondroitin sulfates in articular and growth cartilages of human bones. *Biochimica et Biophysica Acta.* **428 (1):** 19-26.

- Morrissey J.H. (1981) Silver stain for proteins in polyacrylamide gels: A modified procedure with enhanced uniform sensitivity. *Analytical Biochemistry.* **117:** 307-310.
- Munakata H., Takagaki K., Majima M. & Endo M. (1999) Interaction between collagens and glycosaminoglycans investigated using a surface plasmon resonance biosensor. *Glycobiology.* **9(10):** 1023-7.
- Naito Z., Ishiwata T., Kurban G., Teduka K., Kawamoto Y., Kawahara K. & Sugisaki Y. (2002) Expression and accumulation of lumican protein in uterine cervical cancer cells at the periphery of cancer nests. *International Journal of Oncology.* **20 (5):** 943-948.
- Nakamura M., Kobayashi M., Hirano K., Kobayashi K., Hoshino T. & Awaya S. (1992) Assembly of 100 nm periodic fibrils (type VI collagen) in human infant corneal stroma. *Japanese Journal of Ophthalmology.* **36 (4):** 458-464.
- Nakamura M., Kimura S., Kobayashi M., Hirano K., Hoshino T. & Awaya S. (1997) Type VI collagen bound to collagen fibrils by chondroitin/dermatan sulfate glycosaminoglycan in mouse corneal stroma. *Japanese Journal of Ophthalmology.* **41(2):** 71-6
- Nakazawa K. & Suzuki S. (1975). Purification of keratan sulfate-endogalactosidase and its action on keratan sulfates of different origin. *The Journal of Biological Chemistry.* **250 (3):** 912-917.
- Nakazawa K., Suzuki N. & Suzuki S. (1975). Sequential degradation of keratan sulfate by bacterial enzymes and purification of a sulfatase in the enzymatic system. *Journal of Biological Chemistry.* **250 (3):** 905-911.
- Nakazawa K., Newsome D.A., Nilsson B., Hascall V. & Hassell J.R. (1983) Purification of keratan sulphate proteoglycan from monkey cornea. Isolation of

the keratan sulphate linkage region and mannose-containing oligosaccharides. *The Journal of Biological Chemistry.* **258 (10):** 6051 – 6055.

- Nakazawa K., Hassell J.R., Hascall V.C., Lohmander L.S., Newsome D.A. & Krachmer J. (1984) Defective processing of keratan sulfate in macular corneal dystrophy. *The Journal of Biological Chemistry.* **259(22):** 13751-13757.
- Nakazawa K., Ito M., Yamagata T. & Suzuki S. (1989) Substrate specificity of keratan sulphate-degrading enzymes (endo-β-galactosidase, keratanase and keratanase II) from microorganisms. *Keratan Sulphate: chemistry, biology and chemical pathology.* Greiling H. & Scott J.E., Editors. The Biochemical Society, London. **Pages 99-110.**
- Nakazawa K., Takahashi I. & Yamamoto Y. (1998) Glycosyltransferase and sulfotransferase activities in chick corneal stromal cells before and after in vitro culture. *Archives of Biochemistry and Biophysics.* **359 (2):** 269-82.
- Newsome D.A., Gross J. & Hassell J.R. (1982) Human corneal stroma contains three distinct collagens. *Investigative Ophthalmology and Vision Science.* **22 (3):** 376 – 381.
- Nieduszynski I.A., Huckerby T.N., Dickenson J.M., Brown G.M., Tai G.H. & Bayliss M.T. (1990 A) Structural aspects of skeletal keratan sulphates. *Biochemical Society Transactions.* **18(5):** 792-793.
- Nieduszynski I.A., Huckerby T.N., Dickenson J.M., Brown G.M., Tai G.H., Morris H.G. & Eady S. (1990 B) There are two major types of skeletal keratan sulphates. *Biochemical Journal.* **271:** 243-245.
- Nilsson B., Nakazawa K., Hassell J.R., Newsome D.A. & Hascall V.C. (1983) Structure of oligosaccharides and the linkage region from between keratan

sulphate and the core protein on proteoglycans from monkey cornea. *The Journal of Biological Chemistry.* **258:** 6056-6063.

- O'Connell J. (2001) The role of Fas-FasL in inflammatory diseases. *Expert Reviews in Molecular Medicine.* 10 December. Electronic resource, URL http://www-ermm.cbcu.cam.ac.uk/01003969h.htm#45. Accessed February 2005.
- Oeben M., Keller R., Sthulsatz H.W. & Greiling H. (1987) Constant and variable domains of different disaccharide structure in corneal keratan sulphate chains. *Biochemical Journal.* **248 (1):** 85-93.
- Oguma T., Toyoda H., Toida T. & Imanari T. (2001) Analytical method for keratan sulfates by high-performance liquid chromatography/turbo-ion spray tandem mass spectrometry. *Analytical Biochemistry.* **290 (1):** 68-73.
- Ottonello L., Tortolina G., Amelotti M. & Dallegri F. (1999) Soluble Fas ligand is chemotactic for human neutrophilic polymorphonuclear leukocytes. *Journal of Immunology* **162:** 3601–6.
- Papageorgakopoulou N., Theocharis A.D., Skandalis S.S., Vynios D.H., Theocharis D.A. & Tsiganos C.P. (2001). Keratan sulphate in cerebrum, cerebellum and brainstem of sheep brain. *Biochimie.* **83 (10):** 973-978.
- Papageorgakopoulou N., Theocharis A.D., Skandalis S.S., Vynios D.H., Theocharis D.A. & Tsiganos C.P. (2002) Immunological studies of sheep brain keratan sulphate proteoglycans. *Biochimie.* **84 (12):** 1225-1228.
- Pfirrmann C.W., Metzdorf A., Zanetti M., Hodler J. & Boos N. (2001) Magnetic resonance classification of lumbar intervertebral disc degeneration. *Spine.* **26(17):** 1873-8.

- Perkins S.J., Nealis A.S., Dudhia J. & Hardingham T.E. (1989) Immunoglobulin fold and tandem repeat structures in proteoglycan N-terminal domains and link protein. *Journal of Molecular Biology.* **206 (4):** 737-753.
- Plaas A.H., Neame P.J., Nivens C.M. & Reiss L. (1990) Identification of the keratan sulphate attachment sites on bovine fibromodulin. *The Journal of Biological Chemistry.* **265 (33):** 20634-20640.
- Plaas A.H. & Wong-Palms S. (1993) Biosynthetic mechanisms for the addition of polylactosamine to chondrocyte fibromodulin. *The Journal of Biological Chemistry.* **268 (35):** 26634-26644.
- Plaas A.H., West L.A., Wong-Palms S. & Nelson F.R. (1998) Glycosaminoglycan sulfation in human osteoarthritis. Disease-related alterations at the non-reducing termini of chondroitin and dermatan sulfate. *The Journal of Biological Chemistry.* **273 (20):** 12642-12649.
- Plaas A.H., West L.A., Thonar E.J.A., Karcioglu Z.A., Smith C.J., Klintworth G.K. & Hascall V.C. (2001) Altered fine structures of corneal and skeletal keratan sulphate and chondroitin / dermatan sulphates in macular corneal dystrophy. *The Journal of Biological Chemistry.* **276 (43):** 39788-39796.
- Pontecorvo G. (1975). Production of mammalian somatic cell hybrids by means of PEG treatment. *Somatic Cell Genetics.* **1:** 397-400.
- Poon C.J., Plaas A.H., Keene D.R., McQuillan D.J., Last K. & Fosang A.J. (2005) N-linked keratan sulfate in the aggrecan interglobular domain potentiates aggrecanase activity. *The Journal of Biological Chemistry.* **280 (25):** 23615-21.

- Pratta M.A., Tortorella M.D. & Arner E.C. (2000). Age-related changes in aggrecan glycosylation affect cleavage by aggrecanase. *The Journal of Biological Chemistry.* **275 (50):** 39096-39102.
- Prehm P. (1984) Hyaluronate is synthesized at plasma membranes. *Biochemical Journal.* **220 (2):** 597-600.
- Quantock A.J., Meek K.M. & Chakravarti S. (2001) An X-ray diffraction investigation of corneal structure in lumican - deficient mice. *Investigative Ophthalmology and Vision Science.* **42 (8):** 1750-1756.
- Rada J.A., Cornuet P.K. & Hassell J.R. (1993) Regulation of corneal fibrillogenesis in vitro by corneal proteoglycan (lumican and decorin) core proteins. *Experimental Eye Research.* **56:** 635-648.
- Raouf A., Ganss B., McMahon C., Vary C., Roughley P.J. & Seth A. (2002) Lumican is a major proteoglycan component of the bone matrix. *Matrix Biology.* **21:** 361 – 367.
- Rauch U., Gao P., Janetzko A., Flaccus A., Hilgenberg L., Tekotte H., Margolis R.K. & Margolis R.U. (1991) Isolation and characterization of developmentally regulated chondroitin sulphate and chondroitin/keratan sulphate proteoglycans of brain identified with monoclonal antibodies. *The Journal of Biological Chemistry.* **266:** 14785 – 14801.
- Rauch U., Karthikeyan L., Maurel P., Margolis R.U. & Margolis R.K. (1992) Cloning and primary structure of neurocan, a developmentally regulated, aggregating chondroitin sulphate proteoglycan of brain. *The Journal of Biological Chemistry.* **267:** 19536 – 19547.
- Robert L., Legeais A.M. & Renard R.G. (2001) Corneal collagens. *Pathologie Biologie.* **49:** 353-363.

- Roberts S. & Urban J.P.G. Intervertebral Discs. Electronic resource, URL http://www.ilo.org/encyclopaedia/?doc&nd=857400144&nh=0&ssect=0. Accessed January 2005.
- Roughley P.J. & Lee E.R. (1994) Cartilage proteoglycans: structure and potential functions. *Microscopy Research and Techniques.* **28:** 385-397.
- Roughley P.J. (2001) Articular cartilage and changes in arthritis: noncollagenous proteins and proteoglycans in the extracellular matrix of cartilage. *Arthritis Research.* **3:** 342-347.
- Ruter ER, Kresse H. (1984) Partial purification and characterization of 3'-phosphoadenylylsulfate: keratan sulfate sulfotransferases. *The Journal of Biological Chemistry.* **259(19):** 11771-6.
- Saamanen A.M., Salminen H.J., Rantakokko A.J., Heinegard D. & Vuorio E.I. (2001) Murine fibromodulin: cDNA and genomic structure, and age-related expression and distribution in the knee joint. *Biochemical Journal.* **355(Pt 3):** 577-85.
- Sasaki K., Kurata-Miura M., Ujita M., Angata K., Nakagawa S., Sekine S., Nishi T. & Fukuda M. (1997) Expression cloning of cDNA encoding a human β-1,3-N-acetyllactosaminyltransferase that is essential for poly-N-acetyllactosamine synthesis. *Proceedings of the National Academy of Science, USA.* **94:** 14294 – 14299.
- Sashima S., Takahashi I. & Nakazawa K. (2002) Identification and characterization of β-D-galactosyl-transferase in chick corneas. *Japanese Journal of Ophthalmology.* **46 (6):** 607-615.
- Sato K., Yomogida K., Wada T., Yorihuzi T., Nishimune Y., Hosokawa N. & Nagata K. (2002) Type XXVI collagen, a new member of the collagen family,

is specifically expressed in the testis and ovary. *The Journal of Biological Chemistry.* **277 (40):** 37678-37684.

- Sato T., Gotoh M., Kiyohara K., Akashima T., Iwasaki H., Kameyama A., Mochizuki H., Yada T., Inaba N., Togayachi A., Kudo T., Asada M., Watanabe H., Imamura T., Kimata K. & Narimatsu H. (2003). Differential roles of two N-acetyl-galactosaminyltransferases, CSGalNAcT-1, and a novel, CSGalNcT-2. Initiation and elongation in synthesis of chondroitin sulfate. *The Journal of Biological Chemistry.* **278 (5):** 3063-3071.
- Schanbacher F.L. & Ebner K.E. (1970) Galactosyltransferase acceptor specificity of the lactose synthetase A protein. *The Journal of Biological Chemistry.* **245 (19):** 5057 – 5061.
- Schwartz N.B. & Roden L (1974). Biosynthesis of chondroitin sulphate. Purification of UDP-D-xylose: core protein β-D-xylosetransferase by affinity chromatography. *Carbohydrate Research.* **37 (1):** 167-180.
- Scott J.E. & Haigh M. (1988) Keratan sulphate and the ultrastructure of cornea and cartilage: a 'stand-in' for chondroitin sulphate in conditions of oxygen lack? *Journal of Anatomy.* **158:** 95-108.
- Scott J.E. & Bosworth T.R. (1990) A comparative biochemical and ultrastructural study of proteoglycan-collagen interactions in corneal stroma. *Biochemical Journal.* **270:** 491 – 497.
- Scott J.E. (1991) Proteoglycans: collagen interactions and corneal ultrastructure. *Biochemical Society Transactions.* **19:** 877-881.
- Scott J.E. (1992) Supra-molecular organization of extracellular matrix glycosaminoglycans, in vitro and in the tissues. *The Federation of American Societies for Experimental Biology Journal.* **6:** 2639 – 2645.

- Scott J.E. (1994) Keratan sulphate – a 'reserve' polysaccharide? *European Journal of Clinical Chemistry and Clinical Biochemistry.* **32 (4):** 217-223.
- Seidenbecher C.I., Richter K., Rauch U., Fassler R., Garner C.C. & Gundelfinger E.D. (1995) Brevican, a chondroitin sulfate proteoglycan of rat brain, occurs as secreted and cell surface glycosylphosphatidylinositol-anchored isoforms. *The Journal of Biological Chemistry.* **270 (45):** 27206-27212.
- Seko A., Dohmae N., Takio K. & Yamashita K. (2003) β1,4-galactosyltransferase (β4GalT)-IV is specific for GlcNAc 6-0-sulphate. *The Journal of Biological Chemistry.* **278 (11):** 9150 – 9158.
- Seko A. & Yamashita K. (2004) β1,3,-N-acetylglucosaminyltransferase-7 (β3Gn-T7) acts efficiently on keratan sulphate-related glycans. *Federation of European Biochemical Societies Letters* **556:** 216 – 220.
- Seno N., Meyer K., Anderson B. & Hoffman P. (1965) Variations in keratosulfates. *The Journal of Biological Chemistry.* **240:** 1005-1010.
- Sharif M., Osborne D.J., Meadows K., Woodhouse S.M., Colvin E.M., Shepstone L. & Dieppe P.A. (1996) The relevance of chondroitin and keratan sulphate markers in normal and arthritic synovial fluid. *British Journal of Rheumatology.* **35(10):** 951-957.
- Shaw L.M. & Olsen B.R. (1991) FACIT collagens: diverse molecular bridges in extracellular matrices. *Trends in Biochemical Sciences.***16 (5):** 191-194.
- Shiozawa T., Tsukahara Y., Nakayama J., Ishii K. & Katsuyama T. (1991) Immunohistochemical reactivity of antikeratan sulfate monoclonal antibody 5D4 to various conditions of human endometrial tissues and its application as a

useful marker for identifying endometrial epithelia. *Gynecologic and Obstetric Investigation* **32(4):** 239-42.

- Shiraishi N., Natsume A., Togayachi A., Endo T., Akashima T., Yamada Y., Imai A., Nakagawa S., Koizumi S., Sekine S., Narimatsu H. & Sasaki K. (2001) Identification and characterisation of three novel β1,3-N-acetylglucosaminyltransferases structurally related to the β1,3-galactosyltransferase family. *The Journal of Biological Chemistry.* **276(5):** 3498 – 3507.
- Sorrell J.M., Lintala A.M., Mahmoodian F. & Caterson B. (1988) Epitope-specific changes in chondroitin sulfate/dermatan sulfate proteoglycans as markers in the lymphopoietic and granulopoietic compartments of developing bursae of Fabricius. *Journal of Immunology.* **140(12):** 4263-70.
- Sorrell M.J. & Caterson B. (1989) Detection of age-related changes in the distributions of keratan sulphates and chondroitin sulphates in developing chick limbs: an immunocytochemical study. *Development.* **106:** 657-663.
- Sorrell M.J., Caterson B., Caplan A.I., Davis B. & Schafer I.A. (1990) Human keratinocytes contain carbohydrates that are recognized by keratan sulphate-specific monoclonal antibodies. *The Journal of Investigative Dermatology.* **95 (3):** 347-352.
- Steele C. (1999) Corneal wound healing: a review. *Optometry Today.* **24:** 28 – 32.
- Stockwell R.A. (1970) Changes in the acid glycosaminoglycan content of the matrix of ageing human articular cartilage. *Annals of Rheumatic Diseases.* **5:** 509-515.

- Stuhlsatz H.W., Keller R., Becker G., Oeben M., Lennartz L., Fisher D.C. & Greiling H. (1989) Structure of keratan sulphate proteoglycans: core proteins, linkage regions, carbohydrate chains. *Keratan Sulphate: Chemistry, Biology, Chemical Pathology.* Greiling H. & Scott J.E., Editors. London: The Biochemical Society. **Pages 1 – 11.**
- Sugahara K. & Kitagawa H. (2002). Heparin and heparan sulfate biosynthesis. *International Union of Biochemistry and Molecular Biology Life.* **54 (4):** 163-75.
- Suzuki M. (1939) Biochemical studies on carbohydrates. L prosthetic group of corneamucoid. *Journal of Biochemistry* **30:** 185 – 191.
- Svensson L., Aszodi A., Reinholt F.P. Fassler R., Hienegard D. & Oldberg A. (1999) Fibromodulin-null mice have abnormal collagen fibrils, tissue organisation, and altered lumican deposition in tendon. *The Journal of Biological Chemistry.* **274(14):** 9636 – 9647.
- Sweet M.B.E., Thonar E.J.-M.A. & Marsh J. (1979) Age related changes in proteoglycan structure. *Archives of Biochemistry and Biophysics.* **198 (2):** 439-448.
- Sztrolovics R., Alini M., Mort J.S. & Roughley P.J. (1999 A) Age-related changes in fibromodulin and lumican in human intervertebral discs. *Spine.* **24(17):** 1765-1771.
- Sztrolovics R., Grover J., Cs-Szabo G., Shui-Liang S., Zhang Y., Mort J.S. & Roughley P. (2002) The characterization of versican and its message in human articular cartilage and intervertebral disc. *Journal of Orthopaedic Research.* **20:** 257 – 266.

- Tai G.H., Huckerby T.N. & Nieduszynski I.A. (1993) N.m.r. spectroscopic studies of fucose-containing oligosaccharides derived from keratanase digestion of articular cartilage keratan sulphates. Influence of fucose residues on keratanase cleavage. *The Biochemical Journal.* **291 (Pt 3):** 889-94.
- Tai G.H., Huckberby T.N. & Nieduszynski I.A. (1996) Multiple non-reducing chain termni isolated from bovine corneal keratan sulphates. *The Journal of Biological Chemistry.* 271 (38): 23535-23546.
- Tai G.-H., Nieduszynski I.A., Fullwood N.J. & Huckerby T.N. (1997) Human corneal keratan sulphates. *The Journal of Biological Chemistry.* **272 (45):** 28227-28231.
- Takagi M., Maeno M., Yamada T., Miyashita K. & Otsuka K. (1996) Nature and distribution of chondroitin sulphate and dermatan sulphate proteoglycans in rabbit alveolar bone. *Histochem Journal.* **28(5):** 341-51.
- Tang L.H., Buckwalter J.A. & Rosenberg L.C. (1996) Effect of link protein concentration on articular cartilage proteoglycan aggregation. *Journal of Orthopaedic Research.* **14 (2):** 334-339.
- Tasheva E.S., Koester A., Paulsen A.Q., Garrett A.S., Boyle D.L., Davidson H.J., Song M., Fox N. & Conrad G.W. (2002) Mimecan / osteoglycin-deficient mice have collagen fibril abnormalities. *Molecular Vision.* **8:** 407-415.
- Telser A., Robinson H.C. & Dorfman A. (1965) The biosynthesis of chondroitin-sulphate protein complex. *Proceedings of the National Academy of Science, USA.* **54 (3):** 912-919.

- Thonar E.J. & Sweet M.B.E. (1981) Maturation-related changes in proteoglycans of fetal articular cartilage. *Archives of Biochemistry and Biophysics.* **208 (2):** 535-547.
- Thonar E.J., Lenz M.E., Klintworth G.K., Caterson B., Pachman L.M., Glickman P., Katz R., Huff J. & Kuettner K.E. (1985) Quantification of keratan sulfate in blood as a marker of cartilage catabolism. *Arthritis and Rheumatism.* **28(12):** 1367-76.
- Thonar E.J., Buckwalter J.A. & Kuettner K.E. (1986). Maturation-related differences in the structure and composition of proteoglycans synthesized by chondrocytes from bovine articular cartilage. *The Journal of Biological Chemistry.* **261 (5):** 2467-2474.
- Thornton D.J., Morris H.G., Cockin G.H., Huckerby T.N.,, Nieduszynski I.A., Carlstedt I., Hardingham T.E. & Ratcliffe A. (1989) Structural and immunological studies of keratan sulphate from mature bovine articular cartilage. *Biochemical Journal.* **260:** 277-282.
- Tuckwell D. (2002) Identification and analysis of collagen α1(XXI), a novel member of the FACIT collagen family. *Matrix Biology.* **21:** 63 – 66.
- Uchimura K., Muramatsu H., Kadomatsu K., Fan Q.W., Kurosawa N., Mitsuoka C., Kannagi R., Habuchi O. & Muramatsu T. (1998) Molecular cloning and characterization of an N-acetylglucosamine-6-0-sulphotransferase. *The Journal of Biological Chemistry.* **273 (35):** 22577 – 22583.
- Ujita M., McAuliffe J., Suzuki M., Hindsgaul O., Clausen H., Fukuda M. & Fukuda M. (1999) Regulation of I-branched poly-N-acetyllactosamine synthesis. Concentrated actions by i-extension enzyme, I-branching enzyme

and β1,4-galactosyltransferase I. *The Journal of Biological Chemistry.* **274(14):** 9296 – 9304.

- Urban J.P.G. & Roberts S. (2003) Degeneration of the Intervertebral Disc. *Arthritis Research & Therapy.* **5 (3):** 120 – 130.
- Van der Rest M., Mayne R., Ninomiya Y., Seidah N.G., Chretien M. & Olsen B.R. (1985). The structure of type IX collagen. *The Journal of Biological Chemistry.* **260 (1):** 220-225.
- Vertel B.M., Walters L.M., Flay N., Kearns A.E. & Schwartz N.B. (1993) Xyloseylation is an endoplasmic reticulum to golgi event. *The Journal of Biological Chemistry.* **268 (15):** 11105-11112.
- Vij N., Roberts L., Joyce S & Chakravarti S. (2005 A) Lumican regulates corneal inflammatory responses by modulating Fas-Fas Ligand signalling. *Investigative Ophthalmology & Vision Science.* **46 (1):** 88 – 95.
- Vij N., Roberts L., Joyce S & Chakravarti S. (2005 B) Lumican binds FasL and modulates Fas-FasL signalling in the cornea. *The Association for Research in Vision and Ophthalmology.* **Program number 2806.**
- Vogel K.G., Paulsson M. & Heinegard D. (1984) Specific inhibition of type I and type II collagen fibrillogenesis by the small proteoglycan of tendon. *Biochemical Journal.* **223(3):** 587 – 597.
- Von der Mark K., Kirsch T., Nerlich A., Kuss A., Weseloh G., Gluckert K. & Stoss H. (1992) Type X collagen synthesis in human osteoarthritic cartilage. Indication ofchondrocyte hypertrophy. *Arthritis and Rheumatism.* **35 (7):** 806-811.

- Wolf B., Gressner A.M., Nevo Z. & Greiling H. (1982) Age related decrease in the activity of UDP-xylose: core protein xylose transferase in red costal cartilage. *Mechanisms of Ageing and Development.* **19:** 181-190.
- Wu J.J., Woods P.E. & Eyre D.R. (1992) Identification of cross-linking sites in bovine cartilage type IX collagen reveals an antiparallel type II –type IX molecular relationship and type IX to type IX bonding. *Journal of Biochemistry.* **267 (32):** 23007-23014.
- Wu J.J. & Eyre D.E. (1995) Structural analysis of cross-linking domains in cartilage type XI collagen. *The Journal of Biological Chemistry.* **270 (32):** 18865-18870.
- Yamada H., Watanabe K., Shimonaka M. & Yamaguchi Y. (1994) Molecular cloning of Brevican, a novel brain proteoglycan of the aggrecan/versican family. *The Journal of Biological Chemistry.* **269:** 10119 – 10126.
- Yamada H., Watanabe K., Shimonaka M., Yamasaki M. & Yamaguchi Y. (1995). cDNA cloning and the identification of an aggrecanase-like cleavage site in rat brevican. *Biochemical and Biophysical Research Communications.* **216 (3):** 957-963.
- Yamagishi K., Suzuki K., Imai K., Mochizuki H., Morikawa K., Kyogashima M., Kimata K. & Watanabe H. (2003) Purification, characterization, and molecular cloning of a novel keratan sulfate hydrolase, endo-β-N-acetylglucosaminidase, from *Bacillus circulans. The Journal of Biological Chemistry.* **278 (28):** 25766-25772.
- Yeh L.K., Chen W.L., Li W., Espana E.M., Ouyang J., Kawakita T., Kao W.W., Tseng S.C., Liu C.Y. (2005) Soluble lumican glycoprotein purified from

human amniotic membrane promotes corneal epithelial wound healing. Invest *Ophthalmol Vis Sci.* **46(2):** 479-86.

- Young R.D., Lawrence P.A., Duance V.C., Aigner T. and Monaghan P. (2000) Immunolocalization of collagen types II and III in single fibrils of human articular cartilage. *The Journal of Histochemistry and Cytochemistry.* **48:** 423 – 432.
- Young B.B., Zhang G., Koch M. & Birk D.E. (2002) The roles of types XII and XIV collagen in fibrillogenesis and matrix assembly in the developing cornea. *Journal of Cellular Biochemistry.* **87(2):** 208-220.
- Young A.A., Smith M.M., Smith S.M., Cake M.A., Ghosh P., Read R.A., Melrose J., Sonnabend D.H., Roughley P.J. & Little C.B. (2005 A) Regional assessment of articular cartilage gene expression and small proteoglycan metabolism in an animal model of osteoarthritis. *Arthritis Research and Therapy* **7:** R852 – R861.
- Young R.D., Tudor D., Hayes T.J., Kerr B.C., Hayashida Y., Nishida K., Meek K.M., Caterson B. & Quantock A.J. (2005 B) Atypical composition and ultrastructure of proteoglycans in the mouse corneal stroma. *Investigative Ophthalmology and Vision Science.* **46(6):** 1973-1978.
- Zhou D., Dinter A., Gutierrez Gallego R., Kamerling J.P., Vliegenthart J.F., Berger E.G. & Hennet T. (1999) A β-1,3-N-acetylglucosaminyltransferase with poly-N-acetyllactosamine synthase activity is structurally related to β-1,3-galactosyltransferases. *Proceedings of the National Academy of Science, USA.* **96:** 406 – 411.

- Ziegler C. & Mersmann G. (1984) Influence of effectors of the complex-type-oligosaccharide biosynthesis on the formation of proteokeratan sulfate in bovine cornea. *Biochimica et Biophysica Acta.* **799 (3):** 203-208.
- Zimmermann D.R., Trueb B., Winterhalter K.H., Witmer R. & Fischer R.W. (1986) Type VI collagen is a major component of the human cornea. *Federation of European Biochemical Society Letters.* **197 (1-2):** 55-58.
- Zimmermann D.R. & Ruoslahti E. (1989) Multiple domains of the large fibroblast proteoglycan, versican. *European Molecular Biology Organization Journal.* **8 (10):** 2975-2981.

Bibliography

- Alberts B., Bray D., Lewis J., Raff M., Roberts K. & Watson J.D. (1994) *Molecular Biology of the Cell.* Third edition. Garland Publishing, Inc. New York and London.
- Devlin TM (Editor) (1997) *A Text Book of Biochemistry, with clinical correlations.* 4th edition. New York, Chichester, Weinheim, Brisbane, Singapore, l Toronto, Wiley-Liss.
- Greiling H. & Scott J.E. (Editors) (1989). *Keratan Sulphate: Chemistry, Biology, Chemical Pathology.* London: The Biochemical Society.
- Hay E.D. & Revel J.P. (1969) *Fine structure of the developing avian cornea.* Basel (Switzerland), S. Karger, New York.
- Wright T.N. & Mecham R.P. (Editors) (1987). *Biology of Proteoglycans.* Academic Press Inc. Harcourt Brace Jovanovich, Publishers. Orlando, San Diego, New York, Austin, Boston, London, Sydney, Tokyo, Toronto.

Appendices

Appendix A – List of suppliers

Supplier	Materials/Equipment
Amersham Pharmacia Biotech, St Albans, Herts, UK.	UltroSpec2000 spectrophotometer; Akta explorer
Anachem Ltd. Luton, UK	0.5ml & 1.5ml eppendorf tubes
Applied Biosystems, Perkin-Elmer UK, Warrington, UK	$MgCl_2$; Gene Amp dNTPs; Gene Amp 10x PCR buffer; RNase inhibitor; MuLV reverse transcriptase; big dye terminator v 1.1 cycle sequence kit
Becton Dickenson	16 & 27.5 gauge needles
Bio-Rad Laboratories, Hemel Hemsted, UK	Transfer tanks; power packs; molecular weight protein standards
Cambio, Cambridge, UK	DNA ladder (1kb); 6x tracking dye; ethidium bromide
Corning Costar Ltd., High Wycombe, UK	Tissue culture plastic
Elkay, UK	96 well flat bottom EIA microtitre plates
Fisher Scientific, Loughborough, UK	Urea; acetic acid; hydrochloric acid; sodium hydroxide; methanol; ethanol
Gibco Brl (now invitrogen)	RPMI 1640 media; fetal bovine serum (FBS); PBS Dulbecco's; L-glutamine; penicillin streptomycin, fungizone (PSF) & hypoxanthine (100 μM), aminopterin (0.4 μm), thymidine (1.6 μm) [HAT]; Freunds complete adjuvant & Freunds incomplete adjuvant
Invitrogen	Pre-cast 4 - 12% and 4 - 20% Tris glycine gradient gels; Oligonucleotides; electrophoresis tanks
Millipore Ltd., Watford, UK	0.22 μM filters; milli Q Plus 185 unit; Milli RO unit;
MP Biomedical	Keratanase; keratanase II; endo-β-galactosidase; Agarose (genetic technology grade)
National Diagnostics, Hessle, UK	Acrylagel and bisacrylagel
Pierce	Bicinchoninic Acid (BCA) protein assay reagent kit
Promega Corporation, Southampton, UK	Anti-mouse IgG (H+L) alkaline phosphatase conjugated secondary antibody; NBT: nitro blue tetrazolium; BCIP: 5-bromo-4-chloro-3-indoylphosphate; Taq DNA polymerase
Qiagen Ltd., Crawley,UK	RNeasy mini kit; QIA quick PCR purification kit; RNase free DNase set

Roche Diagnostics Ltd., Lewes, UK	Digoxigenin (DIG) glycan differentiation kit
Schleicher & Schuell Bioscience	0.22 μm Protran BA 83 nitrocellulose membrane
Sigma- Aldrich Ltd., Poole, UK	General laboratory chemicals; Tri-reagent; EDGLY protein deglycosylation kit; Chondroitin sulphate C, sodium salt from shark cartilage; L-(tosylamido-2-phenyl) ethyl chloromethyl ketone (TPCK) treated trypsin; Chondroitinase ABC; Polyethylene glycol ($_{Mw}$ 3,000 – 3,700); dimethyl sulphoxide (DMSO); β-mercaptoethanol
Spectrum Laboratories, Rancho Dominguez, CA, USA	Spectra/Por dialysis membrane
Techne, Burlington, NJ, USA	Technegene thermal cycler

Appendix B – Papers, abstracts & presentations

Papers

- Young R.D., Tudor D., Hayes T.J., **Kerr B.C.,** Hayashida Y., Nishida K., Meek K.M., Caterson B. & Quantock A.J. (2005) Atypical composition and ultrastructure of proteoglycans in the mouse corneal stroma. *Investigative Ophthalmology and Vision Science*. **46(6):** 1973-1978.
- Grau S., Richards P.J., **Kerr B.C.,** Hughes C., Caterson B., Williams A.S., Junker U., Jones S.A., Clausen T., Ehrmann M. (2005) The role of human HtrA1 in arthritic disease. *Journal of Biological Chemistry.* **Dec 22**

Oral presentations

April 2004 British Society for Matrix Biology 'Grappling with the Glycome', University of Manchester, UK.

July 2004 Eighth Corneal Conference, Cardiff, Wales, UK.

PRIFYSGOL CAERDYDD